

**An Integrated Approach Involving Metabolomics
and Transcriptomics for a System-Wide
Understanding of the Interaction between Tomato
and *Cladosporium fulvum***

Desalegn Woldesenbet Etalo

Thesis committee

Promotor

Prof. Dr H.J. Bouwmeester
Professor of Plant Physiology
Wageningen University

Co-promotors

Dr M.H.A.J. Joosten
Associate professor, Laboratory of Phytopathology
Wageningen University

Dr C.H. de Vos
Senior researcher, Plant Research International
Wageningen University

Other members

Prof. Dr G.C. Angenent, Plant Research International, Wageningen University
Prof. Dr B.J.C. Cornelissen, University of Amsterdam
Dr G. Smant, Wageningen University
Dr R. Mumm, Plant Research International, Wageningen University

This research was conducted under the auspices of the Graduate School of Experimental Plant Science (EPS)

**An Integrated Approach Involving Metabolomics
and Transcriptomics for a System-Wide
Understanding of the Interaction between Tomato
and *Cladosporium fulvum***

Desalegn Woldesenbet Etalo

Thesis

submitted in fulfilment of the requirement for the degree of doctor
at Wageningen University
by the authority of the Rector Magnificus
Prof. Dr M.J. Kropff,
in the presence of the
Thesis Committee appointed by the Academic Board
to be defended in public
on Thursday 20 March 2014
at 11 a.m. in the Aula.

Desalegn Woldesenbet Etalo

An Integrated Approach Involving Metabolomics and Transcriptomics for a System-Wide Understanding of the Interaction between Tomato and *Cladosporium fulvum*,
272 pages.

PhD thesis Wageningen University, Wageningen, NL (2014)
With references, with summary in English, Dutch and Amharic

ISBN 978-94-6173-821-9

TABLE OF CONTENTS

CHAPTER 1	7
General Introduction	
CHAPTER 2	21
System-Wide Hypersensitive Response-Associated Transcriptome and Metabolome Reprogramming in Tomato	
CHAPTER 3	101
Carbon Economy and the Maintenance of Energy Homeostasis during the Hypersensitive Response in Tomato	
CHAPTER 4	149
Genome-Wide Functional Analysis of Wrky Transcription Factors in Resistance of Tomato to <i>Cladosporium fulvum</i>	
CHAPTER 5	183
The Metabolic Arms Race Between Tomato and <i>Cladosporium fulvum</i>	
CHAPTER 6	233
General Discussion	
Summary	253
Samenvatting	256
ግጥቃሊያ (Amharic Summary)	260
Acknowledgements	262
<i>Curriculum vitae</i>	266
Publication list	267
Education statement	268



Chapter 1

General Introduction



The plant immune system

The relationship between plants and fungi is often mutualistic, with only a small minority of fungal species breaking the fine balance of cooperation to become pathogens (Fraser, 2004; Holub, 2006). Modern agricultural practices based on monoculture cultivation of crop plants, which are often selected mainly for consumer-desired traits and not for disease resistance, is breaking the co-evolution cycle between plants and fungi and results in versatile pathogens (Dangl et al., 2013). These pathogens use highly adapted invasion strategies that have led to devastating epidemics. The Irish potato famine of the 1840s, caused by the oomycete *Phytophthora infestans* that causes late blight (Yoshida et al., 2013) and the current wheat stem, leaf and yellow stripe rust epidemics spreading from East Africa to the Indian subcontinent, caused by rust fungi *Puccinia graminis* and *Puccinia striiformis* (Singh et al., 2011), illustrate the recurring impact of plant diseases (Dangl et al., 2013).

Plant immunity is based on two interconnected layers that are surveyed by extracellular plasma membrane-localised receptors, being either receptor-like proteins (RLPs) or receptor-like kinases (RLKs), and intracellular receptors, referred to as nucleotide-binding-leucine-rich repeat (NB-LRR) proteins. These immune receptors play a critical role in perceiving non-self components and subsequent mounting of an adequate defence response to invading pathogens (Jones and Dangl, 2006). The first layer is in fact formed by so-called pattern recognition receptors (PRRs) that recognize highly conserved microbe-associated molecular patterns (MAMPs), such as fungal chitin and bacterial flagellin, and their perception leads to the induction of MAMP-triggered immunity (MTI). However, virulent microbes deliver specific effector proteins into the host cells that suppress MTI and cause effector-triggered susceptibility (ETS). Resistant plants in turn will use the second layer of surveillance that allows specific recognition of these effectors and halts pathogen ingress through the activation of effector-triggered immunity (ETI). Generally, MTI and ETI give rise to similar responses, although in most cases ETI is stronger, faster and more robust and often involves localized programmed cell death, referred to as the hypersensitive response (HR) (Tao et al., 2003; Chisholm et al., 2006; Jones and Dangl, 2006; Dodds and Rathjen, 2010; Thomma et al., 2011; Dangl et al., 2013). Successful pathogens will avoid ETI by deletion or mutation of the effector that is perceived by the host and will cause ETS by the action of yet another effector. This continuous battle between plants and pathogens that has been going on for many millennia has played a vital role in shaping the defensive and offensive machinery of plants and pathogens, respectively. This results in hosts and pathogens that show a continuous and rhythmic loss and gain of resistance and virulence, respectively.

The interaction between tomato and *Cladosporium fulvum*; a model for system-wide studies on plant-microbe interactions

The *Cladosporium fulvum*-tomato pathosystem has been shown to be a versatile model system to study the evolutionary arms race between plants and pathogens (Rivas and Thomas, 2005; Stergiopoulos and de Wit, 2009). *C. fulvum* is a non-obligate biotrophic fungal pathogen that causes leaf mould disease on tomato and the interaction between plant and fungus can be divided into a compatible and an incompatible one, with tomato either being susceptible or resistant to *C. fulvum*, respectively. The interaction is primarily controlled in a gene-for-gene manner in which *Cf* resistance genes of tomato, encoding leucine-rich repeat- receptor-like proteins (LRR-RLPs), mediate recognition of avirulence factors (Avrs) of *C. fulvum* (Joosten and de Wit, 1999; Rivas and Thomas, 2005; Stergiopoulos and de Wit, 2009).

The compatible interaction between tomato and *C. fulvum*

Different races of *C. fulvum* are defined according to their virulence spectrum on tomato lines harbouring specific *Cf* resistance genes, and are named according to the resistance genes that they can overcome. For example, *C. fulvum* race 5, which was used in most of our experiments, successfully colonizes tomato plants expressing either no *Cf* genes (*Cf-0*) or the *Cf-5* resistance gene (Jones et al., 1994). Thus, race 5 has lost the *Avr5* gene, thereby avoiding recognition by the Cf-5 protein. Similarly, *C. fulvum* race 4 lacks *Avr4*, thereby allowing successful colonization of *Cf-4*-expressing tomato, in addition to *Cf-0* plants.

Under conditions of high relative humidity, conidia of *C. fulvum* germinate on the abaxial side of tomato leaves and generate runner hyphae that grow over the leaf surface and enter the leaf apoplast via the stomata. In a compatible interaction (CI), the fungal hyphae continue to grow between the cells in the spongy mesophyll, without forming haustoria (de Wit, 1977) (**Figure 1A, upper panel**), and produce various effectors with the aim to dampen the host immune response (Rooney et al., 2005; van den Burg et al., 2006; van Esse et al., 2008; de Jonge et al., 2010). Upon successful colonization (**Figure 1B, upper panel**), apoplastic sucrose is broken down to glucose and fructose by *C. fulvum*-encoded invertase and these monosaccharides are converted into mannitol by a fungal mannitol dehydrogenase (Joosten et al., 1990). Conidiophores, which originate from aerial hyphae in the sub-stomatal cavities, emerge through the stomata at approximately 10–12 days post inoculation (dpi) (de Wit, 1977)(**Figure 1C, upper panel**) and at later stages extensive degeneration of the leaf tissue takes place.

The incompatible interaction between tomato and *C. fulvum*

In an incompatible interaction (II) between tomato and *C. fulvum*, the fungal hyphae are arrested in their development soon upon penetration of the sub-stomatal cavity,

after the first contact with the leaf spongy mesophyll cells occurs (de Wit, 1977). The incompatible interaction is typically characterized by the induction of the HR, where spongy mesophyll cells that are in close proximity to fungal hyphae collapse and degenerate (**Figure 1A, lower panel**), resulting in containment of the pathogen to the infection site (**Figure 1B, lower panel**) (Hammond-Kosack and Jones, 1994). The HR is controlled by the above-mentioned gene-for-gene interaction between the fungus and its host and detailed analyses have shown that the HR by itself is not always required to arrest fungal growth (Hammond-Kosack and Jones, 1994). The HR is often associated with massive accumulation of secondary metabolites by the host, together with the production of cell wall-degrading enzymes such as glucanases and chitinases that can degrade the fungal cell wall, and other pathogenesis-related (PR) proteins (Joosten and de Wit, 1999). Eventually growth of the fungus is stopped and macroscopically in most cases no symptoms are visible (**Figure 1C, lower panel**).

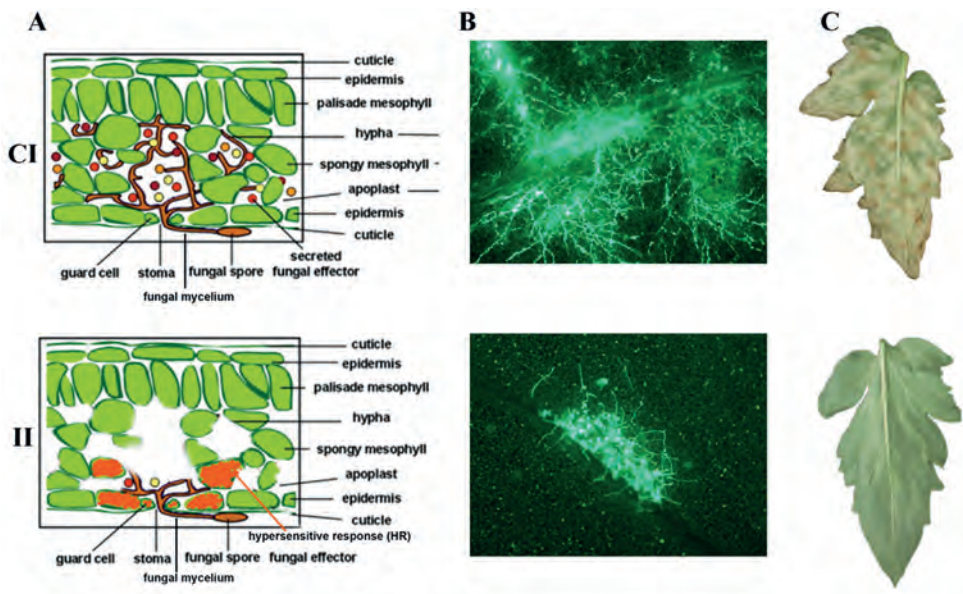


Figure 1. The *Cladosporium fulvum*-tomato interaction.

In a compatible interaction (CI) between tomato and *C. fulvum*, conidia of *C. fulvum* germinate on the leaf surface and randomly penetrate the stomata on the lower side of the tomato leaf. The generated mycelium eventually produces several effectors (small circles filled with different colors) to dampen the host defense response (**CI-A**). Placing micro-droplets of a spore suspension of GFP-labeled *C. fulvum* on the lower side of tomato leaves results in successful colonization of the leaf by the fungus at 13 days post inoculation (dpi) (**CI-B**). Leaflets of susceptible tomato plants show extensive fungal colonization and sporulation at 14 dpi. (**CI-C**).

In an incompatible interaction (II) between tomato and *C. fulvum*, the swift recognition of fungal effectors by tomato Cf resistance proteins induces the hypersensitive response (HR) and stops the ingress of the fungus (**II-A**). Placing micro droplets of a spore suspension of GFP-labeled *C. fulvum* on the lower side of tomato leaves results in the development of hyphae that show limited outgrowth as a result of the induced HR (**II-B**). Leaflets of resistant tomato plants appear healthy as a result of the HR that stops fungal ingress and does not result in macroscopic symptoms (**II-C**).

The dying seedlings; a model system for studying host responses related to the HR

In most pathosystems colonization of host tissues by the pathogen is non-synchronous, rendering the analysis of the chronological order of defense-related, post-inoculation events in resistant plants at the molecular, biochemical, metabolic and cytological level, difficult (Morel and Dangl, 1997). Highly localized sampling of tissue mounting the HR would solve this, but is very laborious and cannot be very precise. A great alternative to this are tomato seedlings that express both a *Cf* resistance gene and the matching *Avr* gene from *C. fulvum*, obtained by crossing *Cf*-expressing tomato with a matching *Avr*-expressing transgenic tomato line (**Figure 2A**). In such *Cf/Avr* “dying seedlings” (DS), the induction of the HR is suppressed by placing the plants at an elevated temperature, in combination with a high relative humidity (RH) (33°C and 100% RH). A subsequent shift to normal growth conditions (20°C and 70% RH) initiates a synchronized and systemic HR in the seedlings that can be monitored at various time points after the temperature shift (**Figure 2B**) (de Jong et al., 2002; Gabriëls et al., 2006; Stulemeijer et al., 2007). Hence, the DS enable us to synchronize and amplify the responses associated with the HR, rendering them an ideal system for integrated, system-wide studies (Stulemeijer et al., 2009).

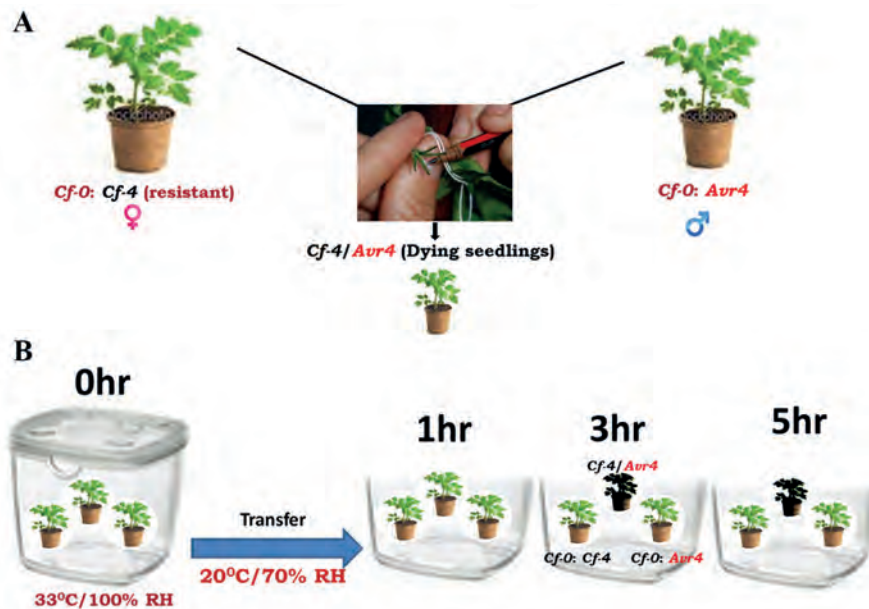


Figure 2. The tomato *Cf-4/Avr4* dying seedlings.

(A) Generation of *Cf-4/Avr4* dying seedlings by crossing transgenic *Cf-0* tomato plants expressing *Avr4* (*Cf-0:Avr4*) to transgenic *Cf-0* tomato plants expressing *Cf-4* (*Cf-0:Cf-4*).

(B) Initiation of a synchronized and systemic HR in the *Cf-4/Avr4* dying seedlings upon a shift from 33°C/100% relative humidity (RH) to lower temperature and RH (20°C/70%).

In the dying seedlings, the activation of the HR is for example associated with an oxidative burst (**Figure 3**), activation of MAP kinases and suppression of photosynthesis and accumulation of secondary metabolites, suggesting that the response typically represents the resistance response of tomato against an avirulent strain of *C. fulvum* (Stulemeijer et al., 2007; Stulemeijer et al., 2009).



Figure 3. The oxidative burst that takes place during mounting of the HR in tomato seedlings that express the *C. fulvum* avirulence gene *Avr9* and the matching resistance gene, *Cf-9*.

Amplex red (10-acetyl-3,7-dihydroxyphenoxazine) was fed to the seedlings through the transpiration stream. In the presence of peroxidase the reagent reacts with H_2O_2 in a 1:1 stoichiometry to produce the red-fluorescent oxidation product, resorufin (Zhou et al., 1997). Resorufin fluorescence was excited by 520 nm irradiation produced by a green light emitting diode (LED), filtered through a 520 nm band pass interference filter and imaged using a CCD camera protected with a 600 nm band-pass interference filter (Etalo et al., 2009).

Integrated system-wide transcriptomics and metabolomics studies in plant-microbe interactions

The activation of the host immune system is associated with a large array of changes in the plant transcriptome, proteome and metabolome. Elucidation of the role of such complex infection-associated changes needs integrated approaches to understand the

underlying mechanisms of plant resistance and strategies used by the pathogen resulting in host susceptibility. Integrated transcriptomics and metabolomics analysis forms a powerful tool to build the relationship between information elements of a system (genes and transcripts) and its functional elements (proteins and metabolites) in cells (Mercke et al., 2004; Li et al., 2010). Recently, the integration of these approaches has shown to be a viable approach in the study of systemic induced resistance in Arabidopsis plants in response to the non-pathogenic rhizobacterium *Pseudomonas fluorescens* SS101 (van de Mortel et al., 2012). Hence, in my PhD research, an integrated approach involving transcriptomics and metabolomics was used for a system-wide understanding of the interaction between tomato and *C. fulvum*.

Transcriptomics

Transcriptomics, is a tool to analyze the pool of mRNA molecules present in a sample (Zhang et al., 2010). It has been more than a decade since the complete sequence of the human genome was published (Lander et al., 2001). Since then, the advent of next generation DNA sequencing technologies revolutionized genome sequencing and comparative genomics studies that focus on the DNA, which represents the static information for any given organism but does not show changes in response to short-term perturbations. Subtle and short-term changes can be monitored through transcriptomics technologies. Recently, RNA sequencing (RNA-Seq) has emerged as an alternative to classical microarrays for quantitative measurement of the dynamic expression of genes (Ye et al., 2001; James et al., 2002; Marioni et al., 2008). In my PhD study, I used both technologies to profile the dynamic changes in the tomato defense-transcriptome, allowing the identification of genes of which the expression changes during the activation of host defense responses.

Metabolomics

The plant metabolome is a representation of the small molecules that are present in the various plant tissues and metabolomics is the high-throughput technology that provides a comprehensive and (semi-)quantitative overview of the metabolites present in an organism (Hall, 2006). Unlike the genome, the transcriptome and the proteome, capturing the metabolome from a complex system requires a number of different extraction, separation and analytical techniques. Moreover, in genomics and transcriptomics, the function and structure of unknown genes and transcripts can be predicted based on their sequence similarity with other known genes of the organism or from other species. The genome sequence of the model plant, *Arabidopsis thaliana* (The Arabidopsis-Genome-Initiative, 2000) and the presence of mutants and T-DNA insertion lines, for example, have been vital for the identification and functional characterization of genes. This propels the prediction process for unknown genes in other species, which is further supported by new genome sequences, including the recently released tomato genome sequence (Sato et al., 2012). These methodologies, however, are not available for

metabolomics and this hinders the identification of metabolites, rendering the biological interpretation of changes in the metabolome difficult.

In plant-microbe interaction studies, plant metabolomics should provide a substantial contribution to the understanding of the pathosystem, as infection of the plant often results in metabolic changes, which may be important for successful deterrence of the invading pathogen (Dixon, 2001; Allwood et al., 2006; Ward et al., 2010). In general, the plant metabolome can be divided into two, partly blurred categories, primary and secondary metabolites. Primary metabolites are required for growth, development, and reproduction of plants while secondary metabolites are defined as not having a direct role in these primary functions, but to contribute to the interaction of the organism with biotic and abiotic factors in its environment.

Secondary metabolites, which are sometimes also referred to as natural products, are highly diverse and the estimated number of these compounds in the Plant Kingdom exceeds 200,000 (Oldiges et al., 2007). These small molecules are known for a range of biological activities, including insect repellence, protection against excessive UV irradiation and antimicrobial activity (Hammerschmidt, 1999; Dixon, 2001). The latter are categorized as phytoanticipins (pre-formed infection inhibitors) and phytoalexins (induced antimicrobials). However, some compounds may be phytoalexins in one species and phytoanticipins in another (Dixon, 2001). Apart from aspects of plant defense itself, such as cell wall thickening (Huckelhoven, 2007) and production of antimicrobial chemicals (Wink, 1988; Osbourn, 1999; Kliebenstein et al., 2005), it is equally important to understand how microbes in turn manipulate host defense metabolism for their own benefit. Indeed, in response to the inherent resistance mechanisms present in plants, pathogenic bacteria and fungi in turn have developed strategies to breach the plant chemical defense line, for example by secreting phytoalexin-detoxifying enzymes (Ford et al., 1977; Roldan-Arjona et al., 1999; Kaup et al., 2005). Re-programming of both host and microbe metabolism is thus core to a biotrophic relationship and metabolomics approaches can play an important role in the exploration of these phenomena (Allwood et al., 2006; Abu-Nada et al., 2007; Allwood et al., 2008; Ward et al., 2010; Draper et al., 2011).

Integrated transcriptomics and metabolomics

In some studies, the correlation between protein and mRNA abundance was shown to be non-significant (Gygi et al., 1999) or only very weak (Ideker et al., 2001; Greenbaum et al., 2002; Nie et al., 2008). Several factors have been suggested to determine the observed discrepancy, including the regulation of protein levels by post-translational modification, post-transcriptional regulation of protein synthesis, differences in the half-lives of mRNA and proteins, specific protein degradation, possible functional requirement for protein binding, and significant levels of experimental errors (Greenbaum et al., 2002; Beyer et al., 2004; Park et al., 2005). Hence, the combination of transcriptomics and metabolomics

will be a viable approach to monitor the relevant transcriptional changes that impact the metabolome, which in most cases reflect the cellular state of the system. Hence, in this thesis a combined transcriptomics and metabolomics approach was employed to gain a system-wide understanding of the molecular interaction between *C. fulvum* and tomato, with a primary focus on integration of the different biological levels. This integration of multilayer information should lay the foundation for a more robust statistical integration of the information that is already available to ultimately develop mathematical models to elucidate how cells function at the system level.

Objectives of the thesis

The objectives of this thesis are to gain insight in the system-wide changes occurring during the interaction between tomato and *C. fulvum*, using metabolomics and transcriptomics. The hypothesis is that the integration of multilayer information allows the identification of important regulators and regulatory mechanisms playing a role during the response of the host to the pathogen. Furthermore, such integrative approaches are anticipated to help unravelling the counter measures taken by pathogens to breach the host defense machinery.

To test these hypotheses, in **Chapter 2** the transcriptional and metabolic changes associated with mounting of the hypersensitive response (HR) are studied, using microarray analysis and metabolomics. For this the dying seedlings that mimic the localized resistance response of tomato plant against *C. fulvum* (**Figure 2**) are employed. Based on the information obtained from Chapter 2, in **Chapter 3** the HR-associated transcriptional changes are further studied. In this case deep sequencing (RNA-seq) is performed, again during HR development in the *Cf/Avr* dying seedlings, but now also in resistant and susceptible tomato plants inoculated with *C. fulvum*. The chapter particularly focuses on processes involved in the regulation of energy homeostasis and carbon economy of the system. These two first experimental chapters contribute to the identification of a number of important regulators of the defense-transcriptome of tomato and using this information, in **Chapter 4** a functional characterization of a number of tomato WRKY transcription factors is performed. This class of transcription factors consists of a group of key regulators, some of which are activating and some of which are suppressing the plant immune response. The results of several experiments support the involvement of the various WRKYs in the defence-associated metabolome reprogramming of tomato upon its colonisation by *C. fulvum*. In **Chapter 5**, to elucidate the major (bio)chemical changes associated with host resistance and the counter measures that are taken by the fungus, a comprehensive metabolic profiling of resistant and susceptible tomato plants inoculated with *C. fulvum* is performed. In addition, several *C. fulvum* enzymes that are involved in the detoxification of antimicrobial tomato metabolites are characterized. In **Chapter 6**, the work that is described in this thesis is discussed and placed in a broader perspective.

References

- Abu-Nada Y, Kushalappa AC, Marshall WD, Al-Mughrabi K, Murphy A (2007) Temporal dynamics of pathogenesis-related metabolites and their plausible pathways of induction in potato leaves following inoculation with *Phytophthora infestans*. *Eur J Plant Pathol* **118**: 375-391
- Allwood JW, Ellis DI, Goodacre R (2008) Metabolomic technologies and their application to the study of plants and plant–host interactions. *Physiol. Plant* **132**: 117-135
- Allwood JW, Ellis DI, Heald JK, Goodacre R, Mur LAJ (2006) Metabolomic approaches reveal that phosphatidic and phosphatidyl glycerol phospholipids are major discriminatory non-polar metabolites in responses by *Brachypodium distachyon* to challenge by *Magnaporthe grisea*. *Plant J* **46**: 351-368
- Beyer A, Hollunder J, Nasheuer HP, Wilhelm T (2004) Post-transcriptional expression regulation in the yeast *Saccharomyces cerevisiae* on a genomic scale. *Mol Cell Proteomics* **3**: 1083-1092
- Chisholm ST, Coaker G, Day B, Staskawicz BJ (2006) Host-microbe interactions: shaping the evolution of the plant immune response. *Cell* **124**: 803-814
- Dangl JL, Horvath DM, Staskawicz BJ (2013) Pivoting the plant immune system from dissection to deployment. *Science* **341**: 746-751
- de Jong CF, Takken FL, Cai X, de Wit PJGM, Joosten MHJ (2002) Attenuation of Cf-mediated defense responses at elevated temperatures correlates with a decrease in elicitor-binding sites. *Mol Plant-Microbe Interact* **15**: 1040-1049
- de Jonge R, van Esse HP, Kombrink A, Shinya T, Desaki Y, Bours R, van der Krol S, Shibuya N, Joosten MHJ, Thomma BPHJ (2010) Conserved fungal LysM effector Ecp6 prevents chitin-triggered immunity in plants. *Science* **329**: 953-955
- de Wit PJGM (1977) A light and scanning-electron microscopic study of infection of tomato plants by virulent and avirulent races of *Cladosporium fulvum*. *Neth J Plant Path.* **83**: 109-122
- Dixon RA (2001) Natural products and plant disease resistance. *Nature* **411**: 843-847
- Dodds PN, Rathjen JP (2010) Plant immunity: towards an integrated view of plant-pathogen interactions. *Nat Rev Genet* **11**: 539-548
- Draper J, Rasmussen S, Zubair H (2011) Metabolite analysis and metabolomics in the study of biotrophic interactions between plants and microbes. *In Annual Plant Reviews Volume 43*. Wiley-Blackwell, pp 25-59
- Etalo DW, Harbinson J, van Meeteren U (2009) Could Wound-Induced Xylem Peroxide Contribute to the Postharvest Loss of Hydraulic Conductivity in Stems? *Ix International Symposium on Postharvest Quality of Ornamental Plants* **847**: 287-293
- Ford JE, McCance DJ, Drysdale RB (1977) The detoxification of α -tomatine by *Fusarium oxysporum* f. sp. *lycopersici*. *Phytochemistry* **16**: 545-546
- Fraser CM (2004) Insights into the evolution of phytopathogens. *Trends Microbiol* **12**: 482-483
- Gabriëls SH, Takken FL, Vossen JH, de Jong CF, Liu Q, Turk SC, Wachowski LK, Peters J, Witsenboer HM, de Wit PJGM, Joosten MHJ (2006) cDNA-AFLP combined with functional analysis reveals novel genes involved in the hypersensitive response. *Mol Plant-Microbe Interact* **19**: 567-576
- Greenbaum D, Jansen R, Gerstein M (2002) Analysis of mRNA expression and protein abundance data: an approach for the comparison of the enrichment of features in the cellular population of proteins and transcripts. *Bioinformatics* **18**: 585-596
- Gygi SP, Rochon Y, Franz A, Aebersold R (1999) Correlation between protein and mRNA abundance in yeast. *Mol Cell Biol* **19**: 1720-1730
- Hall RD (2006) Plant metabolomics: from holistic hope, to hype, to hot topic. *New Phytologist* **169**: 453-468
- Hammerschmidt R (1999) Phytoalexins: What have we learned after 60 years? *Annu Rev Phytopathol* **37**: 285-306
- Hammond-Kosack KE, Jones JDG (1994) Incomplete dominance of tomato Cf Genes for resistance to *Cladosporium fulvum*. *Mol Plant Microbe Interact* **7**: 58-70
- Holub EB (2006) Evolution of parasitic symbioses between plants and filamentous microorganisms. *Curr Opin Plant Biol* **9**: 397-405
- Huckelhoven R (2007) Cell wall-associated mechanisms of disease resistance and susceptibility. *Annu Rev Phytopathol* **45**: 101-127

- Ideker T, Thorsson V, Ranish JA, Christmas R, Buhler J, Eng JK, Bumgarner R, Goodlett DR, Aebersold R, Hood L (2001) Integrated genomic and proteomic analyses of a systematically perturbed metabolic network. *Science* **292**: 929-934
- James TC, Campbell SG, Bond UM (2002) Comparative analysis of global gene expression in lager and laboratory yeast strains grown in Wort. *P IEEE* **90**: 1887-1899
- Jones DA, Thomas CM, Hammond-Kosack KE, Balintkurti PJ, Jones JDG (1994) Isolation of the tomato *Cf-9* gene for resistance to *Cladosporium fulvum* by transposon tagging. *Science* **266**: 789-793
- Jones JDG, Dangl JL (2006) The plant immune system. *Nature* **444**: 323-329
- Joosten MHJ, de Wit PJGM (1999) The tomato-*Cladosporium fulvum* interaction. A versatile experimental system to study plant-pathogen interactions. *Annu Rev Phytopathol* **37**: 335-367
- Joosten MHJ, Hendrickx LJM, de Wit PJGM (1990) Carbohydrate-composition of apoplastic fluids isolated from tomato leaves inoculated with virulent or avirulent races of *Cladosporium fulvum* (*Syn Fulvia fulva*). *Neth J Plant Pathol* **96**: 103-112
- Kaup O, Gräfen I, Zellermann E-M, Eichenlaub R, Gartemann K-H (2005) Identification of a tomatinase in the tomato-pathogenic actinomycete *Clavibacter michiganensis* subsp. *michiganensis* NCPPB382. *Mol Plant Microbe Interact* **18**: 1090-1098
- Kliebenstein DJ, Rowe HC, Denby KJ (2005) Secondary metabolites influence Arabidopsis/Botrytis interactions: variation in host production and pathogen sensitivity. *Plant J* **44**: 25-36
- Lander ES, Consortium IHGS, Linton LM, Birren B, Nusbaum C, Zody MC, Baldwin J, Devon K, Dewar K, Doyle M, FitzHugh W, Funke R, Gage D, Harris K, Heaford A, Howland J, Kann L, Lehoczky J, LeVine R, McEwan P, McKernan K, Meldrum J, Mesirov JP, Miranda C, Morris W, Naylor J, Raymond C, Rosetti M, Santos R, Sheridan A, Sougnez C, Stange-Thomann N, Stojanovic N, Subramanian A, Wyman D, Rogers J, Sulston J, Ainscough R, Beck S, Bentley D, Burton J, Clee C, Carter N, Coulson A, Deadman R, Deloukas P, Dunham A, Dunham I, Durbin R, French L, Grafham D, Gregory S, Hubbard T, Humphray S, Hunt A, Jones M, Lloyd C, McMurray A, Matthews L, Mercer S, Milne S, Mullikin JC, Mungall A, Plumb R, Ross M, Shownkeen R, Sims S, Waterston RH, Wilson RK, Hillier LW, McPherson JD, Marra MA, Mardis ER, Fulton LA, Chinwalla AT, Pepin KH, Gish WR, Chissoe SL, Wendt MC, Delehaunty KD, Miner TL, Delehaunty A, Kramer JB, Cook LL, Fulton RS, Johnson DL, Minx PJ, Clifton SW, Hawkins T, Branscomb E, Predki P, Richardson P, Wenning S, Slezak T, Doggett N, Cheng JF, Olsen A, Lucas S, Elkin C, Uberbacher E, Frazier M, Gibbs RA, Muzny DM, Scherer SE, Bouck JB, Sodergren EJ, Worley KC, Rives CM, Gorrell JH, Metzker ML, Naylor SL, Kucherlapati RS, Nelson DL, Weinstock GM, Sakaki Y, Fujiyama A, Hattori M, Yada T, Toyoda A, Itoh T, Kawagoe C, Watanabe H, Totoki Y, Taylor T, Weissenbach J, Heilig R, Saurin W, Artiguenave F, Brottier P, Bruls T, Pelletier E, Robert C, Wincker P, Rosenthal A, Platzer M, Nyakatura G, Taudien S, Rump A, Yang HM, Yu J, Wang J, Huang GY, Gu J, Hood L, Rowen L, Madan A, Qin SZ, Davis RW, Federspiel NA, Abola AP, Proctor MJ, Myers RM, Schmutz J, Dickson M, Grimwood J, Cox DR, Olson MV, Kaul R, Raymond C, Shimizu N, Kawasaki K, Minoshima S, Evans GA, Athanasiou M, Schultz R, Roe BA, Chen F, Pan HQ, Ramser J, Lehrach H, Reinhardt R, McCombie WR, de la Bastide M, Dedhia N, Blocker H, Hornischer K, Nordsiek G, Agarwala R, Aravind L, Bailey JA, Bateman A, Batzoglou S, Birney E, Bork P, Brown DG, Burge CB, Cerutti L, Chen HC, Church D, Clamp M, Copley RR, Doerks T, Eddy SR, Eichler EE, Furey TS, Galagan J, Gilbert JGR, Harmon C, Hayashizaki Y, Haussler D, Hermjakob H, Hokamp K, Jang WH, Johnson LS, Jones TA, Kasif S, Kasprzyk A, Kennedy S, Kent WJ, Kitts P, Koonin EV, Korf I, Kulp D, Lancet D, Lowe TM, McLysaght A, Mikkelsen T, Moran JV, Mulder N, Pollara VJ, Ponting CP, Schuler G, Schultz JR, Slater G, Smit AFA, Stupka E, Szustakowski J, Thierry-Mieg J, Thierry-Mieg J, Wagner L, Wallis J, Wheeler R, Williams A, Wolf YI, Wolfe KH, Yang SP, Yeh RF, Collins F, Guyer MS, Peterson J, Felsenfeld A, Wetterstrand KA, Patrinos A, Morgan MJ, Conso IHGS (2001) Initial sequencing and analysis of the human genome. *Nature* **409**: 860-921
- Li Y, Zhang Q, Zhang J, Wu L, Qi Y, Zhou JM (2010) Identification of microRNAs involved in pathogen-associated molecular pattern-triggered plant innate immunity. *Plant Physiol* **152**: 2222-2231
- Marioni JC, Mason CE, Mane SM, Stephens M, Gilad Y (2008) RNA-seq: an assessment of technical reproducibility and comparison with gene expression arrays. *Genome Res* **18**: 1509-1517
- Mercke P, Kappers IF, Verstappen FWA, Vorst O, Dicke M, Bouwmeester HJ (2004) Combined transcript and metabolite analysis reveals genes involved in spider mite induced volatile formation in cucumber plants. *Plant Physiol* **135**: 2012-2024

- Morel JB, Dangel JL (1997) The hypersensitive response and the induction of cell death in plants. *Cell Death Differ* 4: 671-683
- Nie L, Wu G, Zhang WW (2008) Statistical application and challenges in global gel-free proteomic analysis by mass spectrometry. *Crit Rev Biotechnol* 28: 297-307
- Oldiges M, Lütz S, Pflug S, Schroer K, Stein N, Wiendahl C (2007) Metabolomics: current state and evolving methodologies and tools. 76: 495-511
- Osborn AE (1999) Antimicrobial phytoprotectants and fungal pathogens: a commentary. *Fungal Genet Biol* 26: 163-168
- Park SJ, Lee SY, Cho J, Kim TY, Lee JW, Park JH, Han MJ (2005) Global physiological understanding and metabolic engineering of microorganisms based on omics studies. *Appl Microbiol Biotechnol* 68: 567-579
- Rivas S, Thomas CM (2005) Molecular interactions between tomato and the leaf mold pathogen *Cladosporium fulvum*. *Annu Rev Phytopathol* 43: 395-436
- Roldan-Arjona T, Perez-Espinosa A, Ruiz-Rubio M (1999) Tomatinase from *Fusarium oxysporum* f. sp. lycopersici defines a new class of saponinases. *Molecular Plant-Microbe Interactions* 12: 852-861
- Rooney HC, Van't Klooster JW, van der Hoorn RA, Joosten MH, Jones JD, de Wit PJGM (2005) *Cladosporium Avr2* inhibits tomato Rcr3 protease required for Cf-2-dependent disease resistance. *Science* 308: 1783-1786
- Sato S, Tabata S, Hirakawa H, Asamizu E, Shirasawa K, Isobe S, Kaneko T, Nakamura Y, Shibata D, Aoki K, Egholm M, Knight J, Bogden R, Li CB, Shuang Y, Xu X, Pan SK, Cheng SF, Liu X, Ren YY, Wang J, Albiero A, Dal Pero F, Todesco S, Van Eck J, Buels RM, Bombarely A, Gosselin JR, Huang MY, Leto JA, Menda N, Strickler S, Mao LY, Gao S, Tecle IY, York T, Zheng Y, Vrebalov JT, Lee J, Zhong SL, Mueller LA, Stiekema WJ, Ribeca P, Alioto T, Yang WC, Huang SW, Du YC, Zhang ZH, Gao JC, Guo YM, Wang XX, Li Y, He J, Li CY, Cheng ZK, Zuo JR, Ren JF, Zhao JH, Yan LH, Jiang HL, Wang B, Li HS, Li ZJ, Fu FY, Chen BT, Han B, Feng Q, Fan DL, Wang Y, Ling HQ, Xue YBA, Ware D, McCombie WR, Lippman ZB, Chia JM, Jiang K, Pasternak S, Gelley L, Kramer M, Anderson LK, Chang SB, Royer SM, Shearer LA, Stack SM, Rose JKC, Xu YM, Eannetta N, Matas AJ, McQuinn R, Tanksley SD, Camara F, Guigo R, Rombauts S, Fawcett J, Van de Peer Y, Zamir D, Liang CB, Spannagl M, Gundlach H, Bruggmann R, Mayer K, Jia ZQ, Zhang JH, Ye ZBA, Bishop GJ, Butcher S, Lopez-Cobollo R, Buchan D, Filippis I, Abbott J, Dixit R, Singh M, Singh A, Pal JK, Pandit A, Singh PK, Mahato AK, Dogra V, Gaikwad K, Sharma TR, Mohapatra T, Singh NK, Causse M, Rothan C, Schiex T, Noirot C, Bellec A, Klopp C, Delalande C, Berges H, Mariette J, Frasse P, Vautrin S, Zouine M, Latche A, Rousseau C, Regad F, Pech JC, Philippot M, Bouzayen M, Pericard P, Osorio S, del Carmen AF, Monforte A, Granell A, Fernandez-Munoz R, Conte M, Lichtenstein G, Carrari F, De Bellis G, Fuligni F, Peano C, Grandillo S, Termolino P, Pietrella M, Fantini E, Falcone G, Fiore A, Giuliano G, Lopez L, Facella P, Perrotta G, Daddiego L, Bryan G, Orozco M, Pastor X, Torrents D, van Schriek KNVMGM, Feron RMC, van Oeveren J, de Heer P, daPonte L, Jacobs-Oomen S, Carriaso M, Prins M, van Eijk MJT, Janssen A, van Haaren MJJ, Jo SH, Kim J, Kwon SY, Kim S, Koo DH, Lee S, Hur CG, Clouser C, Rico A, Hallab A, Gebhardt C, Klee K, Jocker A, Warfsmann J, Gobel U, Kawamura S, Yano K, Sherman JD, Fukuoka H, Negoro S, Bhutty S, Chowdhury P, Chattopadhyay D, Datema E, Smit S, Schijlen EWM, van de Belt J, van Haarst JC, Peters SA, van Staveren MJ, Henkens MHC, Mooyman PJW, Hesselink T, van Ham RCHJ, Jiang GY, Droege M, Choi D, Kang BC, Kim BD, Park M, Kim S, Yeom SI, Lee YH, Choi YD, Li GC, Gao JW, Liu YS, Huang SX, Fernandez-Pedrosa V, Collado C, Zuniga S, Wang GP, Cade R, Dietrich RA, Rogers J, Knapp S, Fei ZJ, White RA, Thannhauser TW, Giovannoni JJ, Botella MA, Gilbert L, Gonzalez R, Goicoechea JL, Yu Y, Kudrna D, Collura K, Wissotski M, Wing R, Schoof H, Meyers BC, Gurazada AB, Green PJ, Mathur S, Vyas S, Solanke AU, Kumar R, Gupta V, Sharma AK, Khurana P, Khurana JP, Tyagi AK, Dalmay T, Mohorianu I, Walts B, Chamala S, Barbazuk WB, Li JP, Guo H, Lee TH, Wang YP, Zhang D, Paterson AH, Wang XY, Tang HB, Barone A, Chiusano ML, Ercolano MR, D'Agostino N, Di Filippo M, Traini A, Sanseverino W, Frusciante L, Seymour GB, Elharam M, Fu Y, Hua A, Kenton S, Lewis J, Lin SP, Najaf F, Lai HS, Qin BF, Qu CM, Shi RH, White D, White J, Xing YB, Yang KQ, Yi J, Yao ZY, Zhou LP, Roe BA, Vezzi A, D'Angelo M, Zimbello R, Schiavon R, Caniato E, Rigobello C, Campagna D, Vitulo N, Valle G, Nelson DR, De Paoli E, Szinay D, de Jong HH, Bai YL, Visser RGF, Lankhorst RMK, Beasley H, McLaren K, Nicholson C, Riddle C, Gianese G, Consortium TG (2012) The tomato genome sequence provides insights into fleshy fruit evolution. *Nature* 485: 635-641

- Singh RP, Hodson DP, Huerta-Espino J, Jin Y, Bhavani S, Njau P, Herrera-Foessel S, Singh PK, Singh S, Govindan V** (2011) The Emergence of Ug99 Races of the Stem Rust Fungus is a Threat to World Wheat Production. *Annu Rev Phytopathol* **49**: 465-481
- Stergiopoulos I, de Wit PJGM** (2009) Fungal Effector Proteins. *In Annual Review of Phytopathology*, Vol 47, pp 233-263
- Stulemeijer IJ, Joosten MHAJ, Jensen ON** (2009) Quantitative phosphoproteomics of tomato mounting a hypersensitive response reveals a swift suppression of photosynthetic activity and a differential role for hsp90 isoforms. *J Proteome Res* **8**: 1168-1182
- Stulemeijer IJS, Stratzmann JW, Joosten MHAJ** (2007) Tomato mitogen-activated protein kinases LeMPK1, LeMPK2, and LeMPK3 are activated during the *Cf-4/Avr4*-induced hypersensitive response and have distinct phosphorylation specificities. *Plant Physiol* **144**: 1481-1494
- Tao Y, Xie ZY, Chen WQ, Glazebrook J, Chang HS, Han B, Zhu T, Zou GZ, Katagiri F** (2003) Quantitative nature of Arabidopsis responses during compatible and incompatible interactions with the bacterial pathogen *Pseudomonas syringae*. *Plant Cell* **15**: 317-330
- The-Arabidopsis-Genome-Initiative** (2000) Analysis of the genome sequence of the flowering plant *Arabidopsis thaliana*. *Nature* **408**: 796-815
- Thomma BPHJ, Nurnberger T, Joosten MHAJ** (2011) Of PAMPs and effectors: the blurred PTI-ETI dichotomy. *Plant Cell* **23**: 4-15
- van de Mortel JE, de Vos RC, Dekkers E, Pineda A, Guillod L, Bouwmeester K, van Loon JJ, Dicke M, Raaijmakers JM** (2012) Metabolic and transcriptomic changes induced in Arabidopsis by the rhizobacterium *Pseudomonas fluorescens* SS101. *Plant Physiol* **160**: 2173-2188
- van den Burg HA, Harrison SJ, Joosten MHAJ, Vervoort J, de Wit PJGM** (2006) *Cladosporium fulvum* Avr4 protects fungal cell walls against hydrolysis by plant chitinases accumulating during infection. *Mol. Plant-Microbe Interact* **19**: 1420-1430
- van Esse HP, van't Klooster JW, Bolton MD, Yadeta KA, van Baarlen P, Boeren S, Vervoort J, de Wit PJGM, Thomma BPHJ** (2008) The *Cladosporium fulvum* virulence protein Avr2 inhibits host proteases required for basal defense. *Plant Cell* **20**: 1948-1963
- Ward JL, Forcat S, Beckmann M, Bennett M, Miller SJ, Baker JM, Hawkins ND, Vermeer CP, Lu C, Lin W, Truman WM, Beale MH, Draper J, Mansfield JW, Grant M** (2010) The metabolic transition during disease following infection of *Arabidopsis thaliana* by *Pseudomonas syringae* pv. tomato. *Plant J*
- Wink M** (1988) Plant-breeding importance of plant secondary metabolites for protection against pathogens and herbivores. *Theor Appl Genet* **75**: 225-233
- Ye RW, Wang T, Bedzyk L, Croker KM** (2001) Applications of DNA microarrays in microbial systems. *J Microbiol Meth* **47**: 257-272
- Yoshida K, Schuenemann VJ, Cano LM, Pais M, Mishra B, Sharma R, Lanz C, Martin FN, Kamoun S, Krause J, Thines M, Weigel D, Burbano HA, Baulcombe D** (2013) The rise and fall of the *Phytophthora infestans* lineage that triggered the Irish potato famine. *Elife* **2**
- Zhang W, Li F, Nie L** (2010) Integrating multiple 'omics' analysis for microbial biology: application and methodologies. *Microbiology* **156**: 287-301
- Zhou M, Diwu Z, Panchuk-Voloshina N, Haugland RP** (1997) A stable nonfluorescent derivative of resorufin for the fluorometric determination of trace hydrogen peroxide: applications in detecting the activity of phagocyte NADPH oxidase and other oxidases. *Anal Biochem* **253**: 162-168



Chapter 2

System-Wide Hypersensitive Response-Associated Transcriptome and Metabolome Reprogramming in Tomato

Desalegn W. Etalo^{1,4,Ω}, Iris J.E. Stulemeijer^{3,6}, H. Peter van Esse³, Ric C.H. de Vos^{2,4,5}, Harro J. Bouwmeester^{1,4*} and Matthieu H.A.J. Joosten^{3,4,5}

¹Laboratory of Plant Physiology, Wageningen University,
6708 PB Wageningen, the Netherlands.

²Plant Research International Bioscience, Wageningen University,
6708 PB Wageningen, the Netherlands.

³Laboratory of Phytopathology, Wageningen University,
6708 PB Wageningen, the Netherlands

⁴Centre for BioSystems Genomics, 6700 AB Wageningen, the Netherlands.

⁵Netherlands Metabolomics Centre, Einsteinweg 55, 2333 CC Leiden, the Netherlands.

⁶Present address: The Netherlands Cancer Institute,
Plesmanlaan 121, 1066 CX Amsterdam, The Netherlands.

^ΩCurrent address: Plant Research International, Bioscience, Wageningen University,
Wageningen, The Netherlands

*Author for correspondence (Harro.Bouwmeester@wur.nl).

Published as Etalo et al., (2013) *Plant Physiology* **162**: 1599-617.

Abstract

The hypersensitive response (HR) is considered to be the hallmark of the resistance response of plants to pathogens. To study HR-associated transcriptome and metabolome reprogramming in tomato (*Solanum lycopersicum*), we used plants that express both a resistance gene to *Cladosporium fulvum* and the matching avirulence gene of this pathogen. In these plants indeed massive reprogramming occurred and we found that the HR and associated processes are highly energy-demanding. Ubiquitin-dependent protein degradation, hydrolysis of sugars, as well as lipid catabolism are used as alternative sources of amino acids, energy and carbon skeletons, respectively. We observed strong accumulation of secondary metabolites, such as hydroxycinnamic acid amides. Co-regulated expression of WRKY transcription factors and genes known to be involved in the HR, in addition to a strong enrichment of the W-box WRKY binding motif in the promoter sequences of the co-regulated genes, point to WRKYs as the most prominent orchestrators of the HR. Our study has revealed several novel HR-related genes and reverse genetics tools will allow to understand the role of each individual component in the HR.

Introduction

Unlike animals, plants do not have a specialized adaptive immune system that recognizes and directly attacks and destroys infectious agents. Instead, plants are endowed with a broad range of sophisticated and efficient innate immunity mechanisms that enable them to recognize and restrain a plethora of pathogenic microbes in their natural habitat (Jones and Dangl, 2006). Plants carry so-called pattern recognition receptors (PRRs) that recognize conserved structural molecules of pathogens, referred to as pathogen-associated molecular patterns (PAMPs), leading to PAMP-triggered immunity (PTI). Invading pathogens, in their turn, secrete virulence proteins (so-called effectors) to suppress PTI, leading to effector-triggered susceptibility (ETS). As a response to this, plants have evolved resistance (R) proteins that recognize these effectors rendering them avirulence factors (Avrs), and subsequently mediate effector-triggered immunity (ETI). In fact, PTI and ETI function in a similar way and both types of immunity are based on the activation of immune receptors that trigger a level of defense that is sufficient to stop colonization by the pathogen (DeYoung and Innes, 2006; Jones and Dangl, 2006; Postel and Kemmerling, 2009; Dodds and Rathjen, 2010; Thomma et al., 2011). The innate immune response of plants often culminates in the hypersensitive response (HR). This particular response, which is considered to be one of the hallmarks of the immunity of plants to pathogens, involves programmed cell death (PCD) and occurs at the site of pathogen entry, resulting in efficient containment of the pathogen (Lam et al., 2001).

The interaction between tomato (*Solanum lycopersicum*) and the biotrophic extracellular fungus *Cladosporium fulvum* is a model pathosystem which is characterized as a typical gene-for-gene interaction, in which *C. fulvum* (Cf) resistance proteins of tomato mediate specific recognition of Avrs of the fungus (de Wit and Joosten, 1999; Rivas and Thomas, 2005; Thomma et al., 2005). In this interaction, the HR is one of the distinctive responses of resistant tomato plants to avirulent strains of the fungus. In most studied pathosystems, pathogen infection is non-synchronous, rendering the chronological ordering of defense-related post-infection events in resistant plants at the molecular, biochemical, metabolic and cytological level difficult (Morel and Dangl, 1997). To obtain insight into the global transcriptome and metabolome reprogramming that occurs in tomato when mounting the HR we studied tomato plants that express both a Cf resistance gene and the matching Avr gene from the fungus, obtained by crossing Cf-expressing tomato with an Avr-expressing tomato line. In such Cf/Avr “dying seedlings” (DS), the induction of the HR can be suppressed at an elevated temperature and high relative humidity (RH) (33°C and 100 % RH). A subsequent shift to normal growth conditions (20°C and 70 % RH) initiates a synchronized and systemic induction of the HR in the seedlings (de Jong et al., 2002; Gabriëls et al., 2006; Stulemeijer et al.,

2007). In contrast, inoculation of *Cf*-expressing tomato plants with *C. fulvum* carrying the matching *Avr* gene results in an HR that is restricted to only a limited number of cells and which is by far not synchronized, which hampers research towards direct and small local effects. Hence, the DS enable us to synchronize and amplify the responses associated with the HR.

Here we performed transcriptome and metabolome profiling of DS expressing both *Cf-4* and *Avr4*, as compared to the parental lines expressing either *Cf-4* or *Avr4*, at various time points after the shift to the permissive condition of 20°C and 70 % RH. Unbiased transcriptome- and metabolome-wide approaches allow to investigate the behavior and relationships between different elements of a particular biological system (Schneider and Collmer, 2010). With the right tools, these approaches allow visualization of the underlying biological processes, leading to a better insight into the biology of the host cells while the plant is mounting defense to the invading pathogen (Bolton et al., 2008; van Baarlen et al., 2008; van Esse et al., 2008; van Esse et al., 2009; Hanssen et al., 2011). We used the Affymetrix® Tomato Genome Array to study changes in the global gene expression profiles in the DS as compared to their parental lines. In addition, we employed untargeted metabolomics, using GC-TOF and LC-PDA-QTOF mass spectrometry for profiling polar primary metabolites (PPM) and semi-polar secondary metabolites (SPSM) of the plant material, respectively. We analyzed and explored the datasets with various bioinformatics and statistics tools to identify major, system-wide transcriptome and metabolome reprogramming events associated with mounting of the HR. We found that the DS undergo a vast and coordinated reprogramming of their transcriptome within several hours after the shift to permissive conditions, on the one hand to induce the HR and on the other hand to control it. We revealed specific interrelationships of various metabolites associated with the HR and a critical role of energy homeostasis during mounting of the HR. Furthermore, we uncover major regulators and regulatory mechanisms of the HR in these tomato plants mounting a synchronous and systemic immune response.

Results

Hypersensitive Response-Associated Global Changes in Gene Expression in Tomato Seedlings

The hierarchical cluster analysis (HCA) presented in **Figure 1A** provides an overview of the relative expression profiles of the genes that were interrogated by the Affymetrix® tomato microarrays in response to transferring the seedlings to environmental conditions permissive for HR. For each time point, the profiles of three independent biological replicates are shown. Before HR induction ($t = 0$ hr), the overall gene

expression profile of the dying seedlings (DS) compared to a 1:1 mixture of their parental lines (PLS; see Materials and Methods) is very similar. At this stage, in both the DS and PLS the majority of the genes with relatively high expression appear to be associated with the initially relatively high temperature of 33°C, as their expression decreases within 1 hr after the shift to 20°C (**Figure 1A**, yellow-boxed gene cluster marked 0_U). This cluster represents a large number of genes, including some of the major marker genes for heat stress, such as genes encoding heat shock proteins (HSPs), heat stress-associated (HAS) proteins, heat shock protein-binding proteins, DNA heat shock proteins and universal stress proteins (USPs). Unlike the greater part of the genes in this cluster, which are further down-regulated at 3 and 5 hr, most of the HSPs show up-regulation at 5 hr after the temperature shift in the DS, when compared to the PLS (**Supplemental Table S1**).

Upon shifting the plants from 33°C to 20°C, within 1 hr moderate changes in gene expression were observed which for the greater part involve slight up-regulation of sets of genes in the DS compared to the PLS. This up-regulation becomes much more pronounced at 3 hr and 5 hr after the temperature shift (**Figure 1A**, yellow boxes marked 35_U1 and 35_U2). In contrast, gene set 35_D is down-regulated in the DS compared to the PLS. **Figure 1B** provides an overview of the numbers of genes that are either significantly up- or down-regulated in the DS compared to the PLS at $t = 0$ hr (33°C/100 % RH) and the different time points after the shift to 20°C/70 % RH, based on the averages between the three biological replicates for the individual time points. From the 10,219 genes represented on the tomato genome array, a total of 1,152 genes (11.3 %) shows differential regulation (a fold change (FC) > 2 and P -value < 0.05), at least under one of the conditions analyzed. Of these genes, 732 genes are up-regulated and 420 genes are down-regulated in the DS when compared to the PLS, representing about 7.2 % and 4.1 % of the total number of genes represented on the array, respectively (**Figure 1B**).

The rescue temperature of 33°C, in combination with 100 % RH, efficiently suppresses the expression of the majority of the defense-related genes (**Figure 1A**, yellow-boxed clusters 0_D1 and 0_D2) (Gabriëls et al., 2006; Stulemeijer et al., 2007). However, in the DS there are six genes that consistently show a higher expression compared to the PLS at all time points (**Figure 1B**, upper panel (0, 1, 3, 5)). These six genes encode a basic endo-chitinase, an acidic 26 kD endo-chitinase, a glycine-rich protein, a photo assimilate-responsive protein (PAR), a disease resistance-responsive family protein and aquaporin NIP1.1, which have all been reported to be involved in the response of plants to biotic stress (Margolles-Clark et al., 1996; Bienert et al., 2007; Hong et al., 2007; Gomes et al., 2009; Mangeon et al., 2010). This implicates that in the DS some level of defense is already induced before the temperature shift without the execution of the HR. One hour after the shift to 20°C, 81 genes show differential regulation in the DS

compared to the PLS, of which the majority (90 %) is up-regulated (**Figure 1B**, upper panel, U_1 hr (73 genes) and lower panel, D_1 hr (8 genes). About 41 % (30 genes) of these up-regulated genes is unique for this time point (**Figure 1B**, upper panel, 1 only), whereas a subset of 20 genes that show early up-regulation continues to exhibit higher expression levels at later time points (**Figure 1B**, upper panel, (1, 3, 5)). In the DS, the overlapping and unique sets of genes that are differentially expressed at 3 hr and 5 hr (see boxes 35_D, 35_U1 and 35_U2 in **Figure 1A**) account for about 91 % of the total number of differentially regulated genes (**Figure 1B**, 3 only and 5 only and (3, 5)), indicating that defense-related transcriptional reprogramming is significantly intensified at time points later than 1 hr after the shift to permissive conditions. Close to 62 % of these genes are up-regulated in the DS compared to the PLS, with the majority (413 genes; 63 %) being unique for t = 5 hr (**Figure 1B**, upper panel, 5 only).

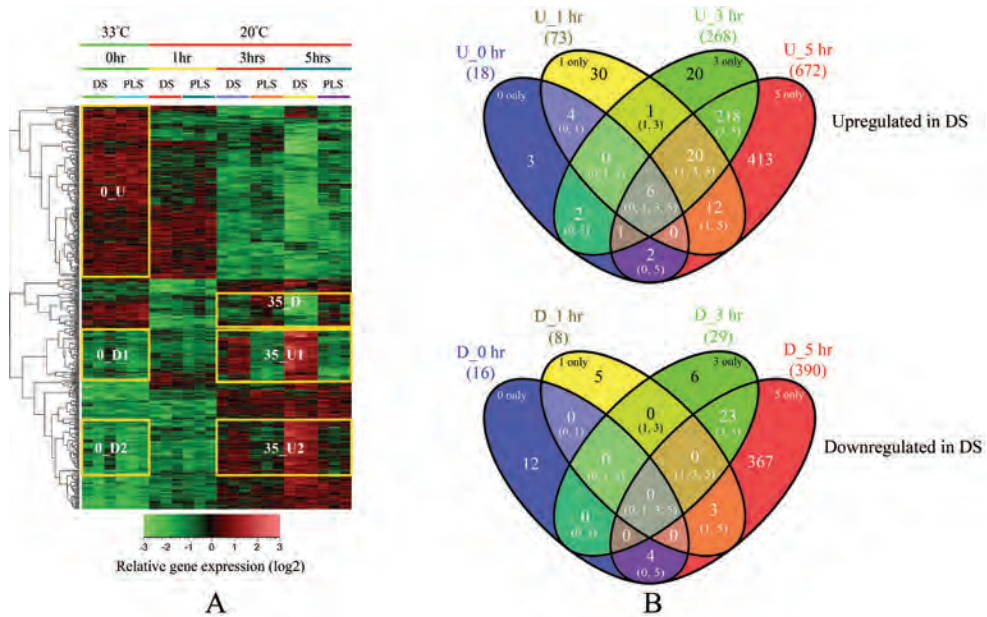


Figure 1. Transcriptome profiles of the Cf-4/Avr4 dying seedlings (DS) and their parental lines (PLS) before (t = 0 hr) and 1 hr, 3 hr and 5 hr after the temperature shift that initiates the hypersensitive response (HR) in the DS. **A**, Hierarchical cluster analysis (HCA) of the transcriptome profile. For each time point, the three columns labeled either "DS" or "PLS", represent the gene expression data obtained in three independent replicate experiments. Marked changes in the gene expression profiles of the DS and the PLS at t = 0 hr and at 3 hr and 5 hr after the temperature shift are indicated by the yellow-boxed gene sets. At t = 0 hr additional gene set selection was performed to group genes based on their expression profiles. 0_U, up-regulated at t = 0 hr; 0_D, down-regulated at t = 0 hr; 35_D, down-regulated at t = 3 hr and t = 5 hr; 35_U, up-regulated at t = 3 hr and t = 5 hr. The bar below the figure indicates the color code for the relative change in gene expression of log2-transformed and auto-scaled data. **B**, Venn diagram showing the temporal distribution of unique and overlapping genes differentially regulated upon comparison of the averages between the three biological replicates of the DS and those of the PLS, for the different time points. Upper panel, genes up-regulated (U) in the DS compared to the PLS. Lower panel, genes down-regulated (D) in the DS compared to the PLS. Numbers between brackets represent the amount of differentially regulated genes that are unique or overlapping at time points 0 hr, 1 hr, 3 hr and/or 5 hr after the temperature shift.

In addition to a large set of up-regulated genes at $t = 5$ hr (U_5 hr; 672 genes), there is also a large number of down-regulated genes at this time point (397, from which 367 are even unique for $t = 5$ hr) (**Figure 1B**, lower panel, D_5 hr and 5 only, respectively).

As visualized by MapMan (Thimm et al., 2004), the massive reprogramming in the DS upon initiation of the HR involves the transcriptional activation of genes encoding receptor-like kinases, G-proteins, MAP kinases, transcription factors and genes involved in calcium regulation, redox pathways, hormone biosynthesis, protein modification and protein degradation (**Figure 2**). Cytoplasmic receptor-like kinase (RLK)-encoding genes are the most prominent among the up-regulated *RLKs*. This group also includes genes encoding leucine-rich repeat (LRR)-containing RLKs, lysin motif (LysM)-containing RLKs, domain of unknown function 26 (DUF26)-containing RLKs, wall-associated kinase (WAK) and an RLK10-like protein. Particularly at 3 and 5 hr, these genes show significantly higher expression in the DS (**Figure 2**, panels $t = 3$ hr and $t = 5$ hr).

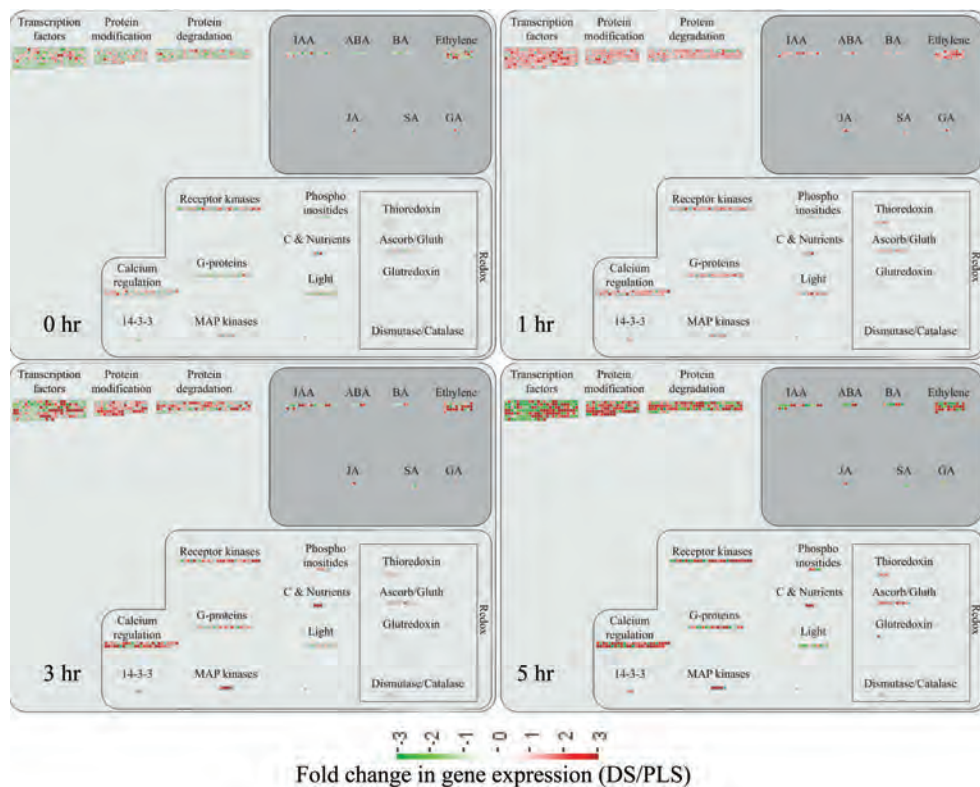


Figure 2. Visualization of the transcriptional reprogramming occurring in the dying seedlings (DS) as compared to their parental lines (PLS), at 0 hr, 1 hr, 3 hr and 5 hr after the temperature shift that induces the HR in the DS. Each panel represents an individual time point and depicts the expression profile of genes (represented by the colored squares) involved in the indicated biological processes. The bar below the figure indicates the color codes for the fold-change in gene expression in the DS compared to the PLS. The map does not represent all differentially regulated genes, as only genes that can be related to specific biological processes are displayed.

Over-Representation Analysis of Differentially Regulated Gene Sets

Over-representation analysis (ORA) of genes within the up- and down-regulated categories (**Figure 1B**) allows making a temporal dissection of the different processes that occur upon mounting of the HR. ORA on gene sets that showed differential regulation at 3 hr and 5 hr after initiating the HR produced a vast list of significantly enriched or under-represented gene ontology (GO): subcategories. To visualize these lists of categories and to reduce the high level of redundancy, we built a similarity matrix using the (Gene x GO: subcategory) matrix, which is an output of GeneTrail software (Backes et al., 2007). In the (Gene x GO: subcategory) matrix, a differentially regulated gene gets a score of 1 when it belongs to a particular functional category, if not its score is 0. Subsequently, the resulting (0, 1) matrix was used to produce a set of manageable “GO: subcategory meta-clusters”, by comparing two GO: subcategories for the characteristic presence of a gene. In such an analysis, the high redundancy level of the GO: annotation is significantly reduced (see **Supplemental Materials** and **Methods S1** for more details). In the panels that are shown, redundant GO: subcategories that have high correlation are indicated in red and fall along the diagonal axis of the similarity matrix (**Figure 3**).

ORA on the set of genes that show early transcriptional activation upon HR induction (**Figure 1B**, top panel, U_1 hr, 73 genes), revealed some significantly over-represented GO: subcategories, such as valine, leucine and isoleucine degradation, oxido-reductase activity, response to chemical stimulus, secondary metabolism and response to stimulus (**Supplemental Table S2**). At time points $t = 3$ hr and $t = 5$ hr, there is massive transcriptional reprogramming in the DS. ORA on the 218 overlapping up-regulated genes at these time points (**Figure 1B**, upper panel, (3, 5)) resulted in 226 significantly enriched GO: subcategories and a similarity matrix analysis on these subcategories produced 25 distinct meta-clusters (**Figure 3A**). Interestingly, functional categories associated with signal perception, signal transduction and activated defense responses are among these meta-clusters. Examples are sets of up-regulated genes associated with aromatic amino acid biosynthesis (phenylalanine and tyrosine), ethylene biosynthesis and signaling, calcium/calmodulin-dependent signaling, protein modification (phosphorylation), phytoalexin biosynthesis, and positive as well as negative regulation of programmed cell death (PCD) (**Figure 3A**).

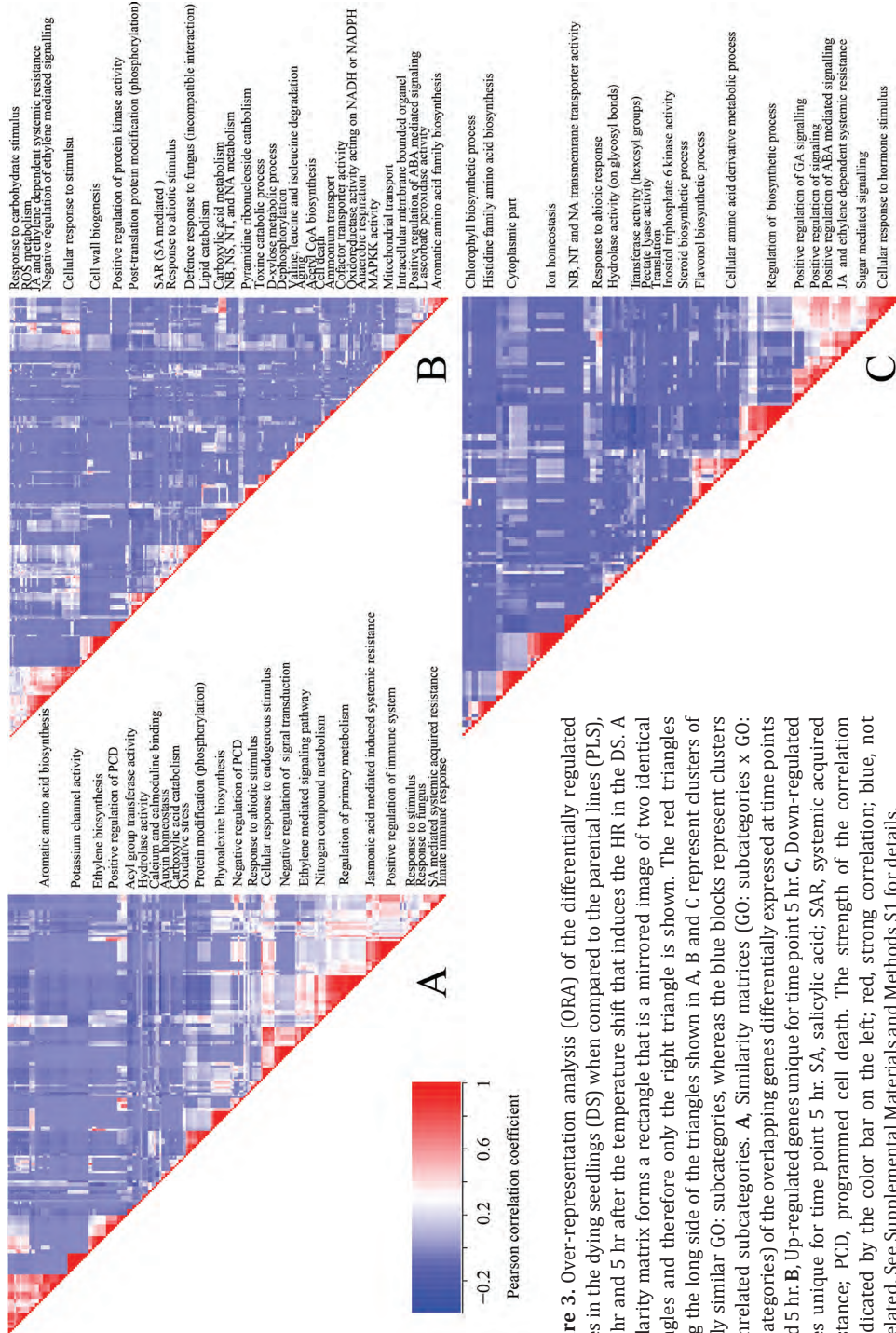


Figure 3. Over-representation analysis (ORA) of the differentially regulated genes in the dying seedlings (DS) when compared to the parental lines (PLS), at 3 hr and 5 hr after the temperature shift that induces the HR in the DS. A similarity matrix forms a rectangle that is a mirrored image of two identical triangles and therefore only the right triangle is shown. The red triangles along the long side of the triangles shown in A, B and C represent clusters of highly similar GO: subcategories, whereas the blue blocks represent clusters of unrelated subcategories. A, Similarity matrices (GO: subcategories x GO: subcategories) of the overlapping genes differentially expressed at time points 3 and 5 hr. B, Up-regulated genes unique for time point 5 hr. C, Down-regulated genes unique for time point 5 hr. SA, salicylic acid; SAR, systemic acquired resistance; PCD, programmed cell death. The strength of the correlation is indicated by the color bar on the left; red, strong correlation; blue, not correlated. See Supplemental Materials and Methods S1 for details.

Time point 5 hr is characterized by the presence of two large differentially regulated gene sets, one up-regulated (**Figure 1A**, sets 35_U1 and 35_U2; **Figure 1B**, upper panel, 5 only, 413 genes) and one down-regulated in the DS (**Figure 1A**, set 35_D; **Figure 1B**, lower panel, 5 only, 367 genes). ORA on these two sets of genes revealed a significant enrichment for a number of GO: subcategories: 32 and 22 major GO: subcategory meta-clusters were identified in the up-regulated and down-regulated categories, respectively (**Figures 3B** and **3C**). In the up-regulated gene set some of the significantly over-represented GO: subcategories are anaerobic respiration, catabolic processes like lipid catabolism and pyrimidine ribonucleoside catabolism, cell wall biogenesis, systemic acquired resistance, mitochondrial transport, positive as well as negative regulation of defense-related processes, aging and cell death. Typically, these categories are indicative for the activation of processes demanding large amounts of energy and the activation of corresponding cellular processes aimed to meet this energy demand. Amongst the down-regulated genes, genes involved in chlorophyll and flavonol biosynthesis, ion homeostasis (related to Ca^{2+} homeostasis), hydrolase activity, response to abiotic stress and positive regulation of signaling and translation, are all significantly over-represented.

Network Analysis Indicates Strong Association between Catabolic Processes, and Carbon Backbone- and Energy-Demanding Biosynthesis-Related Processes, During Activation of the HR

By using Cytoscape software (Shannon et al., 2003) and the plugin Expression Correlation Network (<http://www.baderlab.org/Software/ExpressionCorrelation>), a co-expression network analysis was performed on all 1,152 genes that are differentially regulated between the DS and the PLS under at least one of the conditions that was analyzed. By using the Cytoscape plugin MINE (Rhrissorrakrai and Gunsalus, 2011), four clusters of strongly associated genes were identified within the co-expression network (**Figure 4A**). Clusters 1, 2 and 3 mostly harbor up-regulated genes, whereas cluster 4 consists of mostly down-regulated genes (**Figure 4A**). The expression profile of each gene cluster is shown in **Supplemental Figure S1**. In some cases there is substantial variation in the expression levels of the individual genes belonging to one cluster when the individual replicates for the same conditions are compared. The within sample variation (variation between biological replicates) at early time points is high, resulting in lower numbers of significantly regulated genes (**Figure s 1B, 4A** and **S1**). This variation is much less at time points 3 hr and 5 hr, resulting in high numbers of significantly regulated genes.

We used web-based tools from the Tomato Functional Genomics Database (http://ted.bti.cornell.edu/cgi-bin/TFGD/array/GO_analysis.cgi) and AtCOECIS (<http://bioinformatics.psb.ugent.be/ATCOECIS/>) (Vandepoele et al., 2009; Fei et al., 2011) to

compute GO: enrichment analysis on each cluster. The co-expression network analysis, in combination with the GO: enrichment analyses revealed a strong association between genes involved in protein degradation (encoding proteins involved in proteasome-related pathways) and cell death, with genes involved in the final step of phenylalanine, tyrosine and hydroxycinnamic acid amide (HCAA) biosynthesis. These genes are predominantly present in cluster 1 of **Figure 4A**, together with many genes implicated in the HR, such as genes encoding amino acid transporters, MAP kinases, a number of WRKY transcription factors and genes involved in the calcium and calmodulin signaling network. Furthermore, cluster 1 contains genes encoding receptor-like protein kinases, protein kinases and glycosyl hydrolases, genes involved in phospholipid signaling, the jasmonic acid- and ethylene-mediated signaling pathways, oxidative stress and a number of genes of unknown function (**Figure 4A**, cluster 1; **Supplemental Table S3**, cluster 1 genes and cluster 1 GO:). Genes involved in Ca^{2+} -related signaling are also among the core components of cluster 1. This is evident from the presence of a large number of genes involved in calcium sensing and genes encoding other proteins involved in Ca^{2+} -related signaling. These genes include *GAD2* (*glutamate decarboxylase 2*), *DGK* (*diacylglycerol kinase*), genes encoding phosphatases, *PLD β 1* (*phospholipase D β 1*), *MAPK3* (*mitogen-activated protein kinase 3*), genes encoding a number of protein kinases and calmodulin-binding WRKY transcription factors (Pappan et al., 1997; Snedden and Blumwald, 2000; Snedden and Fromm, 2001; Yang and Poovaiah, 2003; Yap et al., 2003; Du et al., 2009; Leivar et al., 2011) (**Supplemental Table S3**, cluster 1 genes). Unlike genes playing a role in the shikimate pathway, which represents the early steps in the aromatic amino acid biosynthesis (Maeda and Dudareva, 2012), genes encoding enzymes involved in the final steps of the aromatic amino acid biosynthesis, such as *ADT4* (*arogenate dehydratase 4*), *ADT6* (*arogenate dehydratase 6*) and *PDT1* (*prephenate dehydratase 1*), show massive up-regulation (more than 35-fold) in expression in the DS, as compared to the PLS (**Supplemental Table S3**, cluster 1 genes, aromatic amino acid biosynthesis). Most of the genes encoding enzymes of the shikimate pathway that are involved in the generation of chorismate for the biosynthesis of aromatic amino acids (phenylalanine, tryptophan and tyrosine), only show a slight transcriptional up-regulation and predominantly localize in cluster 3 (**Figure 4A**). These genes include *chorismate synthase 1*, *chorismate mutase 1* (*CM1*), *chorismate mutase 3* (*CM3*), *phospho-2-dehydro-3-deoxyheptonate aldolase 2* and *5-enolpyruvylshikimate-3-phosphate synthase* (*EPSP synthase*) (**Supplemental Table S3**, cluster 3 genes).

At 5 hr after the induction of the HR, MapMan-based mapping of the differentially regulated genes clearly illustrates the induction of genes associated with the ubiquitin-dependent protein degradation pathway (**Figure 4B**). In the regulatory network these genes are mainly localized in cluster 1 (**Figure 4A**). Here one of the main differences between the DS and the PLS lays in the final step of ubiquitination (E3), which involves

the ligation of ubiquitin to proteins that are targeted for degradation, with considerably higher related gene expression in the DS (**Figure 4B**, RING and FBOX; **Supplemental Table S3**, cluster 1 genes). There are no clear differences between the DS and PLS concerning the expression of genes involved in processes like ubiquitin activation (E1), whereas at $t = 5$ hr in the DS there is a slight, but significant, down-regulation (about 2 fold) of the E2-related bin representing genes involved in ubiquitin-conjugation (**Figure 4B**).

Network Analysis Indicates WRKY Transcription Factors as Prominent Master Regulators of Transcriptional Reprogramming During the HR

To identify common transcriptional regulators of genes of which the expression profiles are highly similar (**Supplemental Figure S1**), we studied the presence of conserved regulatory motifs in the promoter sequences of genes belonging to the same clusters in **Figure 4A**. One of the significantly over-represented motifs present in the promoter of genes belonging to cluster 1 (**Figure 4A**) is “TGACC/T”; the so-called W-box, a potential binding site for WRKY TFs (Eulgem, 2005). This W-box motif dominates the gene cluster (**Supplemental Table S4** and **Supplemental Figure S2**), as 56 out of the 78 genes present in cluster 1 contain such a “TGACC/T” motif. However, the Y-box motif (redox-dependent transcription activation) and other motifs of unknown function are also among the significantly over-represented motifs (**Supplemental Table S4A**). Validation by the web-based tool POBO (<http://ekhidna.biocenter.helsinki.fi/poxo/pobo/>) confirmed the significant enrichment of the W-box motif in the promoters of the co-regulated gene cluster of the test set (all cluster 1 genes), while the background (the promoter sequences of all Arabidopsis genes) and the second input (the promoter sequences of all genes of cluster 4) have a similar, but low, occurrence of the motif (**Figure 4C**; **Supplemental Table S4A**). Interestingly, in cluster 1, there are a number of genes present that are annotated as WRKY TFs themselves (**Supplemental Table S3**, cluster 1 genes, WRKY). This suggests that there is a network of WRKYs that orchestrates the transcriptome reprogramming related to the induction and amplification of processes leading to the HR.

Cluster 2 harbors genes involved in ethylene biosynthesis and ethylene-triggered signaling, transferases involved in secondary metabolism, genes involved in lipid signaling and others (**Supplemental Table S3**, cluster 2 genes and cluster 2 GO:). For this cluster, POBO validation revealed that binding motifs associated with MYB TFs are abundant in the promoter sequences (**Supplemental Table S4A**). Interestingly, in this cluster there is a gene present with high sequence identity to Arabidopsis MYB78 (*AtMYB78*) (**Supplemental Table S3**, cluster 2 genes). Cluster 3 represents genes involved in the early steps of the aromatic amino acid biosynthesis and the promoter sequences of these genes show enrichment of an ABA-responsive element, which is the ABRE-like binding site motif (**Supplemental Table S4A**).

Cluster 4 is characterized by the presence of genes that are involved in photosynthesis, the biosynthesis of flavonoids, ion homeostasis, circadian rhythm and others (**Figure 3C; Supplemental Table S3**, cluster 4 genes and cluster 4 GO:). One of the fascinating features of this cluster is that there are five genes present that encode unknown proteins and show an inversed expression pattern from the rest of the group. These genes might be involved in the coordinated repression of other genes within this cluster (**Supplemental Figure S1; Supplemental Table S3**, cluster 4 genes). Although the promoter sequences of the genes belonging to cluster 4 contain mostly unknown over-represented motifs, some of the identified motifs that were validated by POBO include AG (MADS) and SORLIP4 (phytochrome A-regulated gene expression) (**Supplemental Table S4A**).

Validation of Gene Expression in *C. fulvum*-Inoculated Tomato and Enhanced Ethylene Production by the DS

We validated our findings concerning up-regulated genes in the DS model system by checking their actual regulation in the interaction between *C. fulvum* and tomato by performing quantitative (q)RT-PCRs on 10 selected genes from clusters 1 and 2, harboring most of the HR-related genes. The selected genes are involved in ethylene biosynthesis, calmodulin binding, oxylipin biosynthesis, proteolysis, transcription factor activity, aromatic amino acid biosynthesis, secondary metabolite (HCAA) biosynthesis and signal transduction (kinase activity), and are categorized into different GO: sub-categories either directly or indirectly linked with plant defense. We inoculated the PLS that were used to generate the DS (MM-Cf0: Cf-4; resistant and MM-Cf0: Avr4; susceptible) with a strain of *C. fulvum* secreting Avr4 and gene expression levels, relative to mock-treated plants, were determined at 6 and 10 days after inoculation (**Supplemental Figure S3A**). The relative expression levels of the selected genes in the *C. fulvum*-tomato interaction are consistent with the microarray results (**Supplemental Figure S3B**), showing an up-regulation in the resistant plants as compared to the susceptible ones at an early stage of infection (t = 6 days after inoculation).

To determine whether the increased expression of genes that encode proteins involved in ethylene production (**Figure s 2, 3 and 4**, cluster 2; **Table 1**) also leads to increased ethylene production, we measured the ethylene emission of both the DS and the PLS before and after the temperature shift. Instead of shifting the plants to 20°C and 70 % RH, plants were now shifted to 20°C/100 % RH as the plants were kept in closed jars to analyze their head space. Upon rescue at 33°C and 100 % RH there was a slow release of ethylene, both by the DS and PLS (**Figure 5A**). Under these particular experimental conditions, lowering the temperature to 20°C did not result in a swift visible HR, indicating that the 100 % RH in the jars is sufficient to suppress this response, at least for a period of 24 hr. Interestingly, although the development of a visual HR is

suppressed, a marked increase in ethylene emission was observed at 4 hr after shifting the seedlings to 20°C/100 % RH, as the DS started to emit significantly higher amounts of ethylene than the PLS (**Figure 5A**). After 24 hr at 20°C/100 % RH, the DS had emitted about three times more ethylene than the PLS.

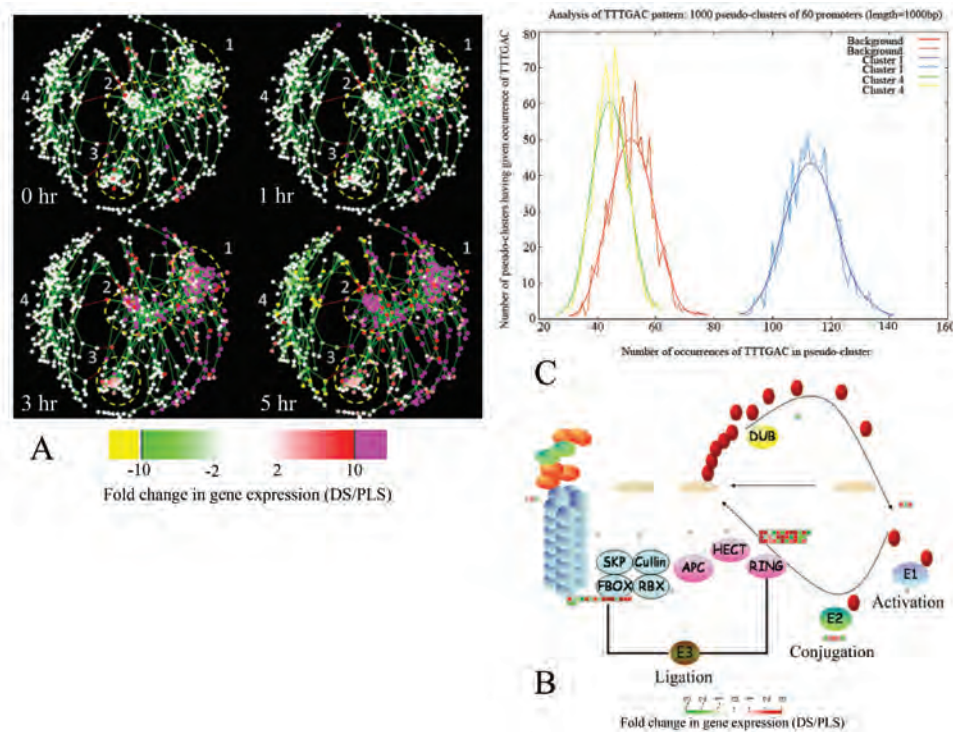


Figure 4. Co-expression analysis of genes differentially regulated during the hypersensitive response and identification of central regulators in the regulatory network. **A**, Co-expression networks, representing all differentially regulated genes that have a correlation coefficient ≥ 0.92 , at 0, 1, 3 and 5 hr after the temperature shift that induces the HR in the dying seedlings (DS). Shown is an output of Cytoscape software that was used to build a co-expression network of all 1,152 genes that are significantly differentially regulated between the DS and the PLS under at least one of the conditions analyzed. The dots represent the individual genes (the “nodes”) and the length of the connecting lines (the “edges”) between them is a measure of their co-expression. Short edges indicate strong co-expression, whereas long edges indicate weak co-expression. Four clusters of strongly co-regulated genes were identified. The bar below the figure indicates the color code for the fold change in gene expression. **B**, MapMan representation of genes involved in the proteasome pathway, depicting differentially regulated genes at 5 hr after the temperature shift involved in ubiquitin activation (E1), ubiquitin-conjugation (E2) and ligation of ubiquitin to proteins that are targeted for degradation (E3). SKP, culin and FBOX together represent the SCF complex. RBX (ring box protein), APC (anaphase-promoting complex), HECT (homology to E6-AP C-terminus) and RING (really interesting new gene) represent different protein complexes in the E3 ubiquitin ligase family. DUB, de-ubiquitinating enzyme. Red ovals represent individual ubiquitin proteins. **C**, POBO output interface indicating a “good” motif with spread sample distribution. In this case, the test set (all cluster 1 genes) and the background (the promoter sequences of all genes of Arabidopsis), as well as cluster 4 gene set (genes with an opposite expression pattern to the test set) are well separated. This indicates a significant difference in the occurrence of the motif searched for among these clusters (in this case “TTTGAC”; the W-box motif). “Bad” motifs are characterized by uniform sample distribution, indicating absence of variation in the occurrence of the motif (cluster 4 and background).

Table 1. Expression profiles of genes involved in ethylene biosynthesis and signaling. Expression levels are given as fold change in gene expression in the dying seedlings (DS) as compared to the parental lines (PLS), at 0 hr, 1 hr, 3 hr and 5 hr after the temperature shift that induces the HR in the DS.

Probe set ID	Arabidopsis ID	Gene name ¹	Fold change (DS/PLS)			
			0 hr	1 hr	3 hr	5 hr
Les.3662.1.S1_at	At1g01480	<i>ACS2</i>	5	2	26	101
LesAffx.3059.1.S1_at	At3g23220	<i>ESE1</i>	-1	1	17	56
Les.3769.1.S1_at	At4g11280	<i>ACS6</i>	-2	2	13	31
Les.3575.1.S1_at	At3g23240	<i>ERF1</i>	4	3	13	31
Les.36.1.S1_at	At3g04580	<i>EIN4</i>	3	2	23	29
Les.274.1.S1_at	At5g61600	<i>ERF104</i>	-1	2	18	22
LesAffx.51274.1.S1_at	At5g47230	<i>ERF5</i>	-1	-1	36	20
Les.3551.1.S1_at	At3g24500	<i>MBF1C</i>	-1	-2	2	20
Les.3818.1.S1_at	At3g23240	<i>ERF1</i>	1	1	4	20
Les.3573.1.S1_at	At5g47220	<i>ERF2</i>	2	2	3	8
Les.4140.1.S1_at	At4g17500	<i>ERF1</i>	-2	2	4	7
Les.3041.1.S1_at	At1g50640	<i>ERF3</i>	-1	2	3	3
Les.3679.1.S1_at	At3g23240	<i>ERF1</i>	2	3	2	2
Les.3500.1.S1_at	At1g66340	<i>ETR1</i>	-1	1	-1	-3
Les.31.1.S1_s_at	At5g03730	<i>CTR1</i>	1	2	1	3

¹*ACS*, 1-aminocyclopropane-1-carboxylate synthase; *CTR1*, constitutive triple response 1; *EIN4*, ethylene insensitive-4; *ETR1*, ethylene response-1; *ERF*, ethylene response factor; *ESE1*, ethylene and salt inducible 1; *MBF1C*, multi protein binding protein-1C.

To verify whether ethylene-induced signaling processes are also activated when tomato is infected with *C. fulvum*, we monitored the expression of *1-aminocyclopropane-1-carboxylate synthase 2 (ACS2)*, which encodes one of the rate-limiting enzymes in ethylene biosynthesis, in the resistant and susceptible parental lines at 6 and 10 days after inoculation with the fungus. In line with our observations in the DS, in resistant tomato *ACS2* expression was strongly up-regulated at 6 dpi when compared to the mock-inoculated plants and was about 2.4 times higher than in the inoculated susceptible plants. *ACS2* continued to exhibit a higher expression level up to 10 dpi, as compared to the susceptible *C. fulvum*-inoculated parental line (**Figure 5B**).

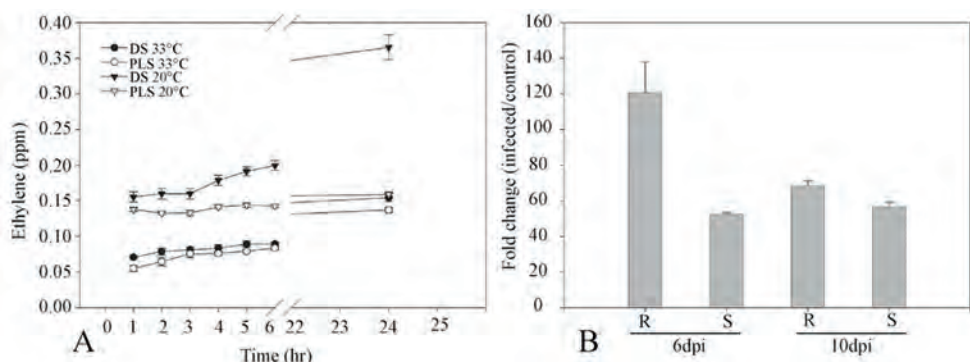


Figure 5. Ethylene emission and *ACC-synthase 2* (*ACS2*) gene expression of the seedlings and *C. fulvum*-inoculated tomato, respectively. A, Ethylene emission patterns of the dying seedlings (DS) and their parental lines (PLS) upon rescue at 33°C and 100 % RH and after a shift to 20°C and 100 % RH. B, Relative expression levels of the *ACS2* gene in resistant (R; MM-Cf0: Cf-4) and susceptible (S; MM-Cf0: Avr4) parental lines, at 6 and 10 days post inoculation (dpi) with *C. fulvum*. Bars represent expression of the gene (fold change) in inoculated plants, relative to the mock-inoculated resistant and susceptible parental lines.

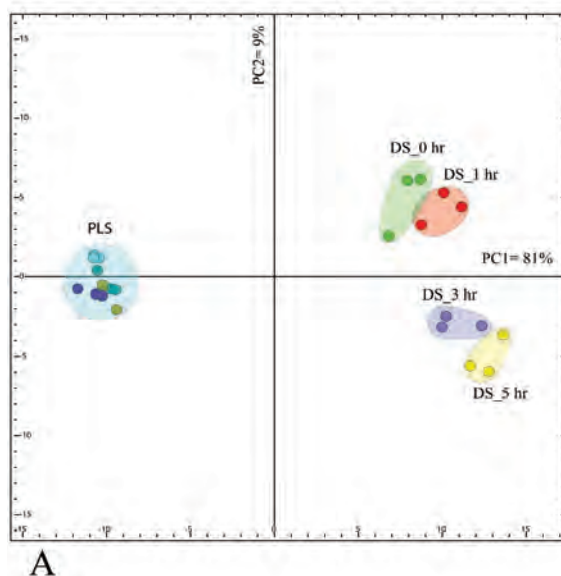
The Dynamics of the Metabolome of the DS, as Compared to the PLS, Upon Mounting of the HR

To further validate the observed HR-associated transcriptional reprogramming in the DS upon mounting of the HR and to determine its effect on the overall metabolome of these plants, we performed untargeted metabolite profiling of both polar primary metabolites (PPM) and semi-polar secondary metabolites (SPSM) of the DS and the PLS using GC-TOF-MS and LC-PDA-QTOF-MS, respectively. We detected a total of 132 different PPM and 250 different SPSM, of which respectively 42 and 144 show differential accumulation ($FC > 1.5$ and $P < 0.05$) in the DS, as compared to the PLS, at least under one of the conditions analyzed. Compared to most of the secondary metabolites, for most of the organic acids and some other primary metabolites the fold change in accumulation is reproducible, but relatively low. Hence, the cut-off value was lowered to an FC of 1.5 in order to retain the organic acids in the analysis (**Supplemental Table S5**).

Based on the differentially accumulating metabolites, we computed a discriminant function analysis (DFA) and performed a hierarchical cluster analysis (HCA) to investigate the temporal accumulation patterns of these metabolites in response to triggering of the HR (**Figure 6A**). The first component (PC1) of the DFA explains already more than two third (81 % variance) of the variation in the entire data set. PC1 predominantly reflects an inherent genotype-dependent difference in metabolite content (DS versus PLS), even before the temperature shift that induces the HR in the DS (**Figure 6A**). The presence of such an inherent difference suggests that, although at $t = 0$ hr (33°C/100 % RH) the differences between the DS and PLS at the transcriptional level are relatively low (**Figure 1**), this condition apparently does not fully suppress the Cf-4/Avr4-triggered responses thereby causing already a substantial difference at

the level of the metabolome (see below). Some of the metabolites that attribute to the separation of the PLS and DS along the first principal component (PC1) include amino acids, alkaloids, some HCAAs, benzenoids, flavonoids and other unidentified metabolites that accumulate to higher amounts in the DS already at $t = 0$ hr. Furthermore, there is a strong depletion of organic acids, and of some flavonoids and several unidentified metabolites in the DS at this time point (**Supplemental Table S5**).

In line with the overall changes in the transcriptome of the DS, there is further reprogramming of the metabolome during mounting of the HR in these plants. This is mainly reflected by the second principal component (9 % variance) that primarily indicates the time-dependent accumulation of HR-associated metabolites that is typical for the DS (**Figure 6A**). In the DS, this group of metabolites shows higher accumulation at time points 3 hr and 5 hr after the temperature shift. All of them are aromatic amino acid-derived metabolites, including benzoic acid (14 fold), salicylic acid (26 fold), tyramine (10 fold), dopamine (5 fold) and the HCAAs coumaroyltyramine-isoform 1 (CT1) (75 fold) and coumaroyldopamine (CD) (116 fold) (**Figure 6B**; **Supplemental Table S5**) and this massive increase reflects the full activation of HR-related defense responses. There is also a clear positive precursor-final product relationship among these metabolites. Other HCAAs, such as feruloyloctapan (FO), coumaroyltyramine-isoform1 (CT1) and -isoform2 (CT2), feruloyltyramine-isoform1 (FT1) and -isoform2 (FT2) and the glycosyl forms of most of these HCAAs showed higher accumulation both before and after the temperature shift that induces the HR in the DS (**Supplemental Table S5A**).



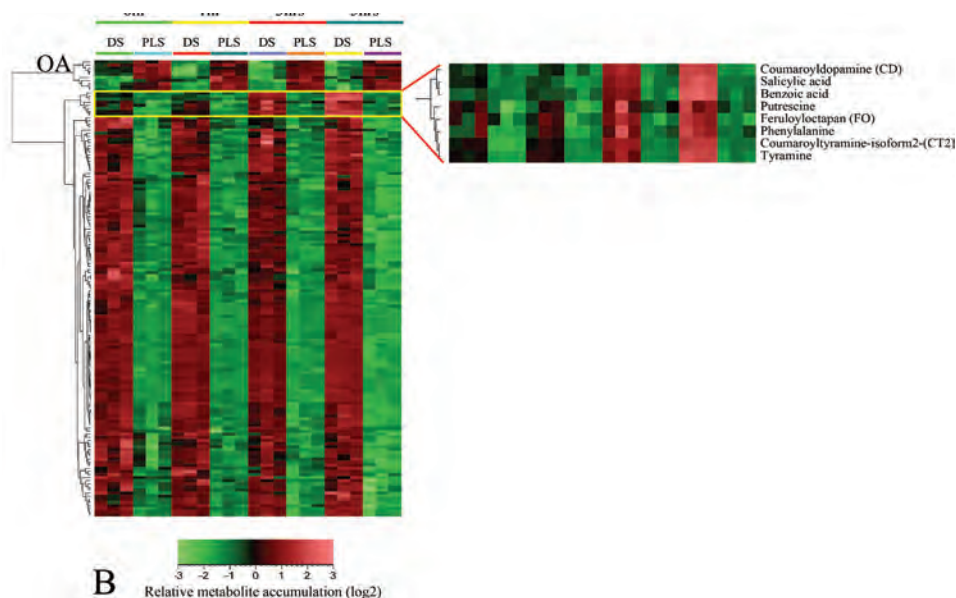


Figure 6. Metabolome reprogramming in the dying seedlings (DS), as compared to their parental lines (PLS). Shown are the metabolome profiles, comprising all differentially regulated primary polar metabolites (PPM) and semi polar secondary metabolites (SPSM), of the DS as compared to the PLS at 0 hr, 1 hr, 3 hr and 5 hr after the temperature shift. **A**, Principal component analysis (PCA), depicting metabolome reprogramming in the DS as compared to the PLS. PC1 and PC2 represent principal component 1 and 2, respectively. **B**, Hierarchical cluster analysis of the PPM and SPSM profiles. The bar below the figure indicates the color code for the relative change in metabolite accumulation of log₂-transformed and auto-scaled data. The blown-up part of the heat map indicates the aromatic amino acid-derived metabolites that differentially accumulate in the DS at time points 3 and 5 hrs after the temperature shift. OA, clade containing most of the organic acids that are differentially down-regulated in the DS.

Moreover, in comparison to other groups of metabolites (amino acids, polyamines, alkaloids, flavonoids and benzenoids), the HCAAs showed by far the highest accumulation in the DS (**Supplemental Table S5**). In the DS, out of the top 20 metabolites showing an increase with a fold change of over 15, 11 metabolites represent HCAAs and their glycosyl forms (**Supplemental Table S5A**).

Discussion

In this study we have used large-scale “-omics” technologies to assess the overall temporal transcriptome and metabolome reprogramming, associated with mounting of the HR in tomato. For this, we used dying seedlings (DS), expressing both the *Cf-4* resistance gene and the matching *Avr4* effector, as a model to study the resistance response of tomato to *C. fulvum*. Our analysis revealed that the induction and execution of the HR is the outcome of the synergistic or antagonistic effects of a number of intertwined cellular and biochemical processes.

Major HR-Associated Signal Transduction and Metabolic Pathways

Our metabolome analysis, combined with the over-representation analysis on the differentially regulated genes, clearly shows the involvement of both ethylene and salicylic acid in intensifying the defense responses at later time points after initiating the HR by shifting the DS to permissive conditions (**Figures 2, 3A and B, 5 and 6B; Table 1; Supplemental Table S5**). The gene *S-adenosyl-L-methionine carboxyl methyltransferase*, which is involved in the conversion of SA to methyl salicylate was slightly upregulated at time points 0 and 1hr and showed dramatic reduction in expression (FC = 5) in the DS at later time points (3 hr and 5 hr). This might be a way to maintain high levels of SA during the HR (**Figure 2, SA**). Other genes such as *MAPK4*, *NPR1*, *GRX480* and *DOX1*, which are involved in SA-mediated signaling, also showed upregulation. However, these genes could not be mapped in **Figure 2**. Ethylene plays an important role in the activation of different forms of programmed cell death (PCD), including the HR (Lund et al., 1998; Ciardi et al., 2000; Ciardi et al., 2001; van Loon et al., 2006; Mur et al., 2009). The well-controlled ethylene release by the DS over time only after HR initiation confirms the robustness of the “dying seedling” system and matches the observed increase in ethylene-related gene expression (**Figure 2**). Ethylene has been shown to be required for the induction of *N-hydroxycinnamoyl-CoA: tyramine N-hydroxycinnamoyl transferase (THT)* gene expression and the accumulation of HCAAs during defense of tomato against the bacterial pathogen *Pseudomonas syringae* (Zacares et al., 2007; Lopez-Gresa et al., 2011). In the latter studies, exogenous application of ethylene led to an increase in the expression of the *THT* genes in tomato, whereas application of the ethylene biosynthesis inhibitor AVG reduced the release of ethylene after *P. syringae* infection and consequently suppressed the expression of the *THT* genes. In potato, tomato and tobacco, THTs play a pivotal regulatory role in the biosynthesis of HCAAs by catalyzing the transfer of hydroxycinnamic acids from the respective CoA esters to tyramine, dopamine, octamine and various other amines (Guillet and De Luca, 2005; Kang et al., 2006).

The changes in the transcriptome and metabolome profiles of the DS revealed the activation of both primary and secondary metabolism during mounting of the HR (**Figures 3 and 6**). Aromatic amino acids (phenylalanine and tyrosine) and various aromatic secondary metabolites derived from these amino acids represent a large portion of the HR-associated metabolites (**Figures 3A and B; Supplemental Table S5**). Phenylalanine and tyrosine, in combination with various amines, are the primary precursors for the induced HCAA biosynthesis during defense of plants against pathogens and wounding (Facchini et al., 2002; von Roepenack-Lahaye et al., 2003; Walters, 2003; López-Gresa et al., 2011). At t = 3 hr and t = 5 hr, hydroxycinnamic acid-derived compounds, such as benzoic acid (14 fold increase), salicylic acid (26 fold increase) and many HCAAs (20 to 116 fold increase) showed massive accumulation in

the DS (**Figure 6B**; **Supplemental Tables S5**). The increase in HCAA levels correlates with an up-regulation of the *THT* genes, as evidenced from the transcriptome of both the DS model and the *C. fulvum*-infected resistant tomato lines (**Supplemental Figure S3**, *THT*; **Supplemental Table S7**). In the DS, most of the induced HCAs have tyramine and dopamine as a backbone. In line with this, tyramine (10 fold increase), dopamine (6 fold increase) and their precursor tyrosine (5 fold increase) were present at higher levels in the DS than in the PLS (**Supplemental Table S5B**). Extraction of HCAs that are present in the form of higher complexes in the plant cell walls is less likely with the extraction technique that we used (see Materials and Methods). However, we detected various HCAs in the leaf extracts of the DS. This might either indicate that there is a massive production of HCAs, exceeding their rate of incorporation into the cell wall, or some of the HCAs in their free form have additional functions, next to cell wall fortification. The increase in the amount of HCAs is considered to be an indicator of the host plant mounting a barrier against the invading pathogen. Accumulation of HCAs in the cell wall for example ensures a durable barrier against pathogens by reducing the cell wall digestibility by hydrolytic enzymes of the pathogen and/or by directly inhibiting further proliferation of the pathogen (Grandmaison et al., 1993; von Röpenack et al., 1998; Facchini et al., 1999). Moreover, the resulting fortified, and less permeable, cell wall ensures exclusion of the pathogen from accessing plant nutrients and water. In support of an additional function, HCAs like coumaroyldopamine (CD) (116 fold) and coumaroyltyramine (CT) (75 fold) have been reported as novel induced HCAs upon colonization of resistant tomato plants by *P. syringae* and were shown to have both antioxidant and antimicrobial activity (Zacares et al., 2007). In conclusion, both our transcriptional network and metabolome analysis indicate the HCAs as a key class of metabolites associated with mounting of the HR in tomato.

The Energy Homeostasis and its Major Regulatory Mechanisms during the HR

During rescue of the DS at 33°C/100 % RH, only a small amount of genes (34) is differentially regulated in these plants, when compared to the PLS (**Figures 1A and B**, $t = 0$ hr). Still, there already is a marked difference in their metabolome when compared to the PLS, including metabolites associated with the HR (**Figure 6**; **Supplemental Table S5**). This is most likely explained by the activation of various defense-associated responses already at $t = 0$ hr (which is after two weeks of rescue), albeit to a low level and without the execution of the HR and without an increased production of ethylene (**Figure 5A**). This suggests that the activation of Cf-4-mediated responses is not completely blocked at elevated temperature and humidity, resulting in a gradual change in the overall metabolome of the DS during the two weeks of rescue before initiating the HR by the temperature and humidity shift. It should be noted that in an earlier experiment, using highly sensitive cDNA-AFLP analysis, it was found that at $t = 0$ hr already 70 % of all 442 Avr4-responsive tomato genes that were selected, were differentially expressed

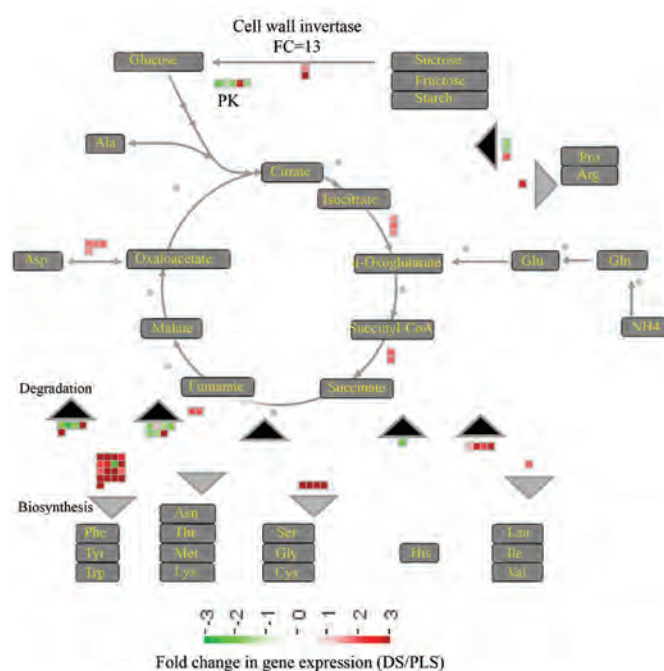
when compared to the PLS at that time point (Gabriëls et al., 2006). This observation supports our findings concerning the “leakiness” of the DS model. Indeed, in addition to the massively altered metabolome at $t = 0$ hr, the DS are smaller in size than the PLS (de Jong et al., 2002), which is in line with the theory that claims reduction in growth to be a consequence of carbon limitation caused by increased biosynthesis of defense-related metabolites. This results in a downward adjustment of growth to a level that can be supported by the new level of carbon availability (Smith and Stitt, 2007).

In an incompatible *C. fulvum*-tomato interaction, once fungal ingress has been resisted and defense responses have again been down-regulated, the plant restores its normal metabolism in order to bring the energy expenditure back to the original situation (Heil and Baldwin, 2002; Bolton, 2009). However, in the DS the introgression of the fungal *Avr4* gene, in combination with the *Cf-4* resistance gene, leads to a continuous systemic triggering of the defense machinery, resulting in an amplification of the responses that occur only locally in *Cf-4* tomato challenged with *C. fulvum* expressing *Avr4*. The associated massive transcriptome and metabolome reprogramming that we observed in the DS costs energy and requires reducing power and carbon skeletons. Disruption of the ion homeostasis (**Figure 3C**, mainly at $t = 5$ hr) reflects the low energy status of the DS, as ATP is normally used to generate the proton motive force to regulate the transport of ions, such as Ca^{2+} across the plasma membrane, and ATP depletion is one of the main causes for the inability of a system to maintain its ion homeostasis (Chanson, 1993; Knickerbocker and Lutz, 2001; Arpagaus et al., 2002). Another marker reflecting ATP imbalance in the system is the up-regulation of adenylate kinase 1 (ADK1) in the DS (3 fold increase as compared to the PLS) at $t = 5$ hr. ADK1 plays a crucial role in maintaining the right equilibrium between ADP and ATP levels (Hardie et al., 2012).

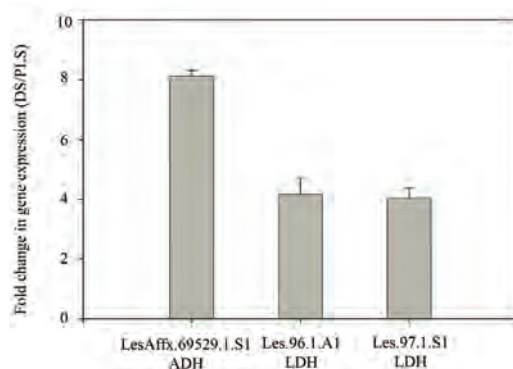
To accommodate the massive metabolome reprogramming, the DS activate various alternative processes generating energy and carbon skeletons. These processes can be categorized into: (1) a switch to catabolism; (2) preferential diversion of precursors towards specific biochemical pathways and (3) increased anaerobic respiration. The first process involves an increased hydrolysis or oxidation of carbohydrates, proteins, nucleic acids and lipids. Increased hydrolysis of carbohydrates (specifically sucrose) into glucose is, for example, caused by transcriptional activation of the gene encoding cell wall invertase (CWI), which is more than 13 fold up-regulated at 5hr in the DS (**Figure 7A**). This ensures a continuous supply of glucose for the energy cycle, as well as for generating carbon skeletons required for the synthesis of primary metabolites, such as aromatic amino acids (**Figure 7A**). The importance of CWI in generating carbohydrates that are catabolized upon the activation of defense responses is shown by RNA interference (RNAi)-mediated knock-down of *CWI* in tobacco leaves. Lowered *CWI* expression resulted in compromised defense responses and a delay in the actual hypersensitive cell death (Essmann et al., 2008). Another form of alternative energy

generation includes lipid- and ribonucleoside-related catabolic processes (**Figure 3B**; lipid and pyrimidine ribonucleoside catabolism). Upon ribonucleoside catabolism, the pentose moiety of the nucleosides serves as a carbon and energy source (Tozzi et al., 2006). Activation of lipid-related catabolic processes was also prominent during mounting of the HR (**Figure 3B**). Under carbohydrate starvation conditions, the respiratory demand for carbon skeletons derived from fatty acid beta-oxidation increases, thereby triggering induction of the fatty acid breakdown pathway (Graham and Eastmond, 2002).

A



B



C

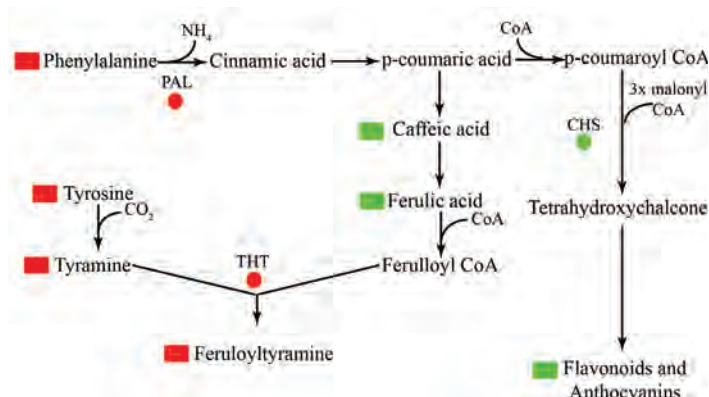


Figure 7. Alternative energy and carbon skeleton generation strategies of tomato dying seedlings (DS) undergoing massive transcriptome and metabolome reprogramming. **A**, Cell wall invertase-mediated generation of glucose from mono, di- and polysaccharides to maintain a continuous supply for the TCA cycle and thereby for amino acid biosynthesis. The grey and black rectangles represent biosynthesis and degradation processes, respectively. **B**, Expression levels of alcohol dehydrogenase (*ADH*) and lactate dehydrogenase (*LDH*) genes in the dying seedlings (DS) as compared to their parental lines (PLS) at $t = 5$ hr. **C**, Redirection of common precursors, such as phenylalanine and tyrosine, towards targeted metabolite pathways (red and green shapes represent up-regulation and down-regulation of a gene (circle) or a metabolite (rectangle), respectively). PAL, phenylalanine ammonia lyase; CHS, chalcone synthase; TyrDC, tyrosine decarboxylase; THT, tyramine N-hydroxycinnamoyl transferase.

It is well established that programmed cell death is an active process that aborts cells, tissues or organs during stress and/or developmental processes, accompanied by re-allocation of the recycled nutrients to new sinks (Jones, 2001; Ameisen, 2002; Kuriyama and Fukuda, 2002). Amino acids derived from proteolysis, especially during acute nutrient restriction, are an important source of carbon skeletons (Vierstra, 1993; Vabulas and Hartl, 2005; Vabulas, 2007). The increased accumulation of aromatic amino acids (such as phenylalanine and tyrosine) in the DS is partly explained by the moderate activation of genes encoding enzymes involved in the shikimate pathway, which is an early step in the aromatic amino acid biosynthesis (**Figure 4A**, cluster 3; **Supplemental Table S3**, cluster 3 genes). In addition to this, also a strong transcriptional activation of genes encoding enzymes involved in the final steps of the biosynthesis of these aromatic amino acids occurs (**Figure 4A**, cluster 1; **Supplemental Table S3**, cluster 1 genes). Remarkably, the latter genes show a high level of co-regulation with genes involved in the protein degradation pathway (**Figure 4A**, cluster 1; **Supplemental Table S3**, cluster 1 genes; **Supplemental Figure S3**). Such a strong association suggests that protein degradation might function as an alternative pathway for the generation of aromatic amino acids required for the biosynthesis of secondary metabolites, such as benzoic acid, salicylic acid, alkaloids and the HCAAs. Another example of a switch to catabolism for the generation of energy- and carbon skeletons is the activation of genes involved in the degradation of branched amino acids (leucine, isoleucine and

valine) (**Figure 7A**; **Supplemental Table S2**). The catabolism of leucine, isoleucine and valine generates acetyl-CoA which in the TCA cycle generates energy, a process widely observed during starvation and stress (Aubert et al., 1996; Fujiki et al., 2001; Taylor et al., 2004; Kochevenko et al., 2012). Our data suggest that the highly induced hydroxycinnamic acid (HCA)-derived secondary metabolite biosynthesis pathways are for the greater part responsible for the alterations in aromatic amino acids and carbon skeleton fluxes. Moreover, the depletion of organic acids (**Figure 6B**) in the DS suggests that these compounds are precursors for many of the primary (aromatic amino acids) and secondary metabolites. Hence, their depletion can be explained by the massive accumulation of the respective primary and secondary metabolites in the DS.

The second way by which the plant deals with the low carbon skeleton and energy supplies, is the preferential diversion of common precursors towards specific metabolic pathways. This is exemplified by suppression of the flavonoid biosynthesis pathway through down-regulation of *chalcone synthase* (*CHS*) gene expression, thereby increasing the availability of precursors like phenylalanine and tyrosine for the HCAA biosynthetic pathway (**Figure 3C**, flavonol biosynthesis; **Figure 7C**), accompanied by up-regulation of the *THT* genes (**Supplemental Table S7**). Similarly, preferential redirection of common flavonoid precursors towards the biosynthesis of HCCAs in onion epidermis upon infection by *Botrytis cinerea* was described (McLusky et al., 1999).

As a third way to obtain energy, the DS activate anaerobic energy production (fermentation) pathways which can be traced by transcriptional activation of *L-lactate dehydrogenase* (*LDH*) and *alcohol dehydrogenase* (*ADH*) genes (Stulemeijer et al., 2009) (**Figure 7C**) and the GABA shunt, evident from high expression of *glutamate decarboxylase 2* (*GAD2*) and accumulation of GABA (**Supplemental Table S3**, cluster 1 genes; **Supplemental Table S5B**). In hypoxic conditions pyruvate is broken down by *LDH* to form lactate and NAD^+ , giving a boost in NAD^+ for the glycolytic anaerobic energy generation (Bolton, 2009). Under particular, energy-demanding conditions, like the systemic activation of defense responses, pyruvate is produced in high amounts and pyruvate dehydrogenase (PDH) activity becomes a limiting step in converting pyruvate into acetyl CoA. Hence, the GABA shunt provides a means to utilize the excess of pyruvate for energy production (Bolton et al., 2008).

Major Regulators and Regulatory Mechanisms of the HR

Our data depict the HR as an active process, regulated at the transcriptional, post-transcriptional, translational and post-translational level, to maintain the cellular homeostasis of the system (**Figures 2-4** and **7**). The robustness of the system is maintained through tightly regulated activation and repression of defense signaling. For example, enhanced activation of 2C-type protein phosphatases that are associated with the regulation of MAPK4 and -6 and potassium channels (Lee et al., 2007; Schweighofer

et al., 2007) can be mentioned as one of the major repression mechanisms of defense signaling during mounting of the HR (**Figure 3B**, de-phosphorylation; **Supplemental Table S6**). Another example is repression of the ethylene-induced signaling pathway through the transcriptional activation of repressors (*RTE1*, *CTR1*) (Huang et al., 2003; Dong et al., 2010) or lowered expression of signal receptors and transducers, such as *EIN2* (Kieber et al., 1993) (**Supplemental Table S6**). Furthermore, repression of programmed cell death is enforced through down-regulation of positive regulators of cell death, such as *LOL1* (*LSD1-like 1*) (Epple et al., 2003) and activation of the immune repressor *RIN4* (Afzal et al., 2011) (**Supplemental Table S6**). Next to this, genes encoding glutathione S-transferases (class III, GST-TAU) that function as protectants against oxidative stress and as potent detoxifiers of toxins are transcriptionally activated (**Figures 3A and B**; **Supplemental Table S6**) (Marrs, 1996; Kilili et al., 2004). In addition to its role in protein turnover, ubiquitin-dependent protein degradation also regulates defense through targeted destruction of proteins involved in intensifying defense signaling (Santner and Estelle, 2009; Vierstra, 2009).

As in the DS massive and highly coordinated transcriptional changes are observed, it is anticipated that master regulators are involved. Some of the major transcription factors implicated in the regulation of the overall transcriptome and metabolome of the plant include WRKYs, AP2/ERFs, bZIPs and MYBs (Daniel et al., 1999; Singh et al., 2002; Eulgem and Somssich, 2007; Lippok et al., 2007; Oñate-Sánchez et al., 2007; Naoumkina et al., 2008; Rushton et al., 2010). Despite the presence of all these, and other, transcription factors in the different hubs of the network (**Figures 4A and B**; **Supplemental Tables S3 and S4**), WRKY transcription factors in particular seem to play a critical role in orchestrating the HR-related transcriptome changes of the DS. This observation is strengthened by the fact that a W-box motif, to which WRKY transcription factors bind, is present in the promoter sequence of 72 % of the genes that are implicated to have an essential role in the HR (**Supplemental Table S4B**) and that fall within the same cluster as these transcription factors themselves (**Figure 4**, cluster 1; **Supplemental Table S3**, cluster 1 genes). The presence of two genes encoding MAP kinases highly homologous to MAPK3 in the same cluster, supports the work that showed some WRKYs to be directly phosphorylated by MAPKs, thereby inducing phytoalexin biosynthesis (Mao et al., 2011). Our findings strengthen the role of WRKYs in plant defense and defense-related secondary metabolite reprogramming. Such a strong association of differentially regulated defense-related genes and the presence of a shared regulatory motif in their promoter region, takes the assumption of “guilt by association” one step further. Furthermore, this co-expression analysis should allow to predict the role of yet uncharacterized genes such as for example Les.113.1.S1_at, which shows 106 fold upregulation in the DS and locates to similar positions in the network as some of the well characterized gene groups (**Supplemental Table S3**, genes in each

cluster listed as “no hit found”). Moreover, most of the genes that we found in our cluster analysis have not been characterized in tomato, although some of them are annotated based on the presence of functional domains and their sequence similarity with other plant genes. Hence, our analysis suggests that these novel genes are also involved in the HR. This approach shows that, based on a robust and synchronized inducible system, it is possible to extract valuable information from the complex biological events that take place during the response of resistant plants to pathogens.

Materials and Methods

Plant Material and Growth Conditions

Dying seedlings (DS) were generated by crossing transgenic tomato MoneyMaker (MM)-Cf0 expressing *Avr4* (Cf0:Avr4), to MM-Cf0 tomato transgenic for the *Hcr9-4D* (*Cf-4*) resistance gene (Cf0:Cf-4) (de Jong et al., 2002; Gabriëls et al., 2006; Stulemeijer et al., 2007). Pre-treatment of the seeds before sowing was carried out as described by (Stulemeijer et al., 2007). Ten seeds were sown per pot of 7 x 7 x 8cm and these were kept in a transparent closed box for 7 days (till the cotyledons had emerged) at 25°C, under a 16 hr/8 hr light/dark regime in an incubator (Elbanton, Kerkdriel, The Netherlands). Plants were rescued at 33°C and 100 % RH for a period of two weeks, after which samples of the *Cf-4/Avr4* DS and as control a 1:1 mixture of the Cf0:Cf-4 and Cf0:Avr4 parental lines (PLS) that were crossed to generate the *Cf-4/Avr4* DS were collected at 0 hr, 1 hr, 3 hr and 5 hr after the initiation of the HR by a transfer of the plants to 20°C and 70 % RH. Samples consisted of cotyledons and just appearing primary leaves and were immediately frozen and ground to a fine powder in liquid nitrogen, and stored at -80°C until further use. Four pots, each containing 10 seedlings, were considered as an experimental unit and three independent biological replicates were generated for the DS and PLS at the individual time points.

To validate gene expression profiles observed in the DS and PLS, the Cf0:Avr4 (susceptible) and Cf0:Cf-4 (resistant) parental tomato lines were also inoculated with a race 5 of *C. fulvum* secreting Avr4 (de Wit, 1977). Four biological replicates were performed, also including mock-treated susceptible and resistant plants and leaflets were harvested at 6 days and 10 days after inoculation with the fungus.

Microarray Experiments

Total RNA was extracted and purified from the collected tomato seedling material using the NucleoSpin RNA/protein kit (Machery-Nagel, GmbH and Co., Dueren, Germany). RNA labeling, hybridization of the microarrays (Affymetrix® Tomato Genome Arrays; GeneChip® Tomato Genome, Affymetrix, Santa Clara, CA, USA) and data extraction were

performed by Service XS (Leiden, The Netherlands), according to standard protocols provided by the manufacturer. For this, the RNA concentration was determined with the Nanodrop (type ND-1000) and RNA quality was assessed with the RNA 6000 Nano Labchip kit (Agilent Technologies, Palo Alto, CA, USA). Biotin-labeled cRNA was synthesized from 2 µg of total RNA using Affymetrix one-cycle target labeling and control agents (Affymetrix, part nr. 900493). GeneChips were hybridized with 20 µg of fragmented biotin-labeled cRNA, followed by automated washing and staining and they were then scanned with an Affymetrix scanner, type G7. Affymetrix GCOS software was used to convert the raw data to CEL files and data analysis was performed by packages from the Bioconductor project (Gentleman et al., 2004), implemented in Genemath XT version 2.12 (Applied Maths, Inc. Austin, TX, USA). The raw array data (CEL files) were normalized using the GCRMA probe summarization algorithm, applying the empirical Bayes approach (Wu et al., 2004). For each time point, three independent biological replicates were performed.

RNA Isolation and qRT-PCR Gene Expression Analysis

RNA was isolated from 100 mg of tomato leaf tissue, using 1 ml of Trizol reagent (Invitrogen) according to the manufacturer's instructions. The total RNA was treated with DNase-I Amplification Grade (Invitrogen) and purified with an RNeasy Mini kit (Qiagen). RNA concentration and integrity was examined and 1 µg of RNA was used for the reverse transcription reaction, using the iScript™ Select cDNA Synthesis Kit (Bio-Rad Laboratories), in a final volume of 20 µl. Quantitative RT-PCR was performed in triplicate reactions, with the same cDNA pool, in the presence of fluorescent dye (iQ SYBR GREEN super mix 2*), using an iCycler iQ instrument (Bio-Rad Laboratories) with specific primer pairs (**Supplemental Table S8**). The constitutively expressed actin gene from tomato (Solyc10g080500.1.1) was used as a reference and the expression levels of other genes were determined relative to this reference.

Extraction and Gas Chromatography Time-of-Flight Mass Spectrometry (GC-TOF-MS) Analysis of Polar Primary Metabolites

Polar primary metabolites were extracted following the procedure described by Lisec and co-workers (Lisec et al., 2006) with minor modifications. Briefly, 50 mg (fresh weight) of frozen leaf tissue was homogenized in an Eppendorf tube and extracted with 700 µl of methanol (100 %), pre-cooled at -20°C and spiked with ribitol (0.2 mg/ml) as an internal standard. The sample was then incubated for 10 min at 70°C and centrifuged at 21,000g for 10 min. The supernatant was transferred to a new Eppendorf tube and 375 µl of chloroform (pre-cooled at -20°C) and 750 µl of water (pre-cooled at 4°C) were added. The mixture was centrifuged at 21,000 g for 10 min and 200 µl of the supernatant was dried in a vacuum concentrator without heating. Online derivatization was performed with methoxyamination reagent (methoxyamine hydrochloride (20

mg/ml pyridine)) and *N*-methyl-*N*-trimethylsilyltrifluoroacetamide (MSTFA) using a CTC CombiPal injection and pipetting robot.

A mixture (5 μ l) containing a series of n-alkanes (C10-C34) was injected into each sample for the calculation of the retention index (RI). A 2 μ l aliquot of each derivatized sample was injected with a gradient of 6°C/s from 70°C to 240°C, using an Optic3 injector (ATAS) in split ratio of 1:20, into an Agilent 6890N gas chromatograph (GC) equipped with a 40 m x 0.25 μ m i.d. fused-silica capillary column with a chemically bonded 0.25 μ m DB 5-MS stationary phase (J and W Scientific, Folsom, CA). The injector temperature was kept at 270°C, the septum purge flow rate was 20 ml/min and the purge was turned on after 60 s. The gas flow rate through the column was 1 ml/min and the column temperature was held at 70°C for 2 min, then increased by 10°C/min to 310°C and held there for 5 min. The column effluent was introduced into the ion source of a Pegasus III time-of-flight mass spectrometer (TOF-MS; Leco Corp., St. Joseph, MI, USA). The transfer line and the ion source temperatures were 270°C and 200°C, respectively. Ions were generated by a 70 eV electron beam at an ionization current of 2.0 mA and compounds were detected at scanning range of 20 spectra/s and recorded in the mass range 50-600 *m/z*. The acceleration voltage was turned on after a solvent delay of 295 s. The detector voltage was 1400 V.

The resulting chromatograms were processed in an untargeted manner using the MetAlign software (Lommen, 2009). Extraction and reconstitution of compound mass spectra were performed according to the method described before (Tikunov et al., 2012). The internal standard (ribitol) was used to normalize the reconstituted metabolites over the samples. Identification of metabolites was performed using NIST-MS Search and retention indices, using the Golm Metabolite database as a reference library (<http://gmd.mpimp-golm.mpg.de/download/>) and further confirmation was obtained through injection of authentic standards.

Extraction and Liquid Chromatography Quadrupole Time-of-Flight Mass Spectrometry (LC-QTOF-MS) Analysis of Semi-Polar Secondary Metabolites

Extraction and liquid chromatography quadrupole time-of-flight mass spectrometry (LC-QTOF-MS) analysis of semi-polar secondary metabolites were performed according to the protocols described by De Vos and co-workers (De Vos et al., 2007) with slight modifications. Briefly, 50 mg of ground frozen leaf tissue was extracted with 150 μ l of a MeOH (99.875 %)-formic acid (0.125 %) mixture (v/v), and sonicated for 15 min. The mixture was centrifuged at 20,000*g* for 10 min and the supernatant was filtered using a 0.45 μ m inorganic membrane filter (Anotop 10; Whatman), fitted onto a disposable syringe, and transferred into a 150 μ l insert in a 1.8 ml glass vial.

The LC-PDA-QTOF-MS platform consisted of a Waters Alliance 2795 HT HPLC system equipped with a Luna C18(2) pre-column (2.0 x 4 mm) and an analytical column (2.0 x 150 mm, pore size 100 Å and particle size 3 µm; Phenomenex), connected to an Ultima V4.00.00 QTOF mass spectrometer (Waters, MS Technologies). Degassed solutions of formic acid in ultrapure water (1:1,000, v/v; eluent A) and formic acid in acetonitrile (1:1,000, v/v; eluent B) were pumped into the HPLC system at 190 µl/min and the gradient was linearly increased from 5 % to 35 % eluent B over a 45 min period, followed by 15 min of washing and equilibration of the column. The column, sample and room temperatures were kept at 40°C, 20°C and 20°C, respectively. Ionization was performed using an electrospray ionization source, and masses were detected in negative mode. A collision energy of 10 eV was used for full-scan LC-MS in the range of m/z 100 to 1,500. For LC-MS/MS, collision energies of 35 eV were applied. Leucine enkephaline, ($M - H$) = 554.2620, was used for online mass calibration (lock mass) using a separate spray inlet. The chromatograms were aligned using the MetAlign (accurate mass option) software package (Lommen, 2009). Extraction and reconstitution of compound mass spectra was performed according to the method described by Tikunov and co-workers (Tikunov et al., 2012).

The identification of the secondary metabolites was based on their detected accurate mass and their corresponding retention time recorded for tomato fruit, as present in the MOTO database (Iijima et al., 2008). We used different public databases (dictionary of natural products <http://dnf.chemnetbase.com> and KNApSACk <http://kanaya.aist-nara.ac.jp/KNApSACk/>) to putatively identify some of the metabolites that are not present in the MOTO database (Moco et al., 2006). For confirmation of the identity of these metabolites we performed MS³ fragmentation of the parent ion using a Thermo LC-LTQ-Orbitrap FTMS system in high-mass resolution mode (van der Hooft et al., 2011). The identification levels were given according to the proposed minimum reporting standards for chemical analysis, Metabolomics Standards Initiative (MSI) (Sumner et al., 2007). The identity of the hydroxycinnamic acid amides (HCAAs) trans-feruloyltyramine (FT) and trans-coumaroyltyramine (CT) present in total extracts of the DS was confirmed by using synthetic trans-FT and trans-CT as standards. For this, trans-FT and trans-CT were synthesized according to López-Gresa et al. (2011) and chromatograms, UV absorption spectra and MS/MS spectra of the FT and CT standards and an extract of the DS obtained at $t = 5$ hr after the temperature shift were compared (**Supplemental Figure S4**).

Ethylene Measurements by Gas Chromatography Coupled to Flame Ionization Detection (GC-FID)

Ethylene was measured using gas chromatography (GC) coupled to flame ionization detection (FID), on a focus GC (Thermo Scientific), equipped with a FID detector and a

RT QPLOT (15m x 0.53mm ID) column (Restek), using helium as carrier gas. First, the seedlings were kept for 24 hr in 1000 ml air-tight glass jars at 33°C and 100 % RH and 2 ml samples were taken regularly from the headspace for analyses. Then the plants were transferred to 20°C /100 % RH and again regularly 2 ml air samples were collected over a period of 24 hrs. Samples were stored in air-tight syringes and were injected in the gas chromatograph using a 500 µl injection loop.

Statistical Analysis and Bioinformatics

For both transcriptome and metabolome studies, three independent biological replicates were performed and analyzed. Differentially expressed genes were filtered based on the following criteria: fold change (FC) in expression > 2 and a *P*-value <0.05, based on two-tailed t-tests on the expression values of the DS and PLS at individual time points. The FC in gene expression was calculated by subtracting the expression value (log2) of the PLS (control) from the DS (treatment). The same procedure was employed to filter both polar primary metabolites and semi-polar secondary metabolites. Here we reduced the fold change cut-off value to 1.5, in order to include most of the tightly regulated primary metabolites in the analysis, and we corrected for the false discovery rate (FDR).

About 80 % to 90 % of the genes on the tomato Affymetrix® genome array are of unknown function. Therefore, to annotate them, the blast output of these genes from the Tomato Functional Genomics Database (http://ted.bti.cornell.edu/cgi-bin/TFGD/array/download_annotation.cgi) was used. In this output list, the potential Arabidopsis orthologues and their respective protein reference sequence IDs were included. Subsequently, this combined information was used to compute an over-representation analysis (ORA), aimed at identifying significantly enriched functional GO: (gene ontology) subcategories of genes that are differentially regulated during the HR. For this analysis, GeneTrail, a web-based tool that compares the frequency of differentially regulated genes belonging to a certain functional category in the test set, with that of a reference set (in this case all genes of Arabidopsis), was used. Separate computation of the ORA was done for the up- and down-regulated gene categories, using the sets of genes that have unique or overlapping expression patterns between the different time points. To reduce the amount of redundant functional categories describing the same biological process, a similarity matrix was built based on the output of GeneTrail using R software (**Supplemental** Materials and Methods S1). In addition to GeneTrail, we used other web-based tools like tomato functional genomics database (TFGD) GO: enrichment analysis (http://ted.bti.cornell.edu/cgi-bin/TFGD/array/GO_analysis.cgi) and AtCOECiS (<http://bioinformatics.psb.ugent.be/ATCOECIS/>) (Vandepoele et al., 2009; Fei et al., 2011) to compute GO: enrichment analysis of gene clusters that are selected from our co-expression network analysis.

Genemaths XT software (Applied Maths, Inc. Austin, TX, USA) was used for discriminant function analysis (DFA) and hierarchical cluster analysis (HCA). For HCA, Pearson's correlation coefficients were used to calculate the distance or similarity between two entries and the resulting clusters were summarized using a complete linkage algorithm. To compare the expression values, both for the transcriptome and the metabolome profile, the raw values of each sample were log-transformed and auto-scaled by the use of the average as an offset and the standard deviation as scale (raw value-average (offset)/SD (scale)).

To gain more insight into the interaction of differentially regulated genes at the systems level, a regulatory network was built using Cytoscape (version 2.6) (Shannon et al., 2003) and the expression correlation network plug-in (<http://www.baderlab.org/Software/ExpressionCorrelation>). Network construction was based on a weighed gene-gene network, in which an edge weight for two genes is given based on the similarity of their expression profiles. A similarity matrix was computed using Pearson's correlation coefficients and was then converted into a sparse network by connecting each gene to its nearest neighbors with a strict similarity cut-off score of 0.92. This type of computation is based on selecting a gene and determining its nearest neighbors in the expression space within the defined distance cut-off value. The Cytoscape plug-in module identification in networks (MINE) was used to identify the major hubs where pathways converge. MINE performs a type of clustering that follows a guilt by association (GBA) approach (Rhissorrakrai and Gunsalus, 2011).

We used *Tair* motif finder (<http://www.arabidopsis.org/tools/bulk/motiffinder/index.jsp>) to identify potential nucleotide patterns (hexamers) in the promoter regions (a 1 kb stretch upstream of the open reading frame) of the co-regulated genes. The web-based tool POBO (Kankainen and Holm, 2004) was used to validate the result from the *Tair* motif finder. MapMan (Thimm et al., 2004) was used to visualize the expression pattern of genes that fall into different functional groups.

Acknowledgements

We are indebted to José María Bellés (Instituto de Biología Molecular y Celular de Plantas (IBMCP), Valencia, Spain) for providing hydroxycinnamic acid amide standards. We wish to thank Anna Undas and Francel Verstappen (Laboratory of Plant Physiology, Wageningen University), Bert Schipper (Plant Research International (PRI)), Arjen Peppel and Uulke van Meeteren (Horticultural Supply Chains Group, Wageningen University) for the technical help we received during primary and secondary metabolite analysis and with ethylene measurements. We are grateful for the technical advice we obtained from Chris Maliepaard on multivariate analysis of both the metabolome and transcriptome data. The excellent plant care by Bert Essenstam is highly appreciated. We are grateful for all technical and intellectual support we received from the Metabolomics groups of the Laboratory of Plant Physiology (Wageningen University) and of PRI.

References

- Afzal AJ, da Cunha L, Mackey D (2011) Separable fragments and membrane tethering of Arabidopsis RIN4 regulate its suppression of PAMP-triggered immunity. *Plant Cell* **23**: 3798-3811
- Ameisen JC (2002) On the origin, evolution, and nature of programmed cell death: a timeline of four billion years. *Cell Death Differ* **9**: 367-393
- Arpagaus S, Rawlyer A, Braendle R (2002) Occurrence and characteristics of the mitochondrial permeability transition in plants. *J Biol Chem* **277**: 1780-1787
- Aubert S, Alban C, Bligny R, Douce R (1996) Induction of β -methylcrotonyl-coenzyme A carboxylase in higher plant cells during carbohydrate starvation: evidence for a role of MCCase in leucine catabolism. *FEBS Lett* **383**: 175-180
- Backes C, Keller A, Kuentzer J, Kneissl B, Comtesse N, Elnakady YA, Muller R, Meese E, Lenhof HP (2007) GeneTrail--advanced gene set enrichment analysis. *Nucleic Acids Res* **35**: 186-192
- Bienert GP, Möller ALB, Kristiansen KA, Schulz A, Möller IM, Schjoerring JK, Jahn TP (2007) Specific aquaporins facilitate the diffusion of hydrogen peroxide across membranes. *J Biol Chem* **282**: 1183-1192
- Bolton MD (2009) Primary metabolism and plant defense—fuel for the fire. *Mol Plant-Microbe Interact* **22**: 487-497
- Bolton MD, Kolmer JA, Xu WW, Garvin DF (2008) Comparative transcript profiling of Lr1- and Lr34-mediated leaf rust resistance in wheat. *Phytopathology* **98**: S24-S24
- Bolton MD, Kolmer JA, Xu WW, Garvin DF (2008) Lr34-mediated leaf rust resistance in wheat: transcript profiling reveals a high energetic demand supported by transient recruitment of multiple metabolic pathways. *Mol Plant-Microbe Interact* **21**: 1515-1527
- Chanson A (1993) Active-transport of proton and calcium in higher-plant cells. *Plant Physiol and Bioch* **31**: 943-955
- Ciardi JA, Tieman DM, Jones JB, Klee HJ (2001) Reduced expression of the tomato ethylene receptor gene LeETR4 enhances the hypersensitive response to *Xanthomonas campestris* pv. *vesicatoria*. *Mol Plant-Microbe Interact* **14**: 487-495
- Ciardi JA, Tieman DM, Lund ST, Jones JB, Stall RE, Klee HJ (2000) Response to *Xanthomonas campestris* pv. *vesicatoria* in tomato involves regulation of ethylene receptor gene expression. *Plant Physiol* **123**: 81-92
- Daniel X, Lacomme C, Morel J-B, Roby D (1999) A novel myb oncogene homologue in *Arabidopsis thaliana* related to hypersensitive cell death. *Plant J* **20**: 57-66

- de Jong CF, Takken FL, Cai X, de Wit PJ, Joosten MH (2002) Attenuation of Cf-mediated defense responses at elevated temperatures correlates with a decrease in elicitor-binding sites. *Mol Plant-Microbe Interact* **15**: 1040-1049
- De Vos RCH, Moco S, Lommen A, Keurentjes JJB, Bino RJ, Hall RD (2007) Untargeted large-scale plant metabolomics using liquid chromatography coupled to mass spectrometry. *Nat Protoc* **2**: 778-791
- de Wit PJGM (1977) A light and scanning-electron microscopic study of infection of tomato plants by virulent and avirulent races of *Cladosporium fulvum*. *Eur J Plant Pathol* **83**: 109-122
- de Wit PJGM, Joosten MH (1999) Avirulence and resistance genes in the *Cladosporium fulvum*-tomato interaction. *Curr Opin Microbiol* **2**: 368-373
- DeYoung BJ, Innes RW (2006) Plant NBS-LRR proteins in pathogen sensing and host defense. *Nat Rev Immunol* **7**: 1243-1249
- Dodds PN, Rathjen JP (2010) Plant immunity: towards an integrated view of plant-pathogen interactions. *Nat Rev Genet* **11**: 539-548
- Dong C-H, Jang M, Scharein B, Malach A, Rivarola M, Liesch J, Groth G, Hwang I, Chang C (2010) Molecular association of the Arabidopsis ETR1 ethylene receptor and a regulator of ethylene signaling, RTE1. *J Biol Chem* **285**: 40706-40713
- Du L, Ali GS, Simons KA, Hou J, Yang T, Reddy ASN, Poovaiah BW (2009) Ca²⁺/calmodulin regulates salicylic-acid-mediated plant immunity. *Nature* **457**: 1154-1158
- Eppl P, Mack AA, Morris VR, Dangl JL (2003) Antagonistic control of oxidative stress-induced cell death in Arabidopsis by two related, plant-specific zinc finger proteins. *Proc Natl Acad Sci U.S.A.* **100**: 6831-6836
- Essmann J, Bones P, Weis E, Scharte J (2008) Leaf carbohydrate metabolism during defense: Intracellular sucrose-cleaving enzymes do not compensate repression of cell wall invertase. *Plant Signal Behav* **3**: 885-887
- Eulgem T (2005) Regulation of the Arabidopsis defense transcriptome. *TRENDS in Plant Science* **10**: 71-78
- Eulgem T, Somssich IE (2007) Networks of WRKY transcription factors in defense signaling. *Curr Opin Plant Biol* **10**: 366-371
- Facchini PJ, Hagel J, Zulak KG (2002) Hydroxycinnamic acid amide metabolism: physiology and biochemistry. *Can J Bot* **80**: 577-589
- Facchini PJ, Yu M, Penzes-Yost C (1999) Decreased cell wall digestibility in canola transformed with chimeric tyrosine decarboxylase genes from opium poppy. *Plant Physiol* **120**: 653-664
- Fei Z, Joung J-G, Tang X, Zheng Y, Huang M, Lee JM, McQuinn R, Tieman DM, Alba R, Klee HJ, Giovannoni JJ (2011) Tomato functional genomics database: a comprehensive resource and analysis package for tomato functional genomics. *Nucleic Acids Res* **39**: 1156-1163
- Fujiki Y, Ito M, Nishida I, Watanabe A (2001) Leucine and its keto acid enhance the coordinated expression of genes for branched-chain amino acid catabolism in Arabidopsis under sugar starvation. *FEBS Lett* **499**: 161-165
- Gabriëls SH, Takken FL, Vossen JH, de Jong CF, Liu Q, Turk SC, Wachowski LK, Peters J, Witsenboer HM, de Wit PJGM, Joosten MH (2006) cDNA-AFLP combined with functional analysis reveals novel genes involved in the hypersensitive response. *Mol Plant-Microbe Interact* **19**: 567-576
- Gentleman R, Carey V, Bates D, Bolstad B, Dettling M, Dudoit S, Ellis B, Gautier L, Ge Y, Gentry J, Hornik K, Hothorn T, Huber W, Iacus S, Irizarry R, Leisch F, Li C, Maechler M, Rossini A, Sawitzki G, Smith C, Smyth G, Tierney L, Yang J, Zhang J (2004) Bioconductor: open software development for computational biology and bioinformatics. *Genome Biol* **5**: R80-80.16
- Gomes D, Agasse A, Thiebaud P, Delrot S, Geros H, Chaumont F (2009) Aquaporins are multifunctional water and solute transporters highly divergent in living organisms. *Biochim Biophys Acta* **1788**: 1213-1228
- Graham IA, Eastmond PJ (2002) Pathways of straight and branched chain fatty acid catabolism in higher plants. *Prog Lipid Res* **41**: 156-181
- Grandmaison J, Olah G.M, Van Calsteren MR, Furlan V (1993) Characterization and localization of plant phenolics likely involved in the pathogen resistance expressed by endomycorrhizal roots. *Mycorrhiza* **3**: 155-164
- Guillet G, De Luca V (2005) Wound-inducible biosynthesis of phytoalexin hydroxycinnamic acid amides of tyramine in tryptophan and tyrosine decarboxylase transgenic tobacco lines. *Plant Physiol* **137**: 692-699

- Hanssen IM, van Esse HP, Ballester AR, Hogewoning SW, Parra NO, Paeleman A, Lievens B, Bovy AG, Thomma BP** (2011) Differential tomato transcriptomic responses induced by pepino mosaic virus isolates with differential aggressiveness. *Plant Physiol* **156**: 301-318
- Hardie DG, Ross FA, Hawley SA** (2012) AMPK: a nutrient and energy sensor that maintains energy homeostasis. *Nat Rev Mol Cell Biol* **13**: 251-262
- Heil M, Baldwin IT** (2002) Fitness costs of induced resistance: emerging experimental support for a slippery concept. *Trends Plant Sci* **7**: 61-67
- Hong W, Xu YP, Zheng Z, Cao JS, Cai XZ** (2007) Comparative transcript profiling by cDNA-AFLP reveals similar patterns of Avr4/Cf-4- and Avr9/Cf-9-dependent defence gene expression. *Mol Plant Pathol* **8**: 515-527
- Huang Y, Li H, Hutchison CE, Laskey J, Kieber JJ** (2003) Biochemical and functional analysis of CTR1, a protein kinase that negatively regulates ethylene signaling in Arabidopsis. *Plant J* **33**: 221-233
- Iijima Y, Nakamura Y, Ogata Y, Tanaka Ki, Sakurai N, Suda K, Suzuki T, Suzuki H, Okazaki K, Kitayama M, Kanaya S, Aoki K, Shibata D** (2008) Metabolite annotations based on the integration of mass spectral information. *Plant J* **54**: 949-962
- Jones AM** (2001) Programmed cell death in development and defense. *Plant Physiol* **125**: 94-97
- Jones JD, Dangl JL** (2006) The plant immune system. *Nature* **444**: 323-329
- Kang S, Kang K, Chung GC, Choi D, Ishihara A, Lee D-S, Back K** (2006) Functional analysis of the amine substrate specificity domain of pepper tyramine and serotonin N-hydroxycinnamoyltransferases. *Plant Physiol* **140**: 704-715
- Kankainen M, Holm L** (2004) POBO, transcription factor binding site verification with bootstrapping. *Nucleic Acids Res* **32**: 222-229
- Kieber JJ, Rothenberg M, Roman G, Feldmann KA, Ecker JR** (1993) CTR1, a negative regulator of the ethylene response pathway in Arabidopsis, encodes a member of the raf family of protein kinases. *Cell* **72**: 427-441
- Kilili KG, Atanassova N, Vardanyan A, Clatot N, Al-Sabarna K, Kanellopoulos PN, Makris AM, Kampranis SC** (2004) Differential roles of tau class glutathione S-transferases in oxidative stress. *J Biol Chem* **279**: 24540-24551
- Knickerbocker DL, Lutz PL** (2001) Slow ATP loss and the defense of ion homeostasis in the anoxic frog brain. *J Exp Biol* **204**: 3547-3551
- Kochevenko A, Araújo WL, Maloney GS, Tieman DM, Do PT, Taylor MG, Klee HJ, Fernie AR** (2012) Catabolism of branched chain amino acids supports respiration but not volatile synthesis in tomato fruits. *Molecular plant* **5**: 366-375
- Kuriyama H, Fukuda H** (2002) Developmental programmed cell death in plants. *Curr Opin Plant Biol* **5**: 568-573
- Lam E, Naohiro K, Lawton M** (2001) Programmed cell death, mitochondria and the plant hypersensitive response. *Nature* **411**: 848-853
- Lee SC, Lan WZ, Kim BG, Li LG, Cheong YH, Pandey GK, Lu GH, Buchanan BB, Luan S** (2007) A protein phosphorylation/dephosphorylation network regulates a plant potassium channel. *Proc Natl Acad Sci U.S.A.* **104**: 15959-15964
- Leivar P, Antolin-Llovera M, Ferrero S, Closa M, Arro M, Ferrer A, Boronat A, Campos N** (2011) Multilevel control of Arabidopsis 3-hydroxy-3-methylglutaryl coenzyme A reductase by protein phosphatase 2A. *Plant Cell* **23**: 1494-1511
- Lippok B, Birkenbihl RP, Rivory G, Brümmer J, Schmelzer E, Logemann E, Somssich IE** (2007) Expression of AtWRKY33 encoding a pathogen- or PAMP-responsive WRKY transcription factor is regulated by a composite DNA motif containing W box elements. *Mol Plant-Microbe Interact* **20**: 420-429
- Lisec J, Schauer N, Kopka J, Willmitzer L, Fernie AR** (2006) Gas chromatography mass spectrometry-based metabolite profiling in plants. *Nat Protoc* **1**: 387-396
- Lommen A** (2009) MetAlign: interface-driven, versatile metabolomics tool for hyphenated full-scan mass spectrometry data preprocessing. *Anal Chem* **81**: 3079-3086
- Lopez-Gresa MP, Torres C, Campos L, Lison P, Rodrigo I, Belles JM, Conejero V** (2011) Identification of defence metabolites in tomato plants infected by the bacterial pathogen *Pseudomonas syringae*. *Env Exp Bot* **74**: 216-228
- López-Gresa MP, Torres C, Campos L, Lisón P, Rodrigo I, Bellés JM, Conejero V** (2011) Identification of defence metabolites in tomato plants infected by the bacterial pathogen *Pseudomonas syringae*. *Environ Exp Bot* **74**: 216-228

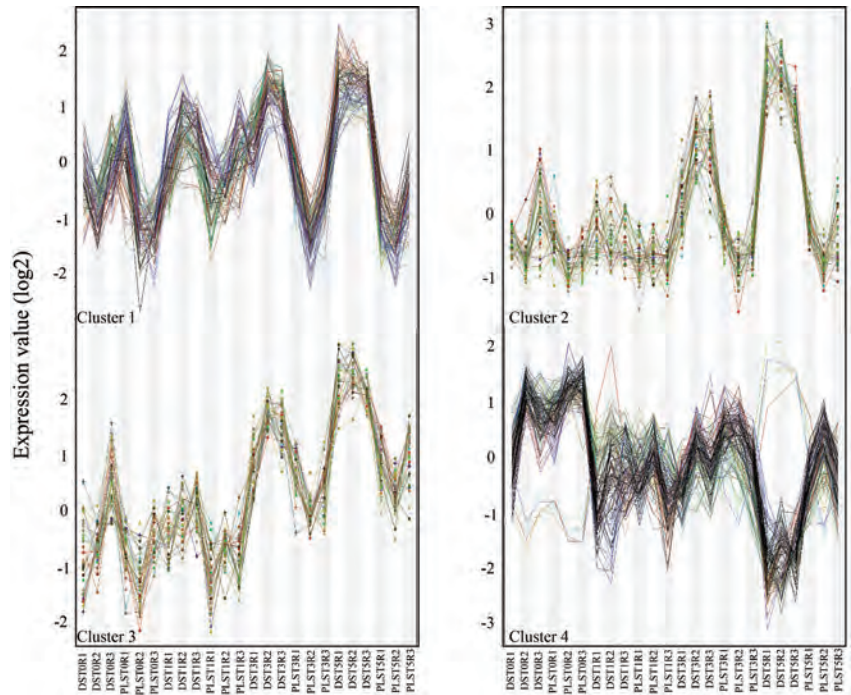
- Lund ST, Stall RE, Klee HJ (1998) Ethylene regulates the susceptible response to pathogen infection in tomato. *Plant Cell* **10**: 371-382
- Maeda H, Dudareva N (2012) The shikimate pathway and aromatic amino acid biosynthesis in plants. *Annu Rev Plant Biol* **63**: 73-105
- Mangeon A, Junqueira RM, Sachetto-Martins G (2010) Functional diversity of the plant glycine-rich proteins superfamily. *Plant Signal Behav* **5**: 99-104
- Mao G, Meng X, Liu Y, Zheng Z, Chen Z, Zhang S (2011) Phosphorylation of a WRKY transcription factor by two pathogen-responsive MAPKs drives phytoalexin biosynthesis in Arabidopsis. *Plant Cell* **23**: 1639-1653
- Margolles-Clark E, Harman GE, Penttilä M (1996) Enhanced expression of endochitinase in *Trichoderma harzianum* with the cbh1 promoter of *Trichoderma reesei*. *Appl Environ Microbiol* **62**: 2152-2155
- Marrs KA (1996) The functions and regulation of glutathione S-transferases in plants. *Annu Rev Plant Physiol Plant Mol Biol* **47**: 127-158
- McLusky SR, Bennett MH, Beale MH, Lewis MJ, Gaskin P, Mansfield JW (1999) Cell wall alterations and localized accumulation of feruloyl-3'-methoxytyramine in onion epidermis at sites of attempted penetration by *Botrytis allii* are associated with actin polarisation, peroxidase activity and suppression of flavonoid biosynthesis. *Plant J* **17**: 523-534
- Moco S, Bino RJ, Vorst O, Verhoeven HA, de Groot J, van Beek TA, Vervoort J, de Vos CHR (2006) A Liquid Chromatography-Mass Spectrometry-Based Metabolome Database for Tomato. *Plant Physiol* **141**: 1205-1218
- Morel JB, Dangl JL (1997) The hypersensitive response and the induction of cell death in plants. *Cell Death Differ* **4**: 671-683
- Mur LA, Lloyd AJ, Cristescu SM, Harren FJ, Hall MA, Smith AR (2009) Biphasic ethylene production during the hypersensitive response in Arabidopsis: a window into defense priming mechanisms? *Plant Signal Behav* **4**: 610-613
- Naoumkina M, He X, Dixon R (2008) Elicitor-induced transcription factors for metabolic reprogramming of secondary metabolism in *Medicago truncatula*. *BMC Plant Biol* **8**: 132
- Oñate-Sánchez L, Anderson JP, Young J, Singh KB (2007) AtERF14, a member of the ERF family of transcription factors, plays a nonredundant role in plant defense. *Plant Physiol* **143**: 400-409
- Pappan K, Qin W, Dyer JH, Zheng L, Wang X (1997) Molecular cloning and functional analysis of polyphosphoinositide-dependent phospholipase D, PLD β , from Arabidopsis. *J Biol Chem* **272**: 7055-7061
- Postel S, Kemmerling B (2009) Plant systems for recognition of pathogen-associated molecular patterns. *Semin Cell Dev Biol* **20**: 1025-1031
- Rhrissorakrai K, Gunsalus K (2011) MINE: module identification in networks. *BMC Bioinf* **12**: 192
- Rivas S, Thomas CM (2005) Molecular interactions between tomato and the leaf mold pathogen *Cladosporium fulvum*. *Annu Rev Phytopathol* **43**: 395-436
- Rushton PJ, Somssich IE, Ringler P, Shen QJ (2010) WRKY transcription factors. *Trends Plant Sci* **15**: 247-258
- Santner A, Estelle M (2009) Recent advances and emerging trends in plant hormone signalling. *Nature* **459**: 1071-1078
- Schneider DJ, Collmer A (2010) Studying plant-pathogen interactions in the genomics era: beyond molecular Koch's postulates to systems biology. *Ann Rev Phytopathol* **48**: 457-479
- Schweighofer A, Kazanaviciute V, Scheikl E, Teige M, Doczi R, Hirt H, Schwanninger M, Kant M, Schuurink R, Mauch F, Buchala A, Cardinale F, Meskiene I (2007) The PP2C-type phosphatase AP2C1, which negatively regulates MPK4 and MPK6, modulates innate immunity, jasmonic acid, and ethylene levels in Arabidopsis. *Plant Cell* **19**: 2213-2224
- Shannon P, Markiel A, Ozier O, Baliga NS, Wang JT, Ramage D, Amin N, Schwikowski B, Ideker T (2003) Cytoscape: a software environment for integrated models of biomolecular interaction networks. *Genome Res* **13**: 2498-2504
- Singh KB, Foley RC, Oñate-Sánchez L (2002) Transcription factors in plant defense and stress responses. *Curr Opin Plant Biol* **5**: 430-436
- Smith AM, Stitt M (2007) Coordination of carbon supply and plant growth. *Plant Cell Env* **30**: 1126-1149
- Snedden WA, Blumwald E (2000) Alternative splicing of a novel diacylglycerol kinase in tomato leads to a calmodulin-binding isoform. *Plant J* **24**: 317-326

- Snedden WA, Fromm H** (2001) Calmodulin as a versatile calcium signal transducer in plants. *New Phytol* **151**: 35-66
- Stulemeijer IJS, Joosten MHAJ, Jensen ON** (2009) Quantitative phosphoproteomics of tomato mounting a hypersensitive response reveals a swift suppression of photosynthetic activity and a differential role for hsp90 isoforms. *J. Proteome Res* **8**: 1168-1182
- Stulemeijer IJS, Stratmann JW, Joosten MHAJ** (2007) Tomato mitogen-activated protein kinases LeMPK1, LeMPK2, and LeMPK3 are activated during the Cf-4/Avr4-induced hypersensitive response and have distinct phosphorylation specificities. *Plant Physiol* **144**: 1481-1494
- Sumner L, Amberg A, Barrett D, Beale M, Beger R, Daykin C, Fan TM, Fiehn O, Goodacre R, Griffin J, Hankemeier T, Hardy N, Harnly J, Higashi R, Kopka J, Lane A, Lindon J, Marriott P, Nicholls A, Reily M, Thaden J, Viant M** (2007) Proposed minimum reporting standards for chemical analysis. *Metabolomics* **3**: 211-221
- Taylor NL, Heazlewood JL, Day DA, Millar AH** (2004) Lipoic acid-dependent oxidative catabolism of α -Keto acids in mitochondria provides evidence for branched-chain amino acid catabolism in Arabidopsis. *Plant Physiol* **134**: 838-848
- Thimm O, Blasing O, Gibon Y, Nagel A, Meyer S, Kruger P, Selbig J, Muller LA, Rhee SY, Stitt M** (2004) MAPMAN: a user-driven tool to display genomics data sets onto diagrams of metabolic pathways and other biological processes. *Plant J* **37**: 914-939
- Thomma BP, Nurnberger T, Joosten MH** (2011) Of PAMPs and effectors: the blurred PTI-ETI dichotomy. *Plant Cell* **23**: 4-15
- Thomma BP, Van Esse HP, Crous PW, De Wit PJ** (2005) *Cladosporium fulvum* (syn. *Passalora fulva*), a highly specialized plant pathogen as a model for functional studies on plant pathogenic Mycosphaerellaceae. *Mol Plant Pathol* **6**: 379-393
- Tikunov YM, Laptinok S, Hall RD, Bovy A, Vos RCH** (2012) MSClust: a tool for unsupervised mass spectra extraction of chromatography-mass spectrometry ion-wise aligned data. *Metabolomics* **8**: 714-718
- Tozzi MG, Camici M, Mascia L, Sgarrella F, Ipata PL** (2006) Pentose phosphates in nucleoside interconversion and catabolism. *FEBS J* **273**: 1089-1101
- Vabulas RM** (2007) Proteasome function and protein biosynthesis. *Curr Opin Clin Nutr Metab Care* **10**: 24-31
- Vabulas RM, Hartl FU** (2005) Protein synthesis upon acute nutrient restriction relies on proteasome function. *Science* **310**: 1960-1963
- van Baarlen P, van Esse HP, Siezen RJ, Thomma BP** (2008) Challenges in plant cellular pathway reconstruction based on gene expression profiling. *Trends Plant Sci* **13**: 44-50
- van der Hooft JJJ, Vervoort J, Bino RJ, Beekwilder J, de Vos RCH** (2011) Polyphenol Identification Based on Systematic and Robust High-Resolution Accurate Mass Spectrometry Fragmentation. *Anal Chem* **83**: 409-416
- van Esse HP, Fradin EF, de Groot PJ, de Wit PJ, Thomma BP** (2009) Tomato transcriptional responses to a foliar and a vascular fungal pathogen are distinct. *Mol Plant-Microbe Interact* **22**: 245-258
- van Esse HP, Van't Klooster JW, Bolton MD, Yadeta KA, van Baarlen P, Boeren S, Vervoort J, de Wit PJ, Thomma BP** (2008) The *Cladosporium fulvum* virulence protein Avr2 inhibits host proteases required for basal defense. *Plant Cell* **20**: 1948-1963
- van Loon LC, Geraats BPJ, Linthorst HJM** (2006) Ethylene as a modulator of disease resistance in plants. *Trends Plant Sci* **11**: 184-191
- Vandepoele K, Quimbaya M, Casneuf T, De Veylder L, Van de Peer Y** (2009) Unraveling transcriptional control in Arabidopsis using cis-regulatory elements and coexpression networks. *Plant Physiol* **150**: 535-546
- Vierstra RD** (1993) Protein-degradation in plants. *Annu Rev Plant Physiol Plant Mol Biol* **44**: 385-410
- Vierstra RD** (2009) The ubiquitin-26S proteasome system at the nexus of plant biology. *Nat Rev Mol Cell Biol* **10**: 385-397
- von Roepenack-Lahaye E, Newman MA, Schornack S, Hammond-Kosack KE, Lahaye T, Jones JDG, Daniels MJ, Dow JM** (2003) P-coumaroylnoradrenaline, a novel plant metabolite implicated in tomato defense against pathogens. *J Biol Chem* **278**: 43373-43383
- von Röpenack E, Parr A, Schulze-Lefert P** (1998) Structural analyses and dynamics of soluble and cell wall-bound phenolics in a broad spectrum resistance to the powdery mildew fungus in barley. *J Biol Chem* **273**: 9013-9022
- Walters DR** (2003) Polyamines and plant disease. *Phytochemistry* **64**: 97-107

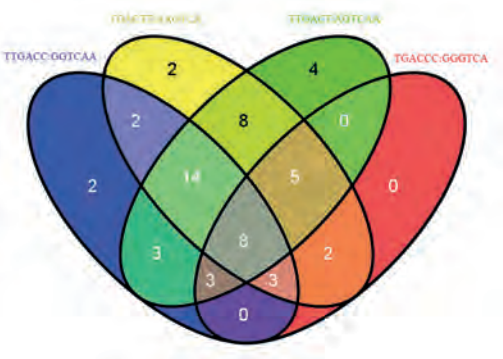
- Wu Z, Irizarry RA, Gentleman R, Martinez-Murillo F, Spencer F** (2004) A model-based background adjustment for oligonucleotide expression arrays. *J Am Stat Assoc* **99**: 909-917
- Yang T, Poovaiah BW** (2003) Calcium/calmodulin-mediated signal network in plants. *Trends Plant Sci* **8**: 505-512
- Yap KL, Yuan T, Mal TK, Vogel HJ, Ikura M** (2003) Structural basis for simultaneous binding of two carboxy-terminal peptides of plant glutamate decarboxylase to calmodulin. *J Mol Biol* **328**: 193-204
- Zacares L, Lopez-Gresa MP, Fayos J, Primo J, Belles JM, Conejero V** (2007) Induction of p-coumaroyldopamine and feruloyldopamine, two novel metabolites, in tomato by the bacterial pathogen *Pseudomonas syringae*. *Mol Plant-Microbe interact* **20**: 1439-1448

Supplemental information

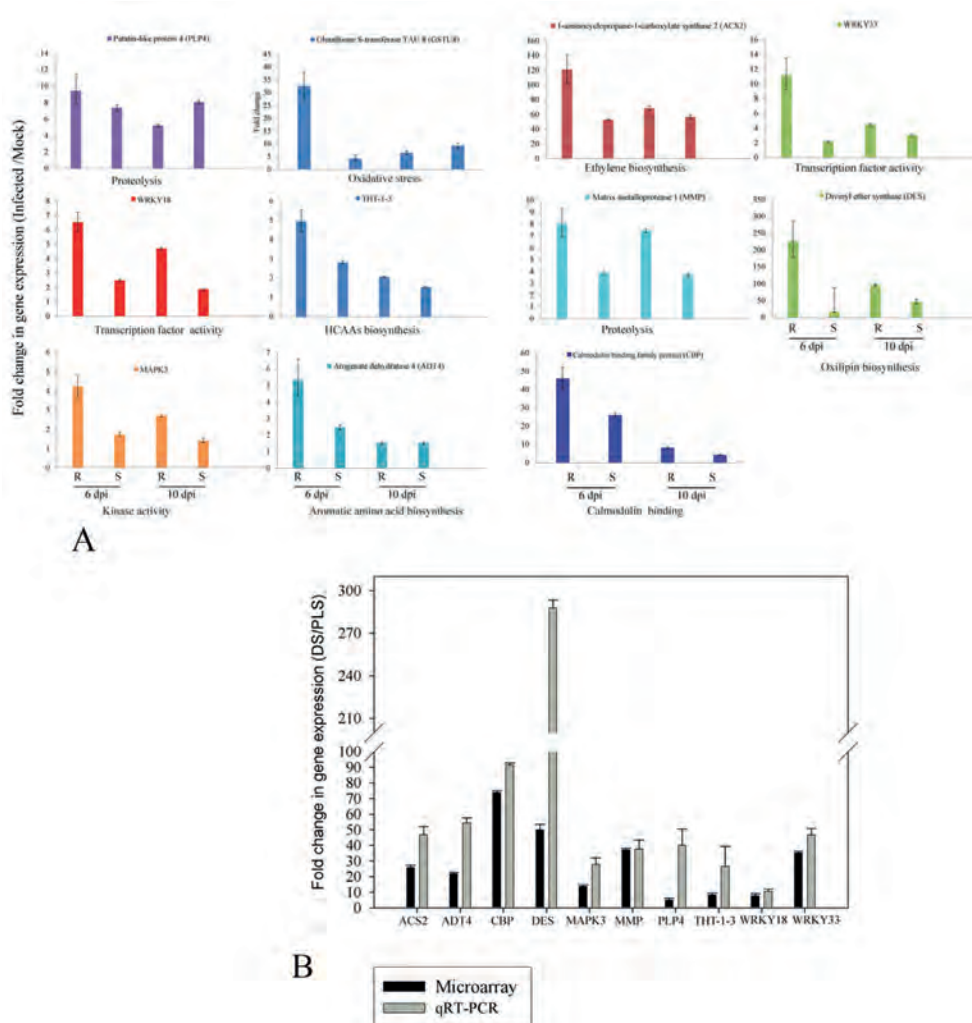
Supplemental Figures



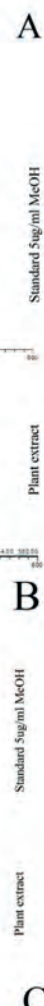
Supplemental Figure S1. Expression profiles of the different gene clusters identified in the co-expression network analysis of differentially regulated genes during mounting of the HR in the dying seedlings (DS), as shown in Fig. 4A. The log2 expression value for every gene in the individual clusters was normalized for offset with the cluster average value and scaled by the standard deviation of the cluster. DS, dying seedlings; PLS, parental lines; T, time after the temperature shift (0 hr, 1 hr, 3 hr or 5hr); R, replicate number (1, 2 or 3). Each time point is represented by three independent biological replicates (see Materials and Methods for details).



Supplemental Figure S2. Venn diagram showing the number and distribution of genes containing the sequence TTTGAC, interrogated for the presence of either a C or a T, following the core sequence TGAC. Note that from the 60 genes that were analyzed (see Supplementary Table S4), 56 contain the TGACC/T W box consensus core motif.



Supplemental Figure S3. Quantitative RT-PCR analysis of the expression of genes, selected from the co-expression network analysis of the dying seedlings (DS), in leaves of *C. fulvum*-inoculated tomato. A, Parental lines (PLS) used to generate the dying seedlings (MM-Cf0: Cf-4, resistant (R) and MM-Cf0: Avr4, susceptible (S)), were inoculated with a strain of *C. fulvum* secreting Avr4. Gene expression levels, in fold change relative to mock-treated plants, were determined at 6 and 10 days after inoculation (dpi). B, Comparison of the relative expression levels of the selected genes, as determined by the microarray analysis and by qRT-PCR, in the DS compared to the PLS, at $t = 3$ hr after the temperature shift that triggers the HR in the DS.



60

Supplementary Materials and Methods S1

Supplementary Method

Reduction of the redundancy of GO: subcategories obtained from GeneTrail

The Gene x GO: subcategory matrix presented in Table I is an output from GeneTrail. When a gene is reported to be involved in one of the listed GO: subcategories it obtains a score of “1”, otherwise the score is “0”.

Table I. Example of a GO: subcategory x Gene matrix, an output from GeneTrail, representing genes reported to be involved in posttranslational protein modification (phosphorylation).

GO: subcategory	Significantly differentially regulated genes										
	ATMPK3	CPK32	AT1G25390	CDPK19	CPK28	APK1B	AT3G09830	ATSIK	AT2G05940	AT3G57700	AT4G17660
protein tyrosine kinase activity (GO:0004713)	0	0	0	0	1	1	0	1	0	0	1
protein modification process (GO:0006464)¹	1	1	1	1	1	1	1	1	1	1	1
post-translational protein modification (GO:0043687)	1	1	1	1	1	1	1	1	1	1	1
macromolecule modification (GO:0043412)	1	1	1	1	1	1	1	1	1	1	1
phosphorus metabolic process (GO:0006793)	1	1	1	1	1	1	1	1	1	1	1
phosphate metabolic process (GO:0006796)	1	1	1	1	1	1	1	1	1	1	1
protein amino acid phosphorylation (GO:0006468) †	1	1	1	1	1	1	1	1	1	1	1
phosphorylation (GO:0016310)	1	1	1	1	1	1	1	1	1	1	1
protein serine/threonine kinase activity (GO:0004674)	1	1	0	1	1	1	0	0	1	1	1
kinase activity (GO:0016301)	1	1	1	1	1	1	1	1	1	1	1
transferase activity, transferring phosphorus-containing groups (GO:0016772)	1	1	1	1	1	1	1	1	1	1	1
protein kinase activity (GO:0004672)	1	1	0	1	1	1	1	1	1	1	1
phosphotransferase activity, alcohol group as acceptor (GO:0016773)	1	1	0	1	1	1	1	1	1	1	1

¹GO: subcategories that share a complete set of genes are indicated in bold. See text below.

Two GO: subcategories “i” and “j” may be compared on the characteristic presence of a differentially regulated gene “k” and are assigned a score S_{ijk} . This score is “0” when the two subcategories are considered to be different as similar genes are not present. The score increases to “1” when more genes common to both functional groups are present. Thus, S_{ijk} is defined by a range between “0” and “1”, in which a value of “1” means that two or more of the functional categories share the same genes (see GO: subcategories that are indicated in bold). This is represented by the red blocks along the diagonal axis in Figure 1. A value of “0” indicates that the functional categories do not share any gene, which is represented by blue in Figure 1. Based on this principle, the similarity between the different GO: subcategories was computed in R program (Figure 1). As the matrix is a mirrored image of itself, only half of the rectangle is shown (see also Figure 3). Categories that represent similar functional processes were given one description. For example, all GO: subcategories merging in the red triangle in the black boxed region in Figure 1 represent protein modification (phosphorylation).

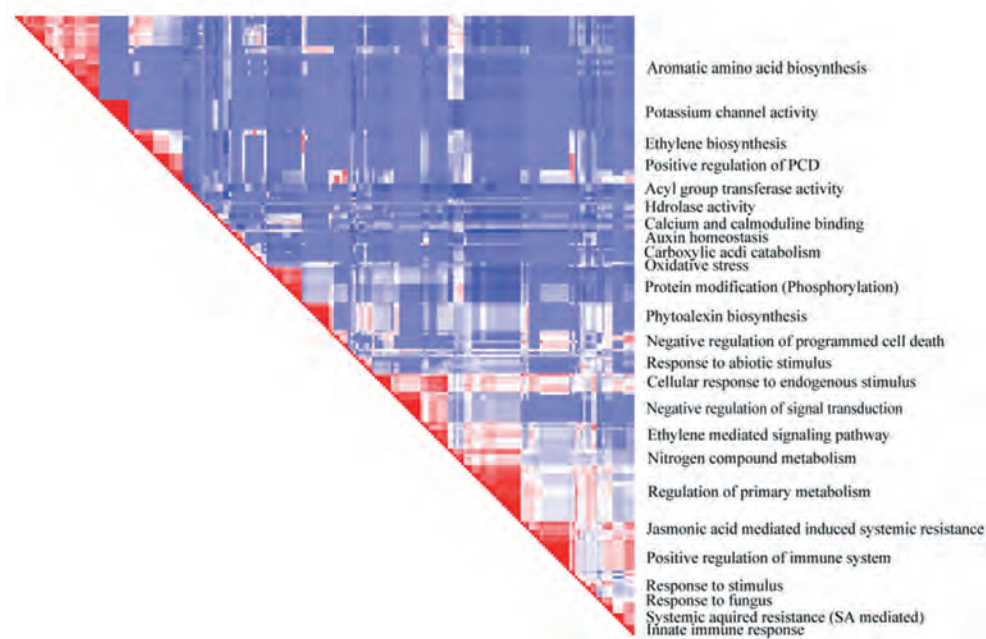


Figure 1. GO: sub-category similarity matrix, resulting from the GeneTrail GO: subcategory x Gene matrix. The red clusters along the diagonal axis represent highly similar GO: sub-categories.

Supplementary Tables

Supplementary Table S1. Expression profiles of genes encoding heat shock proteins. Expression levels are given as fold change (FC) in gene expression in the dying seedlings as compared to the parental lines, at 0, 1, 3 and 5 hr after the temperature shift that induces the HR in the DS.

Probe set ID	Best Arabidopsis hit	Best Arabidopsis hit description	FC, 0hr	FC, 1hr	FC, 3hr	FC, 5hr
Les.3160.3.S1_at	AT3G12580.1	HSP70 (heat shock protein 70); AT binding	1	1	1	3
Les.4819.1.S1_at	AT5G02500.1	HSC70-1 (heat shock cognate protein 70-1); AT binding	1	-1	7	22
Les.3160.2.S1_at	AT3G12580.1	HSP70 (heat shock protein 70); AT binding	1	1	-1	3
Les.3160.1.S1_at	AT1G56410.1	ERD2 (early responsive to dehydration 2); AT binding	1	-1	-1	2
Les.3657.1.S1_at	AT3G12580.1	HSP70 (heat shock protein 70); AT binding	1	1	1	10
Les.14662	At3g14200.1	DNAJ heat shock N-terminal domain-containing protein	1	1	-1	6

Supplementary Table S2. Over representation analysis of significantly induced genes in the DS immediately after the temperature shift.

Category	Subcategory	Expected	Observed	p-value (FDR [†])
Kegg	Valine, leucine and isoleucine degradation	0.0894161	2	0.00959517
Gene Ontology	Oxidoreductase activity, acting on the aldehyde or oxo group of donors, disulfide as acceptor	0.025444	2	0.0267556
Gene Ontology	Response to chemical stimulus	3.71287	12	0.0267556
Gene Ontology	Secondary metabolic process	0.765277	5	0.0483854
Gene Ontology	Response to stimulus	7.03037	16	0.0483854

[†]False discovery rate

Supplemental Table S3. Description of the genes that cluster in groups of strongly associated genes that were identified by co-expression network analysis using Cytoscape, their relative fold change (FC) in expression in the dying seedlings compared to the parental lines at t = 0, 1, 3 and 5 hr, and output of the computation of the GO: enrichment analysis for each cluster:

Cluster 1 genes.

Probe set ID	ATH best hit	Bet hit description	FC 0 hr	FC 1 hr	FC 3 hr	FC 5 hr	Gene bank best hit description	Category
Les.3505.1.S1_at	AT2G15080	AtRLP19 (Receptor Like Protein 19); kinase/ protein binding	2.45	2.20	19.27	17.65	verticillium wilt disease resistance protein [Lycopersicon esculentum]	RLK
Les.2137.1.S1_at	AT2G15080	AtRLP19 (Receptor Like Protein 19); kinase/ protein binding	1.48	2.86	5.83	13.03	EIX receptor 1 [Lycopersicon esculentum]	
Les.4870.1.S1_at	AT4G20780	calcium-binding protein, putative	1.02	1.38	2.37	4.19	RecName: Full=Calcium-binding protein CAST	
LesAffx.63947.2.S1_at	AT3G57530	CPK32 (CALCIUM-DEPENDENT PROTEIN KINASE 32); calcium-dependent protein kinase C/ calmodulin-dependent protein kinase/ kinase/ protein binding	1.03	1.15	3.70	4.20	calcium-dependent protein kinase 4 [Capsicum annuum]	Calcium/ Calmodulin signaling network
LesAffx.30900.1.S1_at	AT5G19450	CDPK19 (CALCIUM-DEPENDENT PROTEIN KINASE 19); ATP binding / calcium ion binding / calmodulin-dependent protein kinase/ kinase/ protein kinase/ protein serine/threonine kinase	1.03	1.31	2.97	4.13	calcium-dependent protein kinase 4 [Capsicum annuum]	
Les.5197.1.S1_at	AT2G18750	calmodulin-binding protein	-1.09	1.36	2.88	3.62	calmodulin binding protein [Zea mays]	
LesAffx.3635.2.A1_at	AT5G57010	calmodulin-binding family protein	2.43	4.09	31.74	69.36	calmodulin-binding protein [Beta vulgaris]	MAPK
LesAffx.69808.1.S1_at	AT2G26190	calmodulin-binding family protein	-1.05	3.08	73.60	268.67	calmodulin binding protein, putative [Ricinus communis]	
LesAffx.66814.1.S1_at	AT1G73805	calmodulin binding	1.19	-1.18	5.15	7.49	calmodulin binding protein, putative [Ricinus communis]	
LesAffx.3635.1.S1_at	AT4G33050	EDA39 (embryo sac development arrest 39); calmodulin binding	1.75	1.92	50.24	137.09	calmodulin binding protein, putative [Ricinus communis]	MAPK
Les.4316.1.S1_at	AT3G45640	ATMPK3 (ARABIDOPSIS THALIANA MITOGEN-ACTIVATED PROTEIN KINASE 3); MAP kinase/ kinase/ protein binding / protein kinase	1.04	1.11	7.33	13.74	mitogen-activated protein kinase 3 [Lycopersicon esculentum]	
LesAffx.16424.1.S1_s_at	AT3G45640	ATMPK3 (ARABIDOPSIS THALIANA MITOGEN-ACTIVATED PROTEIN KINASE 3); MAP kinase/ kinase/ protein binding / protein kinase	-1.01	1.25	7.38	13.27	mitogen-activated protein kinase 3 [Lycopersicon esculentum]	

LesAffx.65273.1.S1_at	AT1G16670	protein kinase family protein	1.09	1.41	1.93	4.00	ATP binding protein, putative [Ricinus communis]	Protein kinases
Les.1806.1.S1_at	AT3G09830	protein kinase, putative	1.25	1.34	2.31	3.86	protein kinase, putative [Arabidopsis thaliana]	
Les.3502.1.S1_at	AT2G05940	protein kinase, putative	-1.59	-1.04	19.44	55.33	auxin-regulated dual specificity cytosolic kinase [Lycopersicon esculentum]	
LesAffx.10313.1.A1_at	AT2G17220	protein kinase, putative	1.55	2.31	4.74	7.93	serine/threonine-protein kinase cx32, putative [Ricinus communis]	
Les.5205.1.S1_at	AT2G31880	leucine-rich repeat transmembrane protein kinase, putative	1.20	1.24	2.13	3.14	receptor-like protein kinase [Nicotiana tabacum]	LRRs
LesAffx.71532.1.S1_at	AT1G33590	disease resistance protein-related / LRR protein-related	1.33	1.25	3.01	4.39	disease resistance protein/LRR protein-related protein [Glycine max]	
Les.3710.1.S1_at	AT1G13580	LAG13 (LAG1 LONGEVITY ASSURANCE HOMOLOG 3)	1.25	2.84	50.45	70.82	RecName: Full=Protein ASC1; AltName: Full=Alternaria stem canker resistance protein 1	
LesAffx.42451.1.S1_at	AT4G00330	CRCK2; ATP binding / kinase/ protein kinase/ protein serine/threonine kinase	2.44	1.99	3.67	18.74	ATP binding protein, putative [Ricinus communis]	
Les.1297.1.S1_at	AT3G21630	CERK1 (CHITIN ELICITOR RECEPTOR KINASE 1); kinase/ receptor signaling protein/ transmembrane receptor protein kinase	1.38	1.19	2.31	5.03	CERK1 (CHITIN ELICITOR RECEPTOR KINASE 1); kinase/ receptor signaling protein/ transmembrane receptor protein kinase [Arabidopsis thaliana]	Phospholipid signaling
LesAffx.37337.1.S1_at	AT1G65960	GAD2 (GLUTAMATE DECARBOXYLASE 2); calmodulin binding / glutamate decarboxylase	1.98	2.76	21.57	36.61	glutamate decarboxylase isozyme 3 [Nicotiana tabacum]	
Les.3526.1.S1_a_at	AT2G20900	diacylglycerol kinase, putative	1.38	1.56	1.97	6.46	diacylglycerol kinase [Lycopersicon esculentum]	
LesAffx.64831.1.S1_at	AT3G26020	serine/threonine protein phosphatase 2A (PP2A) regulatory subunit B', putative	1.41	1.35	1.92	3.80	protein phosphatase 2A regulatory subunit B' [Zea mays]	
Les.3262.2.S1_at	AT2G46500	phosphatidylinositol 3- and 4-kinase family protein / ubiquitin family protein	-1.17	1.16	1.61	2.37	phosphatidylinositol 3- and 4-kinase family protein / ubiquitin family protein [Arabidopsis thaliana]	Phospholipid signaling
Les.3262.3.S1_at	AT2G46500	phosphatidylinositol 3- and 4-kinase family protein / ubiquitin family protein	-1.10	-1.01	1.67	2.20	phosphatidylinositol 3- and 4-kinase family protein / ubiquitin family protein [Arabidopsis thaliana]	
Les.3493.1.S1_at	AT2G42010	PLDBETA1 (PHOSPHOLIPASE D BETA 1); phospholipase D	2.00	2.12	7.28	20.66	phospholipase PLDb1 [Lycopersicon esculentum]	

LesAffx.36712.1.S1_at	AT4G23810	WRKY53; DNA binding / protein binding / transcription activator / transcription factor	1.61	1.40	16.03	19.42	WRKY transcription factor-30 [Capsicum annuum]	WRKY-TFs
LesAffx.51257.1.S1_at	AT5G64810	WRKY51; transcription factor	2.40	3.34	16.84	27.34	putative WRKY transcription factor [Nicotiana tabacum]	
LesAffx.735.1.S1_at	AT2G38470	WRKY33; transcription factor	-1.17	1.92	34.99	53.09	WRKY-like transcription factor [Solanum peruvianum]	
Les.3964.1.S1_at	AT4G31550	WRKY11; calmodulin binding / transcription factor	2.50	1.61	7.88	13.74	PREDICTED: similar to DNA-binding protein [Vitis vinifera]	
LesAffx.33402.1.A1_at	AT1G02170	AMC1 (METACASPASE 1); cysteine-type endopeptidase	1.30	1.47	5.59	6.98	caspase, putative [Ricinus communis]	Protein degradation and programmed cell death
LesAffx.63935.1.S1_at	AT1G24140	matrixin family protein	1.46	1.75	37.08	49.68	matrix metalloprotease 1 [Nicotiana tabacum]	
Les.5240.1.S1_at	AT2G05920	subtilase family protein	1.49	1.57	2.73	5.05	subtilisin-like protease [Solanum lycopersicum]	
LesAffx.57572.1.S1_at	AT4G37060	PLP5 (PATATIN-LIKE PROTEIN 5); nutrient reservoir	2.76	1.37	15.52	33.85	patatin-like protein 3 [Nicotiana tabacum]	
Les.5884.1.S1_at	AT1G17860	trypsin and protease inhibitor family protein / Kunitz family protein	1.61	2.29	5.51	11.45	miraculin-like protein [Solanum brevifolius]	
LesAffx.44417.1.S1_at	AT3G25070	RIN4 (RPM1 INTERACTING PROTEIN 4); protein binding	1.26	1.52	3.70	6.71	RPM1-interacting protein 4 [Arabidopsis thaliana]	
Les.5077.1.S1_at	AT1G28380	NSL1 (necrotic spotted lesions 1)	1.35	1.56	2.01	4.70	NSL1 (necrotic spotted lesions 1) [Arabidopsis thaliana]	
Les.335.1.S1_at	AT5G47910	RBOHD (RESPIRATORY BURST OXIDASE HOMOLOGUE D); NAD(P)H oxidase	1.24	1.50	4.91	5.97	whitefly-induced gp91-phox [Lycopersicon esculentum]	
LesAffx.20391.1.S1_at	AT1G23390	kelch repeat-containing F-box family protein	1.37	1.60	14.34	33.73	F-box/kelch protein [Vitis vinifera]	
LesAffx.30842.1.S1_at	AT2G27310	F-box family protein	-1.19	1.67	12.27	18.53	F-box family protein [Arabidopsis thaliana]	
LesAffx.30842.1.A1_at	AT2G27310	F-box family protein	-1.34	1.05	5.93	6.84	F-box family protein [Arabidopsis thaliana]	
LesAffx.71026.2.S1_at	AT5G62460	zinc finger (C3HC4-type RING finger) family protein	1.48	1.26	3.00	6.37	membrane associated ring finger 1.8, putative [Ricinus communis]	
LesAffx.71026.1.S1_at	AT3G47550	zinc finger (C3HC4-type RING finger) family protein	1.00	1.22	3.20	5.16	zinc finger (C3HC4-type RING finger) family protein [Arabidopsis thaliana]	
Les.4671.1.S1_at	AT4G34040	zinc finger (C3HC4-type RING finger) family protein	-1.11	1.21	1.89	2.44	protein binding protein, putative [Ricinus communis]	
Les.4712.1.S1_at	AT1G49850	zinc finger (C3HC4-type RING finger) family protein	-1.30	1.73	6.87	8.70	RING-H2 finger protein [Glycine max]	
Les.5293.1.S1_at	AT2G26640	RGS11 (3-KETOACYL-COA SYNTHASE 11); acyltransferase / catalytic / transferase, transferring acyl groups other than amino-acyl groups	1.11	1.28	5.55	8.14	beta-ketoacyl-CoA synthase [Helianthus annuus]	

Les.62.1.S1_at	AT4G35670	glycoside hydrolase family 28 protein / polygalacturonase (pectinase) family protein	1.55	2.35	5.94	14.67	polygalacturonase [Lycopersicon esculentum]	Hydrolases
Les.3460.1.S1_at	AT3G52600	AtcwINV2 (Arabidopsis thaliana cell wall invertase 2); hydrolase, hydrolyzing O-glycosyl compounds	2.41	2.45	4.18	13.25	acid invertase [Solanum lycopersicum]	
LesAffx.10955.2.S1_at	AT1G08250	ADT6 (arogenate dehydratase 6); arogenate dehydratase/ prephenate dehydratase	1.88	1.65	17.40	41.82	putative arogenate dehydratase [Capsicum annuum]	Aromatic amino acid biosynthesis and transport
LesAffx.10955.1.S1_at	AT3G44720	ADT4 (arogenate dehydratase 4); arogenate dehydratase/ prephenate dehydratase	1.74	1.79	21.72	67.92	putative arogenate dehydratase [Capsicum annuum]	
Les.5555.1.S1_at	AT1G15710	prephenate dehydrogenase family protein	-1.18	1.29	3.32	5.06	prephenate dehydrogenase, putative [Ricinus communis]	
LesAffx.10955.3.S1_at	AT2G27820	PD1 (PREPHENATE DEHYDRATASE 1); arogenate dehydratase/ prephenate dehydratase	1.32	1.71	14.91	35.09	putative arogenate dehydratase [Capsicum annuum]	
Les.5279.1.S1_at	AT1G47670	amino acid transporter family protein	1.14	1.30	6.40	9.52	amino acid transporter; putative [Ricinus communis]	
LesAffx.71577.1.S1_a_at	AT2G19740	60S ribosomal protein L31 (RPL31A)	1.61	1.73	7.16	10.42	RecName: Full=60S ribosomal protein L31	HCAAs biosynthesis
Les.4822.1.S1_at	AT2G39890	PROT1 (PROLINE TRANSPORTER 1); L-proline transmembrane transporter/ amino acid transmembrane transporter	1.20	1.92	2.81	5.88	proline transporter 1 [Lycopersicon esculentum]	
Les.3686.1.S1_at	AT2G39030	GCN5-related N-acetyltransferase (GNAT) family protein	1.96	1.91	4.56	8.05	N-hydroxycinnamoyl-CoA:tyramine N-hydroxycinnamoyl transferase THT7-8 [Lycopersicon esculentum]	
Les.4038.1.S1_at	AT2G39030	GCN5-related N-acetyltransferase (GNAT) family protein	1.22	1.88	8.28	26.38	N-hydroxycinnamoyl-CoA:tyramine N-hydroxycinnamoyl transferase THT1-3 [Lycopersicon esculentum]	
LesAffx.62617.1.S1_at	AT5G42830	transferase family protein	1.57	1.71	26.90	72.99	Anthranilate N-benzoyltransferase protein, putative [Ricinus communis]	
LesAffx.5435.1.S1_at	AT2G46960	CYP709B1: electron carrier/ heme binding / iron ion binding / monooxygenase/ oxygen binding	1.69	1.67	3.52	6.81	cytochrome P450 [Populus trichocarpa]	HCAAs biosynthesis
Les.5485.1.S1_at	AT2G23810	TET8 (TETRASPANIN8)	-1.09	1.02	2.46	2.91	TET8 (TETRASPANIN8) [Arabidopsis thaliana]	
Les.4429.1.S1_at	AT5G47710	C2 domain-containing protein	1.24	2.08	3.04	5.87	C2 [Medicago truncatula]	
LesAffx.50259.1.S1_at	AT1G78700	brassinosteroid signalling positive regulator-related	1.13	1.07	1.76	2.76	BRASSINAZOLE-RESISTANT 2 protein, putative [Ricinus communis]	
LesAffx.3081.1.S1_at	AT5G35735	auxin-responsive family protein	1.11	1.12	3.32	5.17	putative membrane protein [Solanum tuberosum]	

Les.3574.1.S1_at	AT4G11140	CRF1 (CYTOKININ RESPONSE FACTOR 1); DNA binding / transcription factor	1.12	1.80	3.89	5.94	RecName: Full=Pathogenesis-related genes transcriptional activator PTI6; AltName: Full=PTO-interacting protein 6
Les.3575.1.S1_at	AT3G23240	ERF1 (ETHYLENE RESPONSE FACTOR 1); DNA binding / transcription activator / transcription factor	3.52	2.79	13.32	30.70	RecName: Full=Pathogenesis-related genes transcriptional activator PTI5; AltName: Full=PTO-interacting protein 5
Les.4102.1.S1_at	AT3G16770	ATEBP (ETHYLENE-RESPONSIVE ELEMENT BINDING PROTEIN); DNA binding / protein binding / transcription activator / transcription factor	-1.12	1.42	1.80	4.43	ethylene-binding protein [Lycopersicon esculentum]
LesAffx.37916.1.S1_at	AT1G09155	AtPP2-B15 (Phloem protein 2-B15); carbohydrate binding	1.12	3.31	12.73	37.69	phloem-specific lectin PP2-like protein [Arabidopsis thaliana]
Les.3486.1.S1_at	AT5G59790	unknown protein	1.85	1.69	6.11	11.67	auxin-regulated protein [Lycopersicon esculentum]
LesAffx.344.3.S1_at	AT3G54040	photoassimilate-responsive protein-related	1.61	1.33	5.79	9.21	NEIG-E80 [Nicotiana tabacum]
Les.3735.1.S1_at	AT2G29490	ATGSTU1 (GLUTATHIONE S-TRANSFERASE TAU 1); glutathione transferase	2.50	2.77	3.27	5.65	putative glutathione S-transferase T4 [Lycopersicon esculentum]
LesAffx.22100.1.S1_at	AT5G45710	RHA1 (ROOT HANDEDNESS 1); DNA binding / transcription factor	1.57	2.38	53.20	47.75	Heat shock factor protein, putative [Ricinus communis]
LesAffx.2889.4.S1_at	AT4G39390	NST-K1 (NUCLEOTIDE SUGAR TRANSPORTER-KT 1); nucleotide-sugar transmembrane transporter	-1.12	1.31	1.77	3.17	NST-K1 (NUCLEOTIDE SUGAR TRANSPORTER-KT 1); nucleotide-sugar transmembrane transporter [Arabidopsis thaliana]
LesAffx.67017.1.S1_at	AT5G25220	KNAT3 (KNOTTED1-LIKE HOMEBOX GENE 3); transcription activator / transcription factor	6.40	5.62	12.66	31.43	RecName: Full=Homeobox protein knotted-1-like LET12
Les.5530.1.S1_at	AT5G60800	heavy-metal-associated domain-containing protein	-1.25	2.09	17.22	43.78	metal ion binding protein, putative [Ricinus communis]
Les.5755.1.S1_at	AT5G61210	SNAP33 (SOLUBLE N-ETHYLMALIMIDE-SENSITIVE FACTOR ADAPTOR PROTEIN 33); SNAP receptor / protein binding	1.00	1.62	2.50	5.08	synaptosomal associated protein, putative [Ricinus communis]
Les.5090.1.S1_at	AT3G60450	INVOLVED IN: biological_process unknown; LOCATED IN: cellular component unknown; EXPRESSED IN: 24 plant structures; EXPRESSED DURING: 14 growth stages; CONTAINS InterPro DOMAIN/s: Phosphoglycerate mutase (InterPro:IPR013078), PRIIB5 (InterPro:IPR012398); B	1.39	1.71	2.76	4.83	pRIB5 protein [Arabidopsis thaliana]

LesAffx.68459.2.S1_at	AT3G28630	FUNCTIONS IN: molecular. function unknown; INVOLVED IN: biological_ process unknown; LOCATED IN: endomembrane system; EXPRESSED IN: leaf whorl, male gametophyte, flower, pollen tube; EXPRESSED DURING: L mature pollen stage, M germinated pollen stage, 4 anthe	1.16	1.30	16.69	40.95	unknown [Populus trichocarpa]
Les.5131.1.S1_at	AT5G42050	FUNCTIONS IN: molecular. function unknown; EXPRESSED IN: 22 plant structures; EXPRESSED DURING: 13 growth stages; CONTAINS InterPro DOMAIN/s: Development and cell death domain (InterPro:IPR013989), Kelch related (InterPro:IPR013089); BEST Arabidopsis thali	-1.04	1.37	3.65	6.04	n-rich protein, putative [Ricinus communis]
LesAffx.2934.1.S1_at	AT5G61630	unknown protein	1.09	1.44	3.19	6.63	PREDICTED: hypothetical protein [Vitis vinifera]
LesAffx.64990.1.S1_at	AT3G56180	unknown protein	1.36	2.13	3.59	5.36	conserved hypothetical protein [Ricinus communis]
LesAffx.56634.1.S1_at	AT1G76600	unknown protein	1.39	1.77	5.68	17.88	unnamed protein product [Nicotiana tabacum]
LesAffx.71544.1.S1_at	AT5G11000	unknown protein	1.77	1.77	55.95	58.61	unnamed protein product [Vitis vinifera]
Les.113.1.S1_at	no hit found	no hit found	1.71	4.33	26.08	106.79	no hits found
Les.3262.1A1_at	no hit found	no hit found	-1.02	1.09	1.60	2.22	no hits found
Les.1806.2A1_at	no hit found	no hit found	1.18	1.38	2.14	2.84	no hits found
Les.3334.1.S1_at	no hit found	no hit found	1.01	1.25	1.94	2.67	no hits found
Les.4429.2A1_at	no hit found	no hit found	1.30	2.24	3.17	8.38	no hits found
Les.1826.1A1_at	no hit found	no hit found	-1.23	2.16	12.42	33.00	no hits found
Les.1296.1A1_at	no hit found	no hit found	1.64	2.60	7.42	10.11	no hits found

Cluster 1 GO:Tomato Functional Genomics Database (http://ted.bti.cornell.edu/cgi-bin/TFGD/array/GO_analysis.cgi)

Gene Ontology term	Cluster frequency	Genome frequency of use	Raw P-value	Corrected P-value
protein amino acid phosphorylation	13 out of 90 genes, 14.4%	282 out of 10209 genes, 2.8%	0.00000101	0
hormone-mediated signaling	12 out of 90 genes, 13.3%	238 out of 10209 genes, 2.3%	0.00000107	0
detection of hormone stimulus	4 out of 90 genes, 4.4%	12 out of 10209 genes, 0.1%	0.00000264	0
detection of endogenous stimulus	4 out of 90 genes, 4.4%	12 out of 10209 genes, 0.1%	0.00000264	0
detection of chemical stimulus	4 out of 90 genes, 4.4%	15 out of 10209 genes, 0.1%	0.00000715	0
response to bacterium	9 out of 90 genes, 10.0%	156 out of 10209 genes, 1.5%	0.00000885	0
aromatic amino acid family biosynthetic process, prephenate pathway	4 out of 90 genes, 4.4%	17 out of 10209 genes, 0.2%	0.0000123	0
response to other organism	11 out of 90 genes, 12.2%	270 out of 10209 genes, 2.6%	0.0000235	0
phosphorylation	13 out of 90 genes, 14.4%	382 out of 10209 genes, 3.7%	0.0000276	0
regulation of cellular process	25 out of 90 genes, 27.8%	1216 out of 10209 genes, 11.9%	0.0000328	0
detection of brassinosteroid stimulus	3 out of 90 genes, 3.3%	8 out of 10209 genes, 0.1%	0.0000359	0
defense response	12 out of 90 genes, 13.3%	342 out of 10209 genes, 3.3%	0.0000429	0
signal transduction	15 out of 90 genes, 16.7%	523 out of 10209 genes, 5.1%	0.0000466	0
positive regulation of kinase activity	3 out of 90 genes, 3.3%	9 out of 10209 genes, 0.1%	0.0000535	0
positive regulation of protein kinase activity	3 out of 90 genes, 3.3%	9 out of 10209 genes, 0.1%	0.0000535	0
brassinosteroid mediated signaling	4 out of 90 genes, 4.4%	26 out of 10209 genes, 0.3%	0.0000727	0
steroid hormone mediated signaling	4 out of 90 genes, 4.4%	26 out of 10209 genes, 0.3%	0.0000727	0
positive regulation of transferase activity	3 out of 90 genes, 3.3%	10 out of 10209 genes, 0.1%	0.000076	0.00444
response to hormone stimulus	13 out of 90 genes, 14.4%	425 out of 10209 genes, 4.2%	0.0000829	0.00526
regulation of biological process	25 out of 90 genes, 27.8%	1288 out of 10209 genes, 12.6%	0.0000859	0.005
response to biotic stimulus	11 out of 90 genes, 12.2%	312 out of 10209 genes, 3.1%	0.000088	0.00476

phosphate metabolic process	13 out of 90 genes, 14.4%	434 out of 10209 genes, 4.3%	0.0001	0.00455
intracellular signaling cascade	13 out of 90 genes, 14.4%	434 out of 10209 genes, 4.3%	0.0001	0.00435
phosphorus metabolic process	13 out of 90 genes, 14.4%	435 out of 10209 genes, 4.3%	0.0001	0.00417
cell communication	15 out of 90 genes, 16.7%	562 out of 10209 genes, 5.5%	0.0001	0.004
post-translational protein modification	13 out of 90 genes, 14.4%	439 out of 10209 genes, 4.3%	0.00011	0.00385
detection of stimulus	5 out of 90 genes, 5.6%	56 out of 10209 genes, 0.5%	0.00012	0.0037
defense response to bacterium	7 out of 90 genes, 7.8%	128 out of 10209 genes, 1.3%	0.00013	0.00357
camalexin biosynthetic process	3 out of 90 genes, 3.3%	12 out of 10209 genes, 0.1%	0.00013	0.00345
camalexin metabolic process	3 out of 90 genes, 3.3%	12 out of 10209 genes, 0.1%	0.00013	0.00333
multi-organism process	11 out of 90 genes, 12.2%	333 out of 10209 genes, 3.3%	0.00015	0.00387
response to steroid hormone stimulus	4 out of 90 genes, 4.4%	32 out of 10209 genes, 0.3%	0.00016	0.00375
indole phytoalexin biosynthetic process	3 out of 90 genes, 3.3%	13 out of 10209 genes, 0.1%	0.00017	0.00364
indole metabolic process	3 out of 90 genes, 3.3%	13 out of 10209 genes, 0.1%	0.00017	0.00353
indole phytoalexin metabolic process	3 out of 90 genes, 3.3%	13 out of 10209 genes, 0.1%	0.00017	0.00343
phytoalexin metabolic process	3 out of 90 genes, 3.3%	13 out of 10209 genes, 0.1%	0.00017	0.00333
phytoalexin biosynthetic process	3 out of 90 genes, 3.3%	13 out of 10209 genes, 0.1%	0.00017	0.00324
biological regulation	26 out of 90 genes, 28.9%	1445 out of 10209 genes, 14.2%	0.0002	0.00316
response to endogenous stimulus	13 out of 90 genes, 14.4%	468 out of 10209 genes, 4.6%	0.00021	0.00308
L-phenylalanine biosynthetic process	3 out of 90 genes, 3.3%	14 out of 10209 genes, 0.1%	0.00022	0.003
brassinosteroid homeostasis	3 out of 90 genes, 3.3%	14 out of 10209 genes, 0.1%	0.00022	0.00293
MAPKKK cascade during osmolarity sensing	2 out of 90 genes, 2.2%	3 out of 10209 genes, 0.0%	0.00022	0.00286
activation of MAPK activity during osmolarity sensing	2 out of 90 genes, 2.2%	3 out of 10209 genes, 0.0%	0.00022	0.00279
osmosensory signaling pathway	2 out of 90 genes, 2.2%	3 out of 10209 genes, 0.0%	0.00022	0.00273
response to chitin	5 out of 90 genes, 5.6%	66 out of 10209 genes, 0.6%	0.00027	0.00267

regulation of kinase activity	3 out of 90 genes, 3.3%	15 out of 10209 genes, 0.1%	0.00027	0.00261
regulation of protein kinase activity	3 out of 90 genes, 3.3%	15 out of 10209 genes, 0.1%	0.00027	0.00255
response to brassinosteroid stimulus	4 out of 90 genes, 4.4%	37 out of 10209 genes, 0.4%	0.00029	0.0025
regulation of transferase activity	3 out of 90 genes, 3.3%	16 out of 10209 genes, 0.2%	0.00034	0.00245
response to chemical stimulus	18 out of 90 genes, 20.0%	849 out of 10209 genes, 8.3%	0.00037	0.0024
response to stimulus	27 out of 90 genes, 30.0%	1592 out of 10209 genes, 15.6%	0.0004	0.00275
protein modification process	13 out of 90 genes, 14.4%	499 out of 10209 genes, 4.9%	0.0004	0.00269
vascular transport	2 out of 90 genes, 2.2%	4 out of 10209 genes, 0.0%	0.00045	0.00377
phloem transport	2 out of 90 genes, 2.2%	4 out of 10209 genes, 0.0%	0.00045	0.0037
response to abiotic stimulus	15 out of 90 genes, 16.7%	649 out of 10209 genes, 6.4%	0.0005	0.00364
biopolymer modification	13 out of 90 genes, 14.4%	517 out of 10209 genes, 5.1%	0.00056	0.00357
detection of biotic stimulus	3 out of 90 genes, 3.3%	19 out of 10209 genes, 0.2%	0.00057	0.00351
detection of bacterium	3 out of 90 genes, 3.3%	19 out of 10209 genes, 0.2%	0.00057	0.00345
cellular aromatic compound metabolic process	8 out of 90 genes, 8.9%	218 out of 10209 genes, 2.1%	0.00065	0.00339
activation of MAPK activity	2 out of 90 genes, 2.2%	5 out of 10209 genes, 0.0%	0.00075	0.00567
leaf vascular tissue pattern formation	2 out of 90 genes, 2.2%	5 out of 10209 genes, 0.0%	0.00075	0.00557
positive regulation of MAP kinase activity	2 out of 90 genes, 2.2%	5 out of 10209 genes, 0.0%	0.00075	0.00548
L-phenylalanine metabolic process	3 out of 90 genes, 3.3%	21 out of 10209 genes, 0.2%	0.00078	0.00571
positive regulation of catalytic activity	3 out of 90 genes, 3.3%	22 out of 10209 genes, 0.2%	0.0009	0.00656
abscisic acid mediated signaling	4 out of 90 genes, 4.4%	51 out of 10209 genes, 0.5%	0.00102	0.00708
aromatic amino acid family biosynthetic process	4 out of 90 genes, 4.4%	52 out of 10209 genes, 0.5%	0.0011	0.00818
chorismate metabolic process	4 out of 90 genes, 4.4%	52 out of 10209 genes, 0.5%	0.0011	0.00806
indole derivative biosynthetic process	3 out of 90 genes, 3.3%	25 out of 10209 genes, 0.2%	0.00132	0.00882
positive regulation of flower development	3 out of 90 genes, 3.3%	26 out of 10209 genes, 0.3%	0.00148	0.00957

positive regulation of post-embryonic development	3 out of 90 genes, 3.3%	26 out of 10209 genes, 0.3%	0.00148	0.00943
positive regulation of developmental process	4 out of 90 genes, 4.4%	57 out of 10209 genes, 0.6%	0.00156	0.0107
jasmonic acid and ethylene-dependent systemic resistance, jasmonic acid mediated signaling pathway	2 out of 90 genes, 2.2%	7 out of 10209 genes, 0.1%	0.00156	0.01278
regulation of MAP kinase activity	2 out of 90 genes, 2.2%	7 out of 10209 genes, 0.1%	0.00156	0.0126
MAPKKK cascade	2 out of 90 genes, 2.2%	8 out of 10209 genes, 0.1%	0.00207	0.01595
aromatic amino acid family metabolic process	4 out of 90 genes, 4.4%	62 out of 10209 genes, 0.6%	0.00213	0.016
response to stress	19 out of 90 genes, 21.1%	1077 out of 10209 genes, 10.5%	0.00231	0.01658
indole and derivative metabolic process	3 out of 90 genes, 3.3%	31 out of 10209 genes, 0.3%	0.00249	0.0174
indole derivative metabolic process	3 out of 90 genes, 3.3%	31 out of 10209 genes, 0.3%	0.00249	0.01718
response to fungus	4 out of 90 genes, 4.4%	71 out of 10209 genes, 0.7%	0.00349	0.02759
response to UV	4 out of 90 genes, 4.4%	73 out of 10209 genes, 0.7%	0.00386	0.02875
regulation of transcription, DNA-dependent	11 out of 90 genes, 12.2%	504 out of 10209 genes, 4.9%	0.00462	0.03358
jasmonic acid mediated signaling pathway	3 out of 90 genes, 3.3%	39 out of 10209 genes, 0.4%	0.00481	0.0361
innate immune response	5 out of 90 genes, 5.6%	126 out of 10209 genes, 1.2%	0.00503	0.03614
response to external stimulus	7 out of 90 genes, 7.8%	240 out of 10209 genes, 2.4%	0.00518	0.03762
response to carbohydrate stimulus	5 out of 90 genes, 5.6%	127 out of 10209 genes, 1.2%	0.0052	0.03718
regulation of RNA metabolic process	11 out of 90 genes, 12.2%	514 out of 10209 genes, 5.0%	0.00535	0.03674
defense response, incompatible interaction	4 out of 90 genes, 4.4%	80 out of 10209 genes, 0.8%	0.00536	0.03655
developmental process	14 out of 90 genes, 15.6%	752 out of 10209 genes, 7.4%	0.00585	0.04295
response to osmotic stress	7 out of 90 genes, 7.8%	246 out of 10209 genes, 2.4%	0.00592	0.04247
cell surface receptor linked signal transduction	3 out of 90 genes, 3.3%	43 out of 10209 genes, 0.4%	0.00633	0.044
auxin mediated signaling pathway	4 out of 90 genes, 4.4%	85 out of 10209 genes, 0.8%	0.00664	0.04659
plant-type hypersensitive response	3 out of 90 genes, 3.3%	44 out of 10209 genes, 0.4%	0.00675	0.04674

host programmed cell death induced by symbiont	3 out of 90 genes, 3.3%	44 out of 10209 genes, 0.4%	0.00675	0.04624
regulation of catalytic activity	4 out of 90 genes, 4.4%	86 out of 10209 genes, 0.8%	0.00692	0.04638
immune response	5 out of 90 genes, 5.6%	136 out of 10209 genes, 1.3%	0.00693	0.04589
detection of external stimulus	3 out of 90 genes, 3.3%	45 out of 10209 genes, 0.4%	0.00719	0.04583
programmed cell death	4 out of 90 genes, 4.4%	87 out of 10209 genes, 0.9%	0.0072	0.04557
aromatic compound biosynthetic process	5 out of 90 genes, 5.6%	138 out of 10209 genes, 1.4%	0.00736	0.0451

Cluster 2 genes.

Probe set ID	ATH best hit	Bet hit description	FC 0hr	FC 1 hr	FC 3 hr	FC 5 hr	Gene bank best hit description
Les.5267.1.S1_at	AT5G18480	PGSIP6 (PLANT GLYCOGENIN-LIKE STARCH INITIATION PROTEIN 6); transferase, transferring glycosyl groups / transferase, transferring hexosyl groups	1.16	1.31	1.59	3.50	glycogenin, putative [Ricinus communis]
Les.4482.1.S1_at	AT4G13010	oxidoreductase, zinc-binding dehydrogenase family protein	1.40	1.66	2.56	5.97	ripening regulated protein-like [Solanum tuberosum]
Les.3712.1.S1_at	AT2G43120	pirin, putative	2.55	1.20	8.76	141.04	RecName: Full=Pirin-like protein
LesAffx.64831.1.S1_at	AT3G26020	serine/threonine protein phosphatase 2A (PP2A) regulatory subunit B', putative	1.41	1.35	1.92	3.80	protein phosphatase 2A regulatory subunit B' [Zea mays]
Les.176.1.S1_at	AT1G02130	ARA-5 (ARABIDOPSIS RAS 5); GTP binding	-1.09	1.27	1.91	3.62	small GTP-binding protein
LesAffx.62138.1.S1_at	AT5G49620	AtMYB78 (myb domain protein 78); DNA binding / transcription factor	1.12	1.15	2.66	18.23	Cpm5 [Craterostigma plantagineum]
LesAffx.64689.1.S1_at	AT3G59660	C2 domain-containing protein / GRAM domain-containing protein	1.42	1.72	2.35	10.91	PREDICTED: similar to C2 domain-containing protein / GRAM domain-containing protein [Vitis vinifera]
LesAffx.61402.2.S1_at	AT2G19570	CDA1 (CYTIDINE DEAMINASE 1); cytidine deaminase	-1.03	-1.08	2.81	8.71	cytidine deaminase 1, 2, 7, putative [Ricinus communis]

LesAffx.54536.1.S1_at	AT2G29720	CTF2B; monooxygenase/oxidoreductase	1.46	1.05	2.99	12.05	CTF2B [Arabidopsis thaliana]
LesAffx.38821.1.S1_at	AT4G37310	CYP81H1; electron carrier/heme binding / iron ion binding / monooxygenase / oxygenbinding	1.92	1.48	7.94	32.57	cytochrome P450, putative [Ricinus communis]
LesAffx.23884.1.S1_at	AT2G37820	DC1 domain-containing protein	1.38	1.34	11.20	39.29	DC1 domain-containing protein [Arabidopsis thaliana]
LesAffx.3059.1.S1_at	AT3G23220	DNA binding / transcription factor	-1.04	1.26	17.05	56.27	Ethylene-responsive transcription factor, putative [Ricinus communis]
Les.3818.1.S1_at	AT3G23240	ERF1 (ETHYLENE RESPONSE FACTOR 1); DNA binding / transcription activator / transcription factor	1.08	1.02	3.80	19.91	ethylene responsive element binding protein [Lycopersicon esculentum]
Les.3662.1.S1_at	AT1G01480	ACS2; 1-aminocyclopropane-1-carboxylate synthase	4.65	1.62	25.75	100.57	RecName: Full=1-aminocyclopropane-1-carboxylate synthase 2; Short=ACC synthase 2; AltName: Full=Le-ACS2; Short=ACS-2; AltName: Full=S-adenosyl-L-methionine methylthioadenosine-lyase 2
Les.4623.1.S1_at	AT2G02370	FUNCTIONS IN: molecular_function unknown; INVOLVED IN: biological_process unknown;LOCATED IN: cellular_component unknown; EXPRESSED IN: 22 plant structures; EXPRESSED DURING: 13 growth stages; CONTAINS InterPro DOMAIN/s: SNARE associated Golgi protein (In	1.04	1.29	1.64	3.17	PREDICTED: hypothetical protein [Vitis vinifera]
Les.2668.1.S1_at	AT1G59500	GH3.4; indole-3-acetic acid amido synthetase	1.49	-1.00	8.55	10.76	auxin and ethylene responsive GH3-like protein [Capsicum chinense]
Les.966.1.S1_at	AT1G09560	GLP5 (GERMIN-LIKE PROTEIN 5); manganese ion binding / nutrient reservoir	1.25	1.38	2.20	5.51	germin-like protein [Solanum tuberosum]

Les.5092.1.S1_at	AT3G06350	MEE32 (MATERNAL EFFECT EMBRYO ARREST 32); 3-dehydroquinase dehydratase/ NADP or NADPH binding / catalytic/ shikimate 5-dehydrogenase	1.10	-1.19	4.83	15.40	3-dehydroquinase dehydratase / shikimate dehydrogenase isoform 2 [Nicotiana tabacum]
LesAffx.42561.1.S1_at	AT5G15460	MUB2 (MEMBRANE-ANCHORED UBIQUITIN-FOLD PROTEIN 2)	1.22	1.93	2.48	4.95	MUB2 (MEMBRANE-ANCHORED UBIQUITIN-FOLD PROTEIN 2) [Arabidopsis thaliana]
LesAffx.12670.1.S1_at	AT2G38060	PHT4;2 (PHOSPHATE TRANSPORTER 4;2); carbohydrate transmembrane transporter/ inorganic phosphate transmembrane transporter/ organic anion transmembrane transporter/ sugar:hydrogen symporter	1.09	1.32	12.30	18.43	Sialin, putative [Ricinus communis]
LesAffx.12670.3.S1_at	AT2G38060	PHT4;2 (PHOSPHATE TRANSPORTER 4;2); carbohydrate transmembrane transporter/ inorganic phosphate transmembrane transporter/ organic anion transmembrane transporter/ sugar:hydrogen symporter	1.06	-1.23	37.48	81.25	Sialin, putative [Ricinus communis]
Les.3493.1.S1_at	AT2G42010	PLDBETA1 (PHOSPHOLIPASE D BETA 1); phospholipase D	2.00	2.12	7.28	20.66	phospholipase PLDb1 [Lycopersicon esculentum]
LesAffx.3554.1.A1_at	AT4G37050	PLP4 (PATATIN-LIKE PROTEIN 4); nutrient reservoir	1.24	1.55	4.95	34.60	patatin-like protein 3 [Nicotiana tabacum]
LesAffx.15898.2.S1_at	AT1G05680	UDP-glucuronosyl/UDP-glucosyl transferase family protein	1.16	-1.06	3.09	3.39	UDP-xylose phenolic glycosyltransferase [Solanum lycopersicum]
LesAffx.61149.1.S1_at	AT5G49690	UDP-glucuronosyl/UDP-glucosyl transferase family protein	1.08	1.25	2.52	5.41	UDP-glucuronosyl/UDP-glucosyl transferase family protein [Arabidopsis thaliana]
Les.5481.1.S1_at	AT4G14420	lesion inducing protein-related	1.22	1.38	1.34	2.90	ORF; able to induce HR-like lesions [Nicotiana tabacum]

LesAffx.56130.1.S1_at	AT1G25390	protein kinase family protein	2.02	-1.02	6.80	20.48	wall-associated kinase, putative [Ricinus communis]
Les.3418.1.S1_at	AT3G01980	short-chain dehydrogenase/reductase (SDR) family protein	1.21	1.50	2.24	4.89	short-chain alcohol dehydrogenase [Panax ginseng]
Les.4885.1.S1_at	AT2G39980	transferase family protein	2.37	1.02	16.53	148.30	AER [Nicotiana tabacum]
LesAffx.43640.1.S1_at	AT4G18530	unknown protein	1.48	1.11	1.22	4.50	conserved hypothetical protein [Ricinus communis]
LesAffx.15850.1.S1_a_at	AT1G67060	unknown protein	1.31	-1.43	4.21	11.11	unknown protein [Arabidopsis thaliana]
LesAffx.65135.1.S1_at	AT1G28700	unknown protein	1.58	1.59	7.60	47.70	pentatricopeptide repeat-containing protein, putative [Ricinus communis]
Les.3418.2.S1_a_at	no hits found	unknown protein	1.41	1.43	2.52	5.23	no hits found
Les.2746.2.A1_at	no hits found	unknown protein	1.54	2.36	5.59	67.42	no hits found

Cluster 2 GO:AtCOSCIS (<http://bioinformatics.psb.ugent.be/ATCOSCIS/>)

GO enrichment	Enrichment fold	p-value	Description
GO:0009873	34.51 (2)	1.54E-03	Ethylene mediated signaling pathway
GO:0045735	27.30 (2)	2.45E-03	Nutrient reservoir activity
GO:0000160	25.40 (2)	2.82E-03	Two-component signal transduction system (phosphorelay)
GO:0009723	13.85 (2)	9.15E-03	Response to ethylene stimulus
GO:0009755	9.28 (2)	1.96E-02	Hormone-mediated signaling
GO:0042829	8.09 (2)	2.53E-02	Defense response to pathogen
GO:0009814	8.09 (2)	2.53E-02	Defense response to pathogen, incompatible interaction
GO:0042828	8.09 (2)	2.53E-02	Response to pathogen
GO:0016758	7.65 (2)	2.80E-02	Transferase activity, transferring hexosyl groups
GO:0009613	7.09 (2)	3.22E-02	Response to pest, pathogen or parasite

GO:0016757	6.22 (3)	1.21E-02	Transferase activity, transferring glycosyl groups				
GO:0009725	5.92 (4)	4.39E-03	Response to hormone stimulus				
GO:0009719	4.21 (4)	1.42E-02	Response to endogenous stimulus				
GO:0051707	4.01 (2)	8.84E-02	Response to other organism				
GO:0007242	3.95 (2)	9.07E-02	Intracellular signaling cascade				
GO:0006950	3.44 (4)	2.75E-02	Response to stress				
GO:0042221	3.27 (4)	3.26E-02	Response to chemical stimulus				
GO:0007165	3.25 (3)	6.35E-02	Signal transduction				
GO:0007154	2.99 (3)	7.77E-02	Cell communication				
GO:0006118	2.97 (2)	1.45E-01	Electron transport				
GO:0006355	2.95 (3)	8.03E-02	Regulation of transcription, DNA-dependent				
Cluster 3 genes.							
Probe set ID	ATH best hit	Bet hit description	FC 0hr	FC 1hr	FC 3hr	FC 5 hr	Gene bank best hit description
Les.3039.1.S1_at	AT1G22410	2-dehydro-3-deoxyphosphoheptonate aldolase, putative / 3-deoxy-D-arabino-heptulosonate 7-phosphate synthase, putative / DAHP synthetase, putative	1.38	1.46	2.09	3.70	RecName: Full=Phospho-2-dehydro-3-deoxyheptonate aldolase 2, chloroplastic; AltName: Full=Phospho-2-keto-3-deoxyheptonate aldolase 2; AltName: Full=3-deoxy-D-arabino-heptulosonate 7-phosphate synthase 2; AltName: Full=DAHP synthetase 2; Flags: Precursor
LesAffx.62420.1.S1_at	AT2G15480	UGT73B5 (UDP-glucosyl transferase 73B5); UDP-glucosyltransferase/ UDP-glucosyltransferase/ quercetin 3-O-glucosyltransferase/ transferase, transferring glycosyl groups	4.32	1.84	6.96	16.48	UDP-glucose:glucosyltransferase [Lycium barbarum]
LesAffx.11941.1.S1_at	AT3G49340	cysteine proteinase, putative	1.66	1.84	1.75	2.34	phytophthora-inhibited protease 1 [Solanum lycopersicum]

Les.3672.1.S1_at	AT2G45300	3-phosphoshikimate 1-carboxyvinyltransferase / 5-enolpyruvylshikimate-3-phosphate / EPSP synthase	-1.17	1.29	1.21	2.24	RecName: Full=3-phosphoshikimate 1-carboxyvinyltransferase, chloroplastic; AltName: Full=5-enolpyruvylshikimate-3-phosphate synthase; Short=EPSP synthase; Flags: Precursor
Les.2817.1.S1_at	AT1G10670	ACLA-1; ATP citrate synthase	1.32	1.30	1.92	2.87	ATP-citrate synthase, putative [Ricinus communis]
Les.37.1.S1_at	AT3G12500	ATHCHIB (ARABIDOPSIS THALIANA BASIC CHITINASE); chitinase	7.23	5.47	6.60	6.79	RecName: Full=Basic endochitinase
LesAffx.18587.1.S1_at	AT5G16080	AtCXE17 (Arabidopsis thaliana carboxylesterase 17); hydrolase	1.81	1.70	2.52	2.59	hsr2031 [Solanum tuberosum]
LesAffx.19956.1.S1_at	AT3G29200	CM1 (CHORISMATE MUTASE 1); L-ascorbate peroxidase / chorismate mutase	-1.23	1.22	1.34	2.70	putative chorismate mutase 1 [Capsicum annuum]
LesAffx.44563.1.A1_at	AT1G69370	CM3 (chorismate mutase 3); chorismate mutase	-1.14	1.43	1.46	2.72	putative chorismate mutase 1 [Capsicum annuum]
LesAffx.9038.3.S1_at	AT4G37400	CYP81F3; electron carrier / heme binding / iron ion binding / monooxygenase / oxygenbinding	2.07	1.78	2.65	5.08	CYP81B2v2 [Nicotiana tabacum]
Les.209.1.S1_at	AT1G48850	EMB1144 (embryo defective 1144); chorismate synthase	-1.10	1.18	1.18	2.08	RecName: Full=Chorismate synthase 1, chloroplastic; AltName: Full=5-enolpyruvylshikimate-3-phosphate phosphohyase 1; Flags: Precursor
Les.3774.1.S1_at	AT5G26340	MSS1; carbohydrate transmembrane transporter / hexose:hydrogen symporter / high-affinity hydrogen:glucose symporter / sugar:hydrogen symporter	3.66	2.72	2.80	2.89	hexose transporter [Solanum lycopersicum]
LesAffx.62349.1.S1_at	AT3G27890	NQR (NADPH:QUINONE OXIDOREDUCTASE); FMN reductase	2.24	2.16	2.01	3.49	RecName: Full=NAD(P)H:quinone oxidoreductase; Short=NAD(P)H:QR
Les.2747.1.S1_at	AT5G48880	PKT2 (PEROXISOMAL 3-KETO-ACYL-COA THIOLASE 2); acetyl-CoA C-acyltransferase / catalytic	1.40	1.77	2.65	2.70	PKT2 (PEROXISOMAL 3-KETO-ACYL-COA THIOLASE 2); acetyl-CoA C-acyltransferase / catalytic [Arabidopsis thaliana]

Les.2747.2.S1_at	AT2G33150	PKT3 (PEROXISOMAL 3-KETOACYL-COA THIOLASE 3); acetyl-CoA C-acyltransferase	1.46	1.68	3.04	2.96	3-ketoacyl CoA thiolase 1 [Petunia x hybrida]
Les.3140.3.S1_at	AT2G33150	PKT3 (PEROXISOMAL 3-KETOACYL-COA THIOLASE 3); acetyl-CoA C-acyltransferase	1.65	1.68	3.10	2.89	3-ketoacyl CoA thiolase 1 [Petunia x hybrida]
Les.3140.2.S1_at	AT2G33150	PKT3 (PEROXISOMAL 3-KETOACYL-COA THIOLASE 3); acetyl-CoA C-acyltransferase	1.42	1.72	3.10	2.80	3-ketoacyl CoA thiolase 1 [Petunia x hybrida]
LesAffx.71598.1.S1_at	AT1G75170	SEC14 cytosolic factor family protein / phosphoglyceride transfer family protein	1.40	1.88	1.97	2.15	transporter-like protein [Solanum tuberosum]
Les.4880.1.S1_at	AT5G07990	TT7 (TRANSPARENT TESTA 7); flavonoid 3'-monooxygenase/oxygen binding	2.75	2.31	4.03	4.62	elicitor-inducible cytochrome P450 [Nicotiana tabacum]
LesAffx.9043.1.S1_at	AT2G47650	UXS4 (UDP-XYLOSE SYNTHASE 4); UDP-glucuronate decarboxylase/catalytic	1.28	1.11	1.87	2.52	putative UDP-glucuronate decarboxylase 3 [Nicotiana tabacum]
LesAffx.10235.1.S1_at	AT1G66120	acyl-activating enzyme 11 (AAE11)	1.42	3.70	3.91	3.12	acyl:coa ligase acetate-coa synthetase-like protein [Populus trichocarpa]
LesAffx.16769.1.S1_at	AT1G65870	disease resistance-responsive family protein	4.75	2.79	3.21	3.27	dirigent-like protein pDIR10 [Picea glauca]
LesAffx.51292.1.S1_at	AT5G35200	epsin N-terminal homology (ENTH) domain-containing protein	-1.10	1.25	1.53	2.55	ANTH [Medicago truncatula]
LesAffx.6163.2.S1_at	AT5G52810	ornithine cyclodeaminase/mu-crystallin family protein	1.25	1.52	2.12	2.31	ornithine cyclodeaminase, putative [Ricinus communis]
Les.3635.1.S1_at	AT2G05920	subtilase family protein	1.81	1.95	2.04	2.22	subtilisin-like protease [Solanum lycopersicum]
Les.2529.2.S1_at	AT5G17540	transferase family protein	1.47	1.52	3.09	3.31	benzoyl coenzyme A: benzyl alcohol benzoyl transferase [Petunia x hybrida]
LesAffx.60643.2.S1_at	AT1G67850	unknown protein	1.65	1.47	1.27	2.51	putative lysine ketoglutarate reductase trans-splicing related 1 [Oryza sativa Japonica Group]
LesAffx.60643.1.S1_at	AT1G08040	unknown protein	1.37	1.44	1.30	2.35	lysine ketoglutarate reductase trans-splicing related 1 [Zea mays]
Les.2587.1A1_at			1.34	2.22	1.88	3.73	no hits found
Les.1590.1A1_at			1.13	1.33	1.50	2.07	no hits found
Les.2529.1A1_at			1.41	1.65	2.51	2.58	HRS201-like protein [Solanum melongena]

Cluster 3 GO:

Tomato Functional Genomics Database (http://ted.bti.cornell.edu/cgi-bin/TFGD/array/GO_analysis.cgi)

Gene Ontology term	Cluster frequency	Genome frequency of use	Raw P-value	Corrected P-value
glyoxysome organization	4 out of 31 genes, 12.9%	6 out of 10209 genes, 0.1%	1.03E-09	0
jasmonic acid biosynthetic process	4 out of 31 genes, 12.9%	17 out of 10209 genes, 0.2%	1.61E-07	0
aromatic amino acid family biosynthetic process	5 out of 31 genes, 16.1%	52 out of 10209 genes, 0.5%	4.32E-07	0
chorismate metabolic process	5 out of 31 genes, 16.1%	52 out of 10209 genes, 0.5%	4.32E-07	0
jasmonic acid metabolic process	4 out of 31 genes, 12.9%	22 out of 10209 genes, 0.2%	4.89E-07	0
fatty acid beta-oxidation	4 out of 31 genes, 12.9%	23 out of 10209 genes, 0.2%	5.91E-07	0
oxylipin biosynthetic process	4 out of 31 genes, 12.9%	23 out of 10209 genes, 0.2%	5.91E-07	0
fatty acid oxidation	4 out of 31 genes, 12.9%	26 out of 10209 genes, 0.3%	9.92E-07	0
lipid oxidation	4 out of 31 genes, 12.9%	26 out of 10209 genes, 0.3%	9.92E-07	0
aromatic amino acid family metabolic process	5 out of 31 genes, 16.1%	62 out of 10209 genes, 0.6%	1.05E-06	0
fatty acid catabolic process	4 out of 31 genes, 12.9%	27 out of 10209 genes, 0.3%	1.16E-06	0
oxylipin metabolic process	4 out of 31 genes, 12.9%	28 out of 10209 genes, 0.3%	1.35E-06	0
jasmonic acid and ethylene-dependent systemic resistance	4 out of 31 genes, 12.9%	30 out of 10209 genes, 0.3%	1.80E-06	0
organic acid catabolic process	4 out of 31 genes, 12.9%	30 out of 10209 genes, 0.3%	1.80E-06	0
carboxylic acid catabolic process	4 out of 31 genes, 12.9%	30 out of 10209 genes, 0.3%	1.80E-06	0
cellular lipid catabolic process	4 out of 31 genes, 12.9%	32 out of 10209 genes, 0.3%	2.35E-06	0
lipid modification	4 out of 31 genes, 12.9%	34 out of 10209 genes, 0.3%	3.02E-06	0
aromatic compound biosynthetic process	6 out of 31 genes, 19.4%	138 out of 10209 genes, 1.4%	3.05E-06	0
plastid organization	4 out of 31 genes, 12.9%	42 out of 10209 genes, 0.4%	7.18E-06	0
dicarboxylic acid metabolic process	5 out of 31 genes, 16.1%	98 out of 10209 genes, 1.0%	1.02E-05	0
carboxylic acid metabolic process	9 out of 31 genes, 29.0%	548 out of 10209 genes, 5.4%	2.41E-05	0
organic acid metabolic process	9 out of 31 genes, 29.0%	550 out of 10209 genes, 5.4%	2.48E-05	0
cellular aromatic compound metabolic process	6 out of 31 genes, 19.4%	218 out of 10209 genes, 2.1%	4.16E-05	0
organic acid biosynthetic process	5 out of 31 genes, 16.1%	144 out of 10209 genes, 1.4%	6.58E-05	0.00083
carboxylic acid biosynthetic process	5 out of 31 genes, 16.1%	144 out of 10209 genes, 1.4%	6.58E-05	0.0008
lipid catabolic process	4 out of 31 genes, 12.9%	78 out of 10209 genes, 0.8%	8.48E-05	0.00077
defense response, incompatible interaction	4 out of 31 genes, 12.9%	80 out of 10209 genes, 0.8%	9.36E-05	0.00074
amino acid biosynthetic process	5 out of 31 genes, 16.1%	159 out of 10209 genes, 1.6%	0.0001	0.00071
fatty acid biosynthetic process	4 out of 31 genes, 12.9%	98 out of 10209 genes, 1.0%	0.0002	0.00138

amine biosynthetic process	5 out of 31 genes, 16.1%	191 out of 10209 genes, 1.9%	0.00024	0.00133
nitrogen compound biosynthetic process	5 out of 31 genes, 16.1%	197 out of 10209 genes, 1.9%	0.00028	0.00129
defense response	6 out of 31 genes, 19.4%	342 out of 10209 genes, 3.3%	0.00048	0.00313
response to wounding	4 out of 31 genes, 12.9%	126 out of 10209 genes, 1.2%	0.00053	0.00364
innate immune response	4 out of 31 genes, 12.9%	126 out of 10209 genes, 1.2%	0.00053	0.00353
fatty acid metabolic process	4 out of 31 genes, 12.9%	136 out of 10209 genes, 1.3%	0.00071	0.00514
immune response	4 out of 31 genes, 12.9%	136 out of 10209 genes, 1.3%	0.00071	0.005
immune system process	4 out of 31 genes, 12.9%	152 out of 10209 genes, 1.5%	0.00108	0.00649
cellular amino acid and derivative metabolic process	6 out of 31 genes, 19.4%	403 out of 10209 genes, 3.9%	0.00115	0.00632
response to other organism	5 out of 31 genes, 16.1%	270 out of 10209 genes, 2.6%	0.0012	0.00615
organelle organization	5 out of 31 genes, 16.1%	271 out of 10209 genes, 2.7%	0.00122	0.006
amino acid metabolic process	5 out of 31 genes, 16.1%	279 out of 10209 genes, 2.7%	0.00139	0.00585
response to biotic stimulus	5 out of 31 genes, 16.1%	312 out of 10209 genes, 3.1%	0.00228	0.01048
cellular amine metabolic process	5 out of 31 genes, 16.1%	320 out of 10209 genes, 3.1%	0.00254	0.01023
cellular nitrogen compound metabolic process	5 out of 31 genes, 16.1%	329 out of 10209 genes, 3.2%	0.00287	0.01136
multi-organism process	5 out of 31 genes, 16.1%	333 out of 10209 genes, 3.3%	0.00302	0.01156
nitrogen compound metabolic process	5 out of 31 genes, 16.1%	359 out of 10209 genes, 3.5%	0.00418	0.01783
lipid biosynthetic process	4 out of 31 genes, 12.9%	231 out of 10209 genes, 2.3%	0.00497	0.02085
cellular biosynthetic process	11 out of 31 genes, 35.5%	1599 out of 10209 genes, 15.7%	0.00546	0.02125
response to external stimulus	4 out of 31 genes, 12.9%	240 out of 10209 genes, 2.4%	0.00569	0.02204
monocarboxylic acid metabolic process	4 out of 31 genes, 12.9%	244 out of 10209 genes, 2.4%	0.00603	0.024
metabolic process	19 out of 31 genes, 61.3%	3836 out of 10209 genes, 37.6%	0.0062	0.02471
cellular component organization	6 out of 31 genes, 19.4%	565 out of 10209 genes, 5.5%	0.00629	0.02423
biosynthetic process	11 out of 31 genes, 35.5%	1673 out of 10209 genes, 16.4%	0.00774	0.02868

Cluster 4 genes.

Probe set ID	ATH best hit	Bet hit description	FC 0hr	FC 1hr	FC 3hr	FC 5hr	Gene bank best hit description
Les.1524.1.A1_at			1.04	-1.33	1.80	4.50	no hits found
Les.1297.2.A1_at			1.43	1.11	2.58	4.18	no hits found
Les.4045.1.S1_at			1.29	10.56	2.56	3.74	no hits found
Les.2717.1.S1_at	AT3G48140	senescence-associated protein, putative	1.13	1.64	1.80	3.52	B12D-like protein [Beta vulgaris]
Les.2717.2.A1_at			1.11	1.93	1.68	3.37	no hits found
Les.4566.1.S1_at	AT1G09770	ATDC5 (ARABIDOPSIS THALIANA CELL DIVISION CYCLE 5); DNA binding / transcription factor	-1.54	-1.43	-1.64	-2.01	CDC5-like protein [Solanum lycopersicum]
Les.2230.1.A1_at			-1.17	1.08	-1.21	-2.01	no hits found
Les.2820.2.S1_at	AT3G29320	glucan phosphorylase, putative	-1.28	-1.39	-1.15	-2.01	RecName: Full=Alpha-1,4 glucan phosphorylase L-1 isozyme, chloroplastic/amyloplastic; AltName: Full=Starch phosphorylase L-1; Flags: Precursor
Les.32.1.S1_at	AT4G08920	CRY1 (CRYPTOCHROME 1); ATP binding / blue light photoreceptor/ protein homodimerization/ protein kinase	-1.40	1.10	-1.25	-2.02	cryptochrome 1 [Lycopersicon esculentum]
Les.5307.1.S1_at	AT3G56930	zinc finger (DHHC type) family protein	-1.36	1.09	-1.09	-2.03	zinc finger protein, putative [Ricinus communis]
Les.5108.1.S1_at	AT4G22140	DNA binding / protein binding / zinc ion binding	-1.27	1.49	-1.33	-2.03	phd finger transcription factor; putative [Ricinus communis]
LesAffx.35132.1.S1_at	AT1G54500	rubredoxin family protein	-1.21	1.07	-1.10	-2.05	putative rubredoxin [Musa acuminata]
LesAffx.68801.1.S1_at	AT5G52580	RAB GTPase activator	-1.31	-2.02	-1.32	-2.06	RAB GTPase activator [Arabidopsis thaliana]
LesAffx.55680.1.S1_at	AT5G64380	fructose-1,6-bisphosphatase family protein	-1.14	-1.14	-1.04	-2.07	fructose-1,6-bisphosphatase, putative [Ricinus communis]
Les.1598.1.S1_at	AT3G58800	unknown protein	-1.27	1.56	-1.25	-2.09	unnamed protein product [Vitis vinifera]
Les.2327.1.A1_at			-1.16	1.01	-1.01	-2.10	no hits found
Les.2991.2.S1_at			-1.13	-1.51	-1.31	-2.10	no hits found

Les.4834.1.S1_at	AT1G43710	emb1075 (embryo defective 1075); carboxy-lyase/ catalytic/ pyridoxal phosphate binding	1.02	1.22	-1.06	-2.11	emb1075 (embryo defective 1075); carboxy-lyase/ catalytic/ pyridoxal phosphate binding [Arabidopsis thaliana]
Les.181.1.A1_at			-1.15	1.26	-1.12	-2.12	no hits found
LesAffx.31317.11.S1_at	AT1G64940	CYP89A6; electron carrier/ heme binding / iron ion binding / monooxygenase/ oxygen-binding	-1.41	-1.08	-1.22	-2.15	cytochrome P450 [Capsicum annuum]
LesAffx.65412.1.S1_at	AT4G04770	ATABC1 (ATP BINDING CASSETTE PROTEIN 1); ATPase, coupled to transmembrane movement of substances / protein binding / transporter	-1.23	-1.06	-1.16	-2.15	non-intrinsic ABC protein [Nicotiana benthamiana]
LesAffx.36895.1.S1_at	AT3G10970	haloacid dehalogenase-like hydrolase family protein	-1.20	1.12	-1.08	-2.16	haloacid dehalogenase-like hydrolase family protein [Arabidopsis thaliana]
LesAffx.71493.2.S1_at	AT5G07370	IPK2a (INOSITOL POLYPHOSPHATE KINASE 2 ALPHA); inositol or phosphatidylinositol kinase/ inositol triphosphate 6-kinase	-1.40	1.02	-1.22	-2.17	inositol polyphosphate multikinase [Solanum tuberosum]
Les.2824.1.S1_at	AT3G51840	ACX4 (ACYL-COA OXIDASE 4); acyl-CoA oxidase/ oxidoreductase	-1.25	1.34	-1.29	-2.18	acyl-CoA dehydrogenase, putative [Ricinus communis]
Les.3293.3.S1_at	AT3G48870	HSP93-III; ATP binding / ATPase/ DNA binding / nuclease/ nucleoside-triphosphatase/ nucleotide binding / protein binding	-1.10	-2.02	-1.29	-2.18	RecName: Full=ATP-dependent Clp protease ATP-binding subunit clpA homolog CD4B, chloroplastic; Flags: Precursor
Les.5696.1.S1_at	AT1G29700	unknown protein	-1.27	1.11	-1.20	-2.19	Zn-dependent hydrolases of the beta-lactamase fold [Brachypodium sylvaticum]
LesAffx.64239.1.S1_at	AT1G75460	ATP-dependent protease La (LON) domain-containing protein	-1.13	1.27	-1.31	-2.20	ATP-dependent peptidase, putative [Ricinus communis]
LesAffx.33443.1.S1_at	AT1G56180	unknown protein	-1.35	1.40	-1.22	-2.20	PREDICTED: hypothetical protein [Vitis vinifera]
LesAffx.16672.1.S1_at	AT3G63010	GID1B (GA INSENSITIVE DWARF1B); hydrolase	-1.12	1.18	-1.24	-2.21	GID1-5 [Gossypium hirsutum]
Les.4258.3.S1_at	AT5G64940	ATATH13; transporter	-1.28	-1.30	-1.27	-2.22	ATATH13; transporter [Arabidopsis thaliana]
Les.2875.3.S1_at	AT4G38160	pde191 (pigment defective 191)	-1.02	-1.39	-1.23	-2.23	pde191 (pigment defective 191) [Arabidopsis thaliana]
LesAffx.25786.1.S1_at	AT1G54520	unknown protein	-1.44	-1.05	-1.22	-2.26	hypothetical protein [Vitis vinifera]

LesAffx.61588.1.S1_at	AT3G12560	TRFL9 (TRF-LIKE 9); DNA bending/ DNA binding / telomeric DNA binding	-1.28	1.21	-1.29	-2.29	telomere binding protein [Solanum lycopersicum]
Les.4794.1.S1_at	AT1G76990	ACR3; amino acid binding	-1.38	1.02	-1.22	-2.30	amino acid binding protein, putative [Ricinus communis]
LesAffx.65563.1.S1_at	AT5G63490	CBS domain-containing protein / octicosapeptide/Phox/Bemp1 (PB1) domain-containing protein	-1.54	-1.27	-1.21	-2.32	CBS domain-containing protein / octicosapeptide/Phox/Bemp1 (PB1) domain-containing protein [Arabidopsis thaliana]
Les.112.1.S1_at	AT5G67030	ABA1 (ABA DEFICIENT 1); zeaxanthin epoxidase	-1.47	-1.04	-1.12	-2.33	RecName: Full=Zeaxanthin epoxidase, chloroplastic; Flags: Precursor
Les.3322.3.S1_at	AT5G13630	GUN5 (GENOMES UNCOUPLED 5); magnesium chelatase	-1.35	-1.04	-1.34	-2.35	magnesium chelatase [Capsicum annuum]
LesAffx.1583.1.S1_at	AT3G25805	unknown protein	-1.34	1.13	-1.28	-2.37	hypothetical protein [Vitis vinifera]
LesAffx.39331.1.S1_at	AT4G38160	pde191 (pigment defective 191)	-1.25	1.09	-1.12	-2.37	pde191 (pigment defective 191) [Arabidopsis thaliana]
Les.3488.1.S1_at	AT4G08920	CRY1 (CRYPTOCHROME 1); ATP binding / blue light photoreceptor/ protein homodimerization/ protein kinase	-1.52	1.21	-1.29	-2.37	cryptochrome 1b [Lycopersicon esculentum]
Les.2115.2.S1_at			-1.12	1.52	-1.11	-2.37	no hits found
LesAffx.65209.1.S1_at	AT1G68070	zinc finger (C3HC4-type RING finger) family protein	-1.29	-1.22	-1.02	-2.37	putative RING zinc finger protein [Arabidopsis thaliana]
Les.3522.1.S1_at	AT5G20280	ATSPS1F (sucrose phosphate synthase 1F); sucrose-phosphate synthase/ transferase;transferring glycosyl groups	-1.33	-1.03	-1.45	-2.43	sucrose phosphate synthase [Lycopersicon esculentum]
LesAffx.67008.1.S1_at	AT4G20350	unknown protein	-1.13	1.22	-1.20	-2.43	unnamed protein product [Vitis vinifera]
LesAffx.20922.1.S1_at	AT1G68080	iron ion binding / oxidoreductase, acting on paired donors, with incorporation or reduction of molecular oxygen, 2-oxoglutarate as one donor; and incorporation of one atom each of oxygen into both donors	-1.45	1.84	-1.19	-2.45	iron ion binding / oxidoreductase, acting on paired donors, with incorporation or reduction of molecular oxygen, 2-oxoglutarate as one donor; and incorporation of one atom each of oxygen into both donors [Arabidopsis thaliana]
Les.4760.1.S1_at	AT2G39950	unknown protein	-1.21	1.09	-1.45	-2.45	unnamed protein product [Vitis vinifera]
Les.5758.1.S1_at	AT5G44250	unknown protein	-1.10	1.07	-1.36	-2.45	PREDICTED: hypothetical protein [Vitis vinifera]

Les.5200.1.S1_at	AT5G11580	UVB-resistance protein-related / regulator of chromosome condensation (RCC1) family protein	-1.20	-1.02	-1.23	-2.46	Protein pim1, putative [Ricinus communis]
Les.3500.1.S1_at	AT1G66340	ETR1 (ETHYLENE RESPONSE 1); ethylene binding / protein histidine kinase / two-component response regulator	-1.13	1.01	-1.13	-2.48	RecName: Full=Ethylene receptor 2; Short=LeETR2
Les.4753.1.S1_at	AT3G50210	2-oxoacid-dependent oxidase, putative	-1.15	-1.03	-1.15	-2.48	putative flavonol synthase-like protein [Euphorbia esula]
Les.631.3.S1_at	AT3G30390	amino acid transporter family protein	-1.44	-1.14	-1.11	-2.49	amino acid transporter [Populus trichocarpa]
Les.2620.3.S1_at	AT1G15740	leucine-rich repeat family protein	-1.03	1.05	-1.07	-2.50	F-box-containing protein 1 [Malus x domestica]
Les.2115.2.S1_a_at			-1.11	1.49	-1.15	-2.50	no hits found
Les.1401.3.S1_at	AT5G18670	BMV3; beta-amylase/ catalytic/ cation binding	-1.10	-1.24	-1.48	-2.52	1,4-alpha-glucan-maltohydrolase [Solanum lycopersicum]
LesAffx.68173.1.S1_at	AT1G04970	lipid-binding serum glycoprotein family protein	-1.28	-1.77	-1.08	-2.54	Lipopolysaccharide-binding protein precursor, putative [Ricinus communis]
Les.1401.2.S1_at	AT5G18670	BMV3; beta-amylase/ catalytic/ cation binding	-1.29	-1.18	-1.47	-2.54	1,4-alpha-glucan-maltohydrolase [Solanum lycopersicum]
Les.1493.1.S1_at	AT5G22300	NIT4 (NITRILASE 4); 3-cyanoalanine hydratase/ cyanoalanine nitrilase/ indole-3-acetonitrile nitrilase/ nitrilase/ nitrile hydratase	-1.54	-1.02	-1.48	-2.57	RecName: Full=Bifunctional nitrilase/ nitrile hydratase NIT4B; Short=TNIT4B; AltName: Full=Nitrilase 4B; AltName: Full=Cyanoalanine nitrilase B
LesAffx.67395.1.S1_at	AT5G27320	GID1C (GA INSENSITIVE DWARF1C); hydrolase	-1.04	-1.06	-1.16	-2.58	Gibberellin receptor GID1, putative [Ricinus communis]
Les.2123.2.S1_at	AT3G26100	regulator of chromosome condensation (RCC1) family protein	-1.28	-1.20	-1.07	-2.60	RCC1 and BTB domain-containing protein, putative [Ricinus communis]
Les.1464.1.S1_at	AT5G23050	AAE17 (ACYL-ACTIVATING ENZYME 17); catalytic/ ligase	-1.25	1.03	-1.54	-2.61	acetyl-CoA synthetase, putative [Ricinus communis]
Les.4334.1.A1_at			-1.20	1.67	1.11	-2.61	no hits found
LesAffx.58430.1.S1_at	AT1G22100	ATP binding / inositol pentakisphosphate 2-kinase	-1.55	-1.03	-1.05	-2.62	inositol pentakisphosphate 2-kinase [Glycine max]
Les.2115.1.S1_at	AT1G15340	MBD10; DNA binding / methyl-CpG binding	-1.16	1.49	-1.24	-2.65	MBD10; DNA binding / methyl-CpG binding [Arabidopsis thaliana]

Les.5068.1.S1_at	AT5G23230	NIC2 (NICOTINAMIDASE 2); catalytic/ nicotinamidase	-1.49	1.05	-1.18	-2.69	Isochorismatase, putative [Rcinus communis]
Les.4334.2.S1_at	AT1G73040	jacalin lectin family protein	-1.02	1.39	-1.06	-2.72	jacalin-domain protein [Plantago major]
Les.5354.1.S1_at	AT4G34020	DJ-1 family protein	-1.40	1.15	-1.15	-2.76	DJ-1 family protein [Arabidopsis thaliana]
LesAffx.55080.1.A1_at	AT4G32250	protein kinase family protein	-1.39	1.46	-1.10	-2.76	protein kinase, putative [Rcinus communis]
Les.1977.2.S1_at			-1.23	-1.55	-1.55	-2.77	no hits found
LesAffx.61242.1.S1_at	AT4G36980	unknown protein	1.13	-1.73	-1.27	-2.78	Splicing factor; arginine/serine-rich, putative [Rcinus communis]
LesAffx.17339.1.S1_at	AT1G19870	iqd32 (IQ-domain 32); calmodulin binding	-1.37	-1.08	-1.50	-2.80	iqd32 (IQ-domain 32); calmodulin binding [Arabidopsis thaliana]
LesAffx.66486.1.S1_at	AT3G45620	transducin family protein / WD-40 repeat family protein	-1.31	-1.07	-1.14	-2.82	WD domain containing protein, putative [Solanum demissum]
Les.2493.1.A1_at			-2.30	1.74	-1.39	-2.85	no hits found
LesAffx.50639.1.S1_at	AT5G42210	FUNCTIONS IN: molecular_function unknown; INVOLVED IN: biological_process unknown; LOCATED IN: endomembrane system; CONTAINS InterPro DOMAIN/s: Major facilitator superfamily MFS-1 (InterPro:IPR011701), Major facilitator superfamily, general substrate trans	-2.13	-1.07	-1.87	-2.86	Hippocampus abundant transcript 1 protein, putative [Rcinus communis]
LesAffx.55283.1.S1_at	AT3G20910	NF-YA9 (NUCLEAR FACTOR Y, SUBUNIT A9); specific transcriptional repressor/transcription factor	-1.62	1.35	-1.32	-2.89	YA4 [Antirrhinum majus]
Les.1793.1.A1_at			-1.23	1.17	-1.36	-2.94	no hits found
LesAffx.56656.1.S1_at	AT4G22850	FUNCTIONS IN: molecular_function unknown; INVOLVED IN: biological_process unknown; LOCATED IN: cellular_component unknown; EXPRESSED IN: 23 plant structures; EXPRESSED DURING: 15 growth stages; CONTAINS InterPro DOMAIN/s: SNARE associated Golgi protein (In	-1.02	-1.57	-1.46	-2.95	predicted protein [Populus trichocarpa]

Les.3481.1.S1_a_at	AT3G15730	PLDALPHA1 (PHOSPHOLIPASE D ALPHA 1); phospholipase D	-1.46	1.01	-1.32	-2.99	phospholipase D [<i>Lycopersicon esculentum</i>]
Les.5344.1.S1_at	AT3G26890	unknown protein	-1.27	1.12	-1.32	-3.01	PREDICTED: hypothetical protein [<i>Vitis vinifera</i>]
LesAffx.62465.1.S1_at	AT5G67385	protein binding / signal transducer	-1.54	-1.12	-1.34	-3.01	Root phototropism protein, putative [<i>Ricinus communis</i>]
Les.32.2.S1_a_at	AT4G08920	CRY1 (CRYPTOCHROME 1); ATP binding / blue light photoreceptor/ protein homodimerization/ protein kinase	-1.49	-1.52	-1.45	-3.02	cryptochrome 1 [<i>Lycopersicon esculentum</i>]
Les.5255.1.S1_at	AT1G21680	FUNCTIONS IN: molecular_function unknown; INVOLVED IN: biological_process unknown; LOCATED IN: plasma membrane, vacuole, plant-type cell wall; EXPRESSED IN: 25 plant structures; EXPRESSED DURING: 13 growth stages; CONTAINS InterPro DOMAIN/s: WD40-like Beta	-1.27	-1.13	-1.24	-3.04	tolB protein-related [<i>Arabidopsis thaliana</i>]
LesAffx.71493.1.S1_at	AT5G61760	ATIPK2BETA; inositol or phosphatidylinositol kinase/ inositol triphosphate 6-kinase	-1.44	-1.14	-1.29	-3.04	inositol polyphosphate multikinase [<i>Solanum tuberosum</i>]
LesAffx.44265.1.S1_at	AT4G00560	methionine adenosyltransferase regulatory beta subunit-related	-1.49	-1.04	-1.21	-3.04	dttdp-4-dehydrorhamnose dehydrogenase, putative [<i>Ricinus communis</i>]
Les.5121.1.S1_at	AT3G47430	PEX11B	-1.21	1.32	-1.47	-3.04	peroxisomal biogenesis factor, putative [<i>Ricinus communis</i>]
LesAffx.21904.1.S1_at	AT1G44446	CH1 (CHLORINA 1); chlorophyllide a oxygenase	-1.49	-1.09	-1.37	-3.08	chlorophyll synthase, putative [<i>Ricinus communis</i>]
LesAffx.70505.1.S1_at	AT3G19860	basic helix-loop-helix (bHLH) family protein	-1.08	-1.50	-2.01	-3.10	DNA binding protein, putative [<i>Ricinus communis</i>]
LesAffx.51346.1.S1_at	AT1G54520	unknown protein	-1.80	-1.45	-1.32	-3.11	PREDICTED: hypothetical protein [<i>Vitis vinifera</i>]
Les.2761.1.A1_at			-1.67	1.39	-1.32	-3.11	no hits found
Les.3322.1.S1_at	AT5G13630	GUN5 (GENOMES UNCOUPLED 5); magnesium chelatase	-1.41	-1.49	-1.43	-3.11	Mg protoporphyrin IX chelatase [<i>Nicotiana tabacum</i>]
Les.2298.2.A1_a_at			-1.62	-1.02	-1.33	-3.14	no hits found

LesAffx.69867.3.S1_at	AT3G62110	glycoside hydrolase family 28 protein / polygalacturonase (pectinase) family protein	-2.14	-1.13	-1.71	-3.15	polygalacturonase-like protein-like [Solanum tuberosum]
Les.5311.1.S1_at	AT2G46550	unknown protein	-1.44	1.29	-1.36	-3.29	PREDICTED: hypothetical protein [Vitis vinifera]
Les.5010.1.S1_at	AT3G48110	EDD1 (EMBRYO-DEFECTIVE-DEVELOPMENT 1); glycine-tRNA ligase	-1.13	-2.95	-1.58	-3.32	Glycyl-tRNA synthetase 2, chloroplast/mitochondrial precursor; putative [Ricinus communis]
LesAffx.69782.1.S1_at	AT3G19990	unknown protein	-1.50	-1.50	-1.39	-3.36	predicted protein [Populus trichocarpa]
Les.1064.1.S1_at	AT4G02630	protein kinase family protein	-1.19	1.15	-1.27	-3.36	BRASSINOSTEROID INSENSITIVE 1-associated receptor kinase 1 precursor; putative [Ricinus communis]
Les.5360.1.S1_at	AT1G65660	SMP1 (SWELLMAP 1); nucleic acid binding / single-stranded RNA binding	-1.29	1.15	-1.11	-3.38	step II splicing factor slu7, putative [Ricinus communis]
Les.2594.1.S1_at	AT2G31130	unknown protein	-1.57	-1.01	-1.52	-3.58	fiber protein Fb32 [Gossypium barbadense]
Les.2.1.S1_at	AT2G32810	BGAL9 (Beta galactosidase 9); beta-galactosidase / catalytic / cation binding / sugar binding	-1.40	1.03	-1.16	-3.61	beta-galactosidase [Lycopersicon esculentum]
LesAffx.52470.1.S1_at	AT3G22970	unknown protein	1.05	1.14	-1.38	-3.65	conserved hypothetical protein [Ricinus communis]
Les.640.1.A1_at			-1.21	-1.19	-1.38	-3.86	no hits found
Les.2820.1.S1_at	AT3G29320	glucan phosphorylase, putative	-1.24	-1.65	-1.20	-3.93	RecName: Full=Alpha-1,4 glucan phosphorylase L-1 isozyme, chloroplastic/amyloplastic; AltName: Full=Starch phosphorylase L-1; Flags: Precursor
LesAffx.54132.1.S1_at	AT3G45620	transducin family protein / WD-40 repeat family protein	-1.25	-1.14	-1.23	-4.05	WD domain containing protein, putative [Solanum demissum]
Les.2923.2.S1_at	AT1G32860	glycosyl hydrolase family 17 protein	-1.82	-1.28	-1.44	-4.13	Glucan endo-1,3-beta-glucosidase precursor; putative [Ricinus communis]
Les.4356.3.S1_at	AT4G15530	PPDK (pyruvate orthophosphate dikinase); kinase/ pyruvate, phosphate dikinase	-1.80	-1.75	-1.45	-4.27	pyruvate orthophosphate dikinase [Echinochloa frumentacea]
Les.2923.1.S1_at	AT1G32860	glycosyl hydrolase family 17 protein	-1.58	-1.43	-1.41	-4.28	Glucan endo-1,3-beta-glucosidase precursor; putative [Ricinus communis]

Les.4962.1.S1_at	AT2G19580	TET2 (TETRASPANIN2)	-1.37	-1.00	-1.52	-4.72	TET2 (TETRASPANIN2) [Arabidopsis thaliana]
LesAffx.47386.1.S1_at	AT2G39570	ACT domain-containing protein	-1.91	-1.19	-1.33	-4.81	amino acid binding protein, putative [Ricinus communis]
LesAffx.69931.1.S1_at	AT5G03530	RABC2A (RAB GTPASE HOMOLOG C2A); GTP binding / GTP-dependent protein binding / myosin XI tail binding	-1.70	1.27	-2.20	-4.88	RABC2A (RAB GTPASE HOMOLOG C2A); GTP binding / GTP-dependent protein binding / myosin XI tail binding [Arabidopsis thaliana]
Les.3509.1.S1_at	AT4G13510	AMT1;1 (AMMONIUM TRANSPORTER 1;1); ammonium transmembrane transporter	-1.77	1.03	-1.59	-6.52	RecName: Full=Ammonium transporter 1 member 3; AltName: Full=LeAMT1;3
LesAffx.69867.1.S1_at	AT3G16850	glycoside hydrolase family 28 protein / polygalacturonase (pectinase) family protein	-2.24	-1.77	-1.87	-7.03	polygalacturonase-like protein [Arabidopsis thaliana]
LesAffx.1959.2.S1_at	AT1G74840	myb family transcription factor	-1.03	1.10	-1.40	-7.15	MYB transcription factor [Capsicum annuum]
LesAffx.71242.2.S1_at	AT1G68520	zinc finger (B-box type) family protein	-1.23	1.19	-1.59	-7.47	transcription factor, putative [Ricinus communis]
Les.1784.1.S1_at	AT3G05400	sugar transporter, putative	-2.16	-1.42	-1.63	-8.45	sugar transporter, putative [Arabidopsis thaliana]
Les.2254.1.A1_at			-1.63	1.97	-2.31	-8.56	no hits found
Les.1.1.S1_at	AT3G13750	BGAL1 (Beta galactosidase 1); beta-galactosidase / catalytic / cation binding / hemebinding / peroxidase / sugar binding	-1.14	1.53	-1.24	-9.58	beta-galactosidase [Lycopersicon esculentum]

Cluster 4 GO:

Tomato Functional Genomics Database (http://ted.bti.cornell.edu/cgi-bin/TFGD/array/GO_analysis.cgi)

Gene Ontology term	Cluster frequency	Genome frequency of use	Raw P-value	Corrected p-value (FDR)
cellular ion homeostasis	6 out of 115 genes, 5.2%	30 out of 10209 genes, 0.3%	8.53E-07	0
cellular chemical homeostasis	6 out of 115 genes, 5.2%	30 out of 10209 genes, 0.3%	8.53E-07	0
ion homeostasis	6 out of 115 genes, 5.2%	34 out of 10209 genes, 0.3%	1.86E-06	0
myo-inositol hexakisphosphate biosynthetic process	3 out of 115 genes, 2.6%	4 out of 10209 genes, 0.0%	5.52E-06	0
singlet oxygen-mediated programmed cell death	3 out of 115 genes, 2.6%	4 out of 10209 genes, 0.0%	5.52E-06	0
circadian regulation of calcium ion oscillation	3 out of 115 genes, 2.6%	4 out of 10209 genes, 0.0%	5.52E-06	0
inositol phosphate biosynthetic process	3 out of 115 genes, 2.6%	4 out of 10209 genes, 0.0%	5.52E-06	0
myo-inositol hexakisphosphate metabolic process	3 out of 115 genes, 2.6%	4 out of 10209 genes, 0.0%	5.52E-06	0
cytosolic calcium ion homeostasis	3 out of 115 genes, 2.6%	4 out of 10209 genes, 0.0%	5.52E-06	0
cellular di-, tri-valent inorganic cation homeostasis	4 out of 115 genes, 3.5%	16 out of 10209 genes, 0.2%	2.50E-05	0.002
anthocyanin metabolic process	4 out of 115 genes, 3.5%	16 out of 10209 genes, 0.2%	2.50E-05	0.00182
di-, tri-valent inorganic cation homeostasis	4 out of 115 genes, 3.5%	16 out of 10209 genes, 0.2%	2.50E-05	0.00167
inositol biosynthetic process	3 out of 115 genes, 2.6%	6 out of 10209 genes, 0.1%	2.71E-05	0.00154
chemical homeostasis	6 out of 115 genes, 5.2%	54 out of 10209 genes, 0.5%	2.97E-05	0.00143
cellular calcium ion homeostasis	3 out of 115 genes, 2.6%	7 out of 10209 genes, 0.1%	4.71E-05	0.00133
blue light signaling pathway	3 out of 115 genes, 2.6%	7 out of 10209 genes, 0.1%	4.71E-05	0.00125
calcium ion homeostasis	3 out of 115 genes, 2.6%	7 out of 10209 genes, 0.1%	4.71E-05	0.00118
polyol biosynthetic process	3 out of 115 genes, 2.6%	8 out of 10209 genes, 0.1%	7.48E-05	0.00222
phototropism	3 out of 115 genes, 2.6%	9 out of 10209 genes, 0.1%	0.00011	0.00316
regulation of meristem growth	3 out of 115 genes, 2.6%	9 out of 10209 genes, 0.1%	0.00011	0.003
inositol phosphate metabolic process	3 out of 115 genes, 2.6%	9 out of 10209 genes, 0.1%	0.00011	0.00286
regulation of developmental growth	3 out of 115 genes, 2.6%	9 out of 10209 genes, 0.1%	0.00011	0.00273

cellular cation homeostasis	4 out of 115 genes, 3.5%	26 out of 10209 genes, 0.3%	0.00018	0.00435
cellular homeostasis	6 out of 115 genes, 5.2%	76 out of 10209 genes, 0.7%	0.0002	0.00417
cellular metal ion homeostasis	3 out of 115 genes, 2.6%	11 out of 10209 genes, 0.1%	0.00021	0.004
metal ion homeostasis	3 out of 115 genes, 2.6%	11 out of 10209 genes, 0.1%	0.00021	0.00385
cation homeostasis	4 out of 115 genes, 3.5%	30 out of 10209 genes, 0.3%	0.00033	0.00444
inositol metabolic process	3 out of 115 genes, 2.6%	13 out of 10209 genes, 0.1%	0.00036	0.005
stromatal movement	3 out of 115 genes, 2.6%	15 out of 10209 genes, 0.1%	0.00057	0.0069
response to blue light	3 out of 115 genes, 2.6%	16 out of 10209 genes, 0.2%	0.0007	0.00667
protein-chromophore linkage	3 out of 115 genes, 2.6%	16 out of 10209 genes, 0.2%	0.0007	0.00645
regulation of meristem development	3 out of 115 genes, 2.6%	17 out of 10209 genes, 0.2%	0.00084	0.01375
chromatin remodeling	3 out of 115 genes, 2.6%	19 out of 10209 genes, 0.2%	0.00118	0.01636
regulation of biological quality	10 out of 115 genes, 8.7%	284 out of 10209 genes, 2.8%	0.00134	0.02118
meristem maintenance	3 out of 115 genes, 2.6%	21 out of 10209 genes, 0.2%	0.00159	0.02457
pigment metabolic process	5 out of 115 genes, 4.3%	77 out of 10209 genes, 0.8%	0.00172	0.02389
circadian rhythm	3 out of 115 genes, 2.6%	23 out of 10209 genes, 0.2%	0.00209	0.02865
polyol metabolic process	3 out of 115 genes, 2.6%	24 out of 10209 genes, 0.2%	0.00237	0.03368
homeostatic process	6 out of 115 genes, 5.2%	122 out of 10209 genes, 1.2%	0.00251	0.03333
phagocytosis	2 out of 115 genes, 1.7%	7 out of 10209 genes, 0.1%	0.00254	0.035
positive regulation of flower development	3 out of 115 genes, 2.6%	26 out of 10209 genes, 0.3%	0.00299	0.04537
protein autoproccessing	3 out of 115 genes, 2.6%	26 out of 10209 genes, 0.3%	0.00299	0.04429
protein amino acid autophosphorylation	3 out of 115 genes, 2.6%	26 out of 10209 genes, 0.3%	0.00299	0.04326
positive regulation of post-embryonic development	3 out of 115 genes, 2.6%	26 out of 10209 genes, 0.3%	0.00299	0.04227

Supplemental Table S4. TAIR statistical regulatory element motif analysis of genes present in clusters 1, 2, 3 and 4 of the co-expression network presented in Fig. 4A. A, An over-representation analysis of particular DNA motifs in the 1 kb upstream region of the translation start site of co-expressed genes present in each of the four different clusters was performed and a maximum of 12 significantly enriched motifs is reported.

Motif	Absolute number of this motif in query (test) set	Absolute number in background (genomic set)	Number of sequences in test set containing motif	Number of sequences (out of 33602 in background) containing motif	p-value from binomial distribution	Annotation
Cluster 1						
ATTGCT;AGCAAT*	17	18778	15/78	13961	0.00002	Y-box
CCAATT:AATTGG	87	26725	59/78	17876	0.00003	CArG (MADS)
TTTGAC;GTCAAA*	118	30479	60±/78	19343	0.00017	W/TGA box
GACTTT;AAAGTC*	95	24357	54/78	16819	0.00027	
CTAAAT;ATTAG	103	36518	63/78	21257	0.00039	
GTTGAC;GTCAAC	57	14088	39/78	10999	0.00064	W/TGA box
TTGATA;TATCAA	121	41325	66/78	23223	0.00084	
TTGACC;GGTCAA*	55	15351	40/78	11927	0.00157	W box
TTATCA;TGATAA	102	37518	63/78	22112	0.00159	
AGTCAA;TTGACT*	96	25747	52/78	17171	0.00200	
ACTATT;AATAGT	96	31032	56/78	19110	0.00246	
GGCGGC;GCCGCC	16	3529	14/78	2926	0.00433	GCC box
Cluster 2						
TCCTAC;GTAGGA*	22	8056	16/31	6967	0.00011	MYB
TGCGGC;GCCGCA*	9	2676	9/31	2472	0.00024	
TTCTA;TAGGAA*	29	17181	22/31	13164	0.00026	AG (MADS)
TGAATC;GATTCA	46	27341	25/31	18117	0.00138	EIL (ERF1, ethylene)
TGGGGA;TCCCCA*	17	8583	15/31	7263	0.00064	
TCTTGT;ACAAGA*	17	34064	11/31	20748	0.00190	
GAATTG;CAATTC*	37	23222	23/31	16322	0.00236	
CTTCTT;AAGAAG	34	62234	16/31	25217	0.00276	
ATGGAT;ATCCAT*	39	24022	23/31	16529	0.00287	MYB
TTGGAT;ATCCAA	34	32729	26/31	20368	0.00358	MYB
GTTGGT;ACCAAC	28	18238	20/31	13588	0.00387	MYB
TTGACT;AGTCAA	28	30479	20/31	19343	0.01090	W box
Cluster 3						
GTATGG;CCATAC*	19	8171	15/26	7085	0.00004	
TCACGT;ACGTGA*	17	10218	14/26	8029	0.00072	ABRE-like
TAACGT;ACGTTA*	25	11903	15/26	9235	0.00087	ABRE-like
CATATT;AATATG	52	38354	24/26	21653	0.00108	
TACTTA;TAAGTA	25	24845	21/26	16970	0.00115	
GATTAT;ATAATC	39	32660	23/26	20466	0.00173	
ATATGT;ACATAT	55	43322	24/26	22175	0.00175	
TGTTAT;ATAACA*	51	39503	24/26	22325	0.00200	
CACGTT;AACGTG*	17	9509	13/26	8009	0.00242	ABRE-like
CATACT;AGTATG	20	13369	15/26	10805	0.00440	

CHAPTER 2

Cluster 4						
TTTCCT;AGGAAA*	51	34894	32/36	21201	0.00044	AG (MADS)
GAGAAT;ATTCTC	37	28312	29/36	18699	0.00117	
TAAGAT;ATCTTA	51	32136	30/36	19945	0.00140	
TGATGG;CCATCA*	30	16337	22/36	12437	0.00187	SORLIP4 [†]
ACCTTT;AAAGGT*	12	23122	9/36	16477	0.00193	AG (MADS)
TAATTC;GAATTA	46	29893	29/36	19201	0.00198	
TCCATC;GATGGA*	30	16521	22/36	12574	0.00218	
GCTAAT;ATTAGC*	25	14968	21/36	11804	0.00243	
TTCCCT;AGGGAA	23	14139	20/36	11102	0.00287	
TAAGAC;GTCCTTA	25	14049	20/36	11219	0.00325	

* This motif was validated by POBO and there is significant enrichment of the motif in the co-expressed gene cluster.

± This set of 60 genes contain the core sequence TGAC, representing either a W box or a TGA box. See Supplemental Table S4B and Supplemental Figure S2 for further analysis of this gene set.

† This motif confers light-regulated gene expression.

B, TAIR statistical regulator element motif analysis of genes present in cluster 1 of the co-expression network presented in Fig. 4A that contain the sequence TTTGAC. An over-representation analysis of particular DNA motifs was performed in the 1000 kb upstream region of the translation start site of co-expressed genes present in cluster 1. Details on the occurrence of motifs that contain the W box consensus core motif TGACC/T are reported.

Motif	Absolute number of this motif in query (test) set	Absolute number in background (genomic set)	Number of sequences in query set containing motif	Number of sequences (out of 33602 in genomic set) containing motif	p-value from binomial distribution
TTTGAC:GTCAAA	118	30479	60/60	19343/33602	4.07E-15
TTGACC:GGTCAA	51	15351	37/60	11927/33602	2.22E-05
TGACTT:AAGTCA	76	24289	44/60	16569/33602	8.76E-05
TTGACT:AGTCAA	88	25747	45/60	17171/33602	8.80 E-05
TGACCC:GGGTCA	27	6806	21/60	5934/33602	6.28 E-04

Supplemental Table S5. Metabolites showing differential accumulation in the dying seedlings (DS), as compared to the parental lines (PLS). A, Semi-polar secondary metabolites of which the relative levels are given as fold change (FC) in accumulation in the DS as compared to the PLS, at 0 hr, 1 hr, 3 hr and 5 hr after the temperature shift that induces the HR in the DS.

Compound	MSI	RT* (min)	Mass (D) [M-H ⁺]	Fold change				Group
				0 hr	1 hr	3 hr	5 hr	
Coumaroyldopamine (CD)	2**	28.8	298.1086	3	2	37	116	Hydroxycinnamic acid amides (HCAAs)
Coumaroyltyramine-isoform 1 (CT1) ***	2	21.7	282.1137	19	15	20	30	
Coumaroyltyramine-isoform 2 (CT2)	1	33.4	282.1137	17	7	35	75	
Feruloyloctapan (FO)	2	30.6	328.1198	9	7	17	44	
Feruloyloctapan-hexose-isoform 1 (FO-H1)	2	22.6	490.1713	10	7	12	18	
Feruloyloctapan-hexose-isoform 2 (FO-H2)	2	23.7	490.1723	18	12	28	30	
Coumaroyltyramine-hexose (CT-H)	2	21.8	444.1662	18	15	17	27	
Feruloyltyramine-isoform 1 (FT1)	2	23.0	312.1242	16	16	17	23	
Feruloyltyramine-isoform 2 (FT2)	1	35.1	312.1242	43	14	17	19	
Feruloyltyramine-hexose-isoform 1 (FT-H1)	2	25.0	474.1770	16	15	17	21	
Feruloyltyramine-hexose-isoform 2 (FT-H2)	2	25.8	474.1773	15	16	18	24	
Salicylic acid	1	29.2	137.0245	3	2	13	26	Benzenoids
Salicylate-hexose-hexose	2	9.7	461.1671	7	8	8	11	
3, 4-Dihydroxybenzoic acid ? -D-xylopyranosyl ester	2	11.7	285.0616	3	4	4	5	
Benzyl alcohol-hexose-pentose + FA [†]	2	16.1	447.1512	1	1	1	2	Alkaloids
Benzyl alcohol-hexose-hexose	2	13.2	431.1560	6	6	8	10	
Dehydro tomatine (S) I + FA	2	28.3	1076.5310	2	2	2	2	
Dehydro tomatine (S) II + FA	2	30.7	1076.5330	2	2	1	2	
Dehydro tomatine (S) II + FA	2	31.3	1076.5300	2	2	1	2	
Lycoperoside H or hydroxy tomatine I + FA	2	23.4	1094.5430	2	2	2	2	
Lycoperoside H or hydroxy tomatine III + FA	2	26.5	1094.5420	2	2	2	2	
Lycoperoside H or hydroxy tomatine III + FA	2	26.9	1094.5380	2	3	2	3	
Tomatidine + 2 hexose + 2 pentose + FA	2	33.5	1048.5370	2	2	1	2	
Tomatidine + 4 hexose + FA	2	31.9	1108.5580	2	2	2	2	
Dehydro tomatine (S) I + FA	2	28.3	1076.5310	2	2	2	2	
Dehydro tomatine (S) II + FA	2	30.7	1076.5330	2	2	1	2	
Dehydro tomatine (S) II + FA	2	31.3	1076.5320	2	2	1	2	
Alpha-tomatine	1	31.9	1078.5460	2	2	2	2	
Alpha-tomatine isomer	2	33.0	1078.5480	2	2	2	2	
Lycoperoside H or hydroxy tomatine IV + FA	2	28.0	1094.5420	2	2	2	2	
Leptinidine; Hexose , Hexose, Hexose + FA	2	27.4	944.4875	2	2	2	2	

CHAPTER 2

Quercetin -hexose-hexose (3-O)	2	20.5	625.1403	2	2	2	2	Flavonoids
Quercetin - hexose-hexose-hexose	2	11.8	787.1945	2	2	2	2	
Quercetin 3-O-rutinoside-7-O-glucoside	2	15.4	771.1985	2	2	2	2	
Quercetin-hexose-deoxyhexose, -pentose	2	22.2	741.1882	2	2	2	2	
Quercetin 3-O-rutinoside	2	24.2	609.1456	2	2	1	2	
Quercetin-hexose-deoxyhexose, -hexose	2	29.8	947.2480	2	2	2	2	
Quercetin 3-O-glucoside	2	25.2	463.0877	-1	-2	-2	-1	
Kaempferol-hexose-hexose (3-O)?	2	22.9	609.1459	3	3	3	3	Triterpenoid glycoside
Grossamide	4	47.5	623.2401	11	11	15	20	
Aquilegioside H (C ₄₈ H ₇₈ O ₂₀)	4	35.3	973.5010	38	38	37	56	
Creoside II	4	12.6	305.1614	5	7	7	10	
Sericoside (C ₃₅ H ₅₄ O ₁₂)	4	38.3	665.3907	48	43	40	64	
Esculentoside S (C ₄₂ H ₆₆ O ₁₆)	4	40.5	825.4269	56	55	53	79	Organic acids
3-O-feruloyl quinic acid	2	20.3	367.1039	-1	-2	-2	-2	
Caffeoyl isocitric acid + H ₂ O-isoform 1	2	5.8	371.0623	-1	-2	-2	-2	
Caffeoyl isocitric acid + H ₂ O-isoform 2	2	7.9	371.0621	-1	-2	-2	-2	
Coumaroylquinic acid	2	19.8	337.1504	1	2	1	2	
Melibionic acid	4	45.4	483.2445	-2	-2	-2	-3	Unknown
Unidentified	4	22.7	387.0957	3	4	5	5	
Unidentified	4	31.6	631.2824	3	4	6	6	
Unidentified	4	37.8	1341.6080	4	3	5	3	
Unidentified	4	31.7	1240.6050	4	3	4	3	
Unidentified	4	7.1	329.0876	4	5	7	7	
Unidentified	4	26.7	586.2446	5	4	5	7	
Unidentified	4	16.0	476.1561	5	5	6	9	
Unidentified	4	34.1	453.2350	5	5	5	7	
Unidentified	4	30.5	513.2255	6	5	5	5	
Unidentified	4	21.0	517.1568	6	6	6	8	
Unidentified	4	42.5	463.2630	6	5	7	8	
Unidentified	4	31.1	1181.5700	6	6	7	11	
Unidentified	4	24.8	637.2135	7	6	9	10	
Unidentified	4	40.4	711.3619	10	10	9	15	
Unidentified	4	41.1	857.4556	11	10	9	13	
Unidentified	4	38.9	1165.5700	12	11	13	16	
Unidentified	4	25.5	606.2198	14	10	11	14	
Unidentified	4	38.0	782.2667	14	13	13	19	
Unidentified	4	41.1	785.2931	14	13	13	20	
Unidentified	4	37.3	812.2767	20	20	23	32	
Unidentified (C19H36O10) + FA	4	4.8	469.0301	-4	-3	-5	-2	

HR-associated transcriptome and metabolome changes

Unidentified	4	40.6	617.2621	-3	-6	-9	-6	Unknown
Unidentified (C15H16O11)2	4	9.0	743.1303	-2	-4	-3	-5	
Unidentified	4	45.4	483.2445	-2	-2	-2	-3	
Unidentified (C19H36O10) + FA	4	9.0	469.0293	-2	-2	-2	-3	

* Retention time.

? Position not known.

† Formic acid adduct.

**1, Identified metabolites based on authentic standards; 2, Putatively annotated compounds (e.g. without chemical reference standards, based upon physicochemical properties and/or spectral similarity with public/commercial spectral libraries); 4, Unknown compounds. Although unidentified or unclassified, these metabolites can still be differentiated and quantified based on spectral data. The reporting grades (1, 2 and 4) are assigned according to the proposed minimum reporting standards for chemical analysis (metabolomics standards initiative (MSI)) (Sumner et al., 2007).

***Isoform 1 and isoform 2 are anticipated to refer to the cis- and trans-derivatives of the compound, respectively. Cis-derivatives are more polar than their trans-counterparts and elute earlier than their trans-derivatives. Cis-isomers are generally associated with light-induced isomerization of the natural trans isomers originally synthesized by the plant (Mühlenbeck et al., 1996).

B, Polar primary metabolites of which the relative levels are given as fold change (FC) in accumulation in the DS as compared to the PLS, at 0 hr, 1 hr, 3 hr and 5 hr after the temperature shift that induces the HR in the DS.

Compound	MSI	RT* (min)	RI**	Fold change				Group
				0 hr	1 hr	3 hr	5 hr	
Benzoic acid	1	14.2	1507	2	2	6	14	Benzenoids
Tyramine	1	17.0	1909	3	3	5	10	Polyamines
Putrescine	1	15.1	1730	3	3	3	6	
Dopamine	1	18.0	1909	3	3	3	6	
Tyrosine	1	17.2	1932	4	4	4	5	Amino acids
Phenylalanine	1	13.9	1624	2	2	2	3	
Glutamine	1	15.5	1768	3	3	3	3	
Gamma-aminobutyric acid (GABA)	1	12.7	1525	1	1	2	2	Non protein amino acid
Trehalose	1	23.4	2705	2	7	8	27	Sugars
Xylose	2	14.2	1649	2	3	3	3	
Glucopyranose	2	18.3	2049	8	8	9	13	
Propanoic acid	1	6.3	1054	-2	-2	-2	-1	Organic acids
Phosphoenol pyruvate	1	9.3	1267	-2	-2	-2	-2	
Galactaric acid	2	17.8	1994	-2	-2	-3	-1	
Erythronic acid	2	13.0	1549	2	2	2	2	

*Retention time.

**Retention index.

† 1, Identified metabolites based on authentic standards; 2, Putatively annotated compounds (e.g. without chemical reference standards, based upon physicochemical properties and/or spectral similarity with public/commercial spectral libraries). The reporting grades (1 and 2) are assigned according to the proposed minimum reporting standards for chemical analysis (metabolomics standards initiative (MSI)) (Sumner et al., 2007).

CHAPTER 2

Supplemental Table S6. Expression of genes involved in the repression of defense signal transduction and protection against oxidative damage during mounting of the HR. The fold change in the expression of the genes in the dying seedlings (DS) relative to the parental lines (PLS) is indicated.

Probe set ID	Regulation	Fold change				Best Arabidopsis hit	Best Arabidopsis hit description
		0 hr	1 hr	3 hr	5 hr		
LesAffx.63980.1.S1_at	U_5 ¹	1	1	4	11	AT3G02800	Phosphatase/ phosphoprotein phosphatase/ protein tyrosine phosphatase
Les.4780.1.S1_at	U_5	-1	-1	2	4	AT4G33920	Protein phosphatase 2C (PP2C) family protein
LesAffx.33.1.S1_at	U_5	-1	1	2	2	AT3G62260	PP2C, putative
LesAffx.62321.1.S1_at	U_5	1	1	1	2	AT2G25070	PP2C, putative
LesAffx.344.12.S1_at	U_5	1	2	2	3	AT1G34750	PP2C, putative
Les.3869.1.S1_at	U_35	-2	2	8	7	AT1G07160	PP2C, putative
Les.31.1.S1_s_at	U_5	-2	2	1	3	AT5G03730	CTR1 (constitutive triple response 1)
LesAffx.6422.1.S1_at	U_5	1	3	2	5	AT2G26070	RTE1 (reversion to ethylene sensitivity 1)
Les.4533.1.S1_at	D_5	-1	1	-2	-2	AT5G03280	EIN2 (ethylene insensitive 2)
LesAffx.61034.1.S1_at	D_5	-1	1	-2	-3	AT1G32540	LOL1 (LSD1-like 1)
LesAffx.44417.1.S1_at	U_35	1	2	4	7	AT3G25070	RIN4 (RPM1-interacting protein 4)
LesAffx.57342.1.S1_at	D_5	-1	-1	-2	-8	AT5G17220	ATGSTF12 (glutathione S-transferase (GST) PHI 12)
LesAffx.46036.1.S1_at	U_5	1	1	1	11	AT4G02520	ATGSTF2 (GST PHI 2)
LesAffx.1959.3.S1_at	U_5	2	1	1	7	AT2G47730	ATGSTU8 (GST TAU 8)
LesAffx.24206.1.S1_at	U_5	-1	1	1	3	AT5G41210	ATGSTT1 (GST TAU 1)
Les.3735.1.S1_at	U_5	3	3	3	6	AT2G29490	ATGSTU1 (GST TAU 1)
Les.3734.1.S1_at	U_5	-1	2	2	5	AT1G78380	ATGSTU19 (GST TAU 19)
LesAffx.3002.1.S1_at	U_135	4	3	7	30	AT2G29450	ATGSTU5 (GST TAU 5)
LesAffx.55582.1.S1_at	U_5	2	1	2	11	AT2G29420	ATGSTU7 (GST TAU 7)
Les.123.1.S1_at	U_5	1	1	1	2	AT3G09270	ATGSTU8 (GST TAU 8)
Les.131.1.S1_at	U_135	1	2	4	28	AT3G09270	ATGSTU8 (GST TAU 8)
Les.4501.1.S1_at	U_5	2	2	4	6	AT3G09270	ATGSTU8 (GST TAU 8)
Les.2746.1.S1_at	U_5	2	5	5	35	AT3G09270	ATGSTU8 (GST TAU 8)

¹ U_5, upregulated at t = 5 hr; U_35, upregulated at t = 3 and 5 hr; U_135, upregulated at t = 1, 3 and 5 hr; D_5, downregulated at t = 5 hr.

HR-associated transcriptome and metabolome changes

Supplemental Table S7. Expression of genes involved in the biosynthesis of hydroxycinnamic acid amides (HCAAs) during mounting of the HR. The fold change in the expression of the genes in the dying seedlings (DS) relative to the parental lines (PLS) is indicated.

Probe set ID	Regulation	Fold change				Best Arabidopsis hit	Gene bank best hit description
		0 hr	1 hr	3 hr	5 hr		
LesAffx.62617.1.S1_at	U_35 ¹	2	2	27	73	At5g42830	Anthranilate N-benzoyltransferase, putative [<i>Ricinus communis</i>]
Les.254.1.S1_at	U_135	2	3	6	9	At2g39030	N-hydroxycinnamoyl-CoA: tyramine N-hydroxycinnamoyl transferase (THT) 1-3†
Les.4038.1.S1_at	U_35	1	2	8	26	At2g39030	THT1-3†
Les.3687.1.S1_at	U_35	-1	2	4	7	At2g39030	THT7-1†
Les.3686.1.S1_at	U_35	2	2	5	8	At2g39030	THT7-8†

¹U_35, upregulated at t = 3 and 5 hr; U_135, upregulated at t = 1, 3 and 5 hr.

† Characterized genes in *Solanum lycopersicum*.

Supplemental Table S8. Affymetrix ID, locus ID in the tomato genome sequence, gene description and nucleotide sequences of primers used for qRT-PCR gene expression analysis.

Probe set ID	Transcript locus ID	Best hit description	Forward primer	Reverse primer
Les.3662.1.S1_at	Solyc01g095080.2.1	ACS2 (1-aminocyclopropane-1-carboxylate synthase)	AATGTCAAGAGCCAGGGTGGTTCC	TCCTCGCAGCGCAATATCAAC
LesAffx.10955.1.S1_at	Solyc06g074530.1.1	ADT4 (arogenate dehydratase 4)	AGGAACGAGCGTGTCTCAAG	CGAGACTCGATCTTCGTC AAGCTG
Les.129.1.S1_at	Solyc01g109140.2.1	DES (divinyl ether synthase)	CAAGTCTGCTGTGTCCATGTTGG	GCTTCGCCACAAACCTGAATAG
LesAffx.16424.1.S1_s_at	Solyc06g005170.2.1	MAPK3 (mitogen-activated protein kinase 3)	GCTGCCATAGATGTTTGGTCTGTG	TGTAGGAGTGCCAAGAAGCTCAG
Les.4038.1.S1_at	Solyc08g068770.1.1	THT-1-3 (N-hydroxycinnamoyl-CoA:tyramine N-hydroxycinnamoyl transferase)	GCTTCTATGACAAGCCTGGGTTTC	ACTGCGATTATTCCTCAACCG
LesAffx.3554.1.A1_at	Solyc02g065090.2.1	PLP4 (patatin-like protein-4)	GAGCATTGATGGAGGTGGTATCAG	TGCATTGGTCCATCAAGTTCCTG
LesAffx.9910.1.S1_at	Solyc03g116890.2.1	WRKY18 (transcription factor)	AAGGTTCAAAGAAGCGTGGAAGAC	TTGTAAACAGGGCTGCGGTATC
LesAffx.735.1.S1_at	Solyc09g014990.2.1	WRKY33 (transcription factor)	ACCCGAGGCAAAGAGATGGAAG	AGGTTACGTTACTGTTCTACTTGC
LesAffx.69808.1.S1_at	Solyc07g040710.2.1	CBP (calmodulin-binding family protein)	TGCATCAAGTATCTCGGACCAAAG	TCGACTTGGAACCTCTACTGAC
LesAffx.63935.1.S1_at	Solyc04g005050.1.1	MMP (matrixin metallo family protein)	TGGGAGTCCAGGAGTTATACGG	TCGGAGTCAAATTTGGGTTTGGC



Chapter 3

Carbon Economy and the Maintenance of Energy Homeostasis during the Hypersensitive Response in Tomato

Desalegn W. Etalo^{1,4,Ω}, Thierry L. Delatte¹, Matthew J. Paul⁵, Ric C.H. De Vos^{2,4,6}, Matthieu H.A.J. Joosten^{3,4} and Harro J. Bouwmeester^{1,4}

¹Laboratory of Plant Physiology, Wageningen University, Wageningen, The Netherlands.

²Plant Research International Bioscience, Wageningen University, Wageningen, The Netherlands.

³Laboratory of Phytopathology, Wageningen University, Wageningen, The Netherlands.

⁴Centre for BioSystems Genomics, Wageningen, The Netherlands.

⁵Center for Crop Genetic Improvement, Rothamsted Research, Harpenden, Hertfordshire, AL5 2JQ, United Kingdom.

⁶Netherlands Metabolomics Centre, Einsteinweg 55, 2333 CC Leiden, The Netherlands.

^ΩCurrent address: Plant Research International, Bioscience, Wageningen University, Wageningen, The Netherlands.

To be submitted

Abstract

The hypersensitive response (HR) upon pathogen challenge of resistant plants is characterised by local cell death at the site of pathogen entry, resulting in efficient containment of the invading biotrophic pathogen. *Cladosporium fulvum* is a pathogen of tomato and when an avirulence factor of this fungus is expressed in a tomato line that carries the corresponding resistance gene, the plants will display a synchronized and amplified immune response, culminating in an HR ("dying seedlings", DS). To monitor the HR-associated transcriptional response of these DS, we performed a deep RNA-seq analysis and compared the composition of the transcriptome with that of resistant and susceptible tomato plants inoculated with *C. fulvum*. The RNA-seq analysis revealed that plants that are mounting a resistance response to the fungus undergo massive transcriptional reprogramming that features a shift towards energy generation at the expense of growth. For example, a number of catabolic processes that generate acetyl-CoA, an important intermediate for the energy cycle and the biosynthesis of a wide range of defence-associated primary and secondary metabolites, were up-regulated. The induction of these catabolic processes coincides with a significant reduction in trehalose-6-phosphate, playing a central role in the maintenance of energy homeostasis during carbon starvation, and is accompanied by accumulation of trehalose. Genes regulating the circadian rhythm were down-regulated and this could potentially result in the suppression of genes involved in the biosynthesis and signalling of auxin as well as other hormones that are primarily produced through the isoprenoid pathways (brassinosteroids, cytokinins and gibberellins), resulting in suppression of growth. Our findings shed new light on the processes that are involved in the maintenance of carbon economy and energy homeostasis and that govern the trade-off between growth and the plant immune response.

Introduction

Unlike animals, plants do not have an adaptive immune system, hence they solely rely on innate immunity to recognize and respond to invading pathogens. Innate immunity is generally divided into two blurred classes referred to as microbe-associated molecular pattern (MAMP)- triggered immunity (MTI) and effector-triggered immunity (ETI) (Dodds and Rathjen, 2010; Thomma et al., 2011). MTI is induced upon recognition of MAMPs, such as bacterial flagellin and fungal chitin, which are conserved and essential components of large classes of pathogens, by extracellular pattern recognition receptors (PRRs). In contrast, ETI is induced upon recognition of pathogen virulence molecules, referred to as effectors, and which are species-, race- or strain-specific, mostly by intracellular receptors (Chisholm et al., 2006; Jones and Dangl, 2006; Dodds and Rathjen, 2010; Thomma et al., 2011). Generally, MTI and ETI give rise to similar responses, although ETI in most cases is stronger, faster and more robust and often involves a form of localized cell death, called the hypersensitive response (HR) (Lam et al., 2001; Jones and Dangl, 2006; Dodds and Rathjen, 2010; Thomma et al., 2011).

The interaction between tomato and the biotrophic extracellular fungus *Cladosporium fulvum* is a model pathosystem and is characterized by a typical gene-for-gene interaction (de Wit and Joosten, 1999). In resistant tomato plants, recognition of an avirulence factor (Avr) by the matching *Cf* resistance gene product results in the HR (incompatible interaction). In contrast, in susceptible plants lacking the matching resistance gene the fungus can successfully colonize the leaf apoplastic space and cause disease (compatible interaction). The localized cell death is often associated with resistance response. A thorough investigation of the early molecular, biochemical and cellular changes at the infection site is obscured by the non-synchronous and highly localized response of just a few host cells during the initiation of the HR. However, transgenic tomato plants expressing an effector of *C. fulvum* that are crossed with a tomato line that contains the matching *Cf* resistance gene represent a versatile model system that perfectly mimics the highly localized response of resistant tomato plants to effectors of *C. fulvum*, but now in an amplified and synchronised way (Cai et al., 2001; de Jong et al., 2002; Stulemeijer et al., 2009; Etalo et al., 2013). The offspring of this cross will die soon after germination, due to the systemic HR that will occur as a result of the recognition of the expressed effector by the matching *Cf* protein. However, the HR is suppressed by incubating the plants at an elevated temperature and humidity. Indeed, when the offspring is placed at 33°C and 100% relative humidity (RH) immediately after germination, the seedlings are rescued. Plants can then be grown for a few weeks under these conditions and subsequently, a systemic and highly synchronized HR is induced by placing the plants at permissive conditions (20°C and 70% RH).

Using this “dying seedlings” (DS) system, it was shown that the HR involves a massive reprogramming of the transcriptome, proteome and metabolome (Cai et al., 2001; de Jong et al., 2002; Stulemeijer et al., 2009; Etalo et al., 2013). The defence response coincides with an increased demand for energy, reducing equivalents and carbon skeletons that are provided by the primary metabolism (Bolton, 2009). Hence, tight regulation is required to maintain the carbon economy and the energy homeostasis of the plant in order to preserve the right balance between growth and development on the one hand and the activation of the plant immune response on the other. Several regulatory processes have been shown to be involved in the management of this balance, such as sugar signalling, the circadian clock and several plant hormones (Blasing et al., 2005; Covington and Harmer, 2007; Delatte et al., 2011; Ramsey and Bass, 2011; Wang et al., 2011; Farre and Weise, 2012). For example, at the cellular level, Sucrose non-fermenting-1-Related protein Kinase-1 (SnRK1) is a key player in the plant total energy homeostasis, regulating the switch between growth/development and defence (Baena-Gonzalez et al., 2007). However, the system-wide relationships of these processes remain elusive in the context of resistance of plants to pathogens. Here, taking advantage of the highly synchronised and systemic HR in the DS and using high quality RNA-seq, we analysed the transcriptome of the DS and resistant and susceptible tomato inoculated with *C. fulvum*. Our analysis revealed that the HR is indeed highly energy-demanding and requires a number of strategies to balance the carbon economy and maintain the energy homeostasis of the system. Furthermore, we have monitored the levels of trehalose-6-phosphate (T-6-P) and SnRK1 activity during mounting of the HR, as both of them have been shown to play a crucial role in the maintenance of energy homeostasis during carbon starvation (Baena-Gonzalez et al., 2007; Zhang et al., 2009; Nunes et al., 2013). Pathway analysis indicated that the majority of the genes regulating the circadian rhythm were down-regulated and this could potentially result in the suppression of genes involved in the biosynthesis and signalling of auxin, as well as of other hormones that are primarily produced through the isoprenoid pathway (brassinosteroids, cytokinins and gibberellins), resulting in the suppression of growth and development.

Results and Discussion

Alignment of RNA-seq reads with the tomato reference genome sequence

We performed a deep RNA-seq analysis on RNA obtained from leaf tissue of the dying seedlings (DS) isolated 5 hrs after the temperature shift that induces the HR and compared the results with those obtained from a 1:1 mix of the parental Cf0:Cf-4 and Cf0:Avr4 lines (PLS) subjected to the same treatment and sampled at the same time point. In addition, the RNA-seq data of the *C. fulvum*-inoculated Cf0:Cf-4 (resistant;

incompatible interaction (I)) and Cf0:Avr4 (susceptible; compatible interaction (C)) plants were compared with those of mock-inoculated plants, all sampled at 6 days post inoculation (dpi). Three independent biological replicates were considered for the analysis. The RNA-seq analysis generated approximately 50 million paired-end reads per sample, with the majority of the reads (40 million) individually mapping to one single location within the tomato reference genome sequence (**Figure 1A**). An additional 561,475 ($\pm 27,167$) reads were mapped to multiple locations within the reference genome sequence (**Figure 1A**).

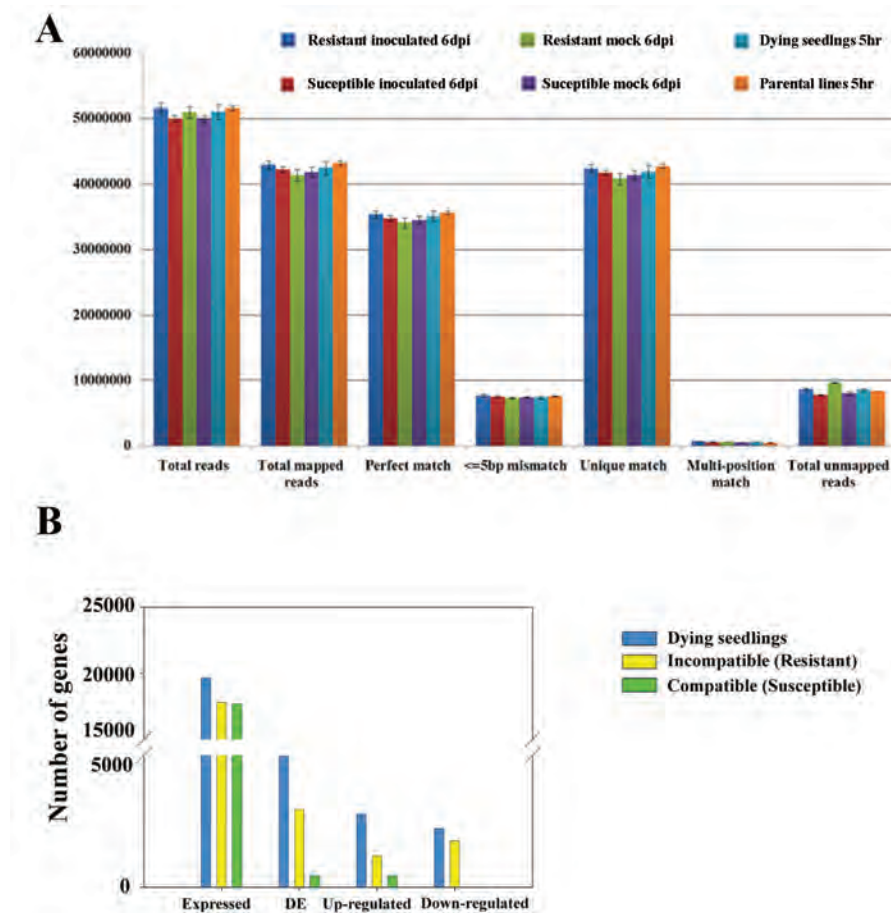


Figure 1. Alignment statistics of the sequence reads obtained by RNA-seq.

(A) The majority of the RNA-seq reads individually map to unique positions in the tomato reference genome sequence. The error bar indicates the standard error of the mean of the three independent biological replicates that were analysed for each condition.

(B) Number of RNA-seq reads matching transcripts of annotated genes in the tomato reference genome originating from the dying seedlings, incompatible interaction and compatible interaction. DE, differentially expressed (Up-regulated and down-regulated genes).

From the total of 34,734 protein-encoding genes predicted to be present in the tomato genome sequence, we identified RNA-seq reads matching the transcripts of respectively 19,643 (~57%), 17,805 (~51%) and 17,692 (~51%) of them in the DS, I and C, respectively, based on the calculation of the unigene expression, the RPKM method (reads per kb per million reads) and gene models reported by the International Tomato Genome Annotation Group (ITAG). The unique set of genes in the DS, both in the up and down-regulated categories (1546 and 1508 genes in the up and down regulated category, respectively) could be regarded as genes that are observed due to the amplified response of the HR in the DS but could not be observed due to dilution effect of the non-synchronous response in the incompatible interaction (**Figure 2**). The genes that are unique for I and C (556 in the I and 12 in C in the upregulated category; 479 in the I in the downregulated category) and these shared between I and C (12 in the upregulated and 3 in the downregulated category) may be linked to responses associated with the presence of the fungus in the plants. The common genes between the DS and the I (808 genes in the upregulated and 704 genes in the downregulated categories) are primarily linked with ETI. Whereas, in the upregulated category the 386 genes that are common between the DS, I and C can be linked to MTI (**Figure 2**).

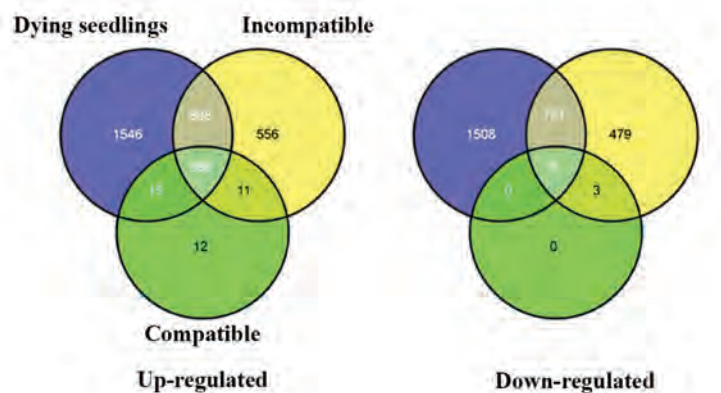


Figure 2. Venn diagram showing the distribution of unique and shared genes that are differentially regulated in the dying seedlings (DS), and resistant (incompatible (I) and susceptible (compatible (C)) tomato inoculated with *C. fulvum*. The transcriptome of the DS was compared with that of the Parental Lines (PLS), while for I and C the transcriptome of respectively resistant and susceptible inoculated plants was compared with that of the mock-inoculated control plants. Three independent biological repeats were analysed. Gene expression was considered to be statistically significantly different when a fold change above 2 was observed with a *P* value of 0.001 after FDR correction. The DS were analysed at 5 hr after the initiation of the HR, whereas the *C. fulvum*-inoculated and control plants were subjected to RNA-seq at 6 dpi.

A quick scan of the identity of the various differentially expressed genes reveals that both in the DS and in I and C a transcriptional reprogramming occurs that will affect many biological processes. Here, we will focus on the biological processes that primarily affect and regulate the carbon economy and energy homeostasis.

Catabolic pathways converge to generate acetyl-CoA for energy and carbon skeleton generation during mounting of the HR

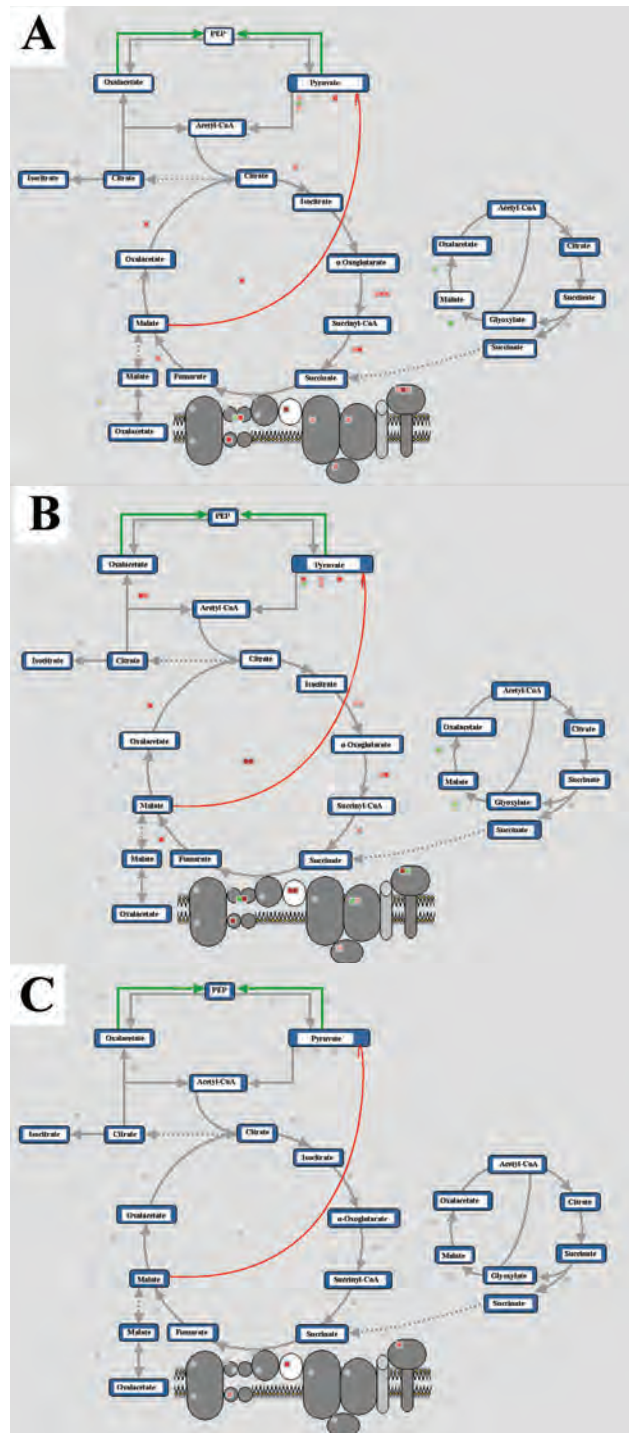
In comparison with the compatible interaction, the expression of genes involved in cellular energy metabolism was considerably up-regulated in the DS and resistant plants inoculated with *C. fulvum* (**Figure 3A and 3B, respectively**). This includes genes involved in the tricarboxylic acid (TCA) cycle, electron transport chain (ETC), oxidative pentose phosphate pathway and anaerobic (fermentative) energy generation (**Figure 3, Supplementary Table S1**). All these up-regulated genes belong to the 808 up-regulated genes that are shared between the DS and I (**Figure 2, Up-regulated**). In the TCA cycle, glucose is catabolised to produce energy in the form of ATP, and molecules that serve as precursors for anabolic reactions such as protein, lipid and carbohydrate biosynthesis. Hence the pathway serves as a link between catabolism and anabolism and which plays an essential role during mounting of the HR. The oxidative pentose phosphate pathway is a primary source of erythrose-4-phosphate (E-4-P), a precursor for aromatic amino acid biosynthesis. Indeed, we earlier observed that aromatic amino acids and secondary metabolites derived from this precursor showed accumulation in the DS (Etalo et al., 2013). Unlike as was observed in the resistant plants, in the susceptible inoculated plants the expression of genes involved in cellular energy metabolism is not significantly different from the control (**Figure 3C**).

Photosynthesis and aerobic oxidation of organic molecules such as fatty acids and sugars are the primary sources of ATP. However, in the DS and incompatible interaction, the HR is clearly associated with significant repression of photosynthesis, as 80 out of the 81 differentially expressed genes (DEGs) that are related to photosynthesis (98.8%) were down-regulated in the DS and 42 out of 46 DEGs related to photosynthesis (91.3%) were downregulated in the incompatible interaction (**Figure 3D, for DS, Supplementary Table S2 and Supplementary Figure S1**). In contrast, in the compatible interaction photosynthesis-related genes did not show significant differential regulation (results not shown). In agreement with our results, previous reports have shown the decrease in photosynthetic activity in the DS and in incompatible interactions between tobacco and *Phytophthora nicotianae*, barley and *Blumeria graminis*, and between Arabidopsis and *Pseudomonas syringae* (Scharte et al., 2005; Bonfig et al., 2006; Swarbrick et al., 2006; Stulemeijer et al., 2009). Chlorophyll fluorescence imaging of tobacco leaves on a macro- and microscopic scale, involved in an incompatible interaction with *P. nicotianae*, revealed that the decline in photosynthesis is a highly localized process which occurs in single mesophyll cells (Scharte et al., 2005).

Although there was a dramatic suppression of the expression of photosynthesis-related genes in the DS, the level of sucrose, which is the product of photosynthesis, was significantly higher in the DS as compared to the PLS at 1, 3 and 5 hrs after the temperature shift that induces the HR in the DS. The glucose and fructose levels were

not significantly different between the DS and PLS (**Supplementary Figure S2**). This observation raises the question how plants undergoing such a massive reprogramming at the transcriptome and metabolome level manage to stabilise their carbohydrate content while at the same time their photosynthesis is strongly repressed. This suggests the induction of alternative carbon and energy generation mechanisms in the DS that are mounting the HR. Some of the induced alternative carbon skeleton and energy generation strategies by the DS include the activation of catabolic processes involving SnRK1-mediated autophagy, ubiquitin-mediated proteolysis, amino acid catabolism, lipid catabolism and hydrolysis of polysaccharides (**Supplementary Table S1, Supplementary Figures S3A and S3B and S4**). Under stress conditions, catabolism could be a more economical strategy of energy and carbon skeleton generation than *de novo* biosynthesis from primary precursors. Moreover, the massive induction of localized catabolic processes at the site of infection has a dual significance in suppressing the proliferation of pathogens through the HR and related responses as the plant kills and recycles part of itself for the regeneration of defensive molecules to combat the fungus and at the same time, the cell death creates an exclusion zone for the biotrophic pathogen.

Acetyl-CoA is one of the most important metabolic intermediates in the pathways regulating cellular energetics and in the biosynthesis of a diverse range of metabolites (**Figure 3A, B and C**). In the TCA cycle, acetyl-CoA is broken down and used for energy and carbon skeleton generation. The products of a number of metabolic pathways such as sugars, amino acids, fatty acids and pyruvate are used to generate this important intermediate. Indeed, genes involved in the degradation of branched-chain amino acids such as valine, leucine and isoleucine showed higher expression in the DS and in the incompatible interaction, while no change in expression was detected in the compatible interaction (**Figure 4A**). These data strongly suggest that these branched-chain amino acids serve as a source of TCA cycle intermediates such as succinyl-CoA and acetyl-CoA, as well as being the direct electron donors of the mitochondrial electron transport chain (Ishizaki et al., 2005; Ishizaki et al., 2006; Araújo et al., 2010; Araujo et al., 2011). HR-associated repression of photosynthesis-related genes forces the cells to use aerobic oxidation as the primary source of energy. Interestingly, genes involved in the aerobic oxidation of organic molecules, in particular those encoding enzymes playing a role in fatty acid oxidation, showed a remarkably higher expression in the DS and incompatible interaction, as compared to the susceptible plants (**Figure 4B, Supplementary Table S3**).



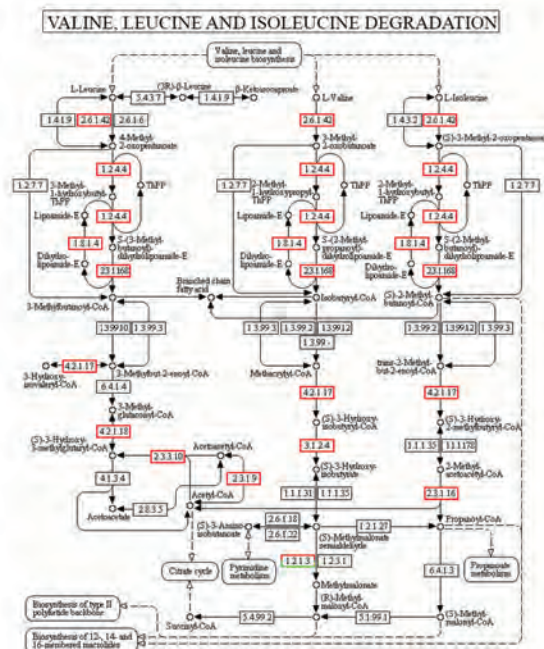
Panels **A**, **B** and **C** represent the expression profiles of genes involved in the TCA cycle and the electron transport chain of cellular energetics in the incompatible, DS and compatible interactions, respectively.

genes in this pathway showed slight up-regulation of their expression (**Supplementary Figure S3C, Supplementary Table S3**). In the DS, expression of genes involved in tryptophan biosynthesis was suppressed, while expression of genes involved in tryptophan degradation was up-regulated (**Supplementary Table S4, Supplementary Figure S4**). The degradation of tryptophan results in the formation of acetyl-CoA, while the suppression of its biosynthesis could potentially result in the enrichment and redirection of shared precursors towards phenylalanine or tyrosine biosynthesis (Penfield et al., 2006). In higher plants the shikimate pathway synthesizes chorismate, which can be converted to tryptophan, phenylalanine or tyrosine. Chorismate is either converted into anthranilate by anthranilate synthase or is directed to tryptophan biosynthesis, or to prephenate by chorismate mutase and then to phenylalanine or tyrosine (Herrmann and Weaver, 1999). The combined transcriptome and metabolome profiling of the DS revealed high expression of genes involved in the biosynthesis of phenylalanine and tyrosine, as well as the accumulation of phenylalanine, tyrosine and secondary metabolites derived from them during mounting of the HR (Etalo et al., 2013).

Similarly, genes involved in the degradation of histidine showed significantly higher levels of expression in the DS and in the incompatible interaction, as compared to the compatible one (**Supplementary Figure S4, Supplementary Table S4**). The degradation of histidine gives rise to glutamate, the precursor for the gamma amino butyric acid (GABA) shunt for the production of GABA. Under energy-demanding conditions, like the systemic activation of defense, pyruvate is produced in high amounts and pyruvate dehydrogenase (PDH) activity becomes a rate-limiting enzyme in converting pyruvate into acetyl-CoA (Bolton et al., 2008). Hence, the GABA shunt provides an alternative means to utilize the excess of pyruvate for energy production. Glutamate decarboxylase (GAD) is the rate-limiting enzyme in the GABA shunt and the encoding gene showed significantly higher expression in the DS (**Supplementary Figure S5A**). The re-channelling of malate to pyruvate can also be traced by the activation of malate dehydrogenase in the DS and the incompatible interaction (**Figures 3A and 3C**, see the arrow that links malate to pyruvate). The product of the GABA shunt, GABA, also strongly accumulated in the DS (**Supplementary Figure S5B**). Indeed, the accumulation of GABA in several plant species upon exposure to various biotic and abiotic related stress conditions has been reported (An et al., 2005; Shelp et al., 2006; van Kan, 2006; Neilson et al., 2013).

In conclusion, the majority of the catabolic processes converge towards the generation of acetyl-CoA that acts as primary precursor for the energy-generating pathway and for the generation of primary and secondary metabolites required during mounting of the defense response.

A



B

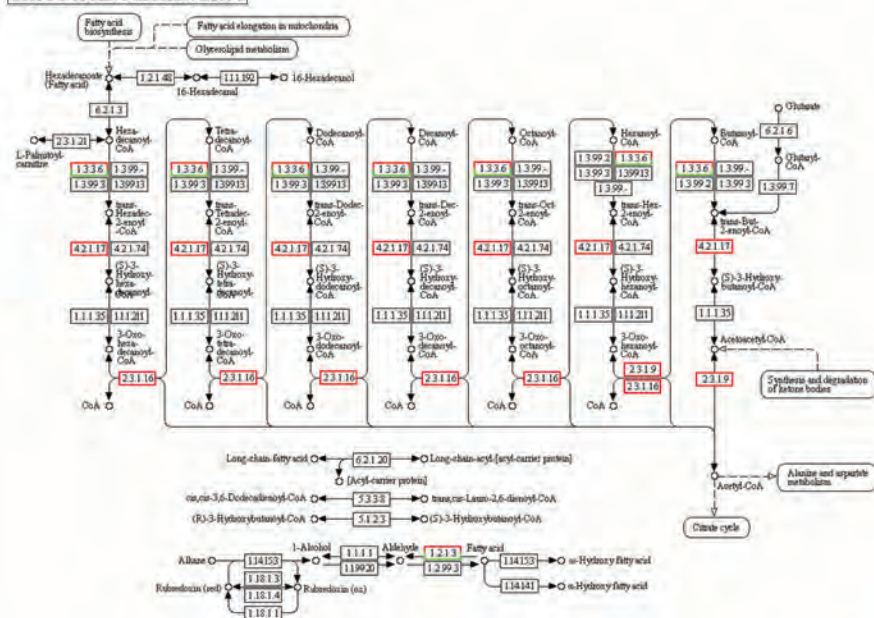
FATTY ACID METABOLISM

Figure 4. Induction of genes involved in the generation of acetyl-CoA from branched-chain amino acids (A) and through fatty acid (B) metabolism. Differentially regulated genes (fold change above 2 and *P* value of 0.001 after FDR correction) in the dying seedlings when compared to the parental lines were mapped to the KEGG pathway. Red boxes indicate that the gene encoding the particular enzyme is up-regulated, while green boxes indicate down-regulation of the encoding genes. Half green/half red boxes indicate that more than one gene was mapped to a particular EC number and that some are up- and some are down-regulated.

The HR is characterised by the suppression of energetically costly cellulose biosynthesis and cell wall modification

The plant cell wall represents a first line of defence against pathogenic microorganisms. It is primarily composed of cellulose, hemicellulose and pectin. This carbon-rich polysaccharide complex represents a useful energy source for pathogen growth and proliferation (Cantu et al., 2008). Through co-evolution, many pathogens developed a strategy to penetrate the plant tissues and to catabolize this carbon source by secreting a mixture of cell wall-degrading enzymes, such as polygalacturonases, pectin methyl esterases, pectin/pectate lyases, xylanases, and endoglucanases (An et al., 2005; Bechtold et al., 2005; Chandra-Shekara et al., 2006; Shelp et al., 2006; van Kan, 2006). Plants use similar enzymes to modify the cell wall during cell wall expansion – occurring during growth – and in fruit ripening (Klessig et al., 2000; Nurnberger et al., 2004; Evrard et al., 2009). These plant cell wall-modifying and -degrading enzymes also represent a potential target for pathogenic microorganisms. In line with this, in the compatible interaction between tomato and *C. fulvum*, the majority of the genes involved in cell wall modification (11 out of the 13 (~85%) DEGs assigned to this biological process in MAPMAN), showed up-regulation, while in the DS and incompatible interaction respectively only 8 out of the 24 DEGs (~33%) and 3 out of the 17 (~18%) DEGs involved in cell wall modification showed up-regulation (**Supplementary Table S5**, bin 10.7).

Actually, in the DS and in the incompatible interaction many cell wall biosynthesis, modification and degradation pathway-related genes were suppressed (**Supplementary Tables S1 and S5 and Figure 5**). In the DS, MAPMAN analysis showed that there were 136 differentially regulated genes involved in cell wall metabolism of which 98 (72%) were down-regulated, while 37 (28%) were up-regulated (**Figure 5, Supplementary Table S5**). Among the down-regulated ones were genes encoding enzymes involved in cellulose biosynthesis, cell wall modification, cell wall precursor biosynthesis and cell wall degradation (cellulases and β -1,4-glucanases, mannan-xylose-arabinose-fucose, pectate lyases and polygalacturonases and pectin methyl esterases) and cell wall proteins (arabinogalactan proteins (AGPs) and LRRs). Among the up-regulated ones were genes involved in hemicellulose biosynthesis, cell wall modification, cell wall precursor biosynthesis, cell wall proteins (reversibly glycosylated polypeptide (RGP)) and cell wall degradation (cellulases and β -1,4-glucanases, pectate lyases and polygalacturonases and pectin methyl esterases) (**Figure 5 and Supplementary Table S5**).

Cellulose is primarily targeted by a cocktail of enzymes produced by pathogens for its degradation, whereas its biosynthesis by the plant is energetically costly. One of the astonishing features of the HR in resistant plants is the strong downregulation of the energetically costly cellulose biosynthesis (**Figure 5A and B, bin 17, Supplementary Table S5**, bin 10.2). Interestingly, genes involved in

hemicellulose biosynthesis, which is a relatively small molecule with less energy and carbon demand for its biosynthesis (Scheller and Ulvskov, 2010), showed up-regulation in the DS (**Figure 5C**, bin 16, **Supplementary Table S5**, bin 10.3).

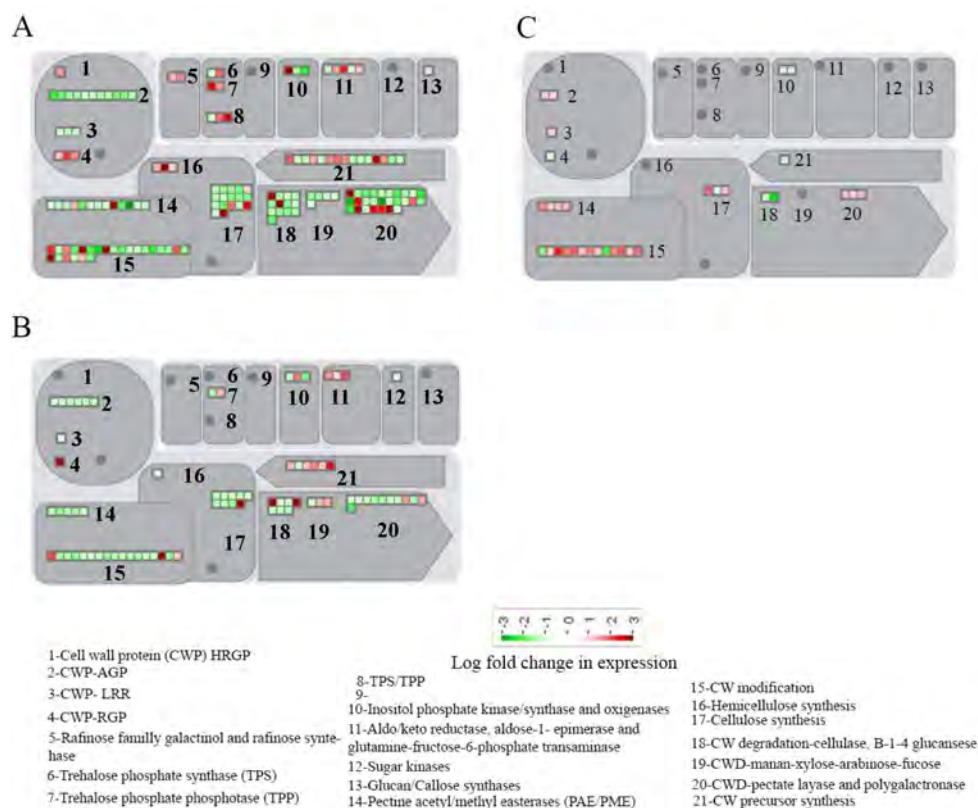


Figure 5. MAPMAN overview of the expression profile of differentially expressed genes (fold change above 2 and P value of 0.001 after FDR correction), involved in carbohydrate and cell wall metabolism in (A) compatible interaction, (B) incompatible interaction and (C) in the dying seedlings.

Hemicellulose plays an important role in strengthening of the cell wall by interaction with cellulose and, in some plants, with lignin (Scheller and Ulvskov, 2010). The low level of reprogramming of cell wall-related processes that does occur in the compatible interaction could be due to the low level of basal defence induction which is also manifest in the low reprogramming of energy metabolism as discussed above (**Figure 3**). The combined transcriptome and metabolome profiling of the DS revealed a strong transcriptional up-regulation of genes involved in the hydroxycinnamic acid amide (HCAA) biosynthesis and the accumulation of these metabolites in the DS during mounting of the HR (Etalo et al., 2013). In the presence of peroxidase activity, these HCAs cross-link within the cell wall and make the cell wall less digestible for pathogenic fungi (Dong, 2004). Indeed, the

majority of the peroxidases (17 out of the 23 differentially regulated ones) showed up-regulation and 14 out of these 17 up-regulated genes showed a fold change in expression above 5 (**Supplementary Table S6**). This result, in combination with the observed down-regulation of cell wall biosynthesis-related genes, could be considered as a less energetically costly strategy of cell wall reinforcement.

The HR is characterised by activation of the mevalonate (MVA) pathway and suppression of the methylerythritol 4-phosphate/ deoxyxylulose 5-phosphate (MEP/DOXP) pathway

All isoprenoids are derived from the common precursor isopentenyl diphosphate (IPP), which in plants is synthesized via the terpenoid backbone biosynthesis pathway (isoprenoid pathway). IPP synthesis involves two pathways, the mevalonate (MVA) pathway that is common to all eukaryotes and is localised in the cytosol, and the methylerythritol 4-phosphate/ deoxyxylulose 5-phosphate (MEP/DOXP) pathway, which is localized in the plastids (Logemann and Hahlbrock, 2002; Griebel and Zeier, 2008; Vranova et al., 2012) (**Figure 6A**). These pathways provide important precursors and intermediates for several biosynthetic pathways involved in almost all biological processes in plants, including the biosynthesis of carotenoids, chlorophylls, phyloquinone, plastoquinone, ubiquinone cytochrome a, steroids, the plant brassinosteroid hormones (BRs), abscisic acid (ABA), gibberellic acid (GA), cytokinins, strigolactones and terpenoids (mono-, sesqui-, di-, and tri-terpenoids) (Vranova et al., 2012). Most of the plant hormones produced through these pathways are involved in growth and development and the terpenoids are known to be amongst the major induced metabolites during the defence response of Solanaceous plants. Hence, the involvement of the pathway in both growth and defence makes it one of the potential pathways where the trade-off between growth and the immune response is determined.

Several hypotheses have been postulated to explain how plants can minimize the overall fitness costs of secondary metabolite biosynthesis (Neilson et al., 2013). One of them is the presence of shared biosynthetic enzymes and intermediates between pathways which is cost-effective and increases the plasticity. Farnesyl diphosphate (FPP) is synthesised through the terpenoid backbone biosynthesis pathway in the cytosol and serves as an intermediate for the biosynthesis of terpenoids, sterols and a number of plant hormones. The mono- and diterpenes and carotenoids are synthesized in the plastid through the MEP/DOXP pathway, whereas sesquiterpenoids and triterpenoids are formed in the cytosol through the MVA pathway. In the DS and incompatible interaction, the carotenoid, chlorophyll and steroid biosynthetic pathways were suppressed, which could favour the availability of precursors for tri- and sesquiterpenoid biosynthesis (**Figures 6A, B and C**). The carotenoids and chlorophylls are generated through the MEP pathway, whereas the steroids are primarily derived through the MVA pathways. Furthermore, within the terpenoid pathway, genes involved in the biosynthesis of monoterpenoids were also significantly down-regulated, while genes involved in the degradation of monoterpenes

showed up-regulation in the DS and incompatible interaction (**Supplementary Table S7**). Unlike genes involved in monoterpene biosynthesis, some genes involved in sesquiterpene and diterpene biosynthesis showed massive up-regulation in the DS and also in the incompatible interaction (**Supplementary Table S7**). In support of the transcriptional up-regulation of these genes, headspace analysis of the DS revealed significantly higher level of α -copaene (a sesquiterpene) emission during mounting of the HR, as compared to the PLS (**Figure 6D**). The induction of α -copaene emission is also reported during the infection of tomato by *Botrytis cinerea* (Genoud et al., 2002). One of the five highly expressed sesquiterpene synthase-encoding genes (soly07g052120.2.1) in the DS and incompatible interaction has high sequence homology (92% identity at nucleotide level) with the well characterized potato α -copaene synthase (Morris et al., 2011).

The suppression of 1-deoxy-D-xylulose-5-phosphate synthase (DXS), the first committed enzyme in the MEP/DOXP pathway that provides the substrate for GA and cytokinin biosynthesis, could represent a mechanism by which the balance between plant defence and growth is maintained (**Figure 6A and 6C, Supplementary Table S7**). Furthermore, in the MVA pathway, the selective suppression of steroid and BRs biosynthesis serves the same purpose. Moreover, BRs are associated with the suppression of PTI, hence their repression ensures an elevated level of basal defence during infection (Albrecht et al., 2012). Considering the importance of these pathways for defence, the major regulators of the MEP/DOXP pathway could potentially be targeted by effectors of pathogens. In support of this observation, GA and BRs biosynthesis are indeed induced in barley roots colonized by the mutualistic fungus *Piriformospora indica* (Zhang et al., 2010).

The HR is characterized by a significant reduction in T-6-P and accumulation of trehalose

Interestingly, the DS contain a high level of trehalose as compared to the PLS, already at $t = 0$ hr when the temperature and humidity shift had not taken place yet (**Figure 7A**). An intermediate in the biosynthesis of trehalose, trehalose-6-phosphate (T-6-P), is derived from glucose-6-phosphate (G-6-P) and UDP-glucose and plays a critical role as a cellular energy gauge of plants. A high level of T-6-P correlates with high cellular sucrose levels and has often been associated with the induction of energy-consuming anabolic processes, like growth (Lunn et al., 2006; Zhang et al., 2009; Paul et al., 2010; Delatte et al., 2011). Although the mechanism of sugar sensing in plants remains elusive, it has been established that a low T-6-P level is tightly linked with the activation of SnRK1, which in its turn activates a wide range of energy-generating and energy-conserving catabolic processes (Baena-Gonzalez et al., 2007; Zhang et al., 2009; Paul et al., 2010; Delatte et al., 2011). In line with this, we quantified the T-6-P levels in the DS at same time points as we used for trehalose quantification and compared the levels with those of the PLS. T-6-P levels in the DS were already much lower than in the PLS prior to the temperature and humidity shift (at $t = 0$ hr) and at 1 hr after transfer, whereas at later time points (5hr) the difference with the PLS was less but T-6-P levels were still significantly lower in the DS (**Figure 7B**).

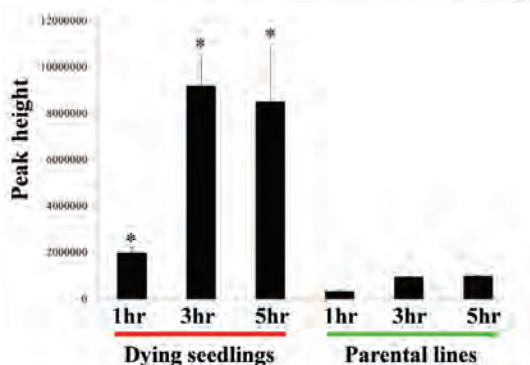
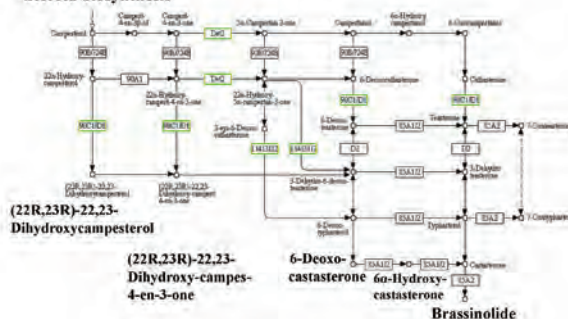


Figure 6. Preferential diversion of precursors and intermediates towards specific metabolic pathways as a means to save energy and restrain growth and development during mounting of the HR. Pathways representing (A) terpenoid backbone biosynthesis, (B) steroid biosynthesis and (C) brassinosteroid biosynthesis and (D) emission of α -copaene (a sesquiterpene) during mounting of the HR. The α -copaene measurements were done at 1, 3 and 5 hr after the temperature shift that induces the HR in the dying seedlings (DS). Differentially regulated genes (fold change above 2 and *P* value of 0.001 after FDR correction) in the dying seedlings when compared to the parental lines are marked by red and green boxes represent up- and down-regulated gene(s), respectively. Boxes marked half red and half green indicate significantly up- and down-regulated gene(s), respectively.

118

We determined the potential activity levels of SnRK1 in the DS and PLS at the various time points after HR initiation in the DS and did not observe any difference between the various treatments. Still, it is clear that SnRK1 activity is suppressed by increasing the amount of T-6-P present in the assay mix (**Figure 7C**). This indicates that the SnRK1 protein abundance in the DS and the PLS is similar and that the regulation of SnRK1 activity is strictly post-translational and could be determined by the cellular level of T-6-P (**Figures 7B and 7C**). Although the potential activity of SnRK1 is the same in the DS and PLS, especially at the early time points the level of T-6-P is significantly lower in the DS than in the PLS, resulting in a higher actual SnRK1 activity (**Figures 7B and C**).

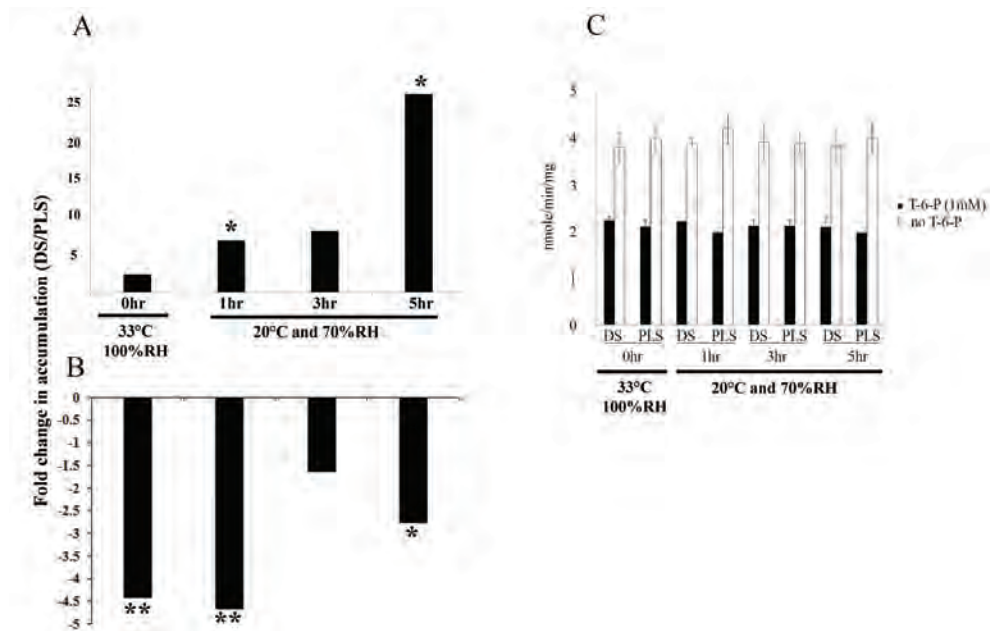


Figure 7. Trehalose and trehalose-6-phosphate (T-6-P) levels and SnRK1 activity during mounting of the HR in the DS, as compared to the PLS.

(A) Temporal fold change in the accumulation of trehalose in the DS as compared to the PLS, during mounting of the HR.

(B) Temporal dynamics of T-6-P in the DS and the PLS.

(C) Potential SnRK1 activity in the DS and PLS over time, in the absence of T-6-P and in the presence of 1 mM T-6-P.

Statistical significance is expressed as (*, $p < 0.05$ and **, $p < 0.01$) when the dying seedlings are compared with the parental lines at each time point.

The correlation that we observe between the T-6-P levels in the DS and the potential SnRK1 activity illustrates the vital role of T-6-P in the regulation of SnRK1 activity, which in turn determines the regulation of anabolic and catabolic processes depending on the physiological condition of the plant (Zhang et al., 2009; Paul et al., 2010; Delatte et al., 2011). To our knowledge this is the first time that defence-associated potential SnRK1 activation is linked with the induction of a whole array of changes in gene

expression, resulting in energy conservation and energy production through catabolic processes and the inhibition of growth during mounting of the HR. At the time of the temperature shift that initiates the HR, the DS are smaller than the PLS (de Jong et al., 2002). This observation shows on the one hand that the DS system is slightly leaky and the activation of defence responses has already been triggered to some extent, as was also demonstrated by the altered metabolome of the DS even before the temperature shift (Etalo et al., 2013). On the other hand, this phenotype is in line with the theory that increased biosynthesis of defence-related metabolites should cause a reduction in growth because of carbon limitation, resulting in a downward adjustment of growth to a level that can be supported by the new level of carbon availability (Smith and Stitt, 2007). The SnRK1-mediated suppressive effect on growth, as a result of the activation of catabolism, could be one of the mechanisms by which plants maintain their energy and carbon homeostasis during the response of plants against pathogens. Moreover, the repression of energy-consuming anabolic processes such as steroid biosynthesis and fatty acid branching and the up-regulation of asparagine synthase and proline dehydrogenase, are additional indicators for increased activation of SnRK1 (**Figure 7B, C and Supplementary Figures S6B, C and D**) (Baena-Gonzalez et al., 2007; Hanson et al., 2008).

Two scenarios could explain the lower T-6-P levels that we observed to be present in the DS (**Figure 7B**). First, these low levels could be attributed to the high consumption of its precursor carbohydrates (G-6-P and UDP-glucose) to support the HR-associated transcriptome and metabolome reprogramming. However, the level of sucrose was even significantly higher in the DS at 1, 3 and 5 hrs after the temperature shift, while fructose and glucose levels were not significantly different between the DS and the PLS (**Supplementary Figure S2**). Maintenance of the relatively high steady-state levels of these mono- and disaccharides could be attributed to the activity of polysaccharide-hydrolysing enzymes in the DS. Indeed, a cell wall invertase (cwINV) was highly transcriptionally up-regulated in the DS and resistant plants inoculated with *C. fulvum* (**Supplementary Table S8, Supplementary Figure S4**). cwINV is found in the cell wall and catalyses the hydrolysis of sucrose into glucose and fructose for energy production and the generation of carbon skeletons for the biosynthesis of large molecules (**Supplementary Figure S4**). One of the cwINVs (soly10g083290.1) that showed extremely high expression in the DS and incompatible interaction (a fold change of 26 and 18, respectively) was down-regulated by 2 fold in the compatible interaction (**Supplementary Table S4**), maybe indicating suppression by virulent *C. fulvum*. Hence, the active conversion of di- and polysaccharides into glucose and its continuous use in the defence-related biosynthesis pool might contribute to the maintenance of low, but stable levels of glucose that would otherwise cause a starvation response in the cell. The second scenario implies an active depletion of T-6-P, as a result of its conversion into

trehalose. Under normal conditions, the level of T-6-P is highly correlated with the levels of sucrose. Possibly, upon the initiation of the HR, and also already before that, high levels of sugars are present for providing the energy to execute the defence response. The continuous presence of sucrose or glucose (**Supplemental Figure S2**) could give rise to relatively high levels of T-6-P, resulting in the suppression of SnRK1 activity that would consequently lead to the activation of energy-consuming, growth-related anabolic processes, which is undesirable during mounting of the defence response. Through an enhanced conversion to trehalose, T-6-P levels could reduce, resulting in the activation of SnRK1 that subsequently leads to the induction of energy-generating and energy-conserving catabolic processes and suppression of energy-demanding growth and development at the same time. Indeed, six genes involved in T-6-P biosynthesis and its subsequent conversion into trehalose were significantly up-regulated in the DS (**Table 1**).

Table 1. Fold change in the expression of genes involved in trehalose-6-phosphate (T-6-P) and trehalose biosynthesis in tomato during mounting of the HR.

ITAG ID	Description (MAPMAN)	ATH best hit and description	FC (DS/PLS)
solyc08g076650.2.1	metabolism.trehalose.TPS	nearly identical to (1422) AT4G17770 AtTPS5, TPS5_Alpha alpha-trehalose-phosphate synthase (UDP-forming)	-2.1
solyc02g072150.2.1	metabolism.trehalose.TPS	nearly identical to (1366) AT1G06410 Symbols: AtTPS7Alpha alpha-trehalose-phosphate synthase (UDP-forming)	3.7
solyc03g007290.2.1	metabolism.trehalose.TPP	moderately similar to (324) AT5G51460 Symbols: AtTPPA Trehalose 6-phosphate phosphatase	5.7
solyc04g072920.2.1	metabolism.trehalose.TPP	moderately similar to AT5G65140 Trehalose-6-phosphate phosphatase	3.0
solyc08g076650.2.1	metabolism.trehalose. potential TPS/TPP	nearly identical to AT4G17770 Symbols: AtTPS5 Alpha alpha-trehalose-phosphate synthase	-2.1
solyc02g072150.2.1	metabolism.trehalose. potential TPS/TPP	nearly identical to AT1G06410 Symbols: AtTPS7-Alpha alpha-trehalose-phosphate synthase (UDP-forming)	3.7
solyc07g006500.2.1	metabolism.trehalose. potential TPS/TPP	nearly identical to AT2G18700 Symbols: AtTPS11_Alpha alpha-trehalose-phosphate synthase (UDP-forming)	6.5

All genes are differentially expressed (fold change above 2 and $P < 0.001$) and corrected for false discovery rate (FDR). The analysis was done based on three independent biological replicates.

ITAG, International Tomato Genome Annotation Group; ATH, *Arabidopsis thaliana*; FC, fold change; DS, dying seedlings; PLS, parental lines; TPS, alpha-trehalose-phosphate synthase; TPP, trehalose-6-phosphate phosphatase.

In conclusion, the high accumulation of trehalose appears to be the consequence of the active lowering of the T-6-P levels, which then results in SnRK1 activation and an increased expression of the genes regulated by SnRK1 kinase. The active depletion of T-6-P suggests a strong autophagic strategy used by the plant to maintain a high level of energy that can be used to mount the HR.

The circadian clock, hormone signalling and photosynthesis during the HR

The co-ordinated repression of auxin, BRs, cytokinins and GA biosynthesis- and signalling-related genes, in addition to genes involved in the circadian clock and in light harvesting and downstream photosynthetic processes, indicates the existence of an interaction between light, stress and hormone signalling pathways (**Figures 6 and 8, Supplementary Figure S1 and Supplementary Table S1**, bins 1, 17.2.2, 17.3, 17.6, 27.3.40 and 30.1) (Nemhauser et al., 2004; Bancos et al., 2006; Covington and Harmer, 2007; Alabadi and Blazquez, 2009; Arana et al., 2011). The circadian clock plays an important role in the interaction of plants with biotrophic pathogens as the life cycle of the pathogen is intimately linked with the host metabolism, which in turn is controlled by the cycle of day and night (Wang et al., 2011). Hence, the interaction of pathogens with their host may also be controlled by the circadian clock. This is especially likely as plants do not have specialized immune cells and their immune response has to be finely balanced with other cellular functions. Auxins, BRs, cytokinins, GA and strigolactones all have been implicated in the modulation of plant growth and development (Brian, 1959; Clouse and Sasse, 1998; Ferguson and Beveridge, 2009; Werner and Schmülling, 2009; Zhao, 2010). Restraining of growth-related processes is essential during the plant defence response to pathogens. The circadian clock has been found to regulate the expression of components involved in nearly every step in the auxin-signalling pathway, from its synthesis to the actual response to the hormone (Covington and Harmer, 2007). A time-dependent transcriptional co-expression analysis of the DS and the PLS also revealed the presence of a cluster of genes with significant SORLIP4 (phytochrome A-regulated gene expression) motif enrichment (Etalo et al., 2013). This cluster represents genes mostly associated with the circadian rhythm and light signalling.

All of the differentially regulated TCP transcription factors (8 genes in total) were down-regulated in the DS (**Supplementary Table S9**). TCP transcription factors are implicated in multiple aspects of developmental control and for example *TCP4* mutants showed a growth-arrest phenotype (Palatnik et al., 2003). Accumulating evidence showed the involvement of the circadian clock in the regulation of the isoprenoid pathway (Rodriguez-Concepcion et al., 2004; Dudareva et al., 2005; Rodriguez-Villalon et al., 2009; Vranová et al., 2013). Furthermore, the MEP/DOXP pathway showed rhythmicity and was shown to be controlled by the circadian clock (Dudareva et al., 2005). The major plant growth regulators such as the BRs, GA, cytokinins, strigolactones, carotenoids and



To validate gene expression profiles observed in the DS and PLS, the Cf0:*Avr4* (susceptible) and Cf0:*Cf-4* (resistant) parental tomato lines were also inoculated with *C. fulvum* race 5, which produces (de Wit, 1977). Three independent biological replicates were used, each consisting of three plants. Mock-treated susceptible and resistant plants were used as controls. Leaves were harvested 6 days after inoculation with the fungus, immediately frozen, ground to a fine powder in liquid nitrogen, and stored at -80°C until further use.

RNA isolation and RNA-seq analysis

The RNA-seq analysis was performed at the Beijing Genome Institute (BGI) (Beijing, China). For this, RNA was isolated from 100 mg of tomato leaf tissue, using 1 ml of Trizol reagent (Invitrogen) according to the manufacturer's instructions. The total RNA was treated with DNase-I Amplification Grade (Invitrogen) and purified with an RNeasy Mini kit (Qiagen). Beads with oligo(dT) were used to isolate poly(A) mRNA from the total RNA. Fragmentation buffer was added to section the mRNA into short fragments. Taking these short fragments as templates, random hexamer primers were used to synthesize the first-strand cDNA. The second-strand cDNA was synthesized using buffer, dNTPs, RNase H and DNA polymerase I. Short fragments were purified with the QiaQuick PCR extraction kit and resolved with EB buffer for end reparation and adding poly(A). After that, the short fragments were connected with sequencing adaptors. For amplification with PCR, suitable fragments were selected, as templates, with respect to the result of agarose gel electrophoresis. The library was sequenced using Illumina HiSeq™ 2000. Clean reads were mapped onto the tomato reference genome and gene sequences, using SOAP2 (Li et al., 2009). Mismatches of no more than 5 bases were allowed in the alignment. For the calculation of Unigene expression the RPKM method (Reads Per Kb per Million reads) was used (Mortazavi et al., 2008). When there was more than one transcript for a gene, the longest one was used to calculate its expression level and coverage. In our analysis, differentially expressed genes (DEGs) with a *P* value after false discovery rate (FDR) correction of ≤ 0.001 and a fold change (treatment/control) ratio larger than 2 were used for GO functional analysis and KEGG Pathway analysis. Hereto, all DEGs were first mapped to GO terms in the database (<http://www.geneontology.org/>), calculating gene numbers for every term. Then the ultra-geometric test was used to find significantly enriched GO terms in DEGs by comparing them to the genome background. Furthermore, pathway enrichment analysis was performed to identify significantly enriched metabolic pathways or signal transduction pathways in DEGs compared with the whole genome background.

Analysis of metabolites and determination of SnRK1 activity

Polar primary metabolites were extracted following the procedure described by Lisec and co-workers (Lisec et al., 2006) with minor modifications, as described by Etalo et

al. (2013). To analyse Volatile Organic Compounds (VOCs), one pot with 10 seedlings was placed in a 1 liter air-tight transparent glass jar and the headspace of the plants was collected using tenax adsorption that are mounted in the glass jar while the system was continuously flushed with fresh air (Tikunov et al., 2007). Headspace samples were analysed with a Thermo Trace gas chromatograph, connected to a Thermo Trace DSQ quadrupole mass spectrometer (Thermo Fisher Scientific, Waltham). Before thermal desorption, cartridges were flushed with helium at 50 ml/min for 20 min to remove moisture and oxygen. After flushing, the collected volatiles were desorbed from the cartridges at 220°C (Ultra; Markes, Llantrisant) for 5 min with a helium flow of 30 ml/min with a split ratio of 1:1. The released compounds were focused on an electrically cooled sorbent trap (Unity; Markes, Llantrisant) at a temperature of 10°C. Volatiles were injected onto the analytical column (ZB-5MSi, 30 m x 0.25 mm ID, 1.0 µm – film thickness, Zebron, Phenomenex) with a split flow of 40 mL/min by ballistic heating of the cold trap to 250°C for 3 min. The temperature program started at 40°C (3 min hold) and rose with 10°C/min to 280°C (3 min hold). The column effluent was ionized by electron impact (EI) at 70 eV. Mass scanning was done from 45 to 450 *m/z* with a scan time of 6 scans/sec. The ion source temperature was set to 250°C and the transfer line was set to 275°C. The eluted compounds were identified using Xcalibur software (Thermo, Waltham) by comparing the mass spectra with those of authentic reference standards.

Samples for trehalose-6-phosphate (T-6-P) quantification were harvested, snap frozen in liquid nitrogen, and ground to a fine powder before extraction. T-6-P was analysed by the combination of liquid- and solid-phase extractions, followed by ion exchange chromatography-mass spectrometry according to Delatte et al. (2009). The method allowed baseline separation of phosphorylated-disaccharides such as: T-6-P, sucrose-6-phosphate, and the internal standard lactose-1-phosphate at the mass-to-charge ratio of T-6-P. Lactose-1-phosphate was used as an internal standard because it is not synthesized by plants. SnRK1 was assayed in the presence or absence of 1 mM T-6-P by determining phosphorylation of the AMARA peptide as described by Zhang et al. (2009).

Acknowledgements

We wish to thank Bert Schipper (Plant Research International (PRI)), for technical assistance with primary and secondary metabolite analysis and Bert Essenstam for taking care of the plants. We thank all people in the Metabolomics groups of the Laboratory of Plant Physiology (Wageningen University) and of PRI for their kind support. This project was (co)financed by the Centre for BioSystems Genomics (CBSG; to DWE, RCHDV, MHAJJ and HJB) and The Netherlands Metabolomics Centre (to RCHDV) which are both part of the Netherlands Genomics Initiative / Netherlands Organisation for Scientific Research.

References

- Alabadi D, Blázquez MA** (2009) Molecular interactions between light and hormone signaling to control plant growth. *Plant Mol Biol* **69**: 409-417
- Albrecht C, Boutrot F, Segonzac C, Schwessinger B, Gimenez-Ibanez S, Chinchilla D, Rathjen JP, de Vries SC, Zipfel C** (2012) Brassinosteroids inhibit pathogen-associated molecular pattern-triggered immune signaling independent of the receptor kinase BAK1. *Proc Natl Acad Sci USA* **109**: 303-308
- An HJ, Lurie S, Greve LC, Rosenquist D, Kirmiz C, Labavitch JM, Lebrilla CB** (2005) Determination of pathogen-related enzyme action by mass spectrometry analysis of pectin breakdown products of plant cell walls. *Anal Biochem* **338**: 71-82
- Arana MV, Marín-de la Rosa N, Maloof JN, Blázquez MA, Alabadí D** (2011) Circadian oscillation of gibberellin signaling in Arabidopsis. *Proc Natl Acad Sci USA* **108**: 9292-9297
- Araújo WL, Ishizaki K, Nunes-Nesi A, Larson TR, Tohge T, Krahnert I, Witt S, Obata T, Schauer N, Graham IA, Leaver CJ, Fernie AR** (2010) Identification of the 2-hydroxyglutarate and isovaleryl-CoA dehydrogenases as alternative electron donors linking lysine catabolism to the electron transport chain of Arabidopsis mitochondria. *Plant Cell* **22**: 1549-1563
- Araujo WL, Tohge T, Ishizaki K, Leaver CJ, Fernie AR** (2011) Protein degradation - an alternative respiratory substrate for stressed plants. *Trends Plant Sci* **16**: 489-498
- Baena-Gonzalez E, Rolland F, Thevelein JM, Sheen J** (2007) A central integrator of transcription networks in plant stress and energy signalling. *Nature* **448**: 938-942
- Bancos S, Szatmári A-M, Castle J, Kozma-Bognár L, Shibata K, Yokota T, Bishop GJ, Nagy F, Szekeres M** (2006) Diurnal regulation of the brassinosteroid-biosynthetic CPD gene in Arabidopsis. *Plant Physiol* **141**: 299-309
- Bechtold U, Karpinski S, Mullineaux PM** (2005) The influence of the light environment and photosynthesis on oxidative signalling responses in plant-biotrophic pathogen interactions. *Plant Cell Environ* **28**: 1046-1055
- Blasing OE, Gibon Y, Gunther M, Hohne M, Morcuende R, Osuna D, Thimm O, Usadel B, Scheible WR, Stitt M** (2005) Sugars and circadian regulation make major contributions to the global regulation of diurnal gene expression in Arabidopsis. *Plant Cell* **17**: 3257-3281
- Bolton MD** (2009) Primary metabolism and plant defense--fuel for the fire. *Mol Plant Microbe Interact* **22**: 487-497
- Bolton MD, Kolmer JA, Xu WW, Garvin DF** (2008) Comparative transcript profiling of Lr1- and Lr34-mediated leaf rust resistance in wheat. *Phytopathology* **98**: S24-S24
- Bonfig KB, Schreiber U, Gabler A, Roitsch T, Berger S** (2006) Infection with virulent and avirulent *Psyringae* strains differentially affects photosynthesis and sink metabolism in Arabidopsis leaves. *Planta* **225**: 1-12
- Brian PW** (1959) Effects of gibberellins on plant growth and development. *Biol Rev* **34**: 37-77

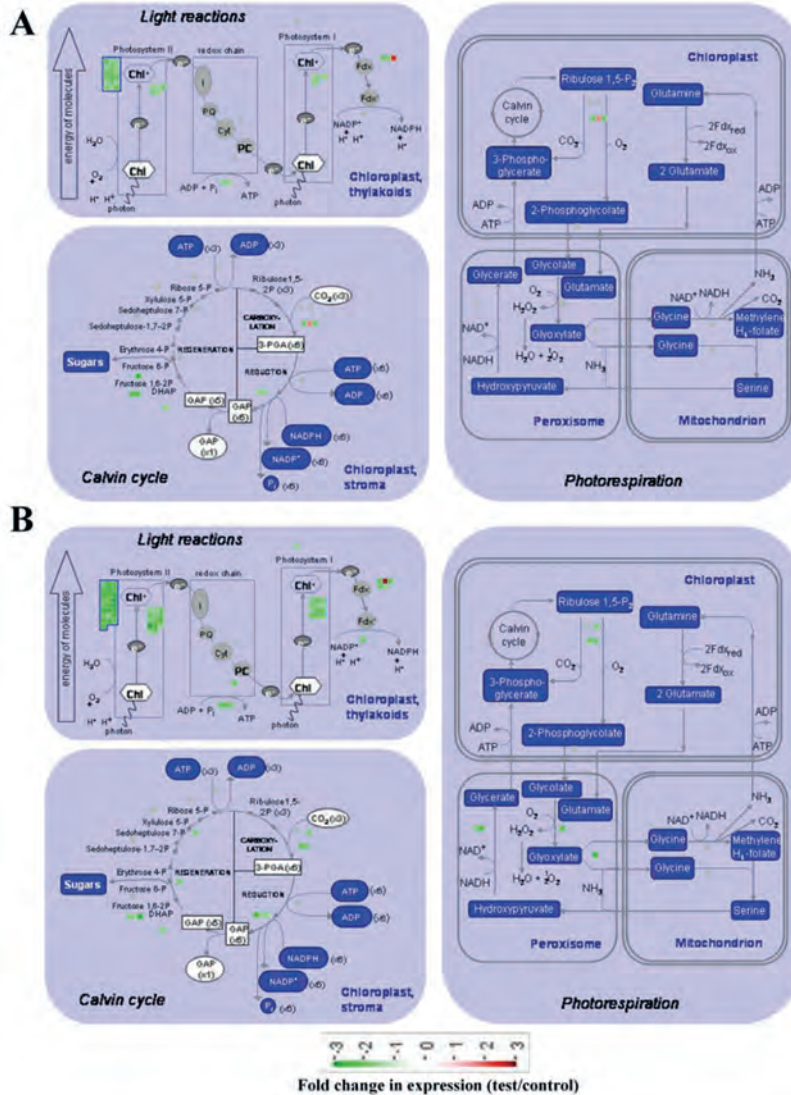
- Cai X, Takken FLW, Joosten MHAJ, De Wit PJGM (2001) Specific recognition of AVR4 and AVR9 results in distinct patterns of hypersensitive cell death in tomato, but similar patterns of defence-related gene expression. *Mol Plant Pathol* **2**: 77-86
- Cantu D, Vicente AR, Labavitch JM, Bennett AB, Powell AL (2008) Strangers in the matrix: plant cell walls and pathogen susceptibility. *Trends Plant Sci* **13**: 610-617
- Chandra-Shekara AC, Gupte M, Navarre D, Raina S, Raina R, Klessig D, Kachroo P (2006) Light-dependent hypersensitive response and resistance signaling against Turnip Crinkle Virus in Arabidopsis. *Plant J* **45**: 320-334
- Chisholm ST, Coaker G, Day B, Staskawicz BJ (2006) Host-microbe interactions: shaping the evolution of the plant immune response. *Cell* **124**: 803-814
- Clouse SD, Sasse JM (1998) Brassinosteroids: Essential regulators of plant growth and development. *Annu Rev Plant Physiol Plant Mol Biol* **49**: 427-451
- Covington MF, Harmer SL (2007) The circadian clock regulates auxin signaling and responses in Arabidopsis. *PLoS Biol* **5**: 1773-1784
- de Jong CF, Takken FLW, Cai XH, de Wit PJGM, Joosten MHAJ (2002) Attenuation of Cf-mediated defense responses at elevated temperatures correlates with a decrease in elicitor-binding sites. *Mol Plant-Microbe Interact* **15**: 1040-1049
- de Wit PJGM (1977) A light and scanning-electron microscopic study of infection of tomato plants by virulent and avirulent races of *Cladosporium fulvum*. *Neth J Plant Pathol* **83**: 109-122
- de Wit PJGM, Joosten MHAJ (1999) Avirulence and resistance genes in the *Cladosporium fulvum*-tomato interaction. *Curr Opin Microbiol* **2**: 368-373
- Delatte TL, Sedijani P, Kondou Y, Matsui M, de Jong GJ, Somsen GW, Wiese-Klinkenberg A, Primavesi LF, Paul MJ, Schlupepmann H (2011) Growth arrest by trehalose-6-phosphate: an astonishing case of primary metabolite control over growth by way of the SnRK1 signaling pathway. *Plant Physiol* **157**: 160-174
- Dodds PN, Rathjen JP (2010) Plant immunity: towards an integrated view of plant-pathogen interactions. *Nat Rev Genet* **11**: 539-548
- Dong X (2004) NPR1, all things considered. *Curr Opin Plant Biol* **7**: 547 - 552
- Dudareva N, Andersson S, Orlova I, Gatto N, Reichelt M, Rhodes D, Boland W, Gershenzon J (2005) The nonmevalonate pathway supports both monoterpene and sesquiterpene formation in snapdragon flowers. *Proc Natl Acad Sci USA* **102**: 933-938
- Etalo DW, Stulemeijer IJE, Peter van Esse H, de Vos RCH, Bouwmeester HJ, Joosten MHAJ (2013) System-wide hypersensitive response-associated transcriptome and metabolome reprogramming in tomato. *Plant Physiol* **162**: 1599-1617
- Evrard A, Ndatimana T, Eulgem T (2009) FORCA, a promoter element that responds to crosstalk between defense and light signaling. *BMC Plant Biol* **9**: 1-13
- Farre EM, Weise SE (2012) The interactions between the circadian clock and primary metabolism. *Curr Opin Plant Biol* **15**: 293-300
- Ferguson BJ, Beveridge CA (2009) Roles for auxin, cytokinin, and strigolactone in regulating shoot branching. *Plant Physiol* **149**: 1929-1944
- Gabriëls SHEJ, Takken FLW, Vossen JH, de Jong CF, Liu Q, Turk SCHJ, Wachowski LK, Peters J, Witsenboer HMA, de Wit PJGM, Joosten MHAJ (2006) cDNA-AFLP combined with functional analysis reveals novel genes involved in the hypersensitive response. *Mol Plant Microbe Interact* **19**: 567-576
- Genoud T, Buchala A, Chua N, Metraux J (2002) Phytochrome signalling modulates the SA-perceptive pathway in Arabidopsis. *Plant J* **31**: 87 - 95
- Griebel T, Zeier J (2008) Light regulation and daytime dependency of inducible plant defenses in Arabidopsis: phytochrome signaling controls systemic acquired resistance rather than local defense. *Plant Physiol* **147**: 790 - 801
- Hanson J, Hanssen M, Wiese A, Hendriks MMWB, Smeekens S (2008) The sucrose regulated transcription factor bZIP11 affects amino acid metabolism by regulating the expression of ASPARAGINE SYNTHETASE1 and PROLINE DEHYDROGENASE2. *Plant J* **53**: 935-949
- Hao L, Wang H, Sunter G, Bisaro DM (2003) Geminivirus AL2 and L2 proteins interact with and inactivate SNF1 kinase. *Plant Cell* **15**: 1034-1048
- Herrmann KM, Weaver LM (1999) The Shikimate Pathway. *Annu Rev Plant Physiol Plant Mol Biol* **50**: 473-503

- Ishizaki K, Larson TR, Schauer N, Fernie AR, Graham IA, Leaver CJ (2005) The critical role of Arabidopsis electron-transfer flavoprotein:ubiquinone oxidoreductase during dark-induced starvation. *Plant Cell* **17**: 2587-2600
- Ishizaki K, Schauer N, Larson TR, Graham IA, Fernie AR, Leaver CJ (2006) The mitochondrial electron transfer flavoprotein complex is essential for survival of Arabidopsis in extended darkness. *Plant J* **47**: 751-760
- Jones JD, Dangl JL (2006) The plant immune system. *Nature* **444**: 323-329
- Klessig D, Durner J, Noad R, Navarre D, Wendehenne D, Kumar D, Zhou J, Shah J, Zhang S, Kachroo P, Trifa Y, Pontier D, Lam E, Silva H (2000) Nitric oxide and salicylic acid signaling in plant defense. *Proc Natl Acad Sci USA* **97**: 8849 - 8855
- Lam E, Kato N, Lawton M (2001) Programmed cell death, mitochondria and the plant hypersensitive response. *Nature* **411**: 848-853
- Li R, Yu C, Li Y, Lam TW, Yiu SM, Kristiansen K, Wang J (2009) SOAP2: an improved ultrafast tool for short read alignment. *Bioinformatics* **25**: 1966-1967
- Lisec J, Schauer N, Kopka J, Willmitzer L, Fernie AR (2006) Gas chromatography mass spectrometry-based metabolite profiling in plants. *Nat Protoc* **1**: 387-396
- Logemann E, Hahlbrock K (2002) Crosstalk among stress responses in plants: pathogen defense overrides UV protection through an inversely regulated ACE/ACE type of light-responsive gene promoter unit. *Proc Natl Acad Sci USA* **99**: 2428 - 2432
- Lunn JE, Feil R, Hendriks JH, Gibon Y, Morcuende R, Osuna D, Scheible WR, Carillo P, Hajirezaei MR, Stitt M (2006) Sugar-induced increases in trehalose 6-phosphate are correlated with redox activation of ADPglucose pyrophosphorylase and higher rates of starch synthesis in *Arabidopsis thaliana*. *Biochem J* **397**: 139-148
- Mano S, Nishimura M (2005) Plant peroxisomes. *Vitam Horm* **72**: 111-154
- Morris WL, Ducreux LJM, Shepherd T, Lewinsohn E, Davidovich-Rikanati R, Sitrit Y, Taylor MA (2011) Utilisation of the MVA pathway to produce elevated levels of the sesquiterpene α -copaene in potato tubers. *Phytochemistry* **72**: 2288-2293
- Mortazavi A, Williams BA, McCue K, Schaeffer L, Wold B (2008) Mapping and quantifying mammalian transcriptomes by RNA-Seq. *Nat Methods* **5**: 621-628
- Neilson EH, Goodger JQD, Woodrow IE, Møller BL (2013) Plant chemical defense: at what cost? *Trends Plant Sci* **18**: 250-258
- Nemhauser JL, Mockler TC, Chory J (2004) Interdependency of brassinosteroid and auxin signaling in Arabidopsis. *PLoS Biol* **2**: 1260-1271
- Nunes C, O'Hara LE, Primavesi LF, Delatte TL, Schluepmann H, Somsen GW, Silva AB, Fevereiro PS, Wingler A, Paul MJ (2013) The trehalose 6-phosphate/SnRK1 signaling pathway primes growth recovery following relief of sink limitation. *Plant Physiol* **162**: 1720-1732
- Nurnberger T, Brunner F, Kemmerling B, Piater L (2004) Innate immunity in plants and animals: striking similarities and obvious differences. *Immunol Rev* **198**: 249 - 266
- Palatnik JF, Allen E, Wu X, Schommer C, Schwab R, Carrington JC, Weigel D (2003) Control of leaf morphogenesis by microRNAs. *425*: 257-263
- Paul MJ, Jhurrea D, Zhang Y, Primavesi LF, Delatte T, Schluepmann H, Wingler A (2010) Upregulation of biosynthetic processes associated with growth by trehalose 6-phosphate. *Plant Signal Behav* **5**: 386-392
- Penfield S, Pinfield-Wells HM, Graham IA (2006) Storage reserve mobilisation and seedling establishment in Arabidopsis. *Arabidopsis Book* **4**: 1-17
- Ramsey KM, Bass J (2011) Circadian clocks in fuel harvesting and energy homeostasis. *Cold Spring Harb Symp Quant Biol* **76**: 63-72
- Rodriguez-Concepcion M, Fores O, Martinez-Garcia JF, Gonzalez V, Phillips MA, Ferrer A, Boronat A (2004) Distinct light-mediated pathways regulate the biosynthesis and exchange of isoprenoid precursors during Arabidopsis seedling development. *Plant Cell* **16**: 144-156
- Rodriguez-Villalon A, Gas E, Rodriguez-Concepcion M (2009) Phytoene synthase activity controls the biosynthesis of carotenoids and the supply of their metabolic precursors in dark-grown Arabidopsis seedlings. *Plant J* **60**: 424-435
- Scharte J, Schon H, Weis E (2005) Photosynthesis and carbohydrate metabolism in tobacco leaves during an incompatible interaction with *Phytophthora nicotianae*. *Plant Cell Environ* **28**: 1421-1435

- Scheller HV, Ulvskov P** (2010) Hemicelluloses. *Annu Rev Plant Biol* **61**: 263-289
- Shelp BJ, Bown AW, Faure D** (2006) Extracellular gamma-aminobutyrate mediates communication between plants and other organisms. *Plant Physiol* **142**: 1350-1352
- Smith AM, Stitt M** (2007) Coordination of carbon supply and plant growth. *Plant Cell Environ* **30**: 1126-1149
- Stulemeijer IJ, Joosten MHJ, Jensen ON** (2009) Quantitative phosphoproteomics of tomato mounting a hypersensitive response reveals a swift suppression of photosynthetic activity and a differential role for hsp90 isoforms. *J Proteome Res* **8**: 1168-1182
- Stulemeijer IJE, Stratmann JW, Joosten MHJ** (2007) Tomato mitogen-activated protein kinases LeMPK1, LeMPK2, and LeMPK3 are activated during the cf-4/Avr4-induced hypersensitive response and have distinct phosphorylation specificities. *Plant Physiol* **144**: 1481-1494
- Swarbrick PJ, Schulze-Lefert P, Scholes JD** (2006) Metabolic consequences of susceptibility and resistance (race-specific and broad-spectrum) in barley leaves challenged with powdery mildew. *Plant Cell Environ* **29**: 1061-1076
- Thimm O, Blasing O, Gibon Y, Nagel A, Meyer S, Kruger P, Selbig J, Muller LA, Rhee SY, Stitt M** (2004) MAPMAN: a user-driven tool to display genomics data sets onto diagrams of metabolic pathways and other biological processes. *Plant J* **37**: 914-939
- Thomma BP, Nurnberger T, Joosten MHJ** (2011) Of PAMPs and effectors: the blurred PTI-ETI dichotomy. *Plant Cell* **23**: 4-15
- Tikunov YM, Verstappen FW, Hall RD** (2007) Metabolomic profiling of natural volatiles: headspace trapping: GC-MS. *Methods Mol Biol* **358**: 39-53
- van Kan JAL** (2006) Licensed to kill: the lifestyle of a necrotrophic plant pathogen. *Trends Plant Sci* **11**: 247-253
- Vranova E, Coman D, Gruissem W** (2012) Structure and dynamics of the isoprenoid pathway network. *Mol Plant* **5**: 318-333
- Vranová E, Coman D, Gruissem W** (2013) Network analysis of the MVA and MEP pathways for isoprenoid synthesis. *Annu Rev Plant Biol* **64**: 665-700
- Wang W, Barnaby JY, Tada Y, Li H, Tor M, Caldelari D, Lee DU, Fu XD, Dong X** (2011) Timing of plant immune responses by a central circadian regulator. *Nature* **470**: 110-114
- Werner T, Schmülling T** (2009) Cytokinin action in plant development. *Curr Opin Plant Biol* **12**: 527-538
- Zhang AP, Liu CF, Sun RC** (2010) Fractional isolation and characterization of lignin and hemicelluloses from triploid of *Populus tomentosa* Carr. *Ind Crop Prod* **31**: 357-362
- Zhang Y, Primavesi LF, Jhurreea D, Andralojc PJ, Mitchell RAC, Powers SJ, Schluepmann H, Delatte T, Wingler A, Paul MJ** (2009) Inhibition of SNF1-related protein kinase1 activity and regulation of metabolic pathways by trehalose-6-phosphate. *Plant Physiol* **149**: 1860-1871
- Zhao Y** (2010) Auxin biosynthesis and its role in plant development. *Annu Rev Plant Biol* **61**: 49-64

Supplemental information

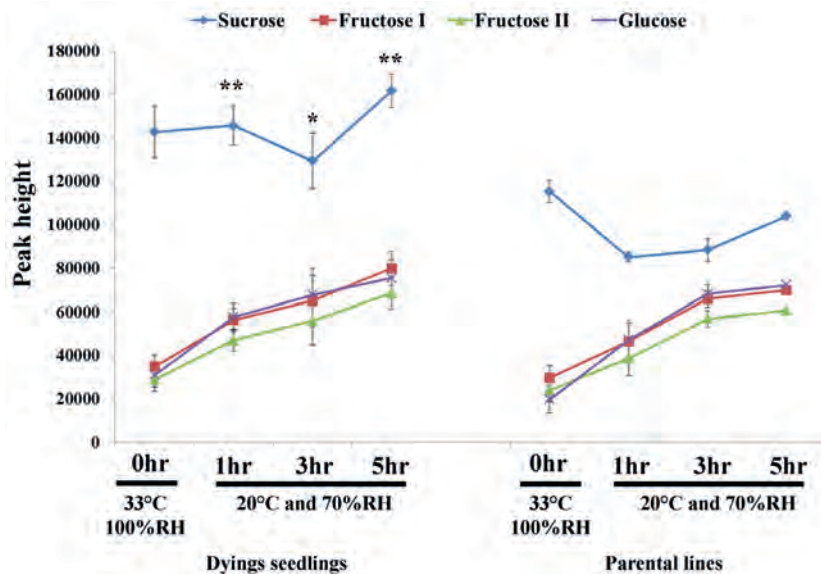
Supplemental Figures



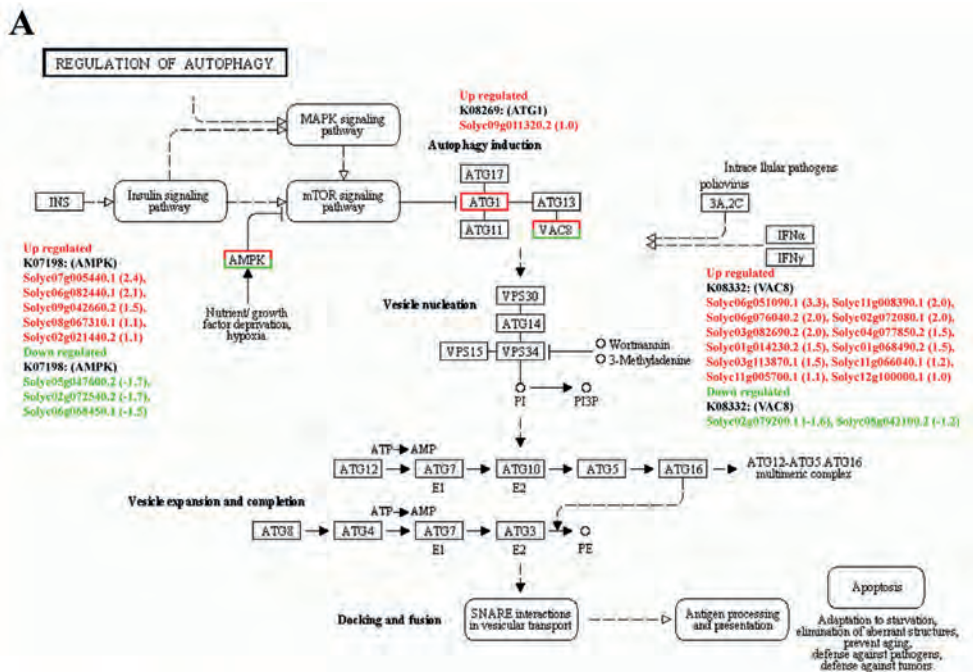
Supplementary Figure S1. Repression of photosynthesis during the incompatible interaction between tomato and *C. fulvum* and in the dying seedlings (DS). The green and red squares in the map represent genes that are down or up-regulated, respectively.

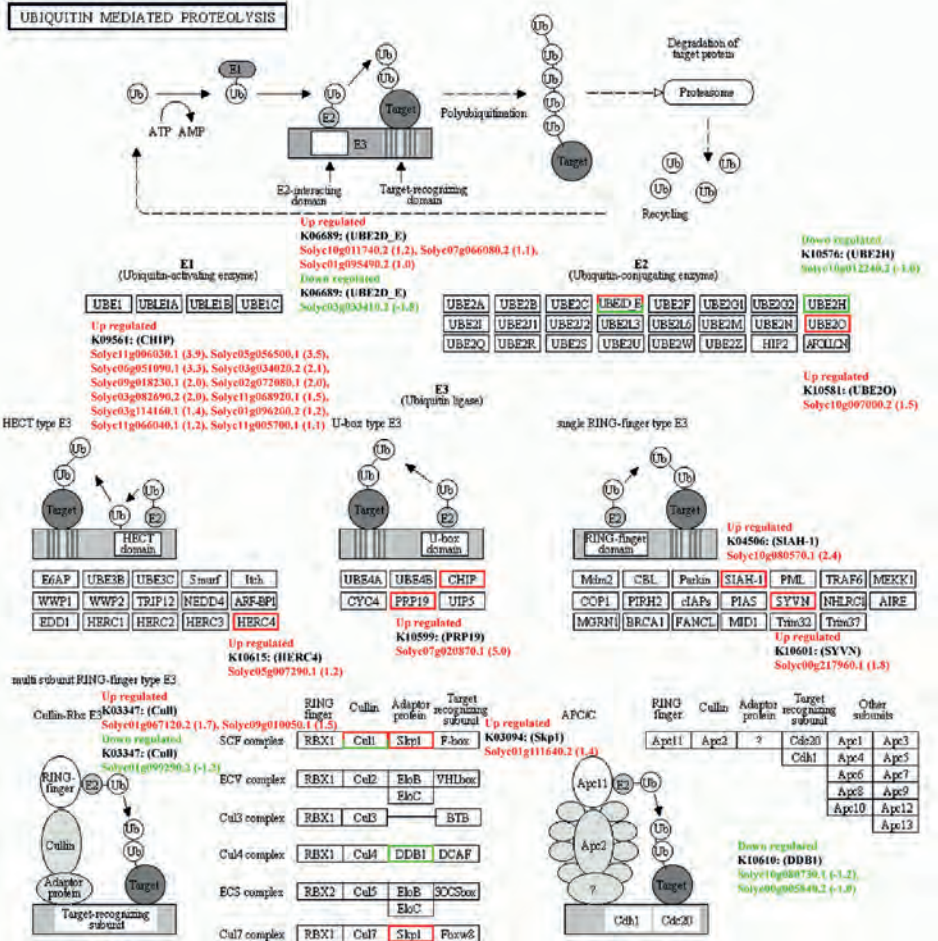
(A) Regulation of photosynthesis-related genes in resistant, inoculated plants (incompatible interaction) compared to mock-inoculated tomato.

(B) Regulation of photosynthesis-related genes in the DS compared to the PLS. All indicated genes are significantly differentially regulated (fold change above 2 and a $P < 0.001$ with FDR correction). Photosynthesis-related processes did not show significant regulation in the compatible interaction (not shown).

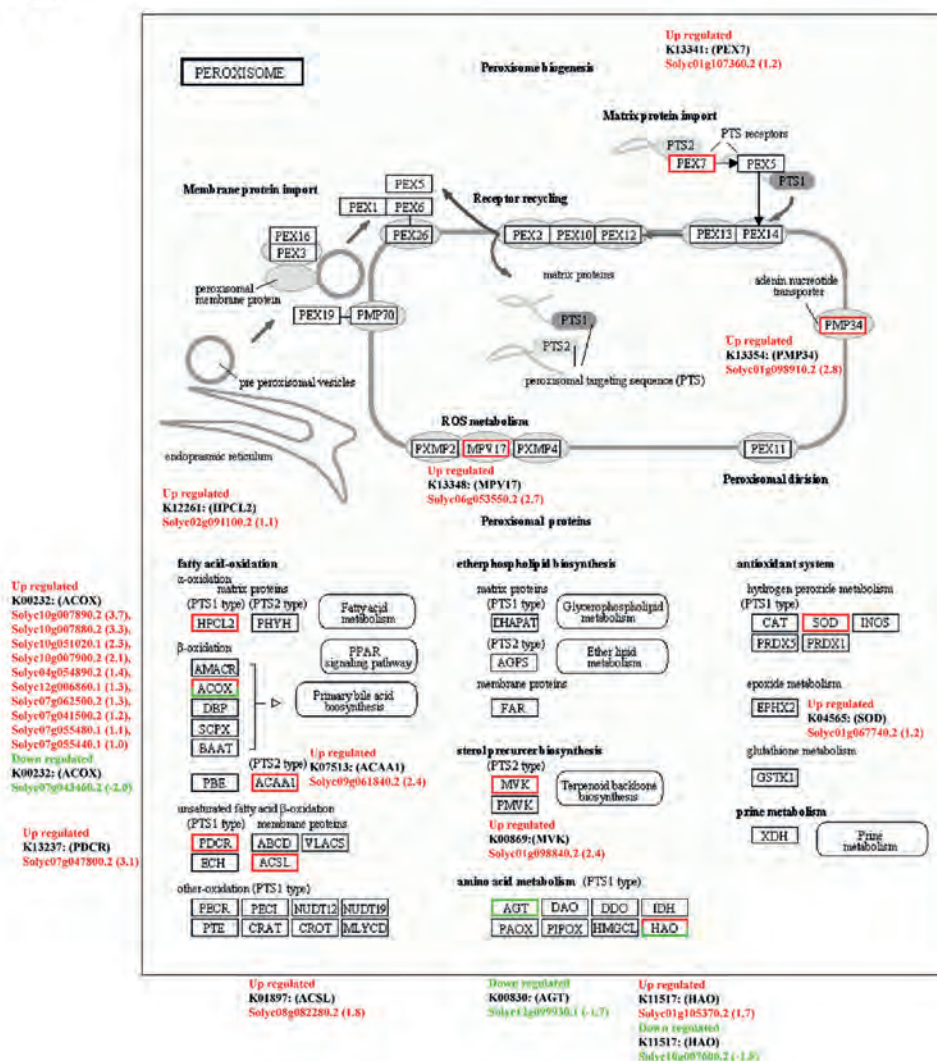


Supplementary Figure S2. The dynamics of sucrose, fructose and glucose levels during the rescue of the dying seedlings (DS) at 33°C and 100% RH and after the temperature shift that induces the HR in the DS, as compared to the parental lines (PLS). Three independent biological replicates were used. The error bars indicate the standard error of the mean. Statistical significance from an independent t-test is expressed as significant (*, $p < 0.05$) and highly significant (**, $p < 0.01$) when the DS are compared to the PLS at the various time points.

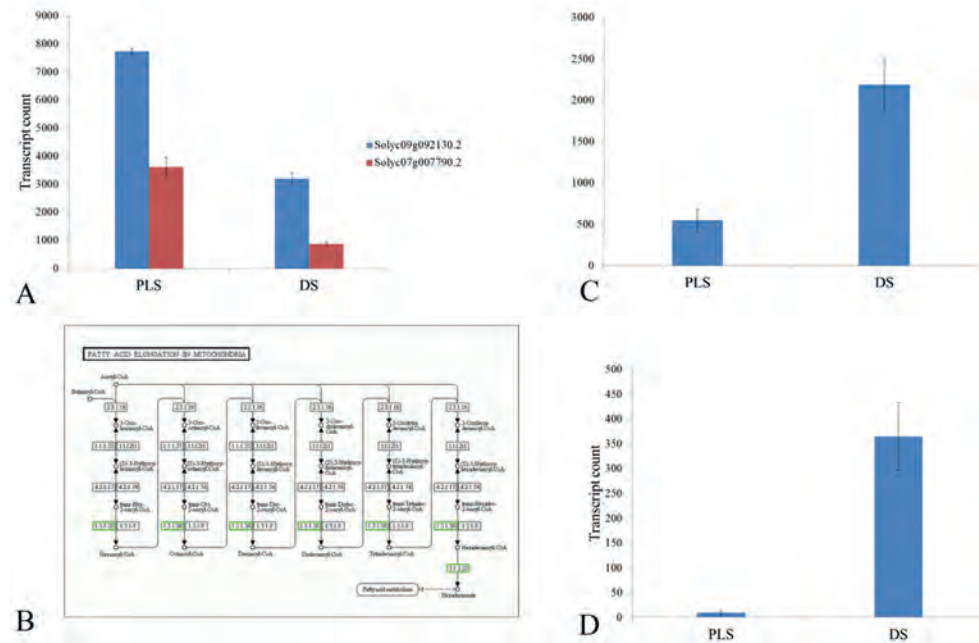


B

C



Supplementary Figure S3. Expression profile of genes involved in autophagy (A), ubiquitin-mediated proteolysis (B) and peroxisomal fatty acid oxidation (C). The green and red boxes represent gene (s) that is/are mapped to the particular bin and are differentially down or up-regulated in the DS, respectively.



Supplementary Figure S6. The behaviour of major indicators of SnRK1 activation and sugar depletion in tomato dying seedlings (DS), as compared to the parental lines (PLS).

(A) Transcript counts for two homologous genes encoding sucrose phosphate synthases in the PLS and the DS, at 5hr after the initiation of the HR in the DS.

(B) Down-regulation of genes involved in fatty acid elongation in DS, as compared to the PLS. Green boxes indicate the genes that are down-regulated in the DS, as compared to the PLS.

(C) Transcript counts for the gene encoding asparagine synthase in the PLS and the DS, at 5hr after the initiation of the HR in the DS.

(D) Transcript counts for the gene encoding proline dehydrogenase in the PLS and the DS, at 5hr after the initiation of the HR in the DS.

Three independent biological replicates were used in all cases. In all cases genes are significantly differentially regulated (fold change above 2 and $P < 0.001$ after FDR correction).

Supplemental Tables

Supplementary Table S1. Wilcoxon rank sum test of differentially regulated genes in the dying seedlings (DS) compared to the PLS, using MAPMAN.

Bin	Name (description)	Elements	Regulation		p-value
			Up	Down	
1	Photosynthesis (PS)	81	1	80	7.34E-15
1.1	PS.lightreaction	65	1	64	1.25E-12
1.1.1	PS.lightreaction.photosystem II	39	0	39	3.98E-11
1.1.1.1	PS.lightreaction.photosystem II.LHC-II	25	0	25	1.70E-09
1.1.1.2	PS.lightreaction.photosystem II.PSII polypeptide subunits	14	0	14	3.10E-03
1.1.2	PS.lightreaction.photosystem I	13	0	13	8.90E-03
1.1.2.2	PS.lightreaction.photosystem I.PSI polypeptide subunits	12	0	12	8.10E-03
1.2	PS.photorespiration	5	0	5	2.60E-02
1.3	PS.calvin cycle	11	0	11	2.20E-02
10	cell wall (CW)	136	38	98	3.00E-09
10.2	CW.cellulose synthesis	17	4	13	1.00E-02
10.2.1	CW.cellulose synthesis.cellulose synthase	6	1	5	4.60E-02
10.5	CW.CW proteins	18	4	14	3.50E-03
10.5.1	CW.CW proteins.AGPs	11	0	11	2.70E-04
10.5.1.1	CW.CW proteins.AGPs.AGP	11	0	11	2.70E-04
10.6	CW.degradation	46	10	36	1.20E-04
10.6.1	CW.degradation.cellulases and beta -1,4-glucanases	13	3	11	1.50E-02
10.6.3	CW.degradation.pectate lyases and polygalacturonases	27	7	20	6.10E-03
10.7	CW.modification	24	8	16	1.20E-02
11.1.8	lipid metabolism (LM).fatty acid (FA) synthesis and FA elongation.acyl coa ligase	8	7	1	4.20E-02
11.2	LM.FA desaturation	9	6	3	2.80E-02
11.2.3	LM.FA desaturation.omega 3 desaturase	7	5	2	1.90E-02
11.8	LM.'exotics' (steroids, squalene etc)	22	7	15	4.70E-02
11.9.4	LM.lipid degradation.beta-oxidation	5	5	0	2.10E-02
13	amino acid metabolism (AAM)	67	44	23	3.10E-04
13.2	AAM.degradation	24	18	6	3.50E-04
13.2.7	AAM.degradation.histidine	8	8	0	1.10E-05
15	metal handling (MH)	18	1	17	1.40E-05
15.2	MH.binding, chelation and storage	12	1	11	2.50E-04
16	secondary metabolism (SM)	98	60	38	1.60E-02
16.2	SM.phenylpropanoids	46	33	13	4.20E-03
16.2.1	SM.phenylpropanoids.lignin biosynthesis	16	15	1	1.60E-04
16.2.1.1	SM.phenylpropanoids.lignin biosynthesis.PAL	7	7	0	9.70E-03
16.2.1.6	SM.phenylpropanoids.lignin biosynthesis.CCoAOMT	4	3	1	4.90E-02

16.7	SM.wax	3	3	0	3.60E-02
17.2.2	hormone metabolism (HM).auxin.signal transduction	6	0	6	1.00E-02
17.3	HM.brassinosteroid (BR)	15	3	12	2.40E-03
17.3.1	HM.BR.synthesis-degradation	12	1	11	1.80E-03
17.3.1.2	HM.BR.synthesis-degradation.sterols	8	1	7	1.50E-02
17.5	HM.ethylene	81	54	27	4.70E-02
17.5.1.1	HM.ethylene.synthesis-degradation.1-aminocyclopropane-1-carboxylate synthase	6	5	1	2.10E-02
17.5.2	HM.ethylene.signal transduction	28	23	5	8.40E-05
17.6	HM.gibberelin (GA)	7	2	5	2.10E-02
17.6.3	HM.GA.induced-regulated-responsive-activated	3	0	3	2.60E-02
18.2	Co-factor and vitamin metabolism.thiamine	3	0	3	3.00E-02
20	Stress	239	169	70	3.00E-06
20.1	stress.biotic	147	113	34	2.70E-07
20.1.1	stress.biotic.respiratory burst	2	2	0	4.30E-02
20.1.7.6	stress.biotic.PR-proteins.proteinase inhibitors	3	3	0	1.50E-02
20.1.7.6.1	stress.biotic.PR-proteins.proteinase inhibitors.trypsin inhibitor	3	3	0	1.50E-02
23.3	nucleotide metabolism (NM).salvage	10	8	2	3.30E-02
23.3.3	NM.salvage.NUDIX hydrolases	10	8	2	2.60E-02
26.12	misc.peroxidases	23	17	6	1.40E-03
26.21	misc.protease inhibitor/seed storage/lipid transfer protein (LTP) family protein	12	3	9	4.60E-02
26.24	misc.GCN5-related N-acetyltransferase	16	13	3	2.20E-02
26.28	misc.GDSL-motif lipase	24	21	3	9.30E-05
26.3	misc.gluco-, galacto- and mannosidases	17	4	13	1.90E-03
26.9	misc.glutathione S transferases	35	33	2	7.80E-08
27.1	RNA.processing	19	12	7	3.20E-02
27.1.19	RNA.processing.ribonucleases	10	9	1	2.80E-04
27.2	RNA.transcription	6	0	6	3.40E-03
27.3.22	RNA.regulation of transcription.HB,Homeobox transcription factor family	18	5	13	9.70E-03
27.3.23	RNA.regulation of transcription.HSF,Heat-shock transcription factor family	13	10	3	2.10E-02
27.3.24	RNA.regulation of transcription.MADS box transcription factor family	3	3	0	4.50E-02
27.3.26	RNA.regulation of transcription.MYB-related transcription factor family	10	2	8	2.50E-02
27.3.27	RNA.regulation of transcription.NAC domain transcription factor family	4	0	4	2.30E-02
27.3.29	RNA.regulation of transcription.TCP transcription factor family	8	0	8	1.80E-03
27.3.32	RNA.regulation of transcription.WRKY domain transcription factor family	38	36	2	1.40E-08
27.3.40	RNA.regulation of transcription.Aux/IAA family	9	2	7	4.20E-03
27.3.6	RNA.regulation of transcription.bHLH,Basic Helix-Loop-Helix family	31	9	22	2.60E-02
27.3.64	RNA.regulation of transcription.PHOR1	9	9	0	6.40E-05

Carbon economy and maintenance of energy homeostasis

27.3.7	RNA.regulation of transcription.C2C2(Zn) CO-like, Constans-like zinc finger family	11	2	9	1.90E-02
27.3.9	RNA.regulation of transcription.C2C2(Zn) GATA transcription factor family	10	2	8	6.80E-03
29.5.9	protein.degradation.AAA type	14	13	1	1.00E-03
30	Signaling	480	331	149	6.20E-14
30.1	signalling.in sugar and nutrient physiology	17	14	3	4.40E-03
30.1.1	signalling.in sugar and nutrient physiology	15	12	3	1.50E-02
30.11	signalling.light	25	2	23	1.50E-06
30.2	signalling.receptor kinases	286	206	80	3.80E-11
30.2.17	signalling.receptor kinases.DUF 26	118	107	11	0.00E+00
30.2.3	signalling.receptor kinases.leucine rich repeat III	15	2	13	1.50E-02
30.3	signalling.calcium	92	77	15	1.20E-10
31.3	cell.cycle	15	1	14	5.70E-04
33	Development	145	58	87	9.80E-04
33.1	development.storage proteins	7	5	2	3.10E-02
33.99	development.unspecified	127	50	77	2.80E-04
34	Transport	315	159	156	3.10E-04
34.13	transport.peptides and oligopeptides	37	7	29	4.40E-09
34.14	transport.unspecified cations	8	7	1	4.00E-02
34.16	transport.ABC transporters and multidrug resistance systems	41	27	14	4.20E-02
34.19	transport.Major Intrinsic Proteins	19	15	4	5.40E-05
34.19.1	transport.Major Intrinsic Proteins.PIP	11	1	10	2.20E-04
34.19.2	transport.Major Intrinsic Proteins.TIP	3	0	3	1.00E-02
34.23	transport.hormones	2	0	2	4.10E-02
34.23.1	transport.hormones.auxin	2	0	2	4.10E-02
34.6	transport.sulphate	6	1	5	4.20E-03

Supplementary Table S2A. Fold change in expression of genes involved in fermentative-related energy generation in the dying seedlings (DS) compared to the parental lines (PLS).

Transcript ID	Description (MAPMAN)	ATH best hit	FC (DS/PLS)
solyc08g007420.2.1	fermentation.LDH	highly similar to AT4G17260 "L-lactate dehydrogenase	3.0
solyc08g078850.2.1	fermentation.LDH	highly similar to L-lactate dehydrogenase	5.3
solyc02g091100.2.1	fermentation.PDC	highly similar to AT5G17380 pyruvate decarboxylase family	2.1
solyc10g076510.1.1	fermentation.PDC	nearly identical to AT4G33070 pyruvate decarboxylase isozyme 2	6.5
solyc02g084640.2.1	fermentation.aldehyde dehydrogenase	highly similar to AT4G36250 Aldehyde Dehydrogenase 3F1	-2.1
solyc06g060250.2.1	fermentation.aldehyde dehydrogenase	highly similar to AT1G44170 3-chloroallyl aldehyde dehydrogenase/ aldehyde dehydrogenase (NAD)	2.1
solyc05g005700.2.1	fermentation.aldehyde dehydrogenase	highly similar to AT1G23800 3-chloroallyl aldehyde dehydrogenase/ aldehyde dehydrogenase (NAD)	3.5

CHAPTER 3

solyc12g007030.1.1	fermentation.aldehyde dehydrogenase	highly similar to AT3G24503 3-chloroallyl aldehyde dehydrogenase/ aldehyde dehydrogenase (NAD)/ coniferyl-aldehyde dehydrogenase	5.3
--------------------	-------------------------------------	--	-----

Supplementary Table S2B. Fold change in expression of genes involved in the TCA in the dying seedlings (DS) compared to the parental lines (PLS).

Transcript ID	Description (MAPMAN)	ATH best hit	FC (DS/PLS)
solyc09g009830.2.1	TCA / org. transformation. carbonic anhydrases	weakly similar to AT3G52720 ALPHA CARBONIC ANHYDRASE 1	-3.7
solyc02g086820.2.1	TCA / org. transformation. carbonic anhydrases	moderately similar to AT3G01500 CARBONIC ANHYDRASE 1	-2.6
solyc05g024160.2.1	TCA / org. transformation.TCA. pyruvate DH.E1	highly similar to AT5G50850pyruvate dehydrogenase (acetyl-transferring)	-2.3
solyc10g074500.1.1	TCA / org. transformation.TCA. IDH	highly similar to AT4G35260 ISOCITRATE DEHYDROGENASE 1	2.0
solyc08g077920.2.1	TCA / org. transformation.TCA. IDH	highly similar to AT5G03290 isocitrate dehydrogenase	2.0
solyc12g005080.1.1	TCA / org. transformation.TCA. pyruvate DH.E2	highly similar to AT5G55070 2-oxoacid dehydrogenase family protein	2.1
solyc01g066520.2.1	TCA / org. transformation.TCA. pyruvate DH.E2	highly similar to AT3G06850 acetyltransferase/ alpha-ketoacid dehydrogenase/ dihydrolipoamide branched chain acyltransferase	2.1
solyc12g005080.1.1	TCA / org. transformation.TCA.2-oxoglutarate dehydrogenase	highly similar to AT5G55070 2-oxoacid dehydrogenase family protein	2.1
solyc01g007910.2.1	TCA / org. transformation.TCA. succinyl-CoA ligase	highly similar to AT5G23250 Symbols: succinyl-CoA ligase (GDP-forming) alpha-chain, mitochondrial, putative / succinyl-CoA synthetase, alpha chain, putative	2.1
solyc11g069640.1.1	TCA / org. transformation. carbonic anhydrases	moderately similar to AT1G08080 ALPHA CARBONIC ANHYDRASE 7	2.1
solyc06g075050.1.1	TCA / org. transformation. carbonic anhydrases	moderately similar to AT1G08080 ALPHA CARBONIC ANHYDRASE 7	2.1
solyc01g059880.2.1	TCA / org. transformation.other organic acid transformaitons.atp-citrate lyase	nearly identical AT5G49460 ATP CITRATE LYASE SUBUNIT B 2	2.3
solyc01g028900.2.1	TCA / org. transformation.TCA. pyruvate DH.E1	highly similar to AT3G13450 DIN4 (DARK INDUCIBLE 4)	2.6
solyc12g099100.1.1	TCA / org. transformation.TCA. pyruvate DH.E3	highly similar to AT1G48030 mtLPD1 mitochondrial lipoamide dehydrogenase 1	2.8
solyc01g073740.2.1	TCA / org. transformation.TCA.CS	highly similar to AT2G44350 ATCS ATP citrate synthase	2.8
solyc04g011350.2.1	TCA / org. transformation.TCA.2-oxoglutarate dehydrogenase	nearly identical AT3G55410 2-oxoglutarate dehydrogenase E1 component	2.8

Carbon economy and maintenance of energy homeostasis

solyc09g075450.2.1	TCA / org. transformation.TCA. fumarase	highly similar to AT5G50950 fumarate hydratase, putative	2.8
solyc05g005160.2.1	TCA / org. transformation.other organic acid transformaitons.atp-citrate lyase	highly similar to AT1G60810 ACLA-2; ATP citrate synthase	3.2
solyc03g120990.2.1	TCA / org. transformation.other organic acid transformaitons. malic	highly similar to AT1G79750 ATNADP-ME4 ATNADP-ME4 (NADP-malic enzyme 4)	5.3
solyc05g050120.2.1	TCA / org. transformation.other organic acid transformations. malic	highly similar to AT5G25880 ATNADP-ME3 (NADP-malic enzyme 3); malate dehydrogenase (oxaloacetate-decarboxylating)	5.3
solyc10g083890.1.1	TCA / org. transformation. carbonic anhydrases	moderately similar to AT1G08080 Symbols: ATACA7(ALPHA CARBONIC ANHYDRASE 7)	14.9

Supplementary Table S2C. Fold change in expression of genes involved in the electron transport chain (ETC) and the oxidative pentose phosphate pathway (OPP) in the dying seedlings (DS) compared to the parental lines (PLS).

Transcript ID	Description (MAPMAN)	ATH best hit	FC (DS/PLS)
solyc06g007160.2.1	MET / ATP synthesis.NADH-DH. type II.internal matrix	highly similar to AT2G29990 NDA2 NDA2 (ALTERNATIVE NAD(P)H DEHYDROGENASE 2)	-1.7
solyc12g044380.1.1	MET / ATP synthesis.cytochrome c oxidase	weakly similar to AT1G66590 ATCOX19-1 cytochrome c oxidase assembly protein COX19	-1.6
solyc05g014120.1.1	MET / ATP synthesis.F1-ATPase	moderately similar to AT1G24480 methyltransferase	-1.2
solyc09g005870.1.1	MET / ATP synthesis.cytochrome c	moderately similar to AT3G51790 ATG1 (ARABIDOPSIS TRANSMEMBRANE PROTEIN G1P-RELATED 1)	1
solyc12g042900.1.1	MET / ATP synthesis.cytochrome c oxidase	weakly similar to AT1G80230	1
solyc01g068640.2.1	MET / ATP synthesis.unspecified	cytochrome c oxidase family protein highly similar to AT4G01660 ATABC1 (ARABIDOPSIS THALIANA ABC TRANSPORTER 1)	1
solyc08g075540.2.1	MET / ATP synthesis.alternative oxidase	moderately similar to AT3G22370 AOX1A (ALTERNATIVE OXIDASE 1A)	1.9
solyc02g078900.2.1	MET / ATP synthesis.NADH-DH. type II.internal matrix	highly similar to AT2G29990 NDA2 (ALTERNATIVE NAD(P)H DEHYDROGENASE 2)	2.1
solyc01g107900.2.1	MET / ATP synthesis.F1-ATPase	moderately similar to AT5G53390 Symbols: unknown protein	2.3
solyc02g079170.2.1	MET / ATP synthesis.NADH-DH. type II.external	highly similar to AT4G05020 NDB2 (NAD(P)H dehydrogenase B2)	2.8
solyc08g075550.2.1	MET / ATP synthesis.alternative oxidase	moderately similar to AT1G32350 AOX1D (alternative oxidase 1D)	3.8

CHAPTER 3

solyc01g093990.2.1	OPP.oxidative PP.6-phosphogluconate dehydrogenase	moderately similar to AT2G45630 Symbols: oxidoreductase family protein Glyoxylate reductase/ hydroxypyruvate reductase	-1.5
solyc02g093830.2.1	OPP.oxidative PP.G6PD	highly similar to AT5G40760 Symbols: G6PD6 G6PD6 (GLUCOSE-6-PHOSPHATE DEHYDROGENASE 6); glucose-6-phosphate dehydrogenase	2.1
solyc12g040570.1.1	OPP.oxidative PP.6-phosphogluconate dehydrogenase	moderately similar to AT3G02360 Symbols: 6-phosphogluconate dehydrogenase family protein	3.4
solyc04g005160.1.1	OPP.oxidative PP.6-phosphogluconate dehydrogenase	highly similar to AT3G02360 Symbols: 6-phosphogluconate dehydrogenase family protein	3.4

Supplementary Table S3. Expression profile of genes involved in fatty acid oxidation in the dying seedlings (DS) compared to the parental lines (PLS).

Transcript ID	Description	Fold change (DS/PLS) log2
solyc04g054890.2.1	acyl-CoA oxidase	1.4
solyc06g053670.1.1	enoyl-CoA hydratase/isomerase family protein	2.5
solyc07g019670.2.1	fatty acid oxidation complex subunit alpha	2.9
solyc05g010720.2.1	enoyl-CoA hydratase	3.0
solyc08g068390.2.1	fatty acid oxidation complex subunit alpha	4.0
solyc09g061840.2	3-ketoacyl-CoA thiolase 1	2.4
solyc07g047800.2	short-chain dehydrogenase/reductase family protein	3.1
solyc08g082280.2	long-chain-fatty-acid-CoA ligase	1.8
solyc10g007890.2	cytochrome p450	3.7
solyc10g007880.2	cytochrome p450	3.3
solyc10g051020.1	cytochrome p450	2.3
solyc10g007900.2	cytochrome p450	2.1
solyc12g006860.1	cytochrome p450	1.3
solyc07g062500.2	cytochrome p450	1.3
solyc07g041500.2	cytochrome p450	1.2
solyc07g055480.1	cytochrome p450	1.1
solyc07g055440.1	cytochrome p450	1

Supplementary Table S4. Expression profile of genes involved in amino acid metabolism in the dying seedlings (DS) compared to the parental lines (PLS).

Transcript ID	Pathway	Description	Fold change (DS/PLS) log2
solyc08g068660.1.1	amino acid metabolism (AAM). degradation.histidine	very weakly similar to AT1G43710 Symbols: emb1075 emb1075 (embryo defective 1075); carboxylyase/ catalytic/ pyridoxal phosphate binding	5.1
solyc08g068640.2.1	AAM.degradation.histidine	highly similar to AT1G43710 Symbols: emb1075 emb1075 (embryo defective 1075); carboxylyase/ catalytic/ pyridoxal phosphate binding	4.2
solyc08g068680.2.1	AAM.degradation.histidine	highly similar to AT1G43710 Symbols: emb1075 emb1075 (embryo-defective 1075); carboxylyase/ catalytic/ pyridoxal phosphate binding	5.1
solyc08g068610.2.1	AAM.degradation.histidine	highly similar to AT1G43710 Symbols: emb1075 emb1075 (embryo-defective 1075); carboxylyase/	4.7
solyc08g006740.2.1	AAM.degradation.histidine	highly similar to AT1G43710 Symbols: emb1075 emb1075 (embryo-defective 1075); carboxylyase	5.0
solyc08g068600.2.1	AAM.degradation.histidine	highly similar to AT1G43710 Symbols: emb1075 emb1075 (embryo-defective 1075); carboxylyase/ catalytic/ pyridoxal phosphate binding	4.4
solyc08g006750.2.1	AAM.degradation.histidine	highly similar to AT1G43710 Symbols: emb1075 emb1075 (embryo-defective 1075); carboxylyase/ catalytic/ pyridoxal phosphate binding	3.3
solyc08g068630.2.1	AAM.degradation.histidine	highly similar to AT1G43710 Symbols: emb1075 emb1075 (embryo-defective 1075); carboxylyase/ catalytic/ pyridoxal phosphate binding	8.4
solyc12g011160.1.1	AAM.degradation.aromatic aa.tryptophan	highly similar to AT1G06550 Symbols: enoyl-CoA hydratase/ isomerase family protein	2.3
solyc06g053670.1.1	AAM.degradation.aromatic aa.tryptophan	moderately similar to AT4G14430 Symbols: IBR10, ATEC12, EC12, ECHIB, PEC12 IBR10 (INDOLE-3-BUTYRIC ACID RESPONSE 10); catalytic/ dodecenoyl-CoA delta-isomerase	2.5
solyc05g010720.2.1	AAM.degradation.aromatic aa.tryptophan	moderately similar to AT1G65520 Symbols: ATEC11, EC11, ECHIC, PEC11 EC11 (DELTA(3), DELTA(2)-ENOYL COA ISOMERASE 1); carnitine racemase/ catalytic/ dodecenoyl-CoA delta-isomerase	3.0

CHAPTER 3

solyc10g080430.1.1	AAM.synthesis.aromatic aa.tryptophan	nearly identical to AT3G57880 Symbols: C2 domain-containing protein	-1.0
solyc10g078680.1.1	AAM.synthesis.aromatic aa.tryptophan	nearly identical to AT3G57880 Symbols: C2 domain-containing protein	-1.5
solyc01g007170.2.1	AAM.synthesis.aromatic aa.tryptophan	highly similar to AT3G03680 Symbols: C2 domain-containing protein	-1.3
solyc11g022460.1.1	AAM.synthesis.aromatic aa.tryptophan	highly similar to AT1G22610 Symbols: C2 domain-containing protein	-1.0

Supplementary Table S5. MAPMAN overview of the regulation of genes involved in cell wall (CW) metabolism in the *C. fulvum*-tomato interaction.

Bin	Description	DS			Incompatible			Compatible		
		Total # DEGs	Up	Down	Total # DEGs	Up	Down	Total # DEGs	Up	Down
10.2	CW.cellulose synthesis	8	1	7	4	0	4	0	0	0
10.3	CW.hemicellulose synthesis	3	3	0	1	0	1	0	0	0
10.6	CW.degradation	1	1	0	0	0	0	0	0	0
10.7	CW.modification	24	8	16	17	3	14	13	11	2
10.1.1.1	CW.precursor synthesis.NDP sugar pyrophosphorylase.GDP mannose	0	0	0	1	1	0	0	0	0
10.1.2	CW.precursor synthesis.UGE	1	1	0	0	0	0	0	0	0
10.1.20	CW.precursor synthesis. phosphomannose isomerase	1	0	1	0	0	0	0	0	0
10.1.21	CW.precursor synthesis. phosphomannomutase	1	0	1	0	0	0	0	0	0
10.1.3	CW.precursor synthesis.AXS	1	0	1	1	0	1	0	0	0
10.1.4	CW.precursor synthesis.UGD	2	1	1	1	1	0	0	0	0
10.1.5	CW.precursor synthesis.UXS	3	2	1	1	1	0	0	0	0
10.1.6	CW.precursor synthesis.GAE	4	1	3	1	1	0	0	0	0
10.1.9	CW.precursor synthesis.MUR4	2	2	0	1	1	0	1	0	1
10.2.1	CW.cellulose synthesis. cellulose synthase	6	1	5	4	0	4	1	1	0
10.2.2	CW.cellulose synthesis.COBRA	3	2	1	1	1	0	2	1	1
10.5.1.1	CW.CW proteins.AGPs.AGP	11	0	11	6	0	6	2	2	0
10.5.3	CW.CW proteins.LRR	3	0	3	1	0	1	1	1	0
10.5.4	CW.CW proteins.HRGP	1	1	0	0	0	0	0	0	0
10.5.5	CW.CW proteins.RGP	3	3	0	1	1	0	1	0	1
10.6.1	CW.degradation.cellulases and beta -1,4-glucanases	13	2	11	7	2	5	2	0	2

Carbon economy and maintenance of energy homeostasis

10.6.2	CW.degradation.mannan-xylose-arabinose-fucose	5	0	5	3	2	1	0	0	0
10.6.3	CW.degradation.pectate lyases and polygalacturonases	27	7	20	11	2	9	3	3	0
10.8.1	CW.pectin*esterases.PME	11	2	9	4	0	4	0	0	0
10.8.2	CW.pectin*esterases.acetyl esterase	2	0	2	1	0	1	4	4	0
	Total # genes	136	38	98	67	16	51	30	23	7

DEGs, differentially expressed genes (fold change > 2 and p < 0.001 with FDR correction); DS, dying seedlings.

Supplementary Table S6. Fold change in expression of peroxidases during mounting of the HR in the dying seedlings (DS), compared to the parental lines (PLS).

Transcript ID	Description	Fold change (DS/PLS) log 2
solyc02g083490.2.1	moderately similar to AT5G42180 Symbols: peroxidase 64 (PER64) (P64) (PRXR4)	-2.2
solyc03g120800.2.1	moderately similar to AT4G33870 Symbols: peroxidase, putative	-1.6
solyc11g010120.1.1	highly similar to AT2G22420 Symbols: peroxidase 17 (PER17) (P17)	-1.4
solyc08g069040.2.1	moderately similar to AT4G30170 Symbols: peroxidase, putative	-1.2
solyc07g052510.2.1	moderately similar to AT1G05260 Symbols: RCI3, RCI3A RCI3 (RARE COLD-INDUCIBLE GENE 3); peroxidase	-1.1
solyc02g087190.1.1	moderately similar to AT5G40150 Symbols: peroxidase, putative	-1.1
solyc01g006300.2.1	moderately similar to AT5G06720 Symbols: peroxidase, putative	1.6
solyc07g055190.2.1	moderately similar to AT5G05340 Symbols: peroxidase, putative	1.7
solyc02g079510.2.1	moderately similar to AT5G05340 Symbols: peroxidase, putative	1.8
solyc04g071890.2.1	moderately similar to AT1G71695 Symbols: peroxidase 12 (PER12) (P12) (PRXR6)	2.6
solyc01g105070.2.1	moderately similar to AT5G64120 Symbols: peroxidase, putative	2.8
solyc02g079500.2.1	moderately similar to AT5G05340 Symbols: peroxidase, putative	2.8
solyc10g084240.1.1	moderately similar to AT2G37130 Symbols: peroxidase 21 (PER21) (P21) (PRXR5)	3.1
solyc02g094180.2.1	moderately similar to AT4G37530 Symbols: peroxidase, putative	3.1
solyc09g007520.2.1	moderately similar to AT2G37130 Symbols: peroxidase 21 (PER21) (P21) (PRXR5)	3.3
solyc06g050440.2.1	moderately similar to AT5G05340 Symbols: peroxidase, putative ascorbate_peroxidase	3.4
solyc05g052280.2.1	moderately similar to AT5G05340 Symbols: peroxidase, putative	3.7
solyc11g018800.1.1	moderately similar to AT1G14550 Symbols: anionic peroxidase, putative	4.1
solyc02g084800.2.1	moderately similar to AT5G66390 Symbols: peroxidase 72 (PER72) (P72) (PRXR8)	4.2

CHAPTER 3

solyc11g072920.1.1	moderately similar to AT5G06720 Symbols: peroxidase, putative	4.2
solyc03g006700.2.1	moderately similar to AT5G05340 Symbols: peroxidase, putative	4.5
solyc01g101050.2.1	moderately similar to AT3G03670 Symbols: peroxidase, putative	5.8
solyc10g076240.1.1	moderately similar to AT5G05340 Symbols: peroxidase, putative	7.5

Supplementary Table S7. Fold change in expression of genes involved in the terpenoid (isoprenoid) pathway in the dying seedlings (DS) compared to the parental lines (PLS).

Transcript ID	Pathway	Description	Fold change (DS/PLS) log2
solyc08g005680.2.1	isoprenoids.mevalonate pathway	moderately similar to AT5G58770 Symbols: dehydrodolichyl diphosphate synthase, putative / DEDOL-PP synthase, putative	-2.8
solyc08g005680.2.1	isoprenoids.terpenoids	moderately similar to AT5G58770 Symbols: dehydrodolichyl diphosphate synthase, putative / DEDOL-PP synthase, putative	-2.8
solyc08g005660.1.1	isoprenoids.mevalonate pathway	very weakly similar to AT5G58770 Symbols: dehydrodolichyl diphosphate synthase, putative / DEDOL-PP synthase, putative	-2.7
solyc08g005640.2.1	isoprenoids.terpenoids	moderately similar to AT1G79460 Symbols: GA2, KS, ATKS GA2 (GA-REQUIRING 2); ent-kaurene synthase	-2.5
solyc01g105880.2.1	isoprenoids.terpenoids	moderately similar to AT3G25810 Symbols: myrcene/ocimene synthase, putative	-1.9
solyc06g084240.1.1	isoprenoids.terpenoids	highly similar to AT4G02780 Symbols: GA1, ABC33, ATCPS1 GA1 (GA-REQUIRING 1); ent-copalyl diphosphate synthase/ magnesium ion binding	-1.7
solyc03g115980.1.1	isoprenoids.non-mevalonate pathway	highly similar to AT1G74470 Symbols: geranylgeranyl reductase	-1.6
solyc08g005720.2.1	isoprenoids.terpenoids	moderately similar to AT1G79460 Symbols: GA2, KS, ATKS GA2 (GA-REQUIRING 2); ent-kaurene synthase	-1.5
solyc01g105920.2.1	isoprenoids.terpenoids	moderately similar to AT3G25810 Symbols: myrcene/ocimene synthase, putative	-1.4
solyc07g042630.2.1	isoprenoids.terpenoids	highly similar to AT1G78960 Symbols: ATLUP2 ATLUP2; beta-amyrin synthase/ lupeol synthase	-1.2
solyc02g081330.2.1	isoprenoids.carotenoids. phytoene synthase	highly similar to AT5G17230 Symbols: phytoene synthase (PSY) / geranylgeranyl-diphosphate geranylgeranyl transferase	-1.2
solyc12g006520.1.1	isoprenoids.terpenoids	nearly identical to AT1G78950 Symbols: beta-amyrin synthase, putative	-1.2
solyc11g010850.1.1	isoprenoids.non-mevalonate pathway.DXS	highly similar to AT4G15560 Symbols: CLA1, DEF, CLA, DXS, DXPS2 CLA1 (CLOROPLASTOS ALTERADOS 1); 1-deoxy-D-xylulose-5-phosphate synthase	-1.2
solyc04g050930.2.1	isoprenoids.carotenoids. violaxanthin de-epoxidase	highly similar to AT1G08550 Symbols: NPQ1, AVDE1 NPQ1 (NON-PHOTOCHEMICAL QUENCHING 1); violaxanthin de-epoxidase	-1.2

Carbon economy and maintenance of energy homeostasis

solyc05g010180.2.1	isoprenoids.carotenoids	highly similar to AT1G57770 Symbols:	-1.1
solyc02g082260.2.1	isoprenoids.mevalonate pathway.HMG-CoA reductase	highly similar to AT1G76490 Symbols: HMG1, HMGR1 HMG1 (HYDROXY METHYLGLUTARYL COA REDUCTASE 1); hydroxymethylglutaryl-CoA reductase	-1.0
solyc04g009600.2.1	Isoprenoids	moderately similar to AT3G11950 Symbols:	1.4
solyc07g045350.2.1	isoprenoids.mevalonate pathway.acetyl-CoA C-acyltransferase	highly similar to AT5G48230 Symbols: EMB1276, ACAT2 ACAT2 (ACETOACETYL-CoA THIOLASE 2); acetyl-CoA C-acetyltransferase	1.6
solyc06g066310.2.1	isoprenoids.mevalonate pathway.phosphomevalonate kinase	highly similar to AT1G31910 Symbols: GHMP kinase family protein	1.7
solyc07g052140.2.1	isoprenoids.terpenoids	weakly similar to AT5G23960 Symbols: ATTPS21, TPS21 TPS21 (TERPENE SYNTHASE 21); (-)-E-beta-caryophyllene synthase/ alpha-humulene synthase	2.0
solyc01g098840.2.1	isoprenoids.mevalonate pathway.mevalonate kinase	moderately similar to AT5G27450 Symbols: MVK, MK MK (MEVALONATE KINASE); mevalonate kinase	2.4
solyc12g006530.1.1	isoprenoids.terpenoids	nearly identical to AT1G78950 Symbols:	2.4
solyc08g007790.2.1	isoprenoids.mevalonate pathway.HMG-CoA synthase	highly similar to AT4G11820 Symbols: MVA1 MVA1; acetyl-CoA C-acetyltransferase/ hydroxymethylglutaryl-CoA synthase	2.7
solyc02g038740.2.1	isoprenoids.mevalonate pathway.HMG-CoA reductase	highly similar to AT1G76490 Symbols: HMG1, HMGR1 HMG1 (HYDROXY METHYLGLUTARYL COA REDUCTASE 1); hydroxymethylglutaryl-CoA reductase	3.3
solyc11g011240.1.1	isoprenoids.non-mevalonate pathway.geranylgeranyl pyrophosphate synthase	moderately similar to AT4G36810 Symbols: GGPS1 GGPS1 (GERANYLGERANYL PYROPHOSPHATE SYNTHASE 1); farnesyltransferase	4.7
solyc07g052120.2.1	Sesquiterpenoid bios.	weakly similar to AT5G23960 Symbols: ATTPS21, TPS21 TPS21 (TERPENE SYNTHASE 21); (-)-E-beta-caryophyllene synthase/ alpha-humulene synthase	6.0
solyc01g101210.2.1	Sesquiterpenoid bios.	moderately similar to AT5G23960 Symbols: ATTPS21, TPS21 TPS21 (TERPENE SYNTHASE 21); (-)-E-beta-caryophyllene synthase/ alpha-humulene synthase	6.3
solyc01g101170.2.1	Sesquiterpenoid bios.	moderately similar to AT5G23960 Symbols: ATTPS21, TPS21 TPS21 (TERPENE SYNTHASE 21); (-)-E-beta-caryophyllene synthase/ alpha-humulene synthase	8.4
solyc01g101190.2.1	Sesquiterpenoid bios.	moderately similar to AT5G23960 Symbols: ATTPS21, TPS21 TPS21 (TERPENE SYNTHASE 21); (-)-E-beta-caryophyllene synthase/ alpha-humulene synthase	10.1
solyc01g101180.2.1	Sesquiterpenoid bios.	moderately similar to AT5G23960 Symbols: ATTPS21, TPS21 TPS21 (TERPENE SYNTHASE 21); (-)-E-beta-caryophyllene synthase/ alpha-humulene synthase	12.8

Supplementary Table S8. Fold change in expression of genes involved in the hydrolysis of polysaccharides in the dying seedlings (DS) compared to the parental lines (PLS) and in *C. fulvum*-inoculated resistant (R) and susceptible (S) tomato compared to the mock-inoculated (M) controls.

Transcript ID	Description	Fold change		
		DS/PLS	RI/RM	SI/SM
solyc01g058020.2.1	moderately similar to AT3G05820 Symbols: beta-fructofuranosidase	2.3	NS	NS
solyc01g058010.2.1	highly similar to AT3G06500 Symbols: beta-fructofuranosidase, putative / invertase	2.2	NS	NS
solyc03g121680.1.1	highly similar to AT3G13790 Symbols: ATINV1, ATBFRUCT1 ATBFRUCT1; beta-fructofuranosidase/hydrolase, hydrolyzing O-glycosyl compounds	6.5	NS	NS
solyc10g083300.1.1	highly similar to AT3G52600 Symbols: AtINV2 AtINV2 (<i>Arabidopsis thaliana</i> cell wall (CW) invertase 2); hydrolase, hydrolyzing O-glycosyl compounds	-2.8	-2.6	NS
solyc10g083290.1.1	highly similar to AT3G52600 Symbols: AtINV2 AtINV2 (<i>Arabidopsis thaliana</i> CW invertase 2); hydrolase, hydrolyzing O-glycosyl compounds	26.4	18.1	-2.0

RI, resistant inoculated; RM, resistant mock-inoculated; SI, susceptible inoculated; SM, susceptible mock-inoculated.

Supplementary Table S9. Fold change in expression of TCP transcription factors involved in the circadian clock in the dying seedlings (DS) compared to the parental lines (PLS).

Transcript ID	Description	Fold change (DS/PLS) log 2
solyc05g007420.1	weakly similar to AT1G58100 Symbols: TCP family transcription factor, putative	-1.9
solyc12g014140.1	moderately similar to AT3G15030 Symbols: TCP4 TCP4 (TCP family transcription factor 4); transcription factor	-1.8
solyc10g008780.1	weakly similar to AT2G31070 Symbols: TCP10 TCP10 (TCP DOMAIN PROTEIN 10); transcription factor	-1.0
solyc08g080150.1	weakly similar to AT5G51910 Symbols: TCP family transcription factor, putative	-1.2
solyc04g009180.1	moderately similar to AT5G23280 Symbols: TCP family transcription factor, putative	-1.6
solyc01g008230.2	moderately similar to AT5G23280 Symbols: TCP family transcription factor, putative	-1.5
solyc06g069460.1	weakly similar to AT5G60970 Symbols: TCP5 TCP5 (TEOSINTE BRANCHED1, CYCLOIDEA AND PCF TRANSCRIPTION FACTOR 5); transcription factor	-1.4
solyc06g070900.2	weakly similar to AT3G47620 Symbols: AtTCP14 AtTCP14 (TEOSINTE BRANCHED1, CYCLOIDEA and PCF (TCP) 14); transcription factor	-2.2

Chapter 4

Genome-Wide Functional Analysis of WRKY Transcription Factors in Resistance of Tomato to *Cladosporium fulvum*

Desalegn W. Etalo^{1,3,Ω}, Wladimir I.L.Tameling^{5†}, Ric C.H. De Vos^{2,3,4}, Harro
J. Bouwmeester^{1,3*} and Matthieu H.A.J. Joosten^{3,5}

¹ Laboratory of Plant Physiology, Wageningen University, Wageningen, the Netherlands.

² Plant Research International, Bioscience, Wageningen University,
Wageningen, The Netherlands.

³ Centre for BioSystems Genomics, Wageningen, The Netherlands.

⁴ Netherlands Metabolomics Centre, Einsteinweg 55, 2333 CC Leiden, the Netherlands.

⁵ Laboratory of Phytopathology, Wageningen University, Wageningen, the Netherlands.

*Corresponding author.

Laboratory of Plant Physiology, Wageningen University,
Droevendaalsesteeg 1, 6708 PB Wageningen, The Netherlands.

Tel.: +31 (0)317-489859.

Fax: +31 (0)317-418094.

E-mail: harro.bouwmeester@wur.nl

† Current address: KEYGENE N.V., 6700 AE Wageningen, The Netherlands

Ω Current address: Plant Research International, Bioscience, Wageningen University,
Wageningen, The Netherlands.

To be submitted

Abstract

The absence of specialized immune cells forces plants to tightly control the immune response. As entire plant organs could potentially mount an immune response (and consequently die), this response has to be strictly regulated. Furthermore, this control is required to balance the allocation of resources, of which the efficiency determines the fitness of plants in their natural habitat. Hence, any response to a perturbation of plant homeostasis should be accompanied by a fast switch between alternative gene transcription programs to ensure an efficient response with the least impact on growth. Transcription factor (TF)-mediated transcriptional regulation shapes the defence transcriptome of resistant plants upon mounting their response to invading pathogens. We study this response in tomato (*Solanum lycopersicum*, *Sl*) carrying *Cf* resistance genes to the pathogenic fungus *Cladosporium fulvum*. Although many different classes of TFs showed differential regulation, genes encoding WRKY TFs (*SIWRKYs*) showed the most pronounced changes at the transcriptional level upon activation of the defence response in tomato resistant to *C. fulvum*. Out of a total of 59 expressed *SIWRKYs*, 36 were transcriptionally up-regulated, whereas the transcription of only two of them was suppressed. Virus-induced gene silencing (VIGS) of selected differentially regulated, and possibly functionally redundant, *SIWRKYs* showed that this class of TFs consists of a group of key regulators, some of which are activating and some of which are suppressing the plant immune response. Untargeted metabolomics showed that inhibition of the expression of *SIWRKY31/33* and *SIWRKY80* (an ortholog of *AtWRKY70*) by VIGS, resulted in an increase in susceptibility, which is comparable with the increased susceptibility when the resistance gene *Cf-4* itself is knocked-down. Targeting of defence repressors (*SIWRKY39/40/45/46*) boosted the basal defence in susceptible plants, thereby resulting in a drastic reduction in *C. fulvum* proliferation. Targeting of the genes encoding these transcription factors and other combinations of *SIWRKYs* resulted in the alteration of the apoplast metabolome towards susceptibility, supporting their involvement in the defence-associated metabolome reprogramming of tomato upon its colonisation by *C. fulvum*.

Introduction

Plants are continuously exposed to a myriad of microbes but only few manage to cause disease. Two interconnected layers of plant immunity surveyed by extracellular plasma membrane-localised receptors and intracellular receptors, referred to as nucleotide-binding-leucine-rich repeat (NB-LRR) proteins, play a critical role in perceiving non-self components and mounting an adequate defence response (Jones and Dangl, 2006). Extracellular pattern recognition receptors (PRRs) recognize highly conserved microbe-associated molecular patterns (MAMPs), such as fungal chitin and bacterial flagellin, and their perception leads to the induction of MAMP-triggered immunity (MTI). However, virulent microbes deliver specific effector proteins into the host cell that suppress the MTI and promote effector-triggered susceptibility (ETS). Resistant plants in turn will use the second layer of surveillance that allows specific recognition of pathogen effectors and halts pathogen ingress through the activation of effector-triggered immunity (ETI). Generally, MTI and ETI give rise to similar responses, although in most cases ETI is stronger, faster and more robust and often involves localized programmed cell death, referred to as the hypersensitive response (HR) (Tao et al., 2003; Chisholm et al., 2006; Jones and Dangl, 2006; Dodds and Rathjen, 2010; Thomma et al., 2011; Dangl et al., 2013).

The absence of specialized immune cells imposes the need for a tight control of the immune response of plants, as otherwise complete tissues could mount this response and undergo an HR. Furthermore, the allocation of resources has to be balanced between various biological processes and an efficient use of energy determines the overall fitness and survival of plants (Kliebenstein and Rowe, 2008; Denance et al., 2013; Neilson et al., 2013). Hence, any response to a perturbation of plant homeostasis should be accompanied by a fast switch to the appropriate gene transcription programme and suppression of other programmes to ensure an economic and efficient reaction. Therefore, factors that are involved in the regulation of this response are essential for plant survival and are subject of studies that use systems biology approaches (Eulgem et al., 1999; Li et al., 2004; Moore et al., 2011; Etalo et al., 2013; Shoji et al., 2013). Key components allowing fast transcriptional reprogramming are transcription factors (TFs). Binding of transcription factors to the appropriate promoter regions in the DNA enables the recruitment of RNA polymerase II to induce gene transcription. Some well-known transcription factors involved in plant defense transcriptome reprogramming include AP2/ERF, bZIP, MYC, MYB and WRKY TFs (Rushton and Somssich, 1998; Pozo et al., 2008; Rushton et al., 2010; Alves et al., 2013; Chang et al., 2013; Meng et al., 2013).

Recently, a system-wide analysis indicated a prominent role of WRKY TFs in orchestrating the HR-associated transcriptome and metabolome reprogramming in tomato (*Solanum lycopersicum*, *Sl*) (Etalo et al., 2013). The WRKY family is among the ten largest families

of TFs in higher plants and is found throughout the green lineage, in green algae as well as land plants (Ulker and Somssich, 2004). WRKYs were regarded to be plant-specific, but the fact that they are also found in the protist *Giardia lamblia* and the slime mold *Dictyostelium discoideum*, suggests an earlier origin (Ulker and Somssich, 2004; Pan et al., 2009). The tomato WRKY (*S*/WRKY) protein family has 81 representatives, which have been categorized into three major groups (I, II and III) based on the number of WRKY domains and the type of zinc finger motifs that are present (Huang et al., 2012). WRKY TFs act as key regulators, both positive and negative, of the two interconnected layers of plant innate immunity, MTI and ETI (Eulgem et al., 1999; Jones and Dangl, 2006; Journot-Catalino et al., 2006; Kim et al., 2006; Wang et al., 2006; Xu et al., 2006; Zheng et al., 2006; Eulgem and Somssich, 2007; Shen et al., 2007; Rushton et al., 2010; Huang et al., 2012). To date, only four *S*/WRKY TFs have been functionally characterized and the biological function of most *S*/WRKYs remains unknown (Bhattarai et al., 2010; Atamian et al., 2012; Li et al., 2012). Functional characterization of this family of TFs has been a major challenge due to the presence of functional redundancy (Xu et al., 2006; Shen et al., 2007; Fradin et al., 2011).

We study the resistance response of tomato to the biotrophic fungal pathogen *Cladosporium fulvum*. The fungus colonizes the intercellular spaces of tomato leaves and in tomato resistant to the fungus, Cf resistance proteins, which are extracellular receptor-like proteins (RLPs), mediate the recognition of extracellular effectors, in this case referred to as avirulence (Avr) proteins, secreted by *C. fulvum*. Upon recognition of these Avr, a typical HR is mounted. To study HR-associated processes in tomato resistant to *C. fulvum* we developed the dying seedling (DS) system, for which a transgenic tomato line expressing the *Avr4* gene of *C. fulvum* is crossed to a plant carrying the matching resistance gene *Cf-4*. The resulting *Cf-4*/*Avr4* offspring generates a systemic HR, which is suppressed by placing the seedlings at elevated temperature and relative humidity (RH) (33°C/100% RH). A synchronized HR can subsequently be induced by moving the plants to 20°C/70% RH (de Jong et al., 2002; Stulemeijer et al., 2007; Etalo et al., 2013). Hence, all changes for example at the level of the transcriptome and metabolome can be associated to the *Cf-4*-mediated recognition of *Avr4*.

To obtain a global overview of the changes in the transcriptome that occur upon mounting of the *Cf-4*/*Avr4*-triggered HR and to further support our earlier findings that were based on the Affymetrix tomato genome array (representing only about one third of all tomato genes), we performed RNA-seq analysis (more than 50 million reads per sample) on selected samples of the DS and resistant *Cf-4* and susceptible *Cf-0* tomato plants inoculated with a strain of *C. fulvum* secreting *Avr4*. From the DS and their parental *Cf-4*- and *Avr4*-expressing tomato lines (PLS) used for generating the DS and subjected to the same treatment, leaf tissue was analysed at 5 hrs after the temperature shift that induces the HR in the DS. At this time point the DS do not show

any visible symptoms of cell death yet, but all HR-related responses are already fully activated (Etalo et al., 2013). For resistant Cf-4 tomato (resulting in an incompatible interaction (II) upon inoculation with *C. fulvum* expressing *Avr4*) and susceptible Cf-0 plants (giving a compatible interaction (CI) with this strain of *C. fulvum*), we decided to analyse leaf samples obtained at 6 days post inoculation (dpi) with the fungus, as at this time point defence responses are fully activated in resistant plants (Joosten and De Wit, 1989; Kan et al., 1992). Our RNA-seq analyses not only point to *SIWRKYs* as the major orchestrators of the massive HR-related transcriptional changes that take place in the DS, but also in *C. fulvum*-inoculated resistant Cf-4 tomato.

In the model plant *Arabidopsis thaliana* the availability of mutants and T-DNA insertion lines facilitates the functional characterization of WRKYs that have redundant functions during the activation of defence responses (Xu et al., 2006; Shen et al., 2007). However, elucidation of their role in economically important crop plants like tomato is hampered as such tools are not available. Hence, to investigate the role of *SIWRKYs* in the defence response of tomato against *C. fulvum*, we performed simultaneous transient virus-induced gene silencing (VIGS) of selected sets of *SIWRKYs* showing high mutual sequence homology and similar differential expression profiles upon mounting of the HR. Here we show that these *SIWRKYs* represent of a group of key regulators, of which some activate and some suppress the plant immune response. Metabolomics analysis of plants in which the genes encoding these TFs were silenced by VIGS also shows their involvement in the swift defence-associated metabolome reprogramming that occurs in the tomato apoplast upon *C. fulvum* ingress.

Results

***SIWRKYs* Are the Most Prominent HR-Associated Up-regulated Transcription Factors**

The defence response of resistant tomato against *C. fulvum* is typically characterized by a massive reprogramming of the transcriptome, proteome and metabolome (Stulemeijer et al., 2009; Etalo et al., 2013). To untangle the major regulators of defence-associated transcriptome reprogramming we used three systems; (1) the Cf-4/*Avr4* dying seedlings (DS) that mount a synchronized and systemic HR under permissive conditions, (2) resistant Cf-4 tomato inoculated with a strain of *C. fulvum* secreting *Avr4* (resulting in an incompatible interaction, II) and (3) susceptible Cf-0 tomato inoculated with the same strain of the fungus (resulting in a compatible interaction, CI). We performed a deep RNA-seq analysis on leaf tissue obtained at 5 hrs after the temperature shift that induces the HR in the DS and compared the results with those obtained from a 1:1 mix of the parental lines (PLS) subjected to the same treatment and sampled at the same time point. In addition, the RNA-seq data of the *C. fulvum*-inoculated Cf-4 and Cf-0 plants were compared with those of mock- inoculated plants, all sampled at 6 dpi.

Three independent biological replicates were considered for the analysis. We compared the expression patterns of the significantly differentially expressed genes (fold change, FC > 2 and $P < 0.001$, with a correction for the false discovery rate, FDR), across the three systems.

From a total of 34,734 protein-coding genes annotated by the International Tomato Annotation Group (ITAG), transcripts of 19,643 (~57%), 17,805 (~51%) and 17,692 (~51%) genes were identified in the DS, II and CI, respectively. Close to 25, 17 and 2% of the expressed genes were differentially expressed in the DS, II and CI, respectively, when compared with the respective controls (**Figure 1A**). Comparison of the global transcriptional changes suggests that the DS amplify the localized, extremely faint and short-lived transcriptional changes occurring in II (**Figures 1B and 1C**). As expected, the DS and the *C. fulvum*-inoculated resistant plants had many of the differentially expressed genes, including the *SIWRKYs*, in common, as in both systems the Cf-4/Avr4-triggered ETI is being activated.

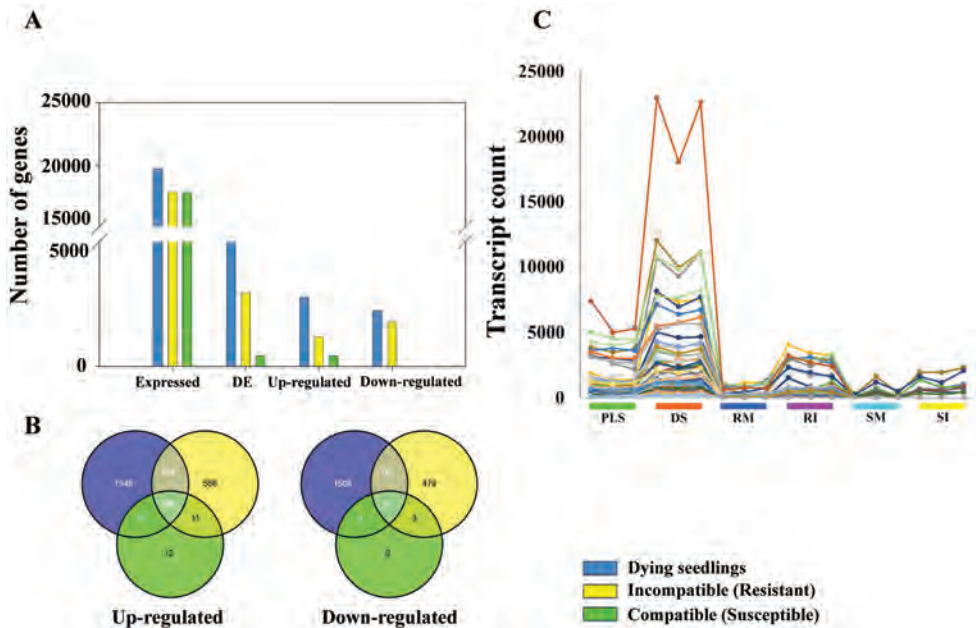


Figure 1. The overall transcriptome landscape of the dying seedlings (DS) and *C. fulvum*-inoculated resistant and susceptible tomato, as compared to their respective controls.

(A) Numbers of expressed, differentially expressed (DE), up-regulated and down-regulated protein-coding genes in the DS and *C. fulvum*-inoculated resistant and susceptible tomato.

(B) Venn diagram depicting the numbers and distribution of differentially expressed genes in the DS and *C. fulvum*-inoculated resistant and susceptible tomato.

(C) Expression profiles of representative gene clusters that showed amplified expression in the DS compared to resistant and susceptible tomato plants inoculated with *C. fulvum*. PLS, parental lines; DS, dying seedlings; RM, resistant tomato mock-inoculated; RI, resistant tomato inoculated with *C. fulvum*; SM, susceptible tomato mock-inoculated and SI, susceptible tomato lines inoculated with *C. fulvum*. Each treatment is represented by three independent biological repeats (Marked by different colours).

As depicted in **Figure 1B**, the response of the DS represents an amplified version of the response of resistant tomato plants inoculated with *C. fulvum*. Based on this observation, we performed most of our detailed analyses on the DS. A total of 2,133 TFs were found to be expressed across the three systems and as visualized by MapMan, in the DS, ~23% (489) of them were differentially regulated (**Figure 2A**). More than half of these (~54%; 265) were up-regulated. A Wilcoxon rank sum test in MapMan revealed some significantly enriched, and predominantly up-regulated families of TFs in the DS, such as the WRKYs, PHOR1s (photoperiod-responsive-1s), MADS box and HSFs (TFs belonging to the heat-shock family), when compared to the PLS (**Table 1** and **Figure 2**).

Table 1. MapMan bins of TFs identified as differentially expressed in dying seedlings and resistant and susceptible tomato inoculated with *C. fulvum*.

Dying seedlings (DS)					
Bin Name*	Bin code	No. of genes	Up	Down	P-value
27.3.32	WRKY domain TF family	38	36	2	1.00E-08
27.3.64	PHOR1	9	9	0	6.00E-05
27.3.29	TCP TF family	8	0	8	2.00E-03
27.3.40	Aux/IAA family	9	2	7	4.00E-03
27.3.9	C2C2(Zn) GATA TF family	10	2	8	7.00E-03
27.3.22	HB, homeobox TF family	18	5	13	1.00E-02
27.3.7	C2C2(Zn) CO-like, Constans-like zinc finger family	11	2	9	2.00E-02
27.3.23	HSF, heat-shock TF family	13	8	3	2.00E-02
27.3.27	NAC domain TF family	4	0	4	2.00E-02
27.3.26	MYB-related TF family	10	3	7	2.00E-02
27.3.6	bHLH, basic helix-loop-helix family	31	9	22	3.00E-02
27.3.24	MADS box TF family	3	3	0	4.00E-02
Total number of TFs		164	79	79	
Incompatible interaction (resistant tomato inoculated with <i>C. fulvum</i>)					
27.3.32	WRKY domain TF family	24	23	1	5.00E-05
27.3.40	Aux/IAA family	8	0	8	6.00E-05
27.3.6	bHLH, basic helix-loop-helix family	15	2	13	5.00E-04
27.3.3	AP2/EREBP, APETALA2/ethylene-responsive element binding protein family	15	2	13	1.00E-03
27.3.22	HB, homeobox TF family	12	2	10	5.00E-03
27.3.28	SBP, squamosa promoter binding protein family	4	0	4	8.00E-03
27.3.64	PHOR1	5	5	0	1.00E-02
27.3.9	C2C2(Zn) GATA TF family	4	0	4	2.00E-02
27.3.21	GRAS TF family	7	2	5	4.00E-02
Total number TFs		94	36	58	
Compatible interaction (susceptible tomato inoculated with <i>C. fulvum</i>)					
27.3.25	MYB domain TF family	3	3	0	2.00E-02

*MapMan bins of genes were identified by comparing the regulation of the genes present in each bin to the transcriptional regulation of the tomato genome as a whole using the Wilcoxon rank sum test.

From the total of 81 *SIWRKYs* encoded by the tomato genome (Huang et al., 2012), 59 (~73%) were expressed in the DS of which 38 (~64%) were differentially regulated, representing about 8% of all 489 differentially expressed TFs. From these 38 *SIWRKYs*, 36 were up- and 2 were down-regulated. Similarly, in *C. fulvum*-inoculated resistant tomato, from the 24 differentially regulated *SIWRKYs* (which represent about 41% of all expressed *SIWRKYs* in this system), 23 were up-regulated compared with the mock-treated plants, while in susceptible tomato only 8 *SIWRKYs* (~14% of all expressed *SIWRKYs*) were upregulated compared to mock treated plants. These 8 *SIWRKYs* were also up-regulated in the DS and resistant plants while their expression was much lower in the susceptible plants (Figure 2B).

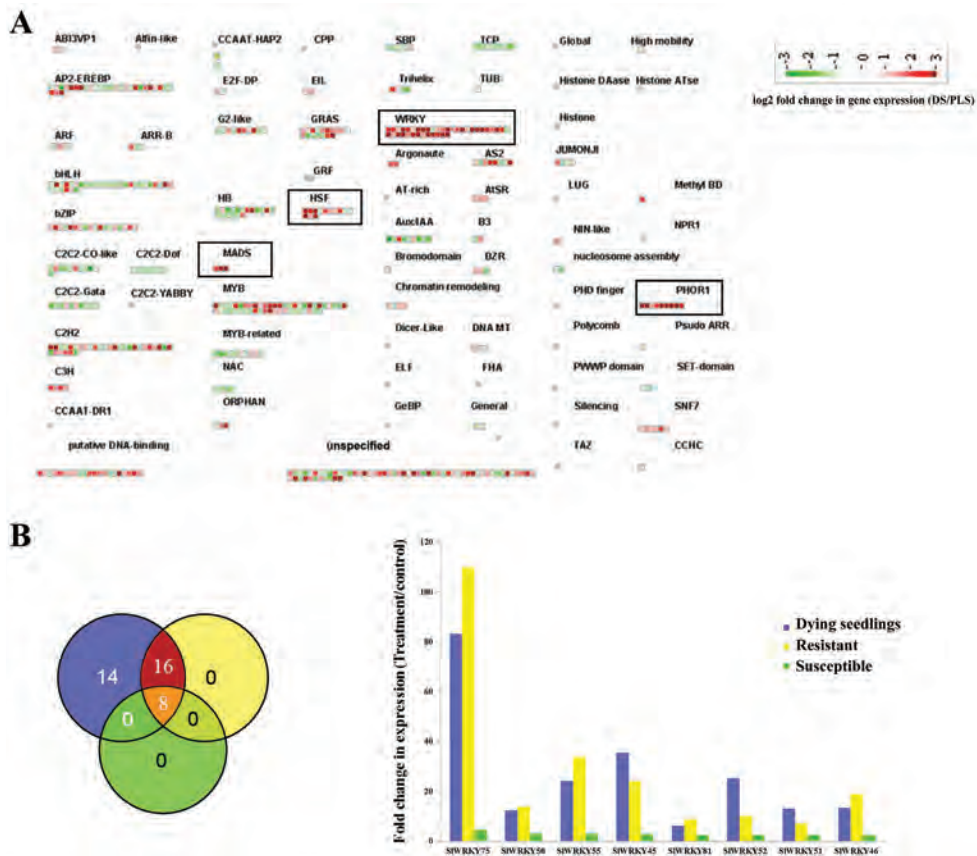


Figure 2. The transcriptional profile of tomato TFs and transcription-related genes during mounting of the HR. (A) TFs and additional transcription-related proteins of which the corresponding genes are differentially regulated (fold change > 2 and $P < 0.001$, with FDR correction) during mounting of the HR in the DS as compared with the PLS. The green and red blocks represent individual genes of which the expression is down- or up-regulated, respectively. The colour code represents the (\log_2) fold change in expression of a gene in the DS compared to the PLS, at 5 hrs after the temperature shift that initiates the HR in the DS. Strongly enriched and upregulated families of TFs are indicated by the black boxes.

(B) Venn diagram showing the amount and distribution of differentially expressed *SIWRKYs* in the DS and *C. fulvum*-inoculated resistant and susceptible tomato.

(C) Bar graph representing the expression profiles of the eight *SIWRKYs* that are differentially expressed in all three systems (see the portion of the Venn diagram shown in (B) marked in orange).

Phylogenetic Tree Analysis and Chromosomal Distribution of Differentially Expressed *SIWRKYs*

To generate an overview of all expressed *SIWRKYs* across the three systems (DS, I and C) and to dissect their transcriptional behaviour across the 12 tomato chromosomes and the different clades of the phylogenetic tree (Huang et al., 2012) during mounting of the HR, we propose the terms “expression index” (EI) and “perturbation index” (PI). EI signifies the portion of expressed *SIWRKYs* present at a particular chromosome or clade of the phylogenetic tree, relative to the total number of *SIWRKYs* that have been assigned to a particular chromosome or clade of the phylogenetic tree. The PI represents the total number of differentially regulated *SIWRKYs*, relative to the total number of expressed *SIWRKYs* that have been assigned to a particular chromosome or clade of the phylogenetic tree. Hence, these two terms are used to describe the quantitative distribution of the expressed and differentially regulated genes located at the various tomato chromosomes and clades of the phylogenetic tree.

The phylogenetic tree of the *SIWRKYs* that was constructed based on the amino acid sequences of the 81 different *SIWRKY* proteins that they encode, resembles the one generated by (Huang et al., 2012) for the WRKYs of tomato, Arabidopsis and rice and reveals a distinct clustering pattern based on the number of WRKY domains that these TFs contain and the variation that exists in their zinc-finger-like motif (**Figure 3A** and **Supplementary Table S1**). In the phylogenetic tree, all the differentially expressed *SIWRKYs* that were identified are labelled by colours corresponding to their distribution over the DS and *C. fulvum*-inoculated resistant (I) and susceptible (C) tomato plants (**Figure 2B**). *SIWRKYs* belonging to group II-e showed the lowest group expression index (GEI). Ten out of the 17 *SIWRKYs* (65%) present in this group were not detected as an expressed transcript in our RNA-seq analysis. However, more than 75% of the *SIWRKYs* belonging to other groups were expressed (**Figure 3B**). Most of the differentially expressed *SIWRKYs* are distributed across all groups except for group II-e, of which none shows differential expression. The 8 differentially expressed *SIWRKYs*, shared between the DS and *C. fulvum*-inoculated resistant and susceptible plants (**Figure 2B**) are evenly distributed over groups II-a, II-c and III, whereas the *SIWRKYs* that are differentially expressed both in the DS and in *C. fulvum*-inoculated resistant plants, are present across all groups (except for group II-e), but show quite exclusive distribution to groups I, II-b and II-d (**Figure 3A**, blue and red labelled leaflets). The highest and lowest number of differentially expressed *SIWRKYs* that correspond to a high PI belong to group III (~91% (9 out of 10)) and group I (~27%), respectively (**Figure 3**). The three *SIWRKYs* that

could not be assigned to any of the groups (*SIWRKY26/27/49*), both in our analysis (**Figure 3A**, leaflets marked by a green box) and in the analysis performed by Huang et al. (2012), did not show any expression according to our RNA-seq analysis.

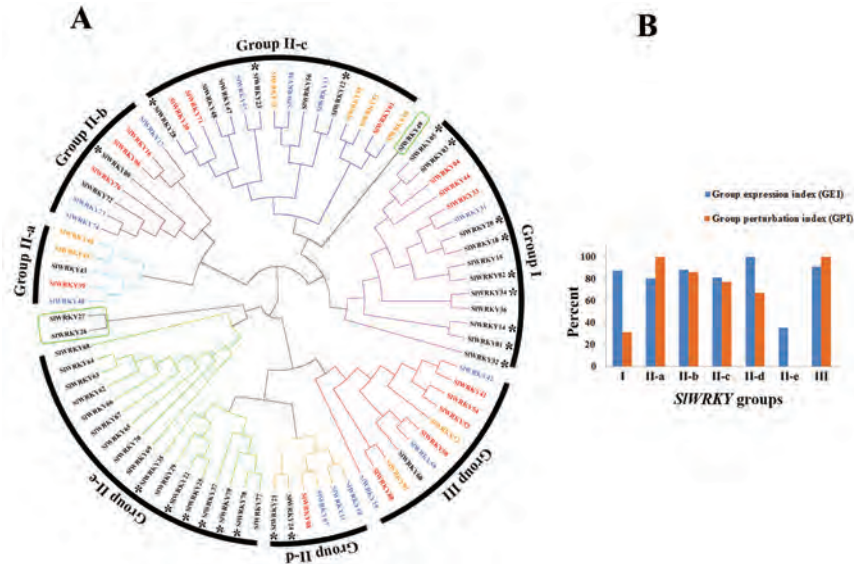


Figure 3. Distribution of the (differentially) expressed *SIWRKY*s across the different groups of *SIWRKY*s.

(A) Phylogenetic tree of the WRKY protein family of tomato, as was also constructed by (Huang et al., 2012). Clades with different colours represent sets of *SIWRKY*s that differ in the amount of WRKY domains that they contain and the type of zinc-finger-like motif that is present (See **Supplementary Table S1**). Differentially expressed genes encoding the *SIWRKY*s (indicated on the leaflets of the tree) are labelled in blue, red or orange, referring to the experimental system(s) (DS, resistant or susceptible tomato inoculated with *C. fulvum*) in which they are differentially regulated (see the corresponding portion of the Venn diagram shown in **Figure 2B**). Genes encoding the *SIWRKY*s that are indicated in black are either not expressed in at least one of the experimental systems or were not found to be differentially expressed when treatment and control were compared. In the latter case these *SIWRKY*s are marked with an asterisk (*). The group names were assigned according to (Huang et al., 2012).

(B) Bar graph depicting the percentage of expressed and differentially regulated genes encoding *SIWRKY*s present in a particular group, as compared with the total number of *SIWRKY*s present in that same clade. These percentages correspond to the group expression index (GEI) and group perturbation index (GPI), respectively (see text for details).

The genes encoding the 81 *SIWRKY*s are distributed across all tomato chromosomes except for chromosome 11, which completely lacks genes encoding *SIWRKY*s (**Figure 4A**). Chromosome 5 contains the highest number of *SIWRKY*s (~20% of them) and 9 out of the 13 tandemly-duplicated *SIWRKY*-encoding genes, which do not show expression according to our RNA-seq dataset. The presence of a large number of tandem-duplicated, unexpressed *SIWRKY*s renders chromosome 5 a *WRKY*-deficient region in the genome, next to chromosome 11 (**Figure 4B**). Six out of the 9 tandem-duplicated *SIWRKY*s present on this chromosome belong to group II-e. Chromosomes

VIGS of *SIWRKYs* Affects the Metabolome of the Apoplast of Tomato Leaves

The metabolome of the leaves of tomato plants is an important indicator of the major biochemical changes that occur during its interaction with *C. fulvum* (Etalo et al., 2013). The fungus exclusively colonizes the apoplast of the leaves of its host and therefore we isolated apoplastic fluids from tomato leaflets (Joosten, 2012) and analysed their metabolome to monitor its changes in resistant and susceptible plants upon inoculation with *C. fulvum*. Analysis of the composition and abundance of the polar and semi-polar secondary metabolites revealed that already at 6 dpi the metabolome of the apoplast of the inoculated tomato leaves is quite distinct from that of the mock-inoculated ones. Moreover, at 6 dpi susceptible inoculated plants have a metabolome profile clearly distinct from their resistant counterparts, which becomes even more clear at 10 dpi (**Supplementary Figure S2**). To study the role of the *SIWRKYs* in defence-associated metabolome reprogramming, we performed metabolomics analyses of apoplastic extracts after silencing of a number of the most interesting *WRKYs* upon inoculation with *C. fulvum*.

Individual characterization of the various *SIWRKYs* is challenging due to the functional redundancy present in this family of TFs (Journot-Catalino et al., 2006; Xu et al., 2006; Eulgem and Somssich, 2007; Shen et al., 2007). To overcome this, we employed a multiple-gene silencing strategy, using a single chimeric VIGS construct that contains 2 to 4 fragments, together targeting a group of *SIWRKYs* predicted to be functionally redundant (**Figure 2** and **Supplementary Figure S3**). The primary screening was performed by analysing the apoplastic metabolome of *C. fulvum*-inoculated resistant plants (Cf-4) at 13 dpi that had been subjected to VIGS of multiple *SIWRKYs* showing significant up-regulation in one or more of the three biological systems (**Figure 2B**) and belonging to the same group in the phylogenetic tree (**Figure 3A**). Furthermore, we also included constructs that target two to three *SIWRKYs* sharing high nucleotide sequence homology with Arabidopsis *WRKYs* reported to be defence activators or repressors (Wang et al., 2006; Lippok et al., 2007) (see **Table S2** for an overview of all chimeric VIGS constructs that have been generated). The metabolome analyses were performed on a mix of the apoplastic fluids that were obtained from five individual, silenced tomato plants for each construct. In all cases, *GUS*-silenced Cf-4 plants were included as controls.

Simultaneous targeting of various *SIWRKYs* resulted in dramatic changes in the tomato apoplast metabolome upon inoculation with *C. fulvum* (**Figure 5A**). Principal component analysis (PCA) of the various apoplast metabolomes indicated that simultaneous targeting of *SIWRKY31/33* (group I) has a comparable effect to targeting of the resistance gene *Cf-4* itself (**Figure 5A**), suggesting that the resistance response is

suppressed. *SIWRKY31* and -33 share high sequence homology (**Figure 3A**) and show strong up-regulation in the DS (**Supplementary Table S1**). The metabolome change caused by targeting *SIWRKY33* alone was slightly less pronounced than targeting both *SIWRKY31* and -33. A similar effect as targeting *SIWRKY31/33*, had targeting of *SIWRKY7/8/10/11* (group II-d, sharing high sequence homology (**Figure 3A**) and all up-regulated in the DS (**Supplementary Table S1**)), *SIWRKY31/33/53* (activators, with *SIWRKY53* belonging to group III and again strongly up-regulated in the DS) (**Supplementary Table S1**), *SIWRKY41/42/53/54* (present in a separate clade of four *SIWRKYs* up-regulated in the DS and Cf-4 tomato inoculated with *C. fulvum*, belonging to group III) (**Figure 3A** and **Supplementary Table S1**) and *SIWRKY80* (belonging to group III and strongly up-regulated in both the DS and resistant tomato inoculated with *C. fulvum* (**Supplementary Table S1**), appears to result in increased susceptibility as illustrated by the resemblance of the metabolome of the various plants to the one of susceptible plants (Cf-0) (**Figure 5A**). Remarkably, in addition to its effect on the infection metabolome, targeting of *SIWRKY41/42/53/54* resulted in a clear phenotype characterized by inverted leaflets morphology (**Supplementary Figure S4**). On the other hand, targeting of *SIWRKY50/51/55/61* (belonging to a separate clade of group II-c, of four *SIWRKYs* upregulated in all three systems except for *SIWRKY61*, which is upregulated both in the DS and resistant Cf-4 tomato inoculated with *C. fulvum* (**Figure 3A** and **Supplementary Table S1**)), *SIWRKY39* (a *WRKY* of group II-a which is upregulated both in the DS and Cf-4 tomato inoculated with *C. fulvum* (**Figure 3A**)) or *SIWRKY10/61* (repressors) (Journot-Catalino et al., 2006; Gao et al., 2011) did not result in alterations in the metabolome as compared to the control (Cf-4-GUS) (**Figure 5A**).

Interestingly, targeting *SIWRKY39/40/45/46*, which are closely related *SIWRKYs* belonging to group II-a that are particularly upregulated in the DS and in resistant tomato (**Figure 3A** and **Supplementary Table S1**), in Cf-0 and Cf-4 tomato resulted in plants showing strong dwarfing and bushy growth and the development of small necrotic lesions (**Figure 6A** and **Supplementary Figure S5**). Upon inoculation with *C. fulvum*, massive lesion formation occurred within 4 dpi (**Figure 6C**). The bushy growth feature of these lines is primarily reflected in the newly emerging small sized leaflets succeeding the first two layers of primary leaves, which have very broad leaflets with thick stems showing downward angular growth. *SIWRKY39* was significantly up-regulated in the DS and the Cf-4 plants inoculated with *C. fulvum*, whereas *SIWRKY45* and -46 were significantly up-regulated in all three systems (**Supplementary Table S1**) and represent the only expressed tandem-duplicated *SIWRKYs* (**Figure 4A**). *SIWRKY40* was differentially up-regulated only in the DS (**Supplementary Table S1** and **Supplementary Figure S6**). The peculiar dwarf phenotype that arises from targeting

SIWRKY39/40/45/46 suggests the activation of a constitutive defence response in tomato. With this consideration, we performed an additional experiment by focusing on this group of WRKYs from the repressor group (Xu et al., 2006; Shen et al., 2007) and we also included *SIWRKY31/33* and *SIWRKY80* from the activator group (Zheng et al., 2006; Gabriels et al., 2007; Vossen et al., 2010). In addition to the resistant (Cf-4) background, targeting of *SIWRKY39/40/45/46* was also performed in the susceptible (Cf-0) background, with the intention of boosting defence in these plants too. Silencing of the activators was only performed in the resistant background (Cf-4), with the expectation of increased susceptibility. Three independent biological replicates were considered and the metabolome of the apoplast was analysed at 9 days after inoculation with *C. fulvum*. Interestingly, targeting *SIWRKY39/40/45/46* in susceptible (Cf-0) or resistant (Cf-4) plants led to increased resistance as manifested by the clear separation of these samples from the control (Cf-4-GUS) (**Figure 5B**).

In contrast, targeting *SIWRKY31/33*, *SIWRKY80* and the resistance gene *Cf-4* itself in Cf-4 tomato caused dramatic changes in the metabolome resulting in the separation of these samples from the Cf-4-GUS control in the other direction (**Figure 5B**). This suggests that the metabolome profile of the resistant plants silenced for these particular activator *SIWRKYs* is an indicator of increased susceptibility (**Figure 5B and 5C**). In the hierarchical cluster analysis (HCA), in general, the metabolome reprogramming is featured by six distinct clusters that determine the spatial separation of the samples in the PCA (indicated with yellow boxes in **Figure 5C**). Cluster II-associated metabolite accumulation in Cf-4 tomato VIGSed for *Cf-4*, *SIWRKY31/33* or *-80*, and cluster III-, V- and VI-related metabolite accumulation in Cf-4 and Cf-0 tomato VIGSed for *SIWRKY39/40/45/46*, results in the separation of the samples in the X-dimension (PC1) that represents the majority of the explained variation (56%; **Figures 5B and 5C**). Furthermore, the accumulation of metabolites depicted in cluster III, V and VI in both Cf-0 and Cf-4 tomato targeted for *SIWRKY39/40/45/46* explains the variation that exists between these targeted lines and the control (Cf-4-GUS) in the Y-dimension (PC2; 14%) (**Figures 5B and 5C**). Cluster IV explains the slight variation that exists between *SIWRKY39/40/45/46*-targeted Cf-0 and Cf-4 tomato (the Z component (PC3) explains nearly 9% of the variation and is not shown in **Figure 5B**).

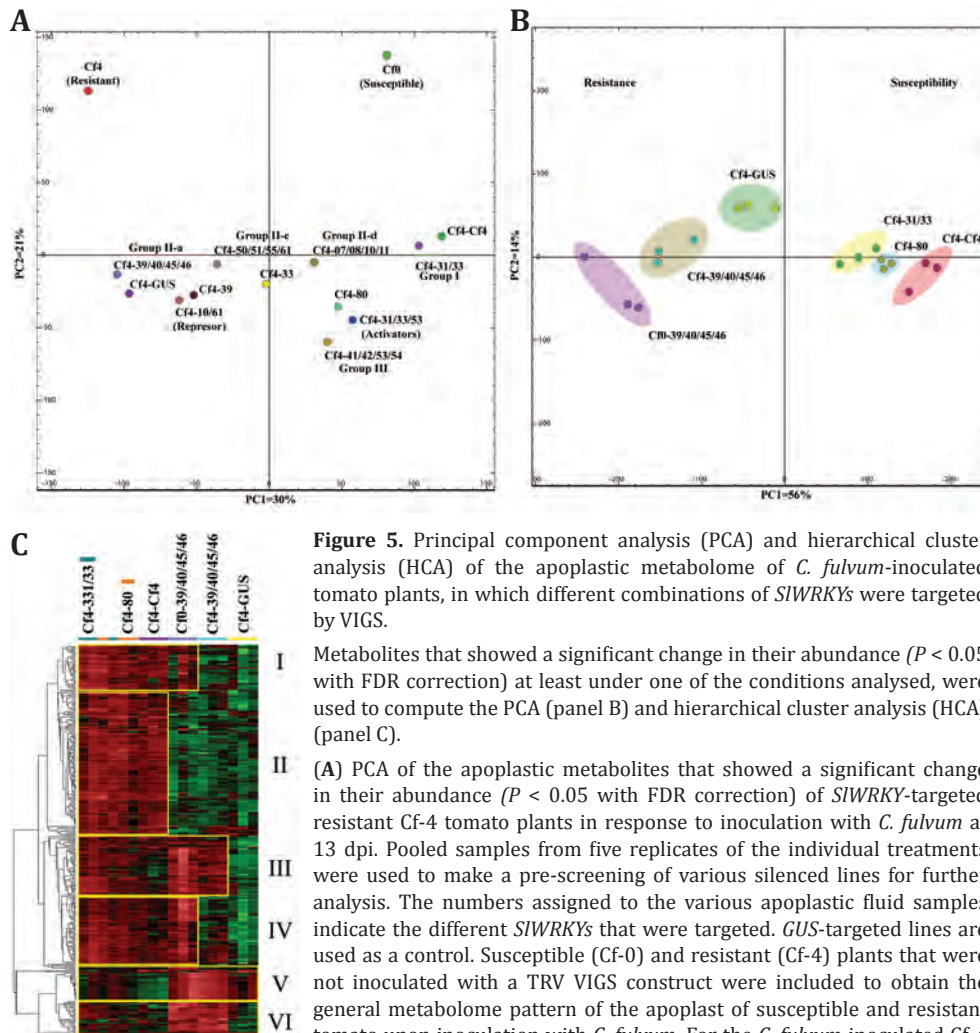


Figure 5. Principal component analysis (PCA) and hierarchical cluster analysis (HCA) of the apoplastic metabolome of *C. fulvum*-inoculated tomato plants, in which different combinations of *SIWRKY*s were targeted by VIGS.

Metabolites that showed a significant change in their abundance ($P < 0.05$ with FDR correction) at least under one of the conditions analysed, were used to compute the PCA (panel B) and hierarchical cluster analysis (HCA) (panel C).

(A) PCA of the apoplastic metabolites that showed a significant change in their abundance ($P < 0.05$ with FDR correction) of *SIWRKY*-targeted resistant Cf-4 tomato plants in response to inoculation with *C. fulvum* at 13 dpi. Pooled samples from five replicates of the individual treatments were used to make a pre-screening of various silenced lines for further analysis. The numbers assigned to the various apoplastic fluid samples indicate the different *SIWRKY*s that were targeted. *GUS*-targeted lines are used as a control. Susceptible (Cf-0) and resistant (Cf-4) plants that were not inoculated with a TRV VIGS construct were included to obtain the general metabolome pattern of the apoplast of susceptible and resistant tomato upon inoculation with *C. fulvum*. For the *C. fulvum*-inoculated Cf-4 plants in which *SIWRKY*s have been silenced, any deviation of the apoplastic metabolome from the Cf-4-*GUS* control is an indicator of increased susceptibility or resistance.

(B) PCA based on the metabolites that showed a significant change in their abundance ($p < 0.05$ with FDR correction) in the apoplast of *SIWRKY*-targeted tomato plants at 9 dpi with *C. fulvum*. Only resistant (Cf-4) tomato was used for targeting the activators *SIWRKY31/33* and *SIWRKY80*, except for targeting defence repressor *SIWRKY*s (*SIWRKY39/40/45/46*), which was performed both in susceptible (Cf-0) and resistant (Cf-4) tomato. Targeting of *GUS* and *Cf-4* served as controls.

(C) HCA based on the metabolites that showed a significant change in their abundance ($p < 0.05$ with FDR correction) in the apoplast of *SIWRKY*-targeted tomato plants at 9 dpi with *C. fulvum*, shown in (B). The boxes indicated in yellow discern the six distinct clusters that determine the spatial separation of the samples in the PCA.

VIGS of *SIWRKY39/40/45/46* in Susceptible Cf-0 Tomato Constitutively Activates Defence and Suppresses *C. fulvum* Proliferation

To investigate the role of the silencing of *SIWRKY39/40/45/46* in Cf-0 tomato beyond the observed metabolome reprogramming, we inoculated the plants with a strain of *C. fulvum* constitutively expressing the *GUS* gene and performed GUS staining of the leaves at 12 dpi. Furthermore, Cf-0 plants only targeted for *SIWRKY39* were included in the analysis to validate if there is functional redundancy between *SIWRKY39*, -40, -45 and -46. Remarkably, the GUS staining revealed a significant reduction in the colonisation by *C. fulvum* of the Cf-0 plants silenced for *SIWRKY39/40/45/46* **Figure 6B**).

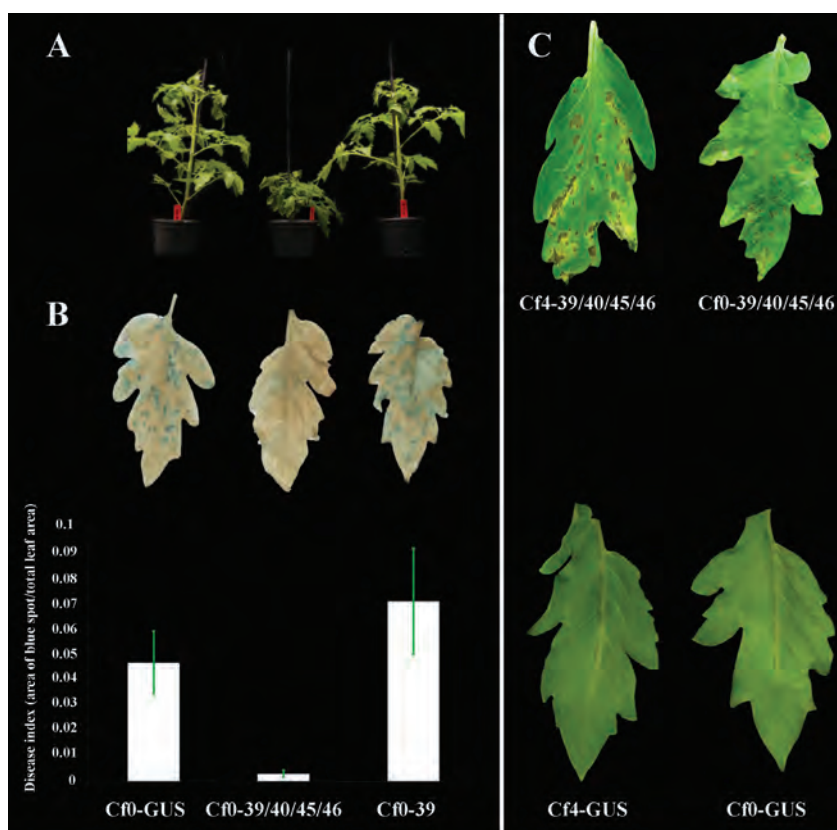


Figure 6. Change in tomato defence against *C. fulvum* through silencing of defence repressors *SIWRKY39/40/45/46* by VIGS.

(A) Severely stunted growth of susceptible tomato lines silenced for *SIWRKY39/40/45/46*, 12 dpi with the recombinant virus.

(B) Representative images of GUS staining, depicting significant reduction in colonization by *C. fulvum* of susceptible Cf-0 tomato silenced for *SIWRKY39/40/45/46*. Blue spots indicate colonization of the tomato leaflet by a strain of the fungus constitutively expressing the *GUS* reporter gene, at 12 dpi. The disease index was calculated using the Image J plugin (Abd-El-Haliem, 2012) and is shown in the bar graph. The average value of 5 independent biological replicates is shown and the standard error of the mean is indicated.

(C) Development of necrotic lesions in resistant (Cf-4) and susceptible (Cf-0) tomato, silenced for *SIWRKY39/40/45/46*, at 8 dpi with *C. fulvum*. The necrotic lesions are already evident at 4 dpi. *GUS*-silenced Cf-4 and Cf-0 leaflets serve as controls.

Discussion

In our system-wide transcriptome analysis, the massive enrichment of *SIWRKYs* in the pool of differentially expressed genes clearly indicates their prominent role in shaping the HR-related transcriptome landscape of tomato during mounting of the HR, in the DS as well as upon inoculation of resistant plants with *C. fulvum* (**Figures 1 and 2** and **Table 1**). It has been postulated that in addition to cis-promoter elements and transcription factors, the organization of the chromosomes into territories within the nucleus also influences the expression level of genes (Cremer and Cremer, 2001; Fraser and Bickmore, 2007; Babu et al., 2008; Gondor and Ohlsson, 2009; De and Babu, 2010; Levesque and Raj, 2013). To have an overview of the genome-wide distribution of the (differentially) expressed *SIWRKYs*, we mapped them onto the 12 tomato chromosomes using the information provided by Huang et al. (2012). The high number of expressed *SIWRKYs* are quite evenly distributed across the various tomato chromosomes, with the exception of chromosome 11, which does not carry any *SIWRKYs* (Huang et al., 2012).

The distribution of (differentially) expressed *SIWRKYs* over a particular chromosome and across different clades in the phylogenetic tree helps to determine whether there is genome-specific regulation and/or regulation related to specific group(s) of *SIWRKYs*. From group and chromosomal expression and perturbation indices, it is evident that there is a considerable variation in the number of differentially expressed *SIWRKYs* in both chromosome-wide and phylogeny-based analyses, suggesting that there is selective upregulation of groups of *SIWRKYs* located in a certain region of the genome (**Figures 3 and 4**). As an example, it is worth considering the *SIWRKYs* belonging to group I, which is believed to represent the most ancestral type of *WRKY* genes (Ulker and Somssich, 2004). However, although in this group a number of expressed *SIWRKYs* are present (high GEI), only a few of them were actually differentially expressed during mounting of the HR (indicated by a low group perturbation index (GPI)) (**Figure 3**). Another example is group II-e of the *SIWRKYs* that showed barely any expression and of which none were differentially expressed (**Figure 3**). Most of them are localized on chromosome 5, representing the majority of the tandem-duplicated *SIWRKY* gene clusters (**Figure 4**). In this group, the *SIWRKYs* that are part of the sub-clade consisting of *SIWRKY62* to -69 have been reported to have expanded only in Solanaceous species (**Figure 3**) (Huang et al., 2012). None of the group II-e *SIWRKYs* showed differential regulation in our dataset as well as in the dataset of Huang et al. (2012) that encompasses various *SIWRKYs* retrieved from publically available microarray experiments involving both

biotic (tomato spotted wilt virus (TSWV), *Clavibacter michiganensis*, fungal ethylene-inducing xylanase (EIX), and inoculation with the fungal necrotrophic pathogen *Botrytis cinerea*) as well as abiotic (salt and drought) stresses suggesting that they are likely to be non-functional WRKYs (**Supplementary Figure S8**, provides information on unique and overlapping upregulated genes between the DS and TSWV, EIX and *Botrytis cinerea*-challenged tomato). *SIWRKYs* belonging to groups I, II-b and II-d specifically showed differential expression in the DS and resistant tomato inoculated with *C. fulvum*. As these experimental systems predominantly represent ETI, this suggests that there could be a specific network of genes that induces the expression of this specific group of *SIWRKYs* upon triggering of ETI.

The timing of the transcriptional reprogramming in response to perturbation of plant homeostasis is critical. However, elucidation of the underlying mechanisms that regulate the switch to an alternative gene transcription programme remains a major challenge. A fast and coordinated transcriptional switch contributes to the fitness of plants by enabling them to maintain the right carbon economy and energy homeostasis. The *SIWRKY* transcriptional network, in combination with other differentially regulated TFs (**Figure 2A**), provides the proper balance to respond quickly and to efficiently activate defence thereby deterring pathogens, but at the same time represses defence responses as their uncontrolled activation will have detrimental consequences on plant fitness. The upregulation of defence repressor genes such as the group II-a *SIWRKY39/40/45/46* (Xu et al., 2006; Shen et al., 2007), together with genes actively required to boost the immune system, creates a fine balance regulating the transcriptional reprogramming associated with mounting of the HR (**Supplementary Figure S6**). In agreement with this, the orthologs of these group II-a *SIWRKYs* in Arabidopsis (*AtWRKY18/40/60*) are also upregulated upon inoculation with an avirulent strain of the bacterial pathogen *Pseudomonas syringae* and upon treatment of the plants with salicylic acid (Dong et al., 2003; Huang et al., 2012). Hence, the observed constitutive defence activation in susceptible tomato upon targeting of *SIWRKY39/40/45/46* by VIGS (**Figure 6B**) strongly supports our argument that an upregulation of defence activators and defence repressors in parallel is essential to boost the immune system but at the same time control it.

The regulatory importance of this group of defence repressors is manifested by the strong dwarf phenotype of the *SIWRKY39/40/45/46*-targeted lines (**Figure 6A**). Our result is consistent with previous studies showing that Arabidopsis double or triple mutants of *wrky18/40* or *wrky18/40/60* exhibit enhanced resistance to the virulent hemi-biotrophic *P. syringae* and powdery mildew *Golovinomyces orontii* (Xu et al., 2006; Shen et al., 2007). In Arabidopsis this group of WRKYs has been reported to have both physical and functional interaction. The functional interaction is more complex, having additive, cooperative and antagonistic effects (Wang et al., 2006; Xu et al., 2006; Shen

et al., 2007; Chen et al., 2010). The leucine zipper motif present at their N-terminus has been shown to be important for homo- and hetero-dimerization of these WRKYs (Xu et al., 2006). Moreover, AtWRKY18/40/60 also interact with group II-b, II-d and III AtWRKYs, signifying their central regulatory role in the WRKY network (Xie et al., 2006; Arabidopsis Interactome Mapping, 2011; Chi et al., 2013). Targeting of *SIWRKY39* only, which is highly similar to *AtWRKY18*, did not result in constitutive defence activation, indicating that this particular *SIWRKY* has a redundant function (**Figure 6**). Similarly, from the group of activators, the impact of targeting only *SIWRKY33* on the tomato apoplast metabolome was low as compared to targeting of both *SIWRKY31* and -33, that both belong to group I (**Figure 3** and **5A**). The impact at the level of the metabolome of targeting *SIWRKY31/33* by VIGS is comparable to that of targeting the resistance gene *Cf-4* itself, suggesting that these two group I *SIWRKY*s act as defence activators. In line with this, in Arabidopsis AtWRKY33, which has a high sequence similarity with *SIWRKY31/33*, has also been suggested to be a positive regulator of defence as it stimulates camalexin biosynthesis during colonization by *Botrytis cinerea* (Mao et al., 2011). The same report showed that AtWRKY33 is a substrate of the MAP kinases MPK3 and MPK6 and mutation of the MPK3/MPK6-targeted phosphorylation sites in AtWRKY33 compromised its ability to complement the lack of induction of camalexin production in a *wrky33* mutant. Furthermore, the impact of targeting *SIWRKY80* alone is also as significant as targeting of the resistance gene *Cf-4* itself (**Figure 5A**). *SIWRKY80* has significant amino acid sequence similarity to AtWRKY70, which has been shown to regulate the balance between salicylic acid- and jasmonic acid- mediated signalling cross talk that plays an important role in defence against biotrophic pathogens and insects (Li et al., 2004).

Comparative analysis of the differentially upregulated *SIWRKY*s in our data set (DS) and datasets produced by Huang et al. (2012) that encompass *B. cinerea*-, TSWV- and EIX-challenged tomato plants, indicates that both *SIWRKY31* and -33 were commonly upregulated in all systems indicating that this set of *SIWRKY*s plays a significant role in defence against a broad range of microbes. Similarly, except for *B. cinerea*-inoculated tomato, *SIWRKY80* showed differential upregulation in all the above-mentioned datasets (**Supplementary Figure 8**). This information and the observed increased susceptibility upon targeting of both *SIWRKY31/33* and *SIWRKY80* in our VIGS experiments signifies the crucial role of this group of *SIWRKY*s in the defence of tomato against a variety of micro-organisms.

Specific clusters of metabolites positioned in different clades of the hierarchical cluster analysis (HCA) could be used as an indicator of compromised/induced immune responses due to targeting of a group of redundant *SIWRKY*s (**Figure 5C**). The metabolite patterns in the *SIWRKY*- and *Cf-4*-targeted plants also could show the link between *Cf-4*-dependent signalling pathways within the *SIWRKY* network. For example, compared

with the Cf-4 plants targeted for *GUS* (Cf-4-GUS), metabolites belonging to cluster II showed higher accumulation when either the gene encoding the upstream receptor Cf-4 itself or the genes encoding the downstream defence regulators *SIWRKY31/33* or *SIWRKY80* were targeted, suggesting that the *SIWRKY31/33*- and *SIWRKY80*-regulated networks are closely linked with Cf-4-mediated defence signalling (**Figure 5C**). However, upon silencing of *SIWRKYs39/40/45/46* in Cf-0, metabolites in cluster II showed the same profile as in Cf-4-GUS or Cf-4-39/40/45/46, suggesting that the response is not solely Cf-4-dependent and also is most likely related to a constitutively induced basal defence response. This observation further strengthens the intricate and inseparable nature of the two blurred layers of the plant immune system (Thomma et al., 2011). In the PCA, this cluster II of metabolites contributes to the separation of the treatments in the X dimension (PC1) that represents Cf-0/Cf-4-39/40/45/46 and Cf-4-GUS on the left and Cf-4-31/33, -80 and -Cf4 on the panel that correspond to either increased resistance or susceptibility, respectively (**Figure 5B**). One possible explanation for the accumulation of this cluster of metabolites in the lines showing compromised defence activation (Cf-4-Cf-4, Cf-4-31/33 and Cf-4-80), is that in resistant Cf-4 plants or in susceptible Cf-0 plants with constitutively induced basal defence (Cf-0-39/40/45/46), these metabolites could be redirected towards the synthesis of defence-related secondary metabolites during the activation of basal defence. Hence, the seemingly high accumulation of these metabolites in Cf-4-Cf-4, Cf-4-31/33 and Cf-4-80 could be linked to compromised defence activation, associated with targeting of the *SIWRKYs* or Cf-4. This is also supported by our previous findings, where in the DS some of the organic acids that act as building blocks for most amino acids and secondary metabolites derived from these amino acids showed an inverse accumulation pattern with that of most of defence related primary and secondary metabolites (Etalo et al., 2013).

Interestingly, metabolite clusters I and IV showed accumulation when Cf-4 or the downstream defence activators *SIWRKY31/33* or *SIWRKY80* were silenced (**Figure 5C**). Unlike the metabolites in cluster II, metabolites in these two clusters also showed accumulation in Cf-0-39/40/45/46, but not in Cf-4-39/40/45/46, indicating that these metabolites are an indicator of increased susceptibility when Cf-4 or Cf-4-WRKY31/33 and WRKY80 circuits is disrupted. Clusters V and VI explain the separation of both Cf-0-39/40/45/46 and Cf-4-39/40/45/46 lines from the Cf-4-GUS and Cf-4 plants in which other groups of *SIWRKYs* have been targeted, in the PCA plots (**Figure 5A** and **5B**). This can be linked to increased resistance due to targeting of the defence repressors *SIWRKY39/40/45/46*. Hence, our work for the first time shows the impact of WRKY TFs on defence-associated global metabolome reprogramming and also underlines the potential of metabolomics to deliver markers that can be used to dissect the different layers of the plant immune system.

Based on our genome-wide analysis, which is supported by deep RNA-seq, untargeted metabolomics and VIGS, the key regulatory function of *SIWRKYs*, both positive and negative, for plant innate immune system is undisputable. The fact that group I, II-b, II-d *SIWRKY* TFs are exclusively expressed in the DS and resistant inoculated tomato suggests that these group of *SIWRKY* TFs are a key regulator of the ETI (**Figure 3**). Group I, II-b, II-d *SIWRKY* TFs are reported to be a substrate for the MAPKs and also to be influenced by CaM and Ca²⁺ fluxes (Menke et al., 2005; Park et al., 2005; Qiu et al., 2008; Popescu et al., 2009; Ishihama et al., 2011; Mao et al., 2011).

The robustness of the DS system helps to amplify small, short lived and non-synchronous plant immune-associated responses to a higher level. The combined use of such a reliable biological system with RNA-seq analysis significantly enhances the amount of biologically relevant information that can be retrieved. This can for example be concluded from the number of differentially expressed *SIWRKYs* identified in the DS, in comparison with the *C. fulvum*-inoculated plants (**Figures 3 and 4** and **Table 1**). In a previous study, using the Affymetrix tomato genome array representing only one third of all tomato genes, we only detected 12 differentially expressed *SIWRKYs*, representing 20% of all expressed *SIWRKYs* (Etalo et al., 2013). In our current analysis more than 64% (38 out of 59) of the expressed *SIWRKYs* showed to be differentially expressed. Our previous and current study establish a solid foundation for demonstrating how systems biology approaches combining a robust biological system with ~omics technologies provides reliable information on how the plant immune system is regulated. Furthermore, VIGS targeting multiple genes at the same time will substantially contribute to functional characterization of redundant gene families in a crop plant like tomato. Hence, future studies focussing on the 38 differentially expressed *SIWRKYs* will surely provide a significant contribution to our quest to understand the role of the WRKY TF network in the immune response of plants to detrimental pathogens.

Materials and Methods

RNA Isolation and RNA-seq Analysis

RNA was isolated from 100 mg of tomato leaf tissue, using 1 ml of Trizol reagent (Invitrogen) according to the manufacturer's instructions. RNA-seq was performed at the Beijing Genome Institute (BGI, Beijing, China), according to the following protocol. Total RNA was treated with DNase-I Amplification Grade (Invitrogen) and purified with an RNeasy Mini kit (Qiagen). Oligo (dT) beads were used to isolate poly (A) mRNA from the total RNA and fragmentation buffer was added to fragment the mRNA into short fragments. Taking these short fragments as templates, random hexamer primers were used to synthesize the first-strand cDNA. Second-strand cDNA was synthesized using buffer, dNTPs, RNase H and DNA polymerase I, respectively. The cDNA fragments were

purified using a QiaQuick PCR extraction kit and resolved with EB buffer for end repair and adding poly (A). After that, sequencing adaptors were added to the short fragments and for amplification by PCR suitable fragments were selected as templates with respect to the result of agarose gel electrophoresis. Lastly, the library was sequenced using Illumina HiSeq™ 2000 technology. Clean reads were mapped to the tomato reference genome and gene sequences respectively using SOAP2 (Li et al., 2009). Mismatches of no more than 5 bases were allowed in the alignments. For the calculation of the Unigene expression, the RPKM method (reads per kb per million reads) was used (Mortazavi et al., 2008). When there is more than one transcript for a certain gene, the longest one is used to calculate its expression level and coverage. In our analysis, differentially expressed genes (DEGs) with a *P*-value (after false discovery rate (FDR) correction) ≤ 0.001 and a fold-change (treatment/control) ratio higher than 2 were used for further studies.

Virus Induced Gene Silencing (VIGS) of Multiple Genes

Generation of VIGS Constructs

The fragments for VIGS of *SIWRKYs* with plausible redundant function (based on sequence similarity, the presence of orthologues in other species with confirmed redundancy and expression patterns), were generated by PCR-mediated specific fragment amplification of the individual *SIWRKYs* to be targeted. For this, cDNA obtained from tomato dying seedlings was employed as a template, using FWD and REV primers that introduce specific restriction enzyme sites (**Supplementary Table S2**). Fragments were checked by sequencing and subjecting them to BLAST searches against the tomato coding sequences present in the recently released tomato genome. All fragments were cloned into pCR4-TOPO (Invitrogen) and chimeric silencing fragments containing the desired specific combination of multiple gene fragments were produced by ligating the individual fragments overnight at 16°C using T4 ligase. Ligation products containing the desired combination of the genes to be targeted were PCR-amplified using the FWD and REV primers from the first and the last gene, respectively (**Supplementary Figure S3**). The chimeric fragment was then cloned into pCR4-TOPO (Invitrogen) and sequenced. Correct fragments were excised from pCR4-TOPO by using restriction enzymes specific for each construct and cloned into pTRV2: RNA2 (pYL156) that was linearized with the same enzymes, to generate the VIGS constructs indicated in **Supplementary Table S2**.

VIGS in Tomato and *C. fulvum* Disease Assays

Tomato was subjected to VIGS as described before (Liebrand et al., 2012). For *C. fulvum* disease assays, tomato plants transformed with the *Hcr9-4D (Cf-4)* gene (Thomas et al., 1997), fully resistant to a race 5 strain of *C. fulvum* (secreting Avr4), were subjected to agroinoculation with various recombinant TRV:VIGS constructs containing a chimeric

fragment to target multiple *SIWRKYs*. Non-agroinoculated MM-Cf-0 and Cf-4 plants served as fully susceptible and resistant controls, respectively. *GUS*-silenced Cf-4 plants (Cf-4-*GUS*) were used as a negative control. Five plants were used per treatment in each experiment. *C. fulvum* inoculations were performed as described (Liebrand et al., 2012) and *C. fulvum* race 5-pGPD:*GUS*, constitutively expressing the *GUS* reporter gene, was used for inoculation (Stulemeijer et al., 2007). Infected leaf samples from the contrasting treatments were destained with ethanol and the extent of the fungal proliferation was quantified by using an image J plugin that compares the blue-stained area to the total leaf area (Abd-El-Haliem, 2012).

Analysis of the Composition and Abundance of Semi-Polar and Polar Secondary Metabolites Present in Apoplastic Fluid Obtained From Tomato Leaves

Apoplastic fluid was isolated from tomato leaves as described by Joosten (2012) and 2 ml aliquots were freeze-dried and extracted with 300 µl of 75% methanol (MeOH) in water, containing 0.1% formic acid. Samples were briefly vortexed, sonicated for 30 min and centrifuged at 21,000g. Supernatants were filtered through a 0.2 µm inorganic membrane filter and transferred to HPLC vials. An LTQ-Orbitrap hybrid mass spectrometer (Thermo Fisher Scientific) was used for the analyses of semi-polar and polar secondary metabolites, with Xcalibur software to control the instrument, and for data acquisition and analysis (van der Hooft et al., 2011). The mass chromatograms that were generated by the LTQ-Orbitrap were processed (peak picking and baseline correction) using the MetAlign software package (Lommen, 2009). Extraction and reconstitution of compound mass spectra were performed according to the method described by Tikunov et al. (2012) and Genemath XT was used for principal component analysis (PCA) as described by Etalo et al. (2013).

Construction of a Phylogenetic Tree of the *SIWRKYs* and Mapping of the Differentially Expressed Genes on the Tomato Chromosomes

For the phylogenetic tree construction, the 81 amino acid sequences that were identified as WRKY transcription factors by Huang et al. (2012) were extracted from the tomato genome (ftp://ftp.sgn.cornell.edu/genomes/Solanum_lycopersicon/annotation/ITAG2.3_release/). The phylogenetic tree was produced in CLCbio main workbench 6 after aligning the sequences using the default settings, followed by phylogenetic tree construction using the UPGMA algorithm with 1,000 bootstrap. The output of the analysis was saved in NETWIK format and further modification of the tree was performed in FigTree (<http://itol.embl.de/Itol.cgi>). The differentially expressed *SIWRKYs* in the three systems (DS, incompatible (I) and compatible (C) interaction) were mapped on the chromosomal map generated by Huang et al. (2012) and indicated in colours that reflect their distribution over these three systems. The Venn diagrams shown in **Figures 1 and 2** have been generated in Venny (<http://bioinfogp.cnb.csic.es/tools/venny/>).

Acknowledgements

We acknowledge Bert Schipper for help with the analysis of the apoplast metabolome and all metabolomics group members of Plant Research International (PRI) and the Laboratory of Plant Physiology (Wageningen University) for their technical and intellectual contribution. We acknowledge Bert Essenstam for excellent plant care. This project was (co)financed by the Centre for BioSystems Genomics (CBSG) and The Netherlands Metabolomics Centre (specifically DWE and RCHDV), which are both part of the Netherlands Genomics Initiative/Netherlands Organisation for Scientific Research.

References

- Abd-El-Haliem A** (2012) An unbiased method for the quantitation of disease phenotypes using a custom-built macro plugin for the program ImageJ. *Methods Mol Biol* **835**: 635-644
- Alves MS, Dadalto SP, Goncalves AB, De Souza GB, Barros VA, Fietto LG** (2013) Plant bZIP transcription factors responsive to pathogens: A review. *Int J Mol Sci* **14**: 7815-7828
- Arabidopsis Interactome Mapping C** (2011) Evidence for network evolution in an Arabidopsis interactome map. *Science* **333**: 601-607
- Atamian H, Eulgem T, Kaloshian I** (2012) SIWRKY70 is required for Mi-1-mediated resistance to aphids and nematodes in tomato. *Planta* **235**: 299-309
- Babu MM, Janga SC, de Santiago I, Pombo A** (2008) Eukaryotic gene regulation in three dimensions and its impact on genome evolution. *Curr Opin Genet Dev* **18**: 571-582
- Bhattacharai KK, Atamian HS, Kaloshian I, Eulgem T** (2010) WRKY72-type transcription factors contribute to basal immunity in tomato and Arabidopsis as well as gene-for-gene resistance mediated by the tomato R gene Mi-1. *Plant J* **63**: 229-240
- Chang C, Yu D, Jiao J, Jing S, Schulze-Lefert P, Shen QH** (2013) Barley MLA immune receptors directly interfere with antagonistically acting transcription factors to initiate disease resistance signaling. *Plant Cell* **25**: 1158-1173
- Chen H, Lai ZB, Shi JW, Xiao Y, Chen ZX, Xu XP** (2010) Roles of arabidopsis WRKY18, WRKY40 and WRKY60 transcription factors in plant responses to abscisic acid and abiotic stress. *Bmc Plant Biol* **10**
- Chi Y, Yang Y, Zhou Y, Zhou J, Fan B, Yu JQ, Chen Z** (2013) Protein-protein interactions in the regulation of WRKY transcription factors. *Mol Plant* **6**: 287-300
- Chisholm ST, Coaker G, Day B, Staskawicz BJ** (2006) Host-microbe interactions: shaping the evolution of the plant immune response. *Cell* **124**: 803-814
- Cremer T, Cremer C** (2001) Chromosome territories, nuclear architecture and gene regulation in mammalian cells. *Nat Rev Genet* **2**: 292-301
- Dangl JL, Horvath DM, Staskawicz BJ** (2013) Pivoting the plant immune system from dissection to deployment. *Science* **341**: 746-751
- de Jong CF, Takken FLW, Cai XH, de Wit PJGM, Joosten MHAI** (2002) Attenuation of Cf-mediated defense responses at elevated temperatures correlates with a decrease in elicitor-binding sites. *Mol Plant Microbe Interact* **15**: 1040-1049
- De S, Babu MM** (2010) Genomic neighbourhood and the regulation of gene expression. *Curr Opin Cell Biol* **22**: 326-333
- Denance N, Sanchez-Vallet A, Goffner D, Molina A** (2013) Disease resistance or growth: the role of plant hormones in balancing immune responses and fitness costs. *Front Plant Sci* **4**: 155
- Dodds PN, Rathjen JP** (2010) Plant immunity: towards an integrated view of plant-pathogen interactions. *Nat Rev Genet* **11**: 539-548
- Dong JX, Chen CH, Chen ZX** (2003) Expression profiles of the Arabidopsis WRKY gene superfamily during plant defense response. *Plant Mol Biol* **51**: 21-37

- Etalo DW, Stulemeijer IJ, van Esse HP, de Vos RC, Bouwmeester HJ, Joosten MHAJ** (2013) System-wide hypersensitive response-associated transcriptome and metabolome reprogramming in tomato. *Plant Physiol* **162**: 1599-1617
- Eulgem T, Rushton PJ, Schmelzer E, Hahlbrock K, Somssich IE** (1999) Early nuclear events in plant defence signalling: rapid gene activation by WRKY transcription factors. *EMBO J*. **18**: 4689-4699
- Eulgem T, Somssich IE** (2007) Networks of WRKY transcription factors in defense signaling. *Curr Opin Plant Biol* **10**: 366-371
- Fradin EF, Abd-El-Hallem A, Masini L, van den Berg GC, Joosten MH, Thomma BP** (2011) Interfamily transfer of tomato Ve1 mediates Verticillium resistance in Arabidopsis. *Plant Physiol* **156**: 2255-2265
- Fraser P, Bickmore W** (2007) Nuclear organization of the genome and the potential for gene regulation. *Nature* **447**: 413-417
- Gabriels SH, Vossen JH, Ekengren SK, van Ooijen G, Abd-El-Hallem AM, van den Berg GC, Rainey DY, Martin GB, Takken FL, de Wit PJGM, Joosten MHAJ** (2007) An NB-LRR protein required for HR signalling mediated by both extra- and intracellular resistance proteins. *Plant J* **50**: 14-28
- Gao QM, Venugopal S, Navarre D, Kachroo A** (2011) Low oleic acid-derived repression of jasmonic acid-inducible defense responses requires the WRKY50 and WRKY51 proteins. *Plant Physiol* **155**: 464-476
- Gondor A, Ohlsson R** (2009) Chromosome crosstalk in three dimensions. *Nature* **461**: 212-217
- Huang S, Gao Y, Liu J, Peng X, Niu X, Fei Z, Cao S, Liu Y** (2012) Genome-wide analysis of WRKY transcription factors in *Solanum lycopersicum*. *Mol Genet Genomics* **287**: 495-513
- Ishihama N, Yamada R, Yoshioka M, Katou S, Yoshioka H** (2011) Phosphorylation of the *Nicotiana benthamiana* WRKY8 transcription factor by MAPK functions in the defense response. *Plant Cell* **23**: 1153-1170
- Jones JDG, Dangl JL** (2006) The plant immune system. *Nature* **444**: 323-329
- Joosten MHAJ** (2012) Isolation of apoplastic fluid from leaf tissue by the vacuum infiltration-centrifugation technique. *Methods Mol Biol*. **835**: 603-610
- Joosten MHAJ, De Wit PJGM** (1989) Identification of several pathogenesis-related proteins in tomato leaves inoculated with *Cladosporium fulvum* (syn. *Fulvia fulva*) as 1,3- β -glucanases and chitinases. *Plant Physiol* **89**: 945-951
- Journot-Catalino N, Somssich IE, Roby D, Kroj T** (2006) The transcription factors WRKY11 and WRKY17 act as negative regulators of basal resistance in *Arabidopsis thaliana*. *Plant Cell* **18**: 3289-3302
- Kan JL, Joosten MHAJ, Wagemakers CM, Berg-Velthuis GM, Wit PJGM** (1992) Differential accumulation of mRNAs encoding extracellular and intracellular PR proteins in tomato induced by virulent and avirulent races of *Cladosporium fulvum*. *Plant Mol. Biol.* **20**: 513-527
- Kim K-C, Fan B, Chen Z** (2006) Pathogen-induced Arabidopsis WRKY7 is a transcriptional repressor and enhances plant susceptibility to *Pseudomonas syringae*. *Plant Physiol* **142**: 1180-1192
- Kliebenstein DJ, Rowe HC** (2008) Ecological costs of biotrophic versus necrotrophic pathogen resistance, the hypersensitive response and signal transduction. *Plant Sci* **174**: 551-556
- Levesque MJ, Raj A** (2013) Single-chromosome transcriptional profiling reveals chromosomal gene expression regulation. *Nat Methods* **10**: 246-248
- Li J-b, Luan Y-s, Jin H** (2012) The tomato SIWRKY gene plays an important role in the regulation of defense responses in tobacco. *Biochem Biophys Res Commun* **427**: 671-676
- Li J, Brader G, Palva ET** (2004) The WRKY70 transcription factor: a node of convergence for jasmonate-mediated and salicylate-mediated signals in plant defense. *Plant Cell* **16**: 319-331
- Li R, Yu C, Li Y, Lam TW, Yiu SM, Kristiansen K, Wang J** (2009) SOAP2: an improved ultrafast tool for short read alignment. *Bioinformatics* **25**: 1966-1967
- Liebrand TW, Smit P, Abd-El-Hallem A, de Jonge R, Cordewener JH, America AH, Sklenar J, Jones AM, Robatzek S, Thomma BP, Tameling WI, Joosten MH** (2012) Endoplasmic reticulum-quality control chaperones facilitate the biogenesis of Cf receptor-like proteins involved in pathogen resistance of tomato. *Plant Physiol.* **159**: 1819-1833
- Lippok B, Birkenbihl RP, Rivory G, Brummer J, Schmelzer E, Logemann E, Somissich IE** (2007) Expression of AtWRKY33 encoding a pathogen- or PAMP-responsive WRKY transcription factor is regulated by a composite DNA motif containing W box elements. *Mol Plant Microbe Interact* **20**: 420-429
- Lommen A** (2009) MetAlign: Interface-driven, versatile metabolomics tool for hyphenated full-scan mass spectrometry data preprocessing. *Anal Chem.* **81**: 3079-3086

- Mao G, Meng X, Liu Y, Zheng Z, Chen Z, Zhang S (2011) Phosphorylation of a WRKY transcription factor by two pathogen-responsive MAPKs drives phytoalexin biosynthesis in Arabidopsis. *Plant Cell* **23**: 1639-1653
- Meng X, Xu J, He Y, Yang KY, Mordorski B, Liu Y, Zhang S (2013) Phosphorylation of an ERF transcription factor by Arabidopsis MPK3/MPK6 regulates plant defense gene induction and fungal resistance. *Plant Cell* **25**: 1126-1142
- Menke FL, Kang HG, Chen Z, Park JM, Kumar D, Klessig DF (2005) Tobacco transcription factor WRKY1 is phosphorylated by the MAP kinase SIPK and mediates HR-like cell death in tobacco. *Mol Plant Microbe Interact* **18**: 1027-1034
- Moore JW, Loake GJ, Spoel SH (2011) Transcription dynamics in plant immunity. *Plant Cell* **23**: 2809-2820
- Mortazavi A, Williams BA, McCue K, Schaeffer L, Wold B (2008) Mapping and quantifying mammalian transcriptomes by RNA-Seq. *Nat. Methods* **5**: 621-628
- Neilson EH, Goodger JQD, Woodrow IE, Moller BL (2013) Plant chemical defense: at what cost? *Trends Plant Sci* **18**: 250-258
- Pan YJ, Cho CC, Kao YY, Sun CH (2009) A novel WRKY-like protein involved in transcriptional activation of cyst wall protein genes in *Giardia lamblia*. *J Biol Chem* **284**: 17975-17988
- Park CY, Lee JH, Yoo JH, Moon BC, Choi MS, Kang YH, Lee SM, Kim HS, Kang KY, Chung WS, Lim CO, Cho MJ (2005) WRKY group IIId transcription factors interact with calmodulin. *FEBS Lett* **579**: 1545-1550
- Popescu SC, Popescu GV, Bachan S, Zhang Z, Gerstein M, Snyder M, Dinesh-Kumar SP (2009) MAPK target networks in *Arabidopsis thaliana* revealed using functional protein microarrays. *Genes Dev* **23**: 80-92
- Pozo MJ, Van Der Ent S, Van Loon LC, Pieterse CMJ (2008) Transcription factor MYC2 is involved in priming for enhanced defense during rhizobacteria-induced systemic resistance in *Arabidopsis thaliana*. *New Phytol* **180**: 511-523
- Qiu JL, Fiil BK, Petersen K, Nielsen HB, Botanga CJ, Thorgrimsen S, Palma K, Suarez-Rodriguez MC, Sandbech-Clausen S, Lichota J, Brodersen P, Grasser KD, Mattsson O, Glazebrook J, Mundy J, Petersen M (2008) Arabidopsis MAP kinase 4 regulates gene expression through transcription factor release in the nucleus. *EMBO J* **27**: 2214-2221
- Rushton PJ, Somssich IE (1998) Transcriptional control of plant genes responsive to pathogens. *Curr Opin Plant Biol* **1**: 311-315
- Rushton PJ, Somssich IE, Ringler P, Shen QJ (2010) WRKY transcription factors. *Trends Plant Sci* **15**: 247-258
- Shen QH, Saijo Y, Mauch S, Biskup C, Bieri S, Keller B, Seki H, Ulker B, Somssich IE, Schulze-Lefert P (2007) Nuclear activity of MLA immune receptors links isolate-specific and basal disease-resistance responses. *Science* **315**: 1098-1103
- Shoji T, Mishima M, Hashimoto T (2013) Divergent DNA-binding specificities of a group of ethylene response factor transcription factors involved in plant defense. *Plant Physiol* **162**: 977-990
- Stulemeijer IJ, Joosten MHJ, Jensen ON (2009) Quantitative phosphoproteomics of tomato mounting a hypersensitive response reveals a swift suppression of photosynthetic activity and a differential role for hsp90 isoforms. *J Proteome Res* **8**: 1168-1182
- Stulemeijer IJ, Stratmann JW, Joosten MH (2007) Tomato mitogen-activated protein kinases LeMPK1, LeMPK2, and LeMPK3 are activated during the Cf-4/Avr4-induced hypersensitive response and have distinct phosphorylation specificities. *Plant Physiol* **144**: 1481-1494
- Tao Y, Xie ZY, Chen WQ, Glazebrook J, Chang HS, Han B, Zhu T, Zou GZ, Katagiri F (2003) Quantitative nature of Arabidopsis responses during compatible and incompatible interactions with the bacterial pathogen *Pseudomonas syringae*. *Plant Cell* **15**: 317-330
- Thomas CM, Jones DA, Parniske M, Harrison K, Balint-Kurti PJ, Hatzixanthis K, Jones JD (1997) Characterization of the tomato Cf-4 gene for resistance to *Cladosporium fulvum* identifies sequences that determine recognition specificity in Cf-4 and Cf-9. *Plant Cell* **9**: 2209-2224
- Thomma BPHJ, Nurnberger T, Joosten MHJ (2011) OfPAMPs and effectors: the blurred PTI-ETI dichotomy. *Plant Cell* **23**: 4-15
- Tikunov YM, Laptinok S, Hall RD, Bovy A, de Vos RCH (2012) MSclust: a tool for unsupervised mass spectra extraction of chromatography-mass spectrometry ion-wise aligned data. *Metabolomics* **8**: 714-718
- Ulker B, Somssich IE (2004) WRKY transcription factors: from DNA binding towards biological function. *Curr Opin Plant Biol* **7**: 491-498

- van der Hooft JJ, Vervoort J, Bino RJ, Beekwilder J, de Vos RC** (2011) Polyphenol identification based on systematic and robust high-resolution accurate mass spectrometry fragmentation. *Anal Chem.* **83**: 409-416
- Vossen JH, Abd-El-Haliem A, Fradin EF, van den Berg GC, Ekengren SK, Meijer HJ, Seifi A, Bai Y, ten Have A, Munnik T, Thomma BP, Joosten MHAJ** (2010) Identification of tomato phosphatidylinositol-specific phospholipase-C (PI-PLC) family members and the role of PLC4 and PLC6 in HR and disease resistance. *Plant J* **62**: 224-239
- Wang D, Amornsiripanitch N, Dong XN** (2006) A genomic approach to identify regulatory nodes in the transcriptional network of systemic acquired resistance in plants. *PLoS Pathog* **2**: 1042-1050
- Xie Z, Zhang ZL, Zou X, Yang G, Komatsu S, Shen QJ** (2006) Interactions of two abscisic-acid induced WRKY genes in repressing gibberellin signaling in aleurone cells. *Plant J* **46**: 231-242
- Xu X, Chen C, Fan B, Chen Z** (2006) Physical and functional interactions between pathogen-induced Arabidopsis WRKY18, WRKY40, and WRKY60 transcription factors. *Plant Cell* **18**: 1310-1326
- Zheng ZY, Abu Qamar S, Chen ZX, Mengiste T** (2006) Arabidopsis WRKY33 transcription factor is required for resistance to necrotrophic fungal pathogens. *Plant J* **48**: 592-605

Supplemental information

Supplemental Figures

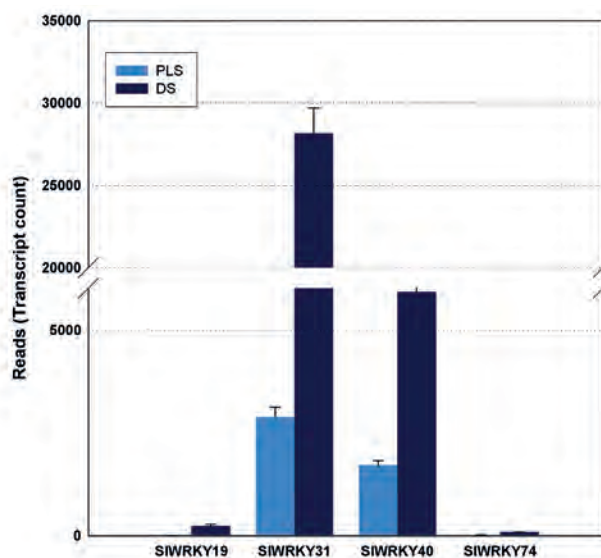


Figure S1. Expression profiles of *SIWRKYs* located on chromosome 6, showing differential expression only in the dying seedlings (DS). PLS, parental lines.

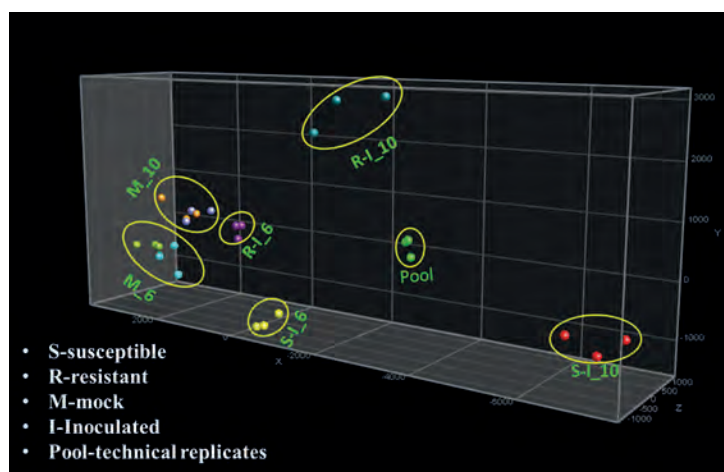


Figure S2. Metabolome reprogramming of the tomato apoplast in response to inoculation with *C. fulvum*. Apoplastic fluid isolated from tomato leaves at 6 and 10 days post inoculation with *C. fulvum* was subjected to untargeted polar and semi-polar metabolite analysis and a principal component analysis (PCA) was performed. M, mock-inoculated; R-I, resistant-inoculated; S-I, susceptible-inoculated; Pool, technical replicates of pooled extract from all samples considered in the analysis. The number refers to the days after inoculation.

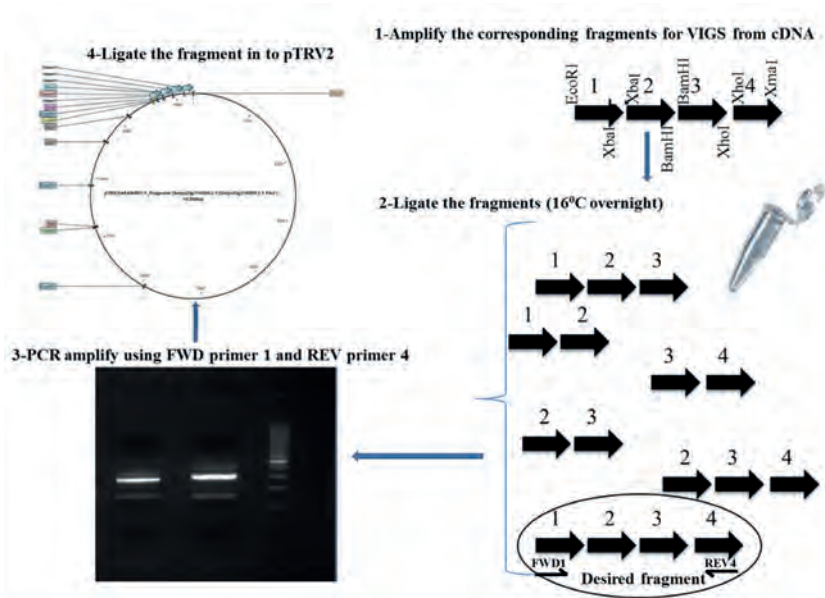


Figure S3. Four step cloning strategy to generate chimeric VIGS constructs for simultaneous silencing of multiple genes in tomato.

(1) Amplification of unique fragments from genes to be targeted by VIGS. The specific restriction enzyme sites that are introduced into the primer sequences and added to both ends of each fragment allow the orderly ligation of the fragments in the next step and prevent the ligation of identical fragments.

(2) All fragments with the specific restriction sites added are ligated overnight. Different possible ligated products and the desired fragment are indicated.

(3) PCR amplification of the desired fragment from the ligation mix is done by using the FWD primer employed for generating the VIGS fragment from gene 1 and the REV primer used for generating the VIGS fragment from gene 4. The PCR product is run on an agarose gel and the fragment corresponding to the right size of the expected chimeric fragment was excised from the gel and sequenced using the same primers.

(4) Finally, the fragment is inserted into pTRV2 using the EcoRI and XmaI sites and the resulting recombinant virus is used for VIGS.



Figure S4. Phenotype resulting from simultaneously targeting group III *SIWRKY*41, -42, -53 and -54. Inverted leaflets are indicated by yellow arrow heads.



Figure S5. Dwarfing phenotype manifested by the *SIWRKY39/40/45/46*-targeted resistant (Cf-4) and susceptible (Cf-0) tomato lines.

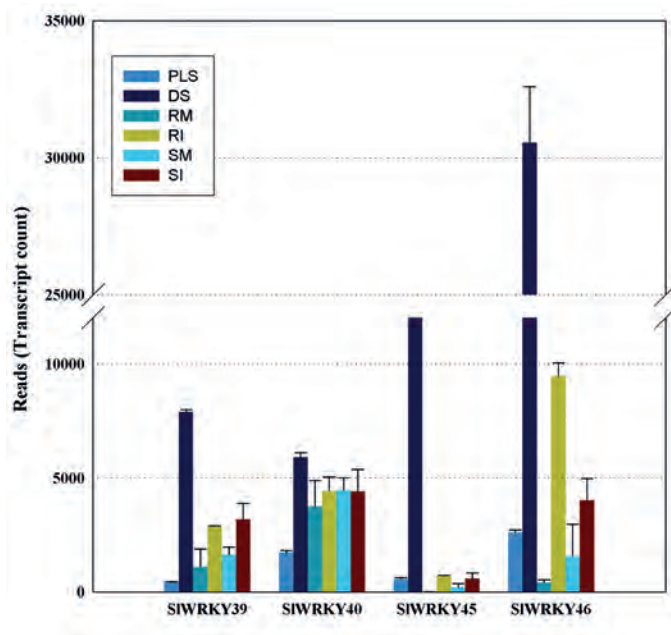


Figure S6. Expression profile of group II-a *SIWRKYs*, acting as defense repressors in tomato (Xu et al., 2006; Shen et al., 2007). PLS, parental lines; DS, dying seedlings (both at 5 hrs after the temperature shift that induces the HR in the DS); RM, resistant tomato mock-inoculated; RI, resistant tomato inoculated with *C. fulvum*, analyzed at 6 dpi; SM, susceptible mock and SI, susceptible inoculated with *C. fulvum*, analyzed at 6dpi. The error bars represent the standard error of the mean of three independent biological replicates.



Figure S7. Leaves of resistant tomato Cf-4, showing epinasty upon targeting of defense repressor *SIWRKY39/40/45/46* by VIGS, at 8 dpi with *C. fulvum* (right). *GUS*-targeted plants were used as a control (left). This typical response of *C. fulvum*-inoculated resistant plants is manifested at 4-5 dpi.

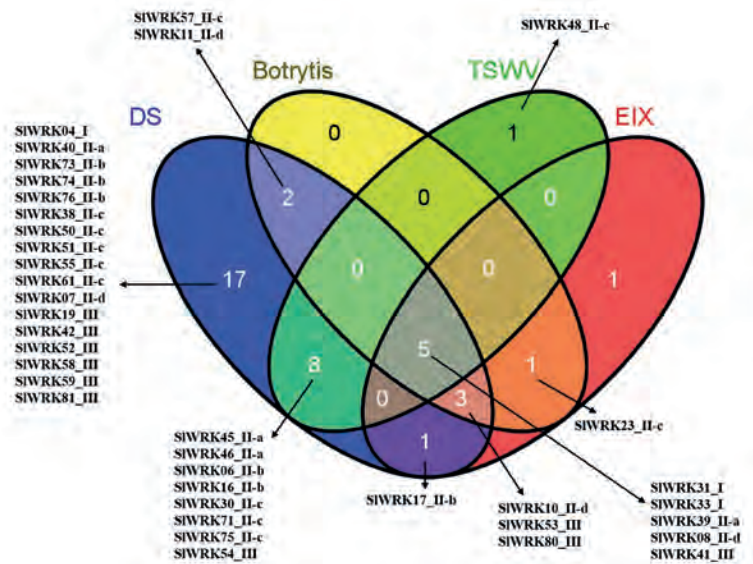


Figure S8. Overlapping and uniquely upregulated *SIWRKY*s in the dying seedlings (DS, data obtained from our RNA-seq analysis) and in tomato exposed to other biotic stresses (invasion by tomato spotted wilt virus (TSWV), treatment with fungal elicitor ethylene-inducing xylanase (EIX) and inoculation with the fungal pathogen *Botrytis cinerea*), as reported by Huang et al. (2012). The analysis performed by Huang et al. (2012) was based on a total of seven independent tomato microarray data sets, belonging to the two microarray platforms (Affymetrix Tomato Genome Array and the TOM2 oligo array), that were downloaded from Tomato Functional Genomics Database (TFGD) (<http://ted.bti.cornell.edu>). Through BLAST analysis, a total of 43 probes corresponding to *SIWRKY* genes accounting for more than 50 % of the gene family were identified (Huang et al., 2012).

Supplemental Tables

Table S1. Differentially expressed *SIWRKY*s in the dying seedlings and resistant and susceptible tomato inoculated with *C. fulvum*.

Gene locus	Gene name	WRKY domain present	Zinc-finger type	Domain number	Group [§]	Fold change in expression (log2)*			Number of <i>SIWRKY</i> s		
						DS/PLS	RI/RM	SI/SM	Total number in tomato genome belonging to group	Total number of DEG	DEG (%)
solyc05g012770.2.1	<i>SIWRKY4</i>	WRKYGQK/WRKYGQK	C2H2	2	I	1.6	1.3	NS [†]			
solyc06g066370.2.1	<i>SIWRKY31</i>	WRKYGQK/WRKYGQK	C2H2	2	I	3.5	NS	NS			
solyc09g014990.2.1	<i>SIWRKY33</i>	WRKYGQK/WRKYGQK	C2H2	2	I	4.6	1.8	NS	15	4	27
solyc10g084380.1.1	<i>SIWRKY44</i>	WRKYGQK/WRKYGQK	C2H2	2	I	-1.6	-1.8	NS			
solyc03g116890.2.1	<i>SIWRKY39</i>	WRKYGQK	C2H2	1	II-a	4.4	1.1	NS			
solyc06g068460.2.1	<i>SIWRKY40</i>	WRKYGQK	C2H2	1	II-a	2.0	NS	NS			
solyc08g067340.2.1	<i>SIWRKY46</i>	WRKYGQK	C2H2	1	II-a	3.7	4.2	1.3	5	4	80
solyc08g067360.2.1	<i>SIWRKY45</i>	WRKYGQK	C2H2	1	II-a	5.1	4.6	1.5			
solyc02g032950.2.1	<i>SIWRKY16</i>	WRKYGQK	C2H2	1	II-b	2.6	1.7	NS			
solyc02g080890.2.1	<i>SIWRKY6</i>	WRKYGQK	C2H2	1	II-b	3.4	2.6	NS			
solyc03g113120.2.1	<i>SIWRKY73</i>	WRKYGQK	C2H2	1	II-b	3.1	NS	NS			
solyc05g007110.2.1	<i>SIWRKY76</i>	WRKYGQK	C2H2	1	II-b	4.1	2.8	NS	8	6	75
solyc06g070990.2.1	<i>SIWRKY74</i>	WRKYGQK	C2H2	1	II-b	2.3	NS	NS			
solyc07g051840.2.1	<i>SIWRKY17</i>	WRKYGQK	C2H2	1	II-b	1.4	NS	NS			
solyc02g071130.2.1	<i>SIWRKY71</i>	WRKYGQK	C2H2	1	II-c	2.4	2.5	NS			
solyc02g094270.1.1	<i>SIWRKY38</i>	WRKYGQK	C2H2	1	II-c	7.2	NS	NS			
solyc04g051540.2.1	<i>SIWRKY13</i>	WRKYGQK	C2H2	1	II-c	-1.4	NS	NS			
solyc04g051690.2.1	<i>SIWRKY51</i>	WRKYGKK	C2H2	1	II-c	3.7	2.8	1.3			
solyc04g072070.2.1	<i>SIWRKY55</i>	WRKYGKK	C2H2	1	II-c	4.6	5.1	1.5			
solyc05g012500.2.1	<i>SIWRKY57</i>	WRKYGQK	C2H2	1	II-c	1.1	NS	NS	15	10	67
solyc05g015850.2.1	<i>SIWRKY75</i>	WRKYGQK	C2H2	1	II-c	6.4	6.8	2.2			
solyc07g056280.2.1	<i>SIWRKY30</i>	WRKYGQK	C2H2	1	II-c	1.2	1.1	NS			
solyc08g062490.2.1	<i>SIWRKY50</i>	WRKYGKK	C2H2	1	II-c	3.6	3.8	1.5			
solyc12g056750.1.1	<i>SIWRKY61</i>	WRKYGKK	C2H2	1	II-c	5.7	6.1	NS			

solyc02g093050.2.1	<i>SIWRKY8</i>	WRKYGQK	C2H2	1	II-d	2.4	2.8	NS			
solyc04g078550.2.1	<i>SIWRKY7</i>	WRKYGQK	C2H2	1	II-d	1.1	NS	NS			
solyc08g006320.2.1	<i>SIWRKY11</i>	WRKYGQK	C2H2	1	II-d	1.5	NS	NS	6	4	67
solyc12g096350.1.1	<i>SIWRKY10</i>	WRKYGQK	C2H2	1	II-d	2.6	NS	NS			
solyc01g095630.2.1	<i>SIWRKY41</i>	WRKYGQK	C2HC	1	III	2.8	1.0	NS			
solyc03g007380.1.1	<i>SIWRKY52</i>	WRKYGQK	C2HC	1	III	4.7	3.3	1.3			
solyc03g095770.2.1	<i>SIWRKY80</i>	WRKYGQK	C2HC	1	III	3.3	2.3	NS			
solyc05g050330.2.1	<i>SIWRKY59</i>	WRKYGQK	C2HC	1	III	1.4	NS	NS			
solyc05g050340.2.1	<i>SIWRKY58</i>	WRKYGQK	C2HC	1	III	1.8	1.1	NS			
solyc06g048870.1.1	<i>SIWRKY19</i>	WRKYGQK	C2HC	1	III	5.4	NS	NS			
solyc08g008280.2.1	<i>SIWRKY53</i>	WRKYGQK	C2HC	1	III	3.0	1.3	NS			
solyc08g082110.2.1	<i>SIWRKY54</i>	WRKYGQK	C2HC	1	III	1.8	1.4	NS			
solyc09g015770.2.1	<i>SIWRKY81</i>	WRKYGQK	C2HC	1	III	2.6	3.1	1.4	11	10	91
solyc10g009550.2.1	<i>SIWRKY42</i>	WRKYGQK	C2HC	1	III	1.4	NS	NS			

[§] The expressed SIWRKYs are grouped according to Eulgem et al. (2000) and Huang et al (2012).

*The fold change in expression corresponds to the log2 fold change in expression of the treatment compared to the control. DS/PLS, dying seedlings versus parental lines; RI/RM, resistant-inoculated versus resistant-mock and SI/SM, susceptible-inoculated versus susceptible-mock.

[†]NS: statistically not significant (fold change < 2 and p > 0.001 after correction for the false discovery rate (FDR)).

CHAPTER 4

Table S2. Chimeric VIGS inserts used for multiple *SIWRKY* silencing

Group II-a <i>SIWRKY39/40/45/46</i>	Gene locus	Unique region in the coding sequence
EcoRI- <i>SIWRKY39</i> -XbaI	Solyc03g116890.2	754-908
XbaI- <i>SIWRKY40</i> -BamHI	Solyc06g068460.2	29-180
BamHI- <i>SIWRKY46</i> -XhoI	Solyc08g067340.2	554-726
XhoI- <i>SIWRKY45</i> -SmaI	Solyc08g067360.2	51-191
Group II-c <i>SIWRKY50/51/55/61</i>		
EcoRI- <i>SIWRKY51</i> -XbaI	Solyc04g051690.2	36-198
XbaI- <i>SIWRKY55</i> -BamHI	Solyc04g072070.2	240-381
BamHI- <i>SIWRKY61</i> -XhoI	Solyc12g056750.1	197-351
XhoI- <i>SIWRKY50</i> -SmaI	Solyc08g062490.2	80-209
Group I <i>SIWRKY31/33</i>		
XbaI- <i>SIWRKY33</i> -BamHI	Solyc09g014990.2	286-557
BamHI- <i>SIWRKY31</i> -XmaI	Solyc06g066370.2	1331-1607
Group II-d <i>SIWRKY07/08/10/11</i>		
EcoRI- <i>SIWRKY11</i> -XbaI	Solyc08g006320.2	859-979
XbaI- <i>SIWRKY07</i> -BamHI	Solyc04g078550.2	596-737
BamHI- <i>SIWRKY10</i> -XhoI	Solyc12g096350.1	254-415
XhoI- <i>SIWRKY08</i> -SmaI	Solyc02g093050.2	6-169
Group III <i>SIWRKY41/42/53/54</i>		
EcoRI- <i>SIWRKY41</i> -XbaI	Solyc01g095630.2	682-826
XbaI- <i>SIWRKY53</i> -BamHI	Solyc08g008280.2	53-227
BamHI- <i>SIWRKY54</i> -XhoI	Solyc08g082110.2	201-335
XhoI- <i>SIWRKY42</i> -SmaI	Solyc10g009550.2	583-726
Activators (Group I (31/33) and III (53)) <i>SIWRKY31/33/53</i>		
EcoRI- <i>SIWRKY31</i> -XbaI	Solyc06g066370.2	1331-1607
XbaI- <i>SIWRKY53</i> -BamHI	Solyc08g008280.2	53-227
BamHI- <i>SIWRKY33</i> -XhoI	Solyc09g014990.2	286-557
Repressors (Group II-d (10) and II-c (61)) <i>SIWRKY10/61</i>		
EcoRI- <i>SIWRKY10</i> -BamHI	Solyc12g096350.1	254-415
BamHI- <i>SIWRKY61</i> -XhoI	Solyc12g056750.1	197-351

Chapter 5

The Metabolic Arms Race between Tomato and *Cladosporium fulvum*

Desalegn W Etalo^{1,4,Ω}, Bilal Ökmen², John K. Meissen⁶, Jérôme Collemare^{2,4},
Oliver Fiehn⁶, Pierre JGM de Wit^{2,4}, Matthieu HAJ Joosten^{2,4}, Ric CH de
Vos^{3,4,5}, Harro J Bouwmeester^{1,4*}

¹ Laboratory of Plant Physiology, Wageningen University,
Droevendaalsesteeg 1, 6708 PB Wageningen, The Netherlands.

² Laboratory of Phytopathology, Wageningen University,
Droevendaalsesteeg 1, 6708 PB Wageningen, The Netherlands.

³ Plant Research International, Bioscience,
P. O. Box 16, 6700 AA Wageningen, The Netherlands.

⁴ Centre for BioSystems Genomics, P.O. Box 98, 6700 AB Wageningen, The Netherlands.

⁵ Netherlands Metabolomics Centre, Einsteinweg 55, 2333 CC Leiden, The Netherlands.

⁶ University of California Davis Genome Centre, University of California Davis,
Davis, California, United States of America.

^ΩCurrent address: Plant Research International, Bioscience,
Wageningen University, Wageningen, The Netherlands

*Corresponding author. Laboratory of Plant Physiology, Wageningen University,
Droevendaalsesteeg 1, 6708 PB Wageningen, The Netherlands.

Tel.: +31 (0)317-489859; Fax: +31 (0)317-418094; E-mail: harro.bouwmeester@wur.nl,

This chapter is a modified version of work published in New Phytologist, by Ökmen et al. (2013) **198**: 1203-1214.

Abstract

The outcome of *Cladosporium fulvum* infection of tomato is determined by the ability of the fungal pathogen to successfully colonize the apoplastic space of tomato leaves. Here, the fungus deploys effectors that suppress the plant immune response, while the plant tries to contain the fungus possibly also using defensive metabolites. To obtain a global view of the major alterations that occur in the metabolome upon successful and unsuccessful infection, we used comprehensive untargeted metabolic profiling of leaf as well as leaf apoplast extracts from resistant (incompatible interaction) and susceptible (compatible interaction) tomato plants challenged with *C. fulvum*. In whole leaf extracts substantial changes were detectable in a large variety of metabolites, including polar, semi-polar and apolar compounds, while in the apoplast extract only the more polar and semi-polar compounds changed. In the incompatible interaction, an early (4-6 days post inoculation (dpi)) increase in the accumulation of a number of phospholipids and secondary metabolites occurred. However, in the compatible interaction the major change was the degradation of a number of fungitoxic glycoalkaloids into their less toxic derivatives and the accumulation of sugar alcohols, in both the whole leaf and apoplast extract. Although α -tomatine, the most abundant tomato glycoalkaloid, is thought to be localized in the vacuole, for the first time we show that it is also present in the apoplast, and we show that it is hydrolyzed by *C. fulvum* tomatinase-1 (CfTom1) upon colonization of the leaf apoplast. CfTom1 belongs to the *glycosyl hydrolase (GH)-10* family and encodes a functional tomatinase, which degrades α -tomatine into its non-toxic aglycone, tomatidine, both *in vitro* and during colonization of tomato leaves. Functional analysis of Δ cftom1 knock-out mutants of *C. fulvum* showed that degradation of α -tomatine is required for full virulence of the fungus on tomato, which is likely due to increased sensitivity of these mutants to α -tomatine, rather than to the presumed suppression of basal defense responses by its breakdown products.

Introduction

The relationship between plants and fungi is often mutually beneficial, with only a small minority of fungal species breaking the fine balance of cooperation to become plant pathogens (Fraser, 2004; Holub, 2006). The genetic background of resistance or susceptibility of plants to pathogens has been an area of intense investigation already for a long time and the studies have provided valuable information on the organization of the plant immune system. However, the intimate cellular, molecular and metabolic interactions occurring at the host-microbe interface as a biotrophic relationship between plant and pathogen is established, remains to be investigated (Perfect and Green, 2001; O'Connell and Panstruga, 2006). Recent advances in molecular plant pathology based on exploiting model pathosystems have significantly increased our understanding of the molecular arms race between plants and pathogens, particularly occurring at the levels of signal perception and signal transduction (Hématy et al., 2009; de Jonge et al., 2010; Caillaud et al., 2012; Howden and Huitema, 2012; Hann et al., 2013; Liebrand et al., 2013). Furthermore, the coupling of these studies with recently developed system biology tools such as genomics, transcriptomics, proteomics and metabolomics, has provided an overview of the great complexity of the ongoing plant-microbe warfare (Stulemeijer et al., 2009; Ward et al., 2010; de Wit et al., 2012; Etalo et al., 2013). This continuous battle for co-existence between plants and pathogens that has been taking place already for millennia plays a vital role in shaping the defense machinery of both plants and pathogens, resulting in versatile organisms that show non-stop, rhythmic loss and gain of resistance and gain and loss of virulence, respectively. In the previous chapters, the defense machineries involved in signal perception and transduction have been discussed. In this chapter, the focus will be on the defense response of the plant that involves the deployment of its phytochemical arsenal and the counter measures that are taken by the fungus.

Chemical plant defense involves the deployment of constitutive chemical barriers (phytoanticipins) and inducible antimicrobials (phytoalexins). In addition to their antimicrobial properties, some of the induced metabolites, for example the hydroxycinnamic acid amides are involved in the reinforcement of the plant cell wall, which is the first line of defense against microbes (Zacares et al., 2007; Etalo et al., 2013). Another interesting group of small molecules are membrane-associated lipids, such as the phospholipids. Beyond their role as a component of the membrane, phospholipids can be co-factors for membrane-associated enzymes, signal precursors, or signaling molecules themselves (de Jong et al., 2004; Park et al., 2004; Vossen et al., 2010). Furthermore, specific phospholipids generated in certain membrane domains can serve as a docking site for cytosolic proteins (Laxalt and Munnik, 2002; van Meer et al., 2008).

A well-known class of preformed antimicrobial compounds present in plants comprises the saponins, which are glycosylated steroids or steroidal alkaloids representing a constitutive chemical barrier against a wide range of fungal and bacterial pathogens (Osbourn, 1996). Saponins cause the loss of membrane integrity in target organisms by forming complexes with sterols, resulting in pore formation and cell lysis (Bowyer et al., 1995; Keukens et al., 1995; Osbourn, 1996). Sensitivity to saponins is correlated with the type of sterols present in the membranes of potential pathogens. Fungal membranes that contain sterols with free 3- β -hydroxy groups are sensitive to saponins, while plant cell membranes are insensitive to these compounds due to the presence of sterol glycosides (Steel and Drysdale, 1988). Similarly, oomycetes are insensitive to saponins because their membranes lack 3- β -hydroxy sterols (Steel and Drysdale, 1988).

Apart from the major aspects of plant defense, such as cell wall thickening (Huckelhoven, 2007) and production of antimicrobial chemicals (Wink, 1988; Osbourn, 1999; Kliebenstein et al., 2005), it is equally important to understand how microbes succeed to manipulate the host defensive metabolism to their benefit. Re-programming of both host and microbe metabolism is thus core to a biotrophic relationship and metabolomics approaches can play an important role in the exploration of these phenomena (Allwood et al., 2006; Abu-Nada et al., 2007; Allwood et al., 2008; Ward et al., 2010; Draper et al., 2011; Etalo et al., 2013). In response to these inherent resistance mechanisms present in plants, pathogenic bacteria and fungi in turn have developed various strategies to breach the plant chemical defense line, for example by secreting detoxifying enzymes (Ford et al., 1977; Roldan-Arjona et al., 1999).

Saponin detoxification by pathogens has mainly been studied for avenacin and α -tomatine, which are present in oat and tomato, respectively. During infection of oat roots, the fungus *Gaeumannomyces graminis* var. *avenae* secretes the avenacinase enzyme that detoxifies avenacin, a triterpenoid saponin. Mutants for the avenacinase are no longer able to infect oat, while they are still virulent on wheat, a host that does not produce saponins (Bowyer et al., 1995; Kaup et al., 2005). In tomato (*Solanum lycopersicum* L.), the major saponin is α -tomatine, a steroidal glycoalkaloid that is present in roots, leaves and green fruits in concentrations as high as 1 mM (Roddick, 1977; Osbourn, 1996). α -Tomatine consists of the aglycone tomatidine and the tetrasaccharide lycotetraose. Toxicity of α -tomatine depends on the presence of a lycotetraose moiety, because removal of one or all four sugar residues renders α -tomatine less toxic (Osbourn, 1996). During tomato infection, bacterial and fungal pathogens secrete various types of tomatinase enzymes that can detoxify α -tomatine by removing one or more sugar residues from the compound (Martin-Hernandez et al., 2000; Kaup et al., 2005; Pareja-Jaime et al., 2008). Tomatinase enzymes secreted by *Septoria lycopersici*, *Botrytis cinerea*, and *Verticillium albo-atrum* belong to the glycosyl hydrolase family 3 (GH3) of carbohydrate-degrading enzymes (CAZY) (Martin-

Hernandez et al., 2000). They remove the terminal β -1,2-D-glucose or β -1,3-D-xylose residues from α -tomatine (Osbourn et al., 1995; Quidde et al., 1998). Other tomato pathogens, such as the fungus *Fusarium oxysporum* f. sp. *lycopersici* and the bacterium *Clavibacter michiganensis* subsp. *michiganensis*, secrete a tomatinase that belongs to the glycosyl hydrolase family 10 (GH10) (Roldan-Arjona et al., 1999; Kaup et al., 2005). GH10 tomatinases remove the complete lycotetraose sugar from α -tomatine to form the aglycone tomatidine (Roldan-Arjona et al., 1999; Pareja-Jaime et al., 2008). Although several knock-out studies have been performed to assess the role of tomatinases in the virulence of bacterial and fungal tomato pathogens (Martin-Hernandez et al., 2000; Kaup et al., 2005), only the GH10 tomatinase FoTom1 from *F. oxysporum* f. sp. *lycopersici* was shown to play a role in virulence of this vascular pathogen (Pareja-Jaime et al., 2008). It has also been suggested that products resulting from tomatinase activity play an indirect role in virulence of tomato pathogens by suppressing the defence responses of the plant. For example, breakdown products of α -tomatine (β -tomatine, tomatidine and lycotetraose) were reported to suppress various defense responses, including the oxidative burst and the hypersensitive response (Bouarab et al., 2002; Ito et al., 2007).

The non-obligate biotrophic fungus *Cladosporium fulvum* is a well-studied tomato pathogen that causes leaf mold. *C. fulvum* enters tomato leaves through stomata and colonizes the apoplastic space surrounding mesophyll cells (Stergiopoulos and de Wit, 2009). Although pathogenic on tomato, it was previously reported that *C. fulvum* is not able to detoxify α -tomatine, possibly because of the vacuolar location of α -tomatine which does not harm the fungus and allows it to infect tomato (Melton et al., 1998). However, heterologous expression of the GH3 tomatinase from *Septoria lycopersici* in *C. fulvum* resulted in transformants showing increased sporulation during colonization of tomato leaves, as compared with the wild-type fungus (Melton et al., 1998). These results suggest that *C. fulvum* might be exposed to α -tomatine during colonization of the apoplastic space of tomato, and that it does not produce functional tomatinase enzymes itself. However, recent sequencing of the *C. fulvum* genome revealed the presence of 19 genes encoding GH3 and two genes encoding GH10 enzymes.

To obtain a global view of the major changes in the infection metabolome, both in whole leaves and in the apoplast, where *C. fulvum* actually resides, we performed large scale metabolic profiling of samples obtained from resistant and susceptible plants that were challenged with *C. fulvum* and compared their metabolome with the respective controls. We used both HILIC-QTOF MS (HILIC-MS) and C18 reversed-phase LC-Orbitrap FTMS (C18-MS) metabolomics platforms, in order to profile both polar, semi-polar and apolar compounds. Our analysis shows that upon infection substantial changes occur in the metabolome of the leaf, while the major change in the apoplast consists of a significantly altered polar and semipolar metabolome. In line with the transcriptome analysis that we performed in chapter four, resistant plants showed an early (6 days post inoculation

(dpi)) reprogramming of both apolar and (semi)-polar metabolites upon inoculation with *C. fulvum*. The onset of this reprogramming was characterized by an increased accumulation of a number of phospholipids and phenylpropanoid-related compounds. In contrast, in the compatible interaction the major metabolome change consisted of the degradation of a number of fungitoxic glycoalkaloids and the accumulation of sugar alcohols in the cells and apoplast of tomato leaflets.

Results

To monitor the major alterations in the infection metabolome of tomato leaves we sampled whole leaf tissue and apoplastic fluid (AF) obtained from susceptible and resistant tomato plants at 4, 6, 10 and 14 days post inoculation (dpi) with race 5 of *C. fulvum*, as well as from mock-treated control plants. The difference in metabolite composition between whole leaf tissue extracts (WLTE) and the AF is assumed to be caused by metabolites that are mainly present inside the cell. The samples were subjected to untargeted metabolic profiling in two different laboratories using different, but complementary, protocols.

Aqueous methanol (75% MeOH)-extracted samples were subjected to profiling by C18-MS (see Materials and Methods). With this platform we analyzed freeze-dried AF collected from tomato plants at 4, 6, 10 and 14 dpi, as well as WLTE collected at 4 and 6 dpi. The AFs and WLTEs obtained at 6 and 10 dpi were also extracted with MeOH:chloroform (CHCl₃):H₂O and subjected to profiling by HILIC-MS (see Materials and Methods). The combination of these extraction and separation techniques enabled us to monitor the temporal changes in a variety of polar and semipolar metabolites and apolar compounds including phospho-, sulpho- and galactolipids. For each time point three independent biological repeats were used.

The Composition and Dynamics of the Metabolome of Tomato Leaflets and Apoplast

In the HILIC-MS analysis of both WLTEs and AFs, a total of 1,095 metabolites were detected in the negative ionisation mode and from these, 495 compounds accumulated differentially under at least one of the conditions analyzed ($P < 0.05$, with false discovery rate (FDR) correction). The hierarchical cluster analysis based on these differentially accumulating metabolites shows that the abundance and composition of metabolites found in the WLTEs and the AFs is clearly distinct (**Figure 1A**, clusters IV and VIII). Nevertheless, some groups of metabolites were present both in WLTEs and AFs and showed similar dynamics (**Figure 1A**, clusters I, II and V). Cluster I represents strongly decreased and Cluster V strongly increased polar and semi-polar metabolites in both WLTEs and AFs of susceptible, inoculated plants (SI) at 10 dpi (**Figure 1A**).

From the total of 61 identified lipid species, comprising phospholipids (PLs; ~80%), galactolipids (GLs; ~5%) and sulpholipids (SLs; ~15%), 57 lipids were exclusively detected in the WLTE, two were detected in both the WLTEs and the AFs, and two were only detected in the AFI (**Figure 1B, Supplementary Figures S1A and B**). The 59 lipid species that are abundant in the WLTEs were dominated by PLs, including phosphatidyl-ethanolamines (PEs; 19 (~33%)), phosphatidyl-serines (PSs; 15 (~26%)), phosphatidyl-inositols (PIs; 7 (~12%)), phosphatidyl-glycerols (PGs; 3 (~5%)), phosphatidic-acids (PAs; 2 (~3%)) and lyso-phosphatidyl-ethanolamines (LysoPEs; 1 (~2%)). The major chloroplast glycosyl-glycerides, such as SLs (sulfoquinovosyl-diacylglycerols, SQDGs; 9 (~16%)) and GLs (monogalactosyl-diacylglycerol).

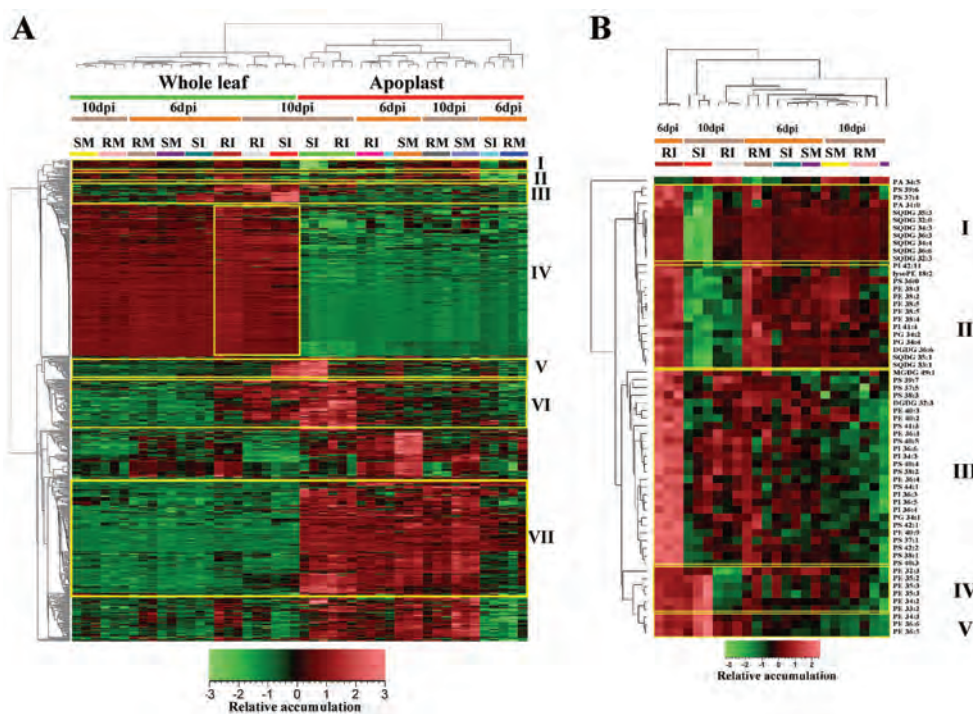


Figure 1. Heatmaps of metabolites isolated from apoplastic and whole leaf extracts obtained from *C. fulvum*-inoculated resistant and susceptible tomato, as compared to their respective controls.

(A) Hierarchical cluster analysis (HCA) based on 495 of the 1,095 metabolites detected by HILIC-LCMS in the negative ionization mode. These 495 metabolites were significantly different in their abundance, at least under one of the conditions analysed ($P < 0.05$ with FDR correction).

(B) Projected view of identified lipids found in clusters II and III shown in (A) that represent lipids and other metabolites exclusively detected in the whole leaf tissue extract. The annotation of the lipids is based on their accurate mass and their MS/MS fragmentation information in the LipidBlast library (Kind et al., 2013).

SM, susceptible, mock-treated; RM, resistant, mock-treated; SI, susceptible, *C. fulvum*-inoculated; RI, resistant, *C. fulvum*-inoculated.

From the total of 61 identified lipid species, comprising phospholipids (PLs; ~80%), galactolipids (GLs; ~5%) and sulpholipids (SLs; ~15%), 57 lipids were exclusively detected in the WLTE, two were detected in both the WLTEs and the AFs, and two were only detected in the AFI (**Figure 1B**, **Supplementary Figures S1A and B**). The 59 lipid species that are abundant in the WLTEs were dominated by PLs, including phosphatidyl-ethanolamines (PEs; 19 (~33%)), phosphatidyl-serines (PSs; 15 (~26%)), phosphatidyl-inositols (PIs; 7 (~12%)), phosphatidyl-glycerols (PGs; 3 (~5%)), phosphatidic-acids (PAs; 2 (~3%)) and lyso-phosphatidyl-ethanolamines (LysoPEs; 1 (~2%)). The major chloroplast glycosyl-glycerides, such as SLs (sulfoquinovosyl-diacylglycerols, SQDGs; 9 (~16%)) and GLs (monogalactosyl-diacylglycerol, MGDG; 1 (~2%)) and digalactosyl diacylglycerol, DGDG; 2 (~3%)), also showed differential dynamics during infection (**Figure 1B** and **Supplementary Figure S1C**).

Early Changes in the Metabolome of *C. fulvum*-Inoculated Tomato leaves

The HILIC-MS analysis of WLTEs showed that in resistant plants, there is an early reprogramming of the lipidome (**Figure 1B**). In contrast, susceptible plants exhibited a much weaker and slower reprogramming of their lipidome. Similarly, in both WLTEs and AFs of resistant plants, the metabolome showed early reprogramming upon inoculation with *C. fulvum* (**Figure 1A**, cluster VI and **Figures 2A and 2B**). The early reprogramming of the lipidome can be divided into two categories; (1) those lipid species that showed early (6 dpi) accumulation in the resistant plants only and exhibited little or no change in their profile at later stages of infection (10 dpi) in both resistant and susceptible plants compared with controls (**Figure 1B**, cluster III), and (2) those lipid species that showed early accumulation in resistant plants only and also show differential accumulation in both resistant and susceptible plants at later stages of infection, as compared to the controls (**Figure 1B**, cluster IV and V). The first group consists of 26 out of the 61 identified lipids species and it contains PS (50%), PE (19%), PI (19%), PG (4%), MGDG (4%) and DGDG (4%). The second group consists of 9 PE species, of which 6 (PE 32:3, 35:2, 35:3 (2x), 34:2, 33:2) had accumulated in susceptible inoculated plants at 10 dpi only, while at this time point they were already decreasing in resistant-inoculated plants. Compared to the controls, in resistant plants the remaining PEs (PE 34:3, 36:6 and 36:5) had accumulated at both 6 and 10 dpi, while in susceptible plants they increased only at 10dpi (**Figure 1B**, clusters IV and V).

With C18-MS analysis of WLTEs obtained at the early stages of infection (4 and 6 dpi; **Supplementary Figure S2A**) a total of 473 metabolites were detected in positive ionization mode, but only two differentially accumulated compared with the controls. The first compound with an elemental formula of $C_{18}H_{19}NO_5$ was significantly higher only in resistant plants at 6 dpi. The same metabolite also accumulated in the AF of resistant plants obtained at 6 dpi, further increased in abundance up to day 10 and

then decreased again at 14 dpi, while in susceptible plants a significant increase of this compound was only observed at the later stages of infection (10 and 14 dpi). The second compound is also a nitrogen-containing metabolite ($C_7H_{13}NO_2$) and this compound significantly accumulated in the WLTEs of resistant plants at both 4 and 6 dpi, while in the WLTEs of susceptible plants accumulation was observed only at 6 dpi (**Supplementary Figures S2A**). Fragmentation analysis of the latter metabolite by LC-MS/MS produced three main fragments at m/z 84, 102 and 58, which corresponded to the reported MS/MS fragments of stachydrine (proline betaine), a pyrrolidine alkaloid identified in a wide variety of plant species. This was further confirmed through the injection of an authentic standard (Dictionary of natural products, <http://dnpc.chemnetbase.com/>) (Gründemann et al., 2005; Shi et al., 2009; Servillo et al., 2011; Li et al., 2013) (**Supplementary Figures S2C and S2D**).

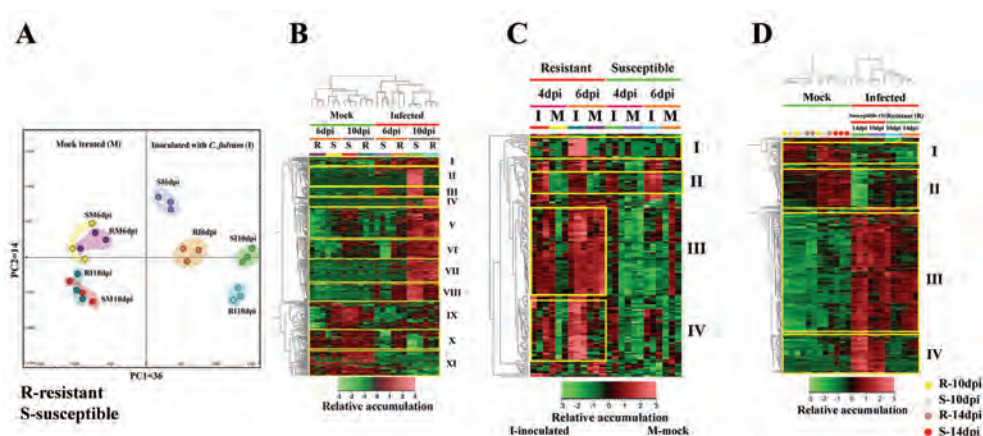


Figure 2. Apoplastic metabolome reprogramming in resistant and susceptible tomato plants inoculated with *C. fulvum*.

(A) Principal component analysis (PCA) based on polar and semi-polar metabolites that showed a significant change in their abundance ($P < 0.05$ with FDR correction) in the apoplast of resistant (R) and susceptible (S) tomato plants at 6 and 10 dpi with *C. fulvum*. Metabolites that were detected in LC (HILIC)-QTOF-MS in positive and negative ion modes were combined to compute the PCA.

(B) Hierarchical cluster analysis (HCA) based on the aforementioned metabolites of which the PCA is shown in panel A. Individual yellow-boxed clusters represent inoculation-associated changes in metabolites, including a small set of phospholipids in the tomato leaf apoplast at 6 and 10 dpi.

(C) and **(D)** represent the early (4 and 6 dpi) and later stages (10 and 14 dpi) of inoculation-related metabolome reprogramming, as shown by the HCA based on metabolites detected by C18-LCMS in the positive ionization mode. The coloured bars indicate the relative abundance of the various metabolites, based on abundance data that are \log_2 -transformed and normalized by the mean and standard deviation (see Materials and Methods for details).

SM, susceptible, mock-treated; RM, resistant, mock-treated; SI, susceptible, *C. fulvum*-inoculated; RI, resistant, *C. fulvum*-inoculated.

Principal component analysis (PCA) based on all metabolites detected by HILIC-MS (272 in negative mode, and 1,077 in positive mode) in the AF showed that there is a temporal reprogramming of the metabolome of the AF in both resistant and susceptible plants depending on the stage of infection (**Figure 2A**). In addition, differences in the metabolome between non-inoculated susceptible and resistant tomato genotypes were observed. For example, in HILIC-MS analysis (**Figure 2B**), cluster IX represents metabolites that were present in higher amounts in susceptible (MM-Cf-0) plants at 6 dpi, while in the C18-MS-based analysis (**Figure 2C**) cluster III metabolites showed a higher abundance in resistant *Cf-4*-expressing (MM-Cf-0: *Hcr9-4D*) plants at 6 dpi. Analysis of the AFs by both platforms showed that, when compared with susceptible-inoculated plants, resistant-inoculated plants showed larger changes in their apoplastic metabolome in the early phases of infection, which are primarily characterized by the accumulation of a number of metabolites at 6 dpi (**Figures 2A and 2B**, cluster VIII and **2C** clusters I and IV). Interestingly, as compared to the controls, in resistant inoculated plants all the 12 identified and putatively annotated aglycone parts of the various glycoalkaloids (GAs) had significantly accumulated at 4 dpi, while in the susceptible plants only one unidentified metabolite had significantly accumulated at this time point. However, at 6 dpi most of these alkaloid aglycones showed significant accumulation in both resistant- and susceptible-inoculated plants, yet in susceptible plants a significant degradation of α -tomatine was apparent (**Supplementary Figure S3A**). Tomatidine ($C_{27}H_{45}NO_2$), tomatidenol ($C_{27}H_{43}NO_2$) and hydroxy-tomatidine ($C_{27}H_{45}NO_3$) are aglycones of the Gas α -tomatine ($C_{50}H_{83}NO_{21}$), dehydro-tomatine ($C_{50}H_{81}NO_{21}$) and hydroxy-tomatine ($C_{50}H_{83}NO_{22}$), respectively. In the AF of resistant plants, stachydrine ($C_7H_{13}NO_2$) had significantly accumulated at both 4 and 6 dpi, while in susceptible plants significant accumulation was only observed at 6 dpi (**Supplementary Figures S3A and S4**), similar to the results obtained with WLTEs (**Supplementary Figure S2**).

Late Infection-Associated Changes in the Metabolome of Whole Leaves and Their Apoplast

At later stages after inoculation, the majority of the reprogramming of the metabolome is associated with susceptibility (**Figures 1A**, clusters I and IV and **1B**, clusters IV and V and **2A**, clusters II, III, VIII and X and **2C** and **2D**, clusters I and IV). In the HILIC-MS analysis, 7 out of the 9 differentially regulated SQDGs showed a drastic depletion in susceptible plants, while the remaining 2 (SQDG 35:1 and SQDG 33:1) were depleted in both resistant- and susceptible-inoculated plants (**Figure 1B**, clusters I and II). Unlike SQDGs, a cluster of PE species significantly increased at later stages after inoculation (**Figure 1B**, clusters IV and V). PS 33:5 was only detected in the AF and had massively accumulated in *C. fulvum*-inoculated susceptible plants at 10 dpi, while in the controls and resistant-inoculated plants the compound was below detection level at both early and later stages of infection (**Supplementary Figure S1B**). In resistant plants, the extent of reprogramming of the lipidome and metabolome at later stages of infection

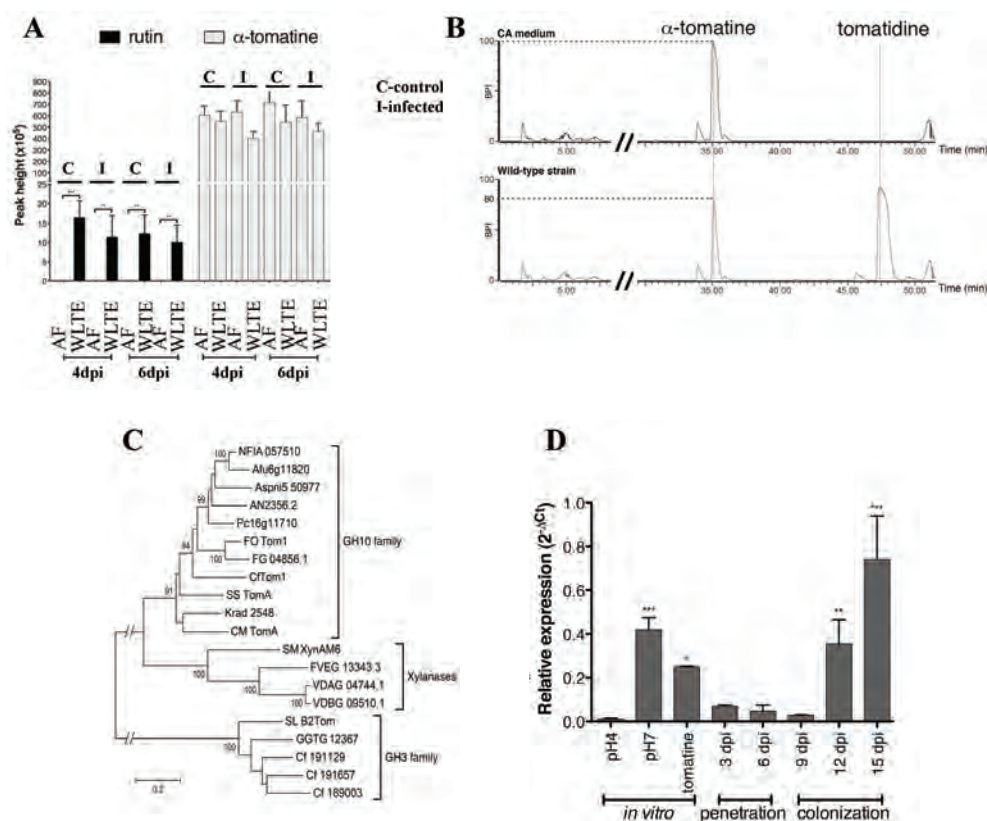
was minimal. Yet, some changes were still evident both at the lipidome and metabolome levels. For example, at 10 dpi PE 38:2 showed a nearly 3-fold increase in the AF obtained from resistant-inoculated plants, as compared to susceptible-inoculated plants, while no significant variation was detected between the mock-treated plants from the resistant and susceptible genotypes (**Supplementary Figure S1A**). Furthermore, the HILIC-MS analysis showed that in resistant-inoculated plants, a cluster of metabolites (of which some are putative phenyl-propanoids) increased significantly in the AF at 10 dpi (**Figure 2B**, cluster II). Besides the observed genotypic differences in the infection metabolome, at the later stages after inoculation, in both susceptible and resistant plants there seems to be a rechanneling of a group of metabolites towards the biosynthesis of defense-related compounds (**Figure 2B**, clusters I and XI and **Figure 2D**, clusters I and III).

Both metabolomics platforms showed that in susceptible-inoculated plants, massive depletion of GAs occurred at the later stages after inoculation (10 and 14 dpi) in both WLTEs and AFs (**Figure 1A**, cluster I; **Figure 2B**, cluster X and **Figure 2D**, cluster II and **Supplementary Figure S3B**). The hydrolysis of the GAs into their respective less toxic aglycone derivatives seems to be the primary cause for their depletion in inoculated susceptible plants. In **Figure 2D**, clusters II and IV represent the depletion of the various GAs and the accumulation of their degradation products, respectively (see **Supplementary Figure S3B** for details). Interestingly, stachydrine ($C_7H_{13}NO_2$), which showed early accumulation in resistant inoculated plants, showed massive accumulation at the later stages in susceptible-inoculated plants (10 and 14dpi) (**Supplementary Figure S4**). This metabolite was detected by both analytical platforms in the positive ionization mode. Moreover, the analysis of the apoplast metabolome of a number of resistant and susceptible tomato genotypes (**Supplementary Figure S5**) revealed that at later stages (14 dpi), when compared to the controls, even in resistant plants there is some level of α -tomatine and dehydro-tomatine degradation. Next to the degradation derivatives of GAs, the HILC-MS analysis showed that in both the WLTEs and AFs of inoculated susceptible plants sugar alcohols had also massively accumulated (**Figure 1**, cluster V), of which the five carbon (xylitol) and six carbon (mannitol) were the predominant forms. Furthermore, we also tentatively identified glycosylated forms of these sugar alcohols (**Supplementary Figure S6**).

C. fulvum* secretes a functional tomatinase enzyme that degrades α -tomatine *in vitro* and *in planta

In contrast to our observations, it was previously reported that *C. fulvum* is unable to degrade α -tomatine (Melton et al., 1998). During infection, *C. fulvum* colonizes the apoplastic space surrounding tomato mesophyll cells without entering them. It was hypothesized that *C. fulvum* does not need a tomatinase, as α -tomatine is residing in the vacuole of the tomato leaf cells. However, AF of tomato leaves has never been critically

inspected for the presence of α -tomatine and here we show that α -tomatine is present in the AF. As a control, we also analyzed rutin, a glycoside of the flavonoid quercetin, which has been reported to be only present in the cytoplasm and/or vacuole of plants (Marrs et al., 1995; Markham et al., 2001). As expected, rutin was abundantly present in WLTEs, but it was undetectable in AFs, while α -tomatine was detected in AFs at a concentration of $0.02 \pm 0.005 \mu\text{mol g}^{-1}$ leaf (FW) (**Figure 3A**). Although this concentration is lower than that of total leaf extracts ($1.0 \pm 0.1 \mu\text{mol g}^{-1}$ fresh leaf), it indicates that α -tomatine is detected at a significant level in AFs. A similar distribution of rutin and α -tomatine was seen in both infected and mock-inoculated leaves (**Figure 3A**). In contrast to what has been reported in the literature, our results show that *C. fulvum* does encounter α -tomatine and additional GAs upon colonization of the tomato apoplastic space. Interestingly, in the leaflets of colonized susceptible plants GAs were degraded and their degradation products significantly accumulated (**Figure 2B**, clusters X and III, **Figure 2D** clusters II and IV, **Supplementary Figures S3B** and **S4**). The observed depletion of α -tomatine and other GAs could be due to the induction of plant-derived GA-degrading enzymes upon inoculation with *C. fulvum*.



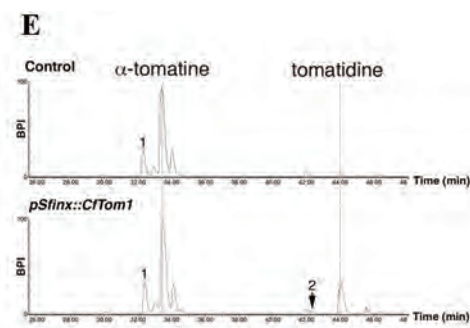


Figure 3. *In vitro* and *in vivo* CfTom1-mediated degradation of α -tomatine.

(A) α -tomatine is found both in whole leaf total extracts (WLTEs) and in apoplastic fluids (AF) obtained from tomato leaves. Cytoplasmic and/or vacuolar rutin was used as a control to confirm that there is no leakage of intracellular metabolites into the apoplast during the isolation procedure.

(B) *In vitro* detoxification of α -tomatine by *C. fulvum*.

(C) Phylogenetic tree of GH3 and GH10 tomatinase enzymes from fungal and bacterial pathogens. Amino acid sequences were aligned using ClustalW2 and a phylogenetic tree was constructed using the minimum evolution algorithm and performing 1,000 bootstraps. The scale bar shows the genetic distance (substitutions per site). NFIA, *Neosartorya fischeri*; Afu6g, *Aspergillus fumigatus*; Aspni5, *Aspergillus niger*; AN, *Aspergillus nidulans*; Pc16g, *Penicillium chrysogenum*; FO, *Fusarium oxysporum* f. sp. *lycopersici*; FG, *Fusarium graminearum*; Cf, *Cladosporium fulvum*; SS, *Streptomyces scabiei*; Krad, *Kineococcus radiotolerans*; CM, *Clavibacter michiganensis*; SM, *Streptomyces megasporus*; FVEG, *Fusarium verticillioides*; VDAG, *Verticillium dahliae*; VDBG, *Verticillium albo-atrum*; SL, *Septoria lycopersici*; GGTG, *Gaeumannomyces graminis* var. *avenae*.

(D) CfTom1 expression levels under three *in vitro* conditions (B5 medium adjusted to pH 4 and pH 7, and B5 medium adjusted to pH 4 and containing 50 μ M α -tomatine), and upon *C. fulvum* inoculation of tomato, were measured by quantitative PCR. Expression was normalized using the actin gene of *C. fulvum* according to the $2^{-\Delta\Delta Ct}$ method. Note that CfTom1 expression is induced at pH 7, in the presence of α -tomatine at pH 4 and during colonization at 12 and 15 days post inoculation (dpi).

(E) CfTom1 is a GH10 tomatinase enzyme. Apoplastic fluids were isolated from plants expressing either CfTom1 or the empty vector (control) using the pSfmx system. The relative base peak intensities (BPI) of α -tomatine and tomatidine were measured by LC-MS. In addition, dehydro-tomatine [1] and the corresponding degradation product, tomatidenol [2] were detected.

In order to prove that the fungus is responsible for this degradation, we firstly incubated culture filtrate from *C. fulvum* grown *in vitro* with α -tomatine (100 μ g ml⁻¹) for 24 h. Subsequently, the relative levels of α -tomatine and its degradation product tomatidine were monitored by LC-MS. The concentration of α -tomatine after incubation with culture filtrate was reduced compared to the incubation with non-inoculated control medium and α -tomatine degradation coincided with the accumulation of tomatidine, which was never detected upon incubation with the non-inoculated control medium (**Figure 3B**). These results suggest that the α -tomatine degradation observed during colonization of tomato leaflets is likely due to the secretion of a tomatinase enzyme by *C. fulvum*. Noteworthy is that in all experiments no β -tomatine could be detected, which suggests that *C. fulvum* does not secrete any functional GH3 tomatinase enzyme. Thus, a secreted GH10 enzyme is expected to be responsible for the degradation of α -tomatine by *C. fulvum*.

Identification of *C. fulvum* CfTom1, a GH10 tomatinase that degrades α -tomatine into tomatidine *in planta*

The availability of the genome sequence of *C. fulvum* facilitated the identification of GH10 enzyme-encoding genes. Only two genes belonging to this family were identified, but no substrate specificity could be assigned (de Wit et al., 2012). However, one of the genes encodes a protein that shares 61% amino acid identity with the *F. oxysporum* f. sp. *lycopersici* GH10 tomatinase enzyme and therefore this gene was named *CfTom1* (JGI protein ID: 188986). Phylogenetic analysis of selected GH3 and GH10 family enzymes confirmed that CfTom1 belongs to the clade of characterized fungal and bacterial GH10 tomatinases (**Figure 3C**). Although no GH3 tomatinase activity could be detected, the *C. fulvum* genome was also found to contain genes encoding enzymes related to the GH3 tomatinase of *Septoria lycopersici* and avenacinase of *G. graminis*. As enzymes in the GH3 clade have been shown to have different substrate specificities, even when they share high sequence similarity, the GH3 enzymes of *C. fulvum* are believed to target other tomato metabolites. Given that the toxicity of α -tomatine is pH-dependent, the expression of *CfTom1* was assessed by quantitative PCR *in vitro* at different pH values and also in the presence or absence of α -tomatine. Consistent with the higher toxicity of α -tomatine at neutral pH, *CfTom1* is expressed to low levels at low pH, whereas its expression is induced at pH 7 (**Figure 3D**) (Dow and Callow, 1978; Roddick and Drysdale, 1984). Similar to tomatinase induction by α -tomatine in *F. oxysporum* (Pareja-Jaime et al., 2008), the presence of α -tomatine also induces the expression of *CfTom1*, even at pH 4 (Fig. 3). *CfTom1* shows a very low expression level during the early stages of infection of tomato, but its expression is significantly induced at 12 and 15 dpi (**Figure 3D**).

In order to verify that CfTom1 is responsible for the degradation of α -tomatine into tomatidine, the *CfTom1* gene was constitutively expressed in tomato seedlings using the Potato Virus X (PVX) expression system (Hammond-Kosack et al., 1995). Five weeks after agroinoculation of the recombinant PVX constructs, AFs were isolated from PVX::*CfTom1*- and empty PVX-expressing tomato plants. LC-MS analysis of AF obtained from control plants showed detectable levels of α -tomatine, but also the presence of dehydro-tomatine (**Figure 3E**). The control AF also contained limited but detectable levels of tomatidine, which points to a low level of α -tomatine degradation by plant enzymes. In contrast, clear accumulation of tomatidine was detected in AF obtained from *CfTom1*-expressing plants, demonstrating that CfTom1 has GH10 tomatinase activity. The LC-MS analysis also revealed accumulation of tomatidenol in AF obtained from *CfTom1*-expressing tomato plants, indicating that CfTom1 can also degrade another glycoalkaloid present in tomato (**Figure 3E**).

Δ *cftom1* knock-out mutants of *C. fulvum* can no longer degrade α -tomatine *in vitro*

Functional analysis of *CfTom1* was continued by targeted gene deletion in the sequenced *C. fulvum* strain. For this, the *CfTom1* gene was replaced by the hygromycin resistance (*HYG*) and green fluorescent protein (*GFP*) genes. Two independent Δ *cftom1* mutants

(*Δcftom1-2.6* and *Δcftom1-5.1*), for which gene replacement was confirmed by Southern blot analysis, were selected (**Supplementary Figure S7**). An ectopic transformant and the wild-type strain were used as controls in all experiments. Both the *Δcftom1-2.6* and *Δcftom1-5.1* mutants did not show any visible phenotype regarding their morphology, *in vitro* growth and sporulation rates when compared to the wild-type strain and the ectopic transformant. To check for altered sensitivity of the mutants to α -tomatine, the compound was tested in a conidium germination assay. Conidia of the wild-type strain, the ectopic transformant and two *Δcftom1* mutants were allowed to germinate in the presence of control solution (1% methanol) or 100 μ M α -tomatine. In the absence of α -tomatine, no difference in the germination of conidia was observed between all strains (about 90% of the conidia germinated; **Figures 4A and B**). However, when incubated in 100 μ M α -tomatine, the germination of conidia of both *Δcftom1* mutants was reduced to about 70% of the original germination rate (**Figure 4A and B**). The higher sensitivity of the mutants is likely due to their inability to degrade α -tomatine.

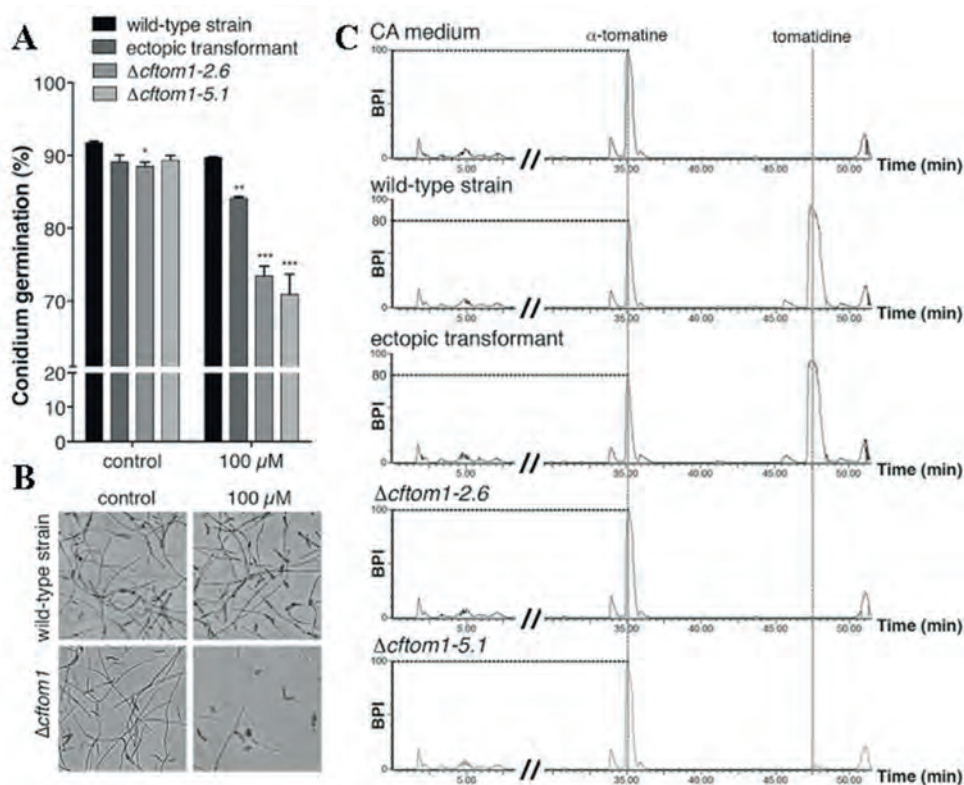


Figure 4. *Δcftom1* mutants of *C. fulvum* are sensitive to α -tomatine.

(A) The sensitivity of *C. fulvum* to α -tomatine was tested by measuring its effect on conidium germination. Conidia from the wild-type strain, an ectopic transformant and two independent *Δcftom1* mutants were incubated in the absence or presence of 100 μ M α -tomatine and the number of germinated conidia out of 100 conidia was determined. A two-way ANOVA analysis was performed and followed by a Bonferroni test. Only significant differences are indicated (* $P < 0.05$; ** $P < 0.01$ and *** $P < 0.001$). Error bars represent the standard deviation of at least three biological repeats.

(B) Representative pictures of the conidium germination assay to assess the sensitivity of the wild-type strain and a *Δcftom1* mutant of *C. fulvum* to α -tomatine.

(C) Sterile CA medium (control) and culture filtrates from the same *C. fulvum* strains as shown in **(A)** were supplemented with 100 $\mu\text{g ml}^{-1}$ α -tomatine. After 24 h of incubation, the relative base peak intensities (BPIs) of α -tomatine and tomatidine were measured by LC-MS.

To verify this hypothesis, culture filtrates of the deletion mutants were incubated with α -tomatine (100 $\mu\text{g ml}^{-1}$), along with culture filtrates of the wild-type strain and ectopic transformant as positive controls, and non-inoculated culture medium as a negative control. After 24 h of incubation, both α -tomatine depletion and tomatidine accumulation were observed for the wild-type strain and the ectopic transformant (**Figure 4C**). In contrast, culture filtrates from both *Δcftom1* knock-out mutants were not able to degrade α -tomatine and no tomatidine accumulation was detected. These results show that the higher sensitivity of the *Δcftom1* mutants to α -tomatine is due to their inability to degrade the compound *in vitro*.

***In planta* degradation of α -tomatine is required for full virulence of *C. fulvum* on tomato**

The ability to degrade α -tomatine appears to be important for successful infection of tomato by fungal pathogens (Pareja-Jaime et al., 2008). The role of *CfTom1* in *C. fulvum* virulence was analyzed by inoculating susceptible tomato plants with the wild-type strain, the ectopic transformant and two *Δcftom1* mutants. The virulence of the various strains was subsequently determined by quantifying the fungal biomass by quantitative PCRs. No significant difference in fungal biomass was observed for the wild-type, the ectopic transformant and two *Δcftom1* mutants during the early stages of infection (until 8 dpi) (**Figure 5A**). However, from 10 dpi onwards, the biomass of the two *Δcftom1* mutants was reduced by approximately 63% when compared to the wild-type strain and the ectopic transformant (**Figure 5A**). The reduction in fungal biomass is correlated with a delay in disease progression at 10 dpi, indicating that *CfTom1* is required for full virulence of *C. fulvum* on tomato.

Depletion of α -tomatine and the accumulation of its degradation product tomatidine were measured at 10 dpi of the wild-type, the ectopic transformant and two *Δcftom1* mutants on susceptible tomato plants. Similar to the *in vitro* results, no tomatidine could be detected in AFs obtained from plants inoculated with the *Δcftom1* mutants, whereas this compound clearly accumulated in the AFs of plants inoculated with the wild-type and the ectopic transformant (**Figure 5B**). Therefore, the reduction in fungal biomass production by the deletion mutants could be explained by their inability to degrade α -tomatine.

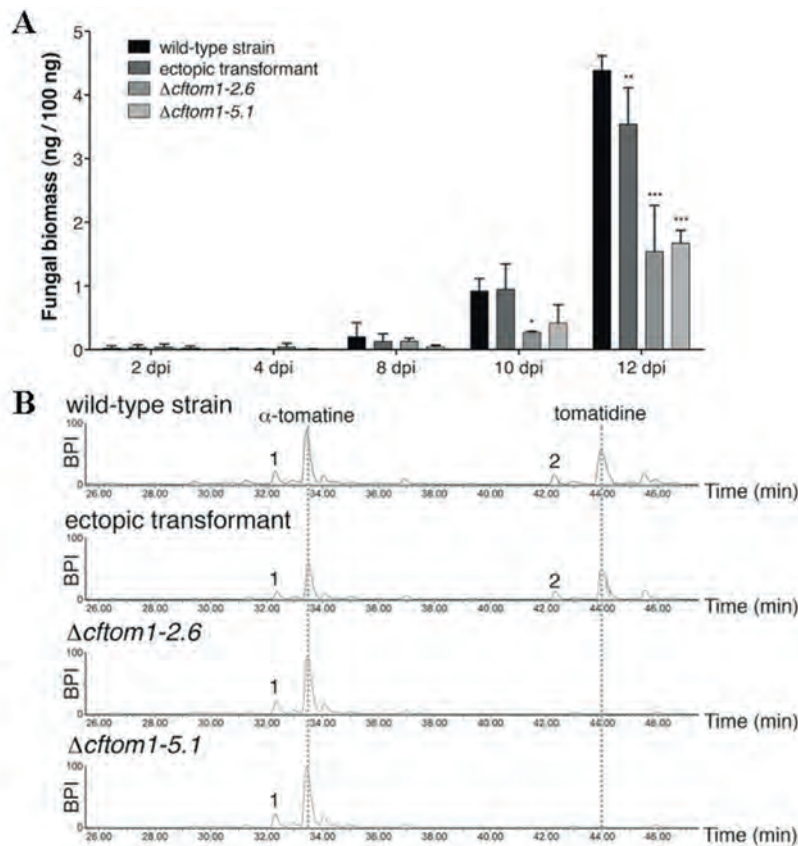


Figure 5. $\Delta cftom1$ mutants show reduced virulence.

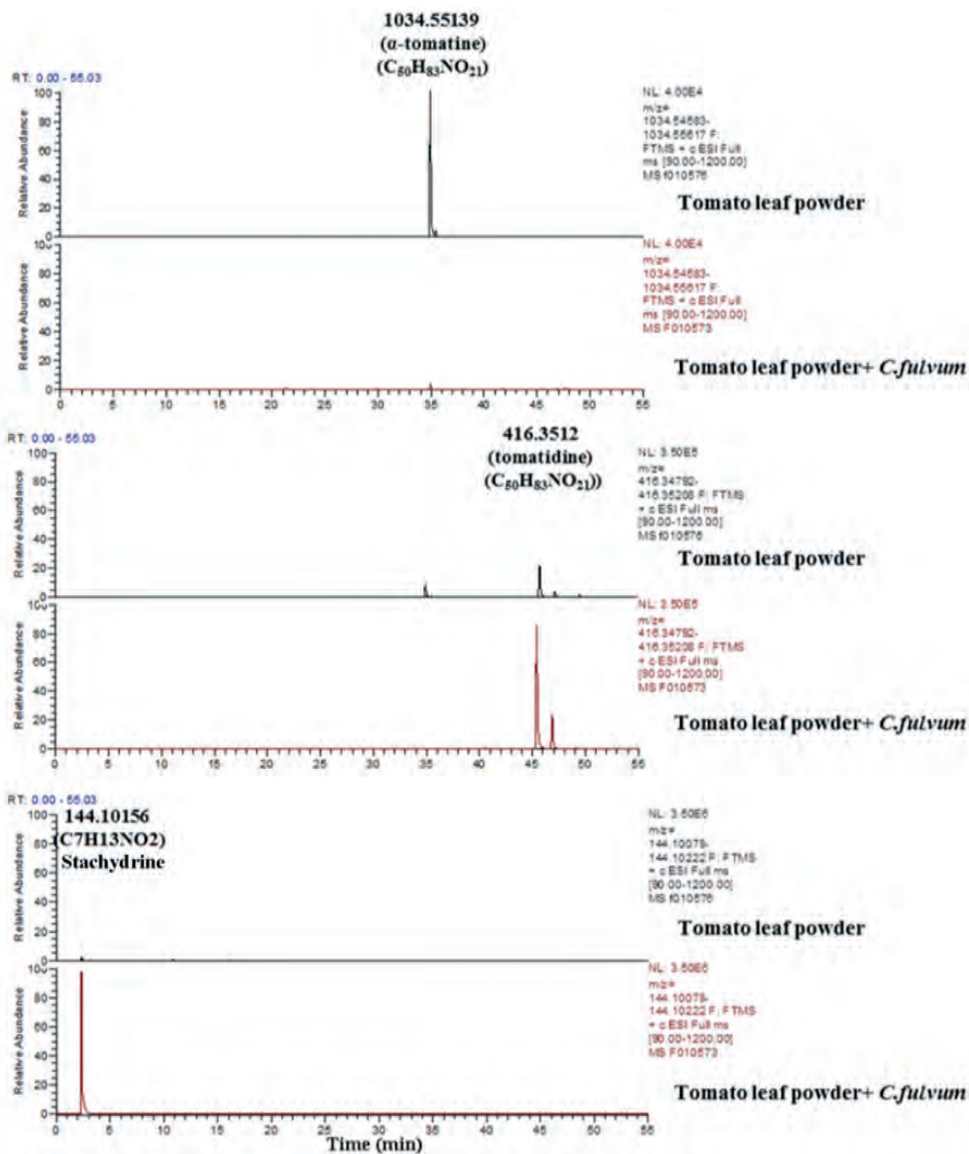
(A) Virulence of the wild-type *C. fulvum* strain, an ectopic transformant and two independent $\Delta cftom1$ mutants was assessed by quantification of the fungal biomass at different time points after inoculation of susceptible tomato plants. Quantitative PCR was performed on total genomic DNA that was isolated, using the *actin* genes from *C. fulvum* and tomato as standards. The fungal biomass was deduced from a standard curve. Inoculated tomato leaves were harvested and analyzed at 2 to 12 days post inoculation (dpi). A two-way ANOVA analysis was performed and followed by a Bonferroni test. Only significant differences are indicated (* $P < 0.05$; ** $P < 0.01$ and *** $P < 0.001$). Error bars represent the standard deviation of at least three biological repeats.

(B) Apoplastic fluids were isolated from tomato plants inoculated with the same *C. fulvum* strains as indicated in (A), at 10 dpi. The depletion of α -tomatine and accumulation of tomatidine were monitored by LC-MS. In addition, dehydro-tomatine [1] and the corresponding degradation product, tomatidenol [2], were detected as well. Note that both $\Delta cftom1$ knock-out mutants have lost their ability to detoxify α -tomatine during colonization of the apoplast of tomato leaflets as no tomatidine is detected.

It has previously been reported that the breakdown products of α -tomatine, such as tomatidine and β -tomatine, can suppress plant defense responses (Bouarab et al., 2002; Ito et al., 2007), suggesting that the accumulation of tomatidine can also indirectly contribute to virulence. Thus, the reduced virulence of the $\Delta cftom1$ mutants could not only be due to their increased sensitivity to α -tomatine, but also

due to their reduced ability to suppress plant defense responses as tomatidine does no longer accumulate. We assayed the presumed defense-suppressing activity of tomatidine on the H_2O_2 production in MSK8 tomato cell suspensions, but such activity was not confirmed in our experiments. On the contrary, MSK8 tomato cells that were incubated with α -tomatine or tomatidine showed higher H_2O_2 production when compared to the negative control (**Supplementary Figure S8A**). Furthermore, α -tomatine and tomatidine even enhanced the H_2O_2 production after treatment of the cells with chitin, showing that they were unable to suppress chitin-triggered basal defense responses. This unexpected effect of tomatidine on H_2O_2 production suggested that it could even be toxic to tomato cells. Indeed, Itkin *et al.* (2011) recently showed that down-regulation of the glycoalkaloid metabolism-1 (*GAME1*) gene, which is responsible for the glycosylation of the aglycone tomatidine into α -tomatine, results in growth retardation of this tomato mutant as a consequence of the accumulation of its precursor tomatidine. To further investigate this observation, different concentrations of α -tomatine and tomatidine (100, 250 and 500 μM) were injected into the intercellular space of tomato leaves. Results clearly show that tomatidine induces cell death in tomato leaves at concentrations of 250 and 500 μM , while α -tomatine does not cause cell death even at the highest concentration (**Supplementary Figure S8B**). These results do not point to a role for tomatidine in plant defense suppression, but rather indicate that the compound is toxic to tomato. Thus, the decrease in virulence of the Δcftom1 mutants is only caused by their inability to degrade α -tomatine.

The toxic effect of tomatidine on the plant would also have indirect consequences for the fungus, as it is highly dependent on the host for its nutrition. Therefore, the fungus has to deal with the excessively accumulating amounts of tomatidine in the tomato apoplast to sustain its existence within the plant. Compared to the situation at 10 dpi, there was a drastic reduction in the amount of apoplastic α -tomatine at 14 dpi in leaves of *C. fulvum*-inoculated susceptible plants (**Supplementary Figure S4**). However, the relative increase in tomatidine at 14 dpi was not proportional, suggesting that tomatidine might be further degraded by the fungus into other derivatives. In line with this hypothesis, stachydrine showed a massive increase in susceptible plants at 14dpi. Furthermore, a similarity matrix analysis based on 330 differentially accumulating metabolites (out of a total of 583 metabolites detected in the AF) across all 48 samples (representing treated and control susceptible and resistant plants at 4, 6, 10 and 14 dpi, in three replicates), indicated a strong association between most of the aglycone derivatives of the GAs and stachydrine (**Figure 6**).



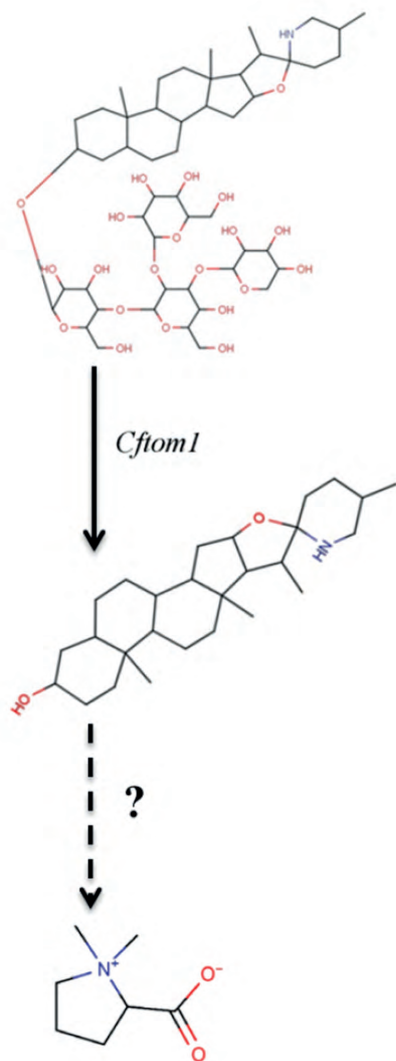


Figure 7. Detoxification of α -tomatine, and accumulation of the degradation products, by *C. fulvum* cultured in 50 mL *Aspergillus* liquid medium supplemented with 50 mg of tomato leaf powder. The $C_7H_{13}NO_2$ compound is proposed to be a degradation derivative of tomatidine and other aglycons of tomato GAs. Samples were collected at 48 hrs after incubating the fungus in the culture medium. An aliquot of 2 ml of the culture filtrate was freeze-dried, extracted with 75% MeOH and subjected to untargeted metabolome profiling using C18-LC/MS. Selected masses at specified retention times that represent tomatine, tomatidine and $C_7H_{13}NO_2$ are selected and are displayed in the chromatogram.

Discussion

In resistant plants, the majority of the changes associated with mounting of the hypersensitive response (HR) occur in the epidermal and mesophyll cells (de Wit, 1977; Thordal-Christensen et al., 1997; Wright et al., 2000; Lam et al., 2001). It is also reasonable to assume that tomato plants deploy a chemical defense arsenal in the apoplast to create a hostile environment for *C. fulvum* that exclusively resides in the extracellular spaces. Metabolites that are changing in abundance in the extracellular

(apoplastic) space hallmark the molecular warfare that takes place between tomato and *C. fulvum*. To monitor the metabolic alterations taking place in the apoplast and in the mesophyll cells, both as a part of the plant defense response and/or as a consequence of the manipulation of the host metabolism by the fungus, apoplastic fluids (AFs) and whole leaf tissue extracts (WLTEs) obtained from resistant and susceptible tomato plants inoculated with *C. fulvum* and their respective mock-inoculated controls, were subjected to untargeted metabolome profiling by two partly overlapping and partly complementary analytical platforms, C18 (reversed-phase) LCMS and HILIC-LCMS. The distinct features of the metabolome of the AFs and WLTEs upon inoculation with *C. fulvum*, reveals the power of local sampling in the study of plant-microbe interactions to elucidate the major alterations that take place locally (**Figure 1**). Furthermore, coupling of local sampling with analytical techniques that employ different extraction and separation procedures is a viable approach to monitor the alteration of different classes of metabolites during the interaction between tomato and *C. fulvum*. For example, phospholipids were predominantly found in WLTEs when obtained using MeOH: CHCl₃: H₂O. On the other hand, sugar alcohols are abundantly found in both WLTEs and AFs and due to their highly polar nature they are better separated by the HILIC column than the RP-C18 column that we used. PS 33:5, which is specific to AF obtained from leaves of *C. fulvum*-inoculated susceptible tomato, could be used as a susceptibility biomarker, particularly in relation to the presence of the fungus. Such lipids could also play a role as a signaling molecule and further studies are needed to confirm whether they are produced by the plant or by the fungus during the interaction. The depletion of SQDGs is another indicator for the progression of the disease (**Figure 1B**, cluster I). SQDGs are most abundant in the thylakoids, the membranous cellular structures that bear the photosynthetic pigments in plants (Walti et al., 2003; Shimojima, 2011). In green algae, SQDGs have been shown to be utilized as a major internal sulfur source for protein synthesis in the early phase of sulfur starvation and are suggested to function as sulfur storage lipids in these cells (Sugimoto et al., 2007; Sugimoto et al., 2010). Likewise, the tomato SQDGs may possibly be targeted by the *C. fulvum* enzymes as a source of sulfur. Further, investigation is needed to identify the fungal enzyme (s) that are involved in these processes and such information may provide more insight in the fungal nutrient acquisition strategies.

In WLTEs obtained from resistant-inoculated plants, the early reprogramming of the infection lipidome, which is characterized by the accumulation of a number of membrane phospholipid species (PEs, PSs, PIs and PGs) that have both a structural and a signaling role as a secondary messengers (Meijer and Munnik, 2003), hallmarks the activation of the host defense response against *C. fulvum* (**Figure 1B** and **Supplementary Figure S1C**). Although phosphatidyl-serines (PSs) represent only a minor phospholipid constituent of the leaves of many plant species (Vance and Steenbergen, 2005), in the

incompatible interaction they represent 50% of the early induced lipid species found in cluster III of **Figure 1B**. In animals, PSs are reported to have a crucial role in the regulation of programmed cell death in response to particular calcium-dependent stimuli, primarily related to their externalization from the inner membrane lipids, giving an “eat me” signal by the dying cells to phagocytes (OBrien et al., 1997; Bell, 2007; Ravichandran, 2010; Segawa et al., 2012). PSs have also been shown to be essential cofactors that bind to and activate a large number of proteins, especially those with signaling activity (Vance and Steenbergen, 2005). Furthermore, a rise in PS levels was reported while the level of other PLs decreased in senescing carrot leaves upon dark treatment, suggesting that the rise in PSs is one of the biochemical events occurring during membrane degradation caused by either starvation or senescence (Manoharan et al., 2000).

In the incompatible interaction and the “Dying Seedlings (DS)” of tomato, a model that represents the amplified localized response of resistant tomato plants to *C. fulvum* (Etalo et al., 2013), the early transcriptional activation of genes involved in lipid metabolism and signaling supports the role of lipids and lipid-derived compounds in the early resistance response of tomato against *C. fulvum* (**Table 1**). Particularly, genes involved in fatty acid desaturation showed higher expression levels in the incompatible interaction and the DS when compared to the compatible interaction. The fatty acid desaturases (FADs) play an important role in the introduction of double bonds into the fatty acid chain. They greatly influence the biosynthesis of membrane phospholipids and have been shown to play an important role in the plant defense response (Kachroo et al., 2001; Kachroo et al., 2003; Walley et al., 2013). Elucidation of the role of these FADs in the reprogramming of the early infection lipidome and its subsequent impact on the tomato defense against *C. fulvum* is an interesting future line of research.

In the incompatible interaction, in addition to the changes in the lipidome dynamics of the WLTEs, our comprehensive time-course studies clearly indicated that at the early phase of infection (4-6 dpi) a number of polar and semi-polar secondary metabolites accumulate in the apoplast (**Figures 1A, 1B, 2A, 2B and 2C**). In agreement with this, in chapter 3 of this thesis, our comparative transcriptional profiling clearly indicated that the incompatible interaction features a fast and massive reprogramming of the host transcriptome at 6 dpi. This indicates that the early transcriptional rewiring is an important factor for the observed reprogramming of the metabolome, suggesting that multiple integrated -omics approaches as applied here, will enable a comprehensive dissection of all metabolic changes occurring during the interaction between tomato and *C. fulvum*.

At the later stages of infection, major changes in the metabolome occur in the compatible interaction, suggesting that the manipulation of the host metabolism by the fungus is

the primary cause for the observed changes. The accumulation of sugar alcohols, both in the WLTEs and in the AFs, is a strong indication of this manipulation of the host metabolism by the fungus, as these compounds are less metabolized by the plant but can readily be used by the fungus. The active manipulation of the AFs carbohydrates involves hydrolysis of sucrose by the host/fungal invertase and the conversion of the resulting hexoses, glucose and fructose into mannitol by the fungus (Joosten et al., 1990). Similarly, in pea plants infected with *Uromyces fabae* a time-dependent increase in mannitol has been observed in both WLTEs and in AFs (Voegelé et al., 2005). Although sugar alcohols have also been found in a number of plant species, fungi are the major producers and accumulators of these compounds (Lewis and Smith, 1967). This group of metabolites is proposed to have several functions in fungi; such as (1) a carbohydrate source (Voegelé et al., 2005; Dulermo et al., 2010), (2) antioxidant activity (Shen et al., 1997; Voegelé et al., 2005) and (3) osmo-protection (Shen et al., 1999; Clark et al., 2003).

Table 1. Expression profiles of genes involved in lipid metabolism and signaling in the “Dying Seedlings” that represent the localized response of resistant tomato plants to *C. fulvum*, and resistant and susceptible tomato plants inoculated with *C. fulvum*.

Locus ID	Description	log2 fold change in expression (treatment/control)		
		Dying Seedlings	Resistant	Susceptible
solyc03g116730.2.1	FAD5†	-1.6	-1.4	NS ^Ω
solyc04g040120.1.1	FAD 2	5.3	5.2	NS
solyc06g007130.2.1	FAD 3	-1.4	NS	NS
solyc12g044950.1.1	FAD 2	4.3	1.6	NS
solyc12g100250.1.1	FAD 2	7.0	6.6	1.7
solyc06g007140.2.1	FAD 7	-1.2	NS	NS
solyc04g040130.1.1	FAD 2	4.5	5.2	1.6
solyc12g049030.1.1	FAD 2	5.6	6.3	1.9
solyc06g051400.2.1	FAD 8	NS	-1.1	NS
solyc12g100260.1.1	FAD 2	5.2	8.1	NS
solyc07g005510.2.1	FAD 6	NS	-1.2	NS
solyc08g080130.2.1	Phospholipase D beta 1	4.6	3.3	NS
solyc02g069750.1.1	Choline kinase	1.4	NS	NS
solyc04g072020.2.1	Choline kinase 1	1.8	NS	NS
solyc06g009270.2.1	Diacyl-glycerol kinase 7	1.8	NS	NS
solyc05g056420.2.1	Diacyl-glycerol kinase 2	2.4	NS	NS
solyc07g054830.2.1	Diacyl-glycerol kinase5	2.5	1.3	NS

† Fatty acid desaturase

Ω Difference is not statistically significant ($P > 0.001$ and $FC < 2$).

The expression of the genes in the Dying Seedlings is compared to those of the parental control. The expression of the genes in resistant and susceptible plants inoculated with *C. fulvum* was compared to the expression of the genes in the respective mock-treated plants.

At later stages of infection, the degradation of GAs is another indicator of the progression of the disease in susceptible plants. GAs are antimicrobial compounds present in plants that provide constitutive protection against a broad range of pathogens (Osbourn, 1996). In tomato, the major GA that has been characterized is α -tomatine, a compound that disrupts fungal membranes. Tomato pathogens, however, can overcome this chemical barrier by production of tomatinases that detoxify α -tomatine into β -tomatine (by GH3 enzymes) or into tomatidine and lycotetraose (by GH10 enzymes) (Roldan-Arjona et al., 1999; Martin-Hernandez et al., 2000).

The concentration of α -tomatine in tomato leaves can reach levels as high as 1 mM, assuming a uniform distribution in all cells (Arneson and Durbin, 1967). In previous reports it was assumed that α -tomatine is localized in the vacuoles (Roddick, 1977). For this reason, and the fact that *C. fulvum* grows in the intercellular space in a biotrophic way (Stergiopoulos and de Wit, 2009), it was expected that this fungus would not need to detoxify α -tomatine during its colonization of tomato leaflets. However, the assumed vacuolar localization is questionable, as the original conclusion of Roddick (1977) was mainly based on the fact that α -tomatine was present in the supernatant after sequential centrifugation, including ultracentrifugation, without taking into account the possibility of possible localization in the apoplast. Our analysis shows for the first time the concentration of α -tomatine in AFs to be $0.02 \pm 0.005 \mu\text{mol g}^{-1}$ fresh leaf. This quantification seems to be reliable because the concentration of α -tomatine in WLTEs ($1.0 \pm 0.1 \mu\text{mol g}^{-1}$ fresh leaf) is comparable to what has been reported by others (Melton et al., 1998). The higher concentration in WLTEs suggests that α -tomatine is indeed more abundant inside the plant cells, but still it also significantly accumulates in the apoplast. Assuming that α -tomatine is not randomly distributed in the apoplast, it is likely that the actual concentration of α -tomatine that *C. fulvum* encounters around the mesophyll cells inside tomato leaves is higher than in the AF extract.

Monitoring α -tomatine degradation and tomatidine accumulation during tomato colonization by *C. fulvum* revealed that the fungus is able to detoxify this GA. This result contrasts with previous reports, which could possibly be explained by a lower sensitivity of the analytical methods used by others. In their analysis, Melton et al., (1998) performed thin-layer chromatography (TLC), which is much less sensitive than LC-MS, to detect breakdown products of α -tomatine after incubation with proteinaceous extracts isolated from culture filtrates of *C. fulvum* (Melton et al., 1998). More importantly, the culture filtrates they used in their assay originate from *C. fulvum* grown on B5 medium, of which the pH is approximately 4.5. Our expression data showed that *CfTom1* is barely expressed in the same medium at pH 4 (**Figure 3D**), suggesting that the absence of tomatinase activity in this earlier study is due to a limited expression of *CfTom1*.

Analysis of the *C. fulvum* genes encoding CAZymes revealed two *GH10* and 19 *GH3* genes

in its genome (de Wit et al., 2012). A phylogenetic analysis showed that only one of the GH10 enzymes belongs to the GH10 tomatinase clade (CfTom1), while three GH3 enzymes belong to the GH3 tomatinase/avenacinase clade. Our results showed that *C. fulvum* degrades α -tomatine into tomatidine, both *in vitro* and during colonization of tomato leaflets, suggesting that CfTom1 is responsible for the observed activity. A specific search for the presence of β -tomatine in the extracts, based on its accurate mass in the LCMS chromatograms, was unsuccessful, suggesting that the enzymes encoded by the three putative *GH3* genes cannot degrade α -tomatine to β -tomatine. Alternatively, CfTom1 could also degrade β -tomatine into tomatidine. However, this is unlikely because the presence of β -tomatine was neither observed *in vitro* nor *in planta* when α -tomatine degradation was determined for the Δ *cftom1* mutants. These results indicate that CfTom1 is probably the only enzyme responsible for degradation of α -tomatine by *C. fulvum* and the three putative GH3 tomatinases cannot complement Δ *cftom1* mutants for α -tomatine degradation. The predicted protein sequences suggest that the GH3 enzymes are functional, but they might be involved in the degradation of other (secondary metabolite) compounds present in tomato. Indeed, although the homology between the GH3 enzymes is high, they could have different substrate specificities. For example, the amino acid identity between *Septoria lycopersici* GH3 tomatinase and *G. graminis* var. *avenae* GH3 avenacinase is only 53% (Osbourn et al., 1995). In addition, recent RNA-seq analysis performed on *C. fulvum*-inoculated leaves of susceptible tomato plants revealed that the three *GH3* genes are poorly expressed, both *in vitro* and *in planta* (unpublished results, P.J.G.M. de Wit).

Our results showed a clear correlation between α -tomatine depletion (**Figure 2D**, cluster II and **Supplementary Figures S3** and **S4**), *CfTom1* gene expression (**Figure 3D**) and *C. fulvum* growth (**Figure 5A**). Therefore, we assume that the depletion of α -tomatine is related to the fungal biomass and the expression level of *CfTom1*. The ability of tomato pathogens to specifically degrade α -tomatine suggests that tomatinase enzymes play an important role in the infection process. Several tomatinases have been characterized from bacterial and fungal tomato pathogens (Martin-Hernandez et al., 2000; Sandroock and Vanetten, 2001; Kaup et al., 2005; Seipke and Loria, 2008). However, neither GH3 tomatinase knock-out mutants in *Septoria lycopersici* (Martin-Hernandez et al., 2000) nor GH10 tomatinase knock-out mutants in *C. michiganensis* subsp. *michiganensis* showed a significant decrease in virulence as compared to wild-type strains (Kaup et al., 2005). These results could be due to only subtle effects on virulence that were difficult to detect, or due to the presence of additional tomatinase-encoding genes in the genomes of these pathogens (Sandroock and Vanetten, 2001; Pareja-Jaime et al., 2008; this study).

So far, the only strong evidence for the involvement of a tomatinase enzyme in fungal pathogenicity was found for the *GH10 tom1* gene of *F. oxysporum* f. sp. *lycopersici*,

although the genome of this fungus also contains putative *GH3* tomatinase genes (Pareja-Jaime et al., 2008). Our study shows that the *GH10 CfTom1* gene of *C. fulvum* is involved in virulence. Colonization of tomato leaves by $\Delta cfTom1$ mutants was reduced as shown by the significant reduction in fungal biomass from 10 dpi onwards (**Figure 5A**). No significant difference in biomass was observed between the mutants, wild-type strain and ectopic transformant at the early stages of infection (2-8 dpi), at which time points the *CfTom1* gene was also only weakly expressed. *CfTom1* gene expression is induced after 9 dpi, which explains the difference in growth between the mutants and controls at later stages of infection. Accordingly, degradation of α -tomatine to tomatidine during infection was found to occur from 10 dpi onwards. This study confirms the previous finding that heterologous expression of the *Septoria lycopersici GH3* tomatinase gene in *C. fulvum* causes increased sporulation in susceptible tomato plants and supports a role for α -tomatine degradation in *C. fulvum* virulence (Melton et al., 1998).

Since it was reported that breakdown products of α -tomatine, such as β -tomatine and tomatidine, suppress plant defense responses (Bouarab et al., 2002; Ito et al., 2007), the absence of this indirect activity may also contribute to the reduction in virulence of the $\Delta cfTom1$ mutants, in addition to the increased sensitivity of the mutant fungus to α -tomatine. However, suppression of plant defense responses by tomatidine could not be confirmed in our experiments. On the contrary, we found that tomatidine was toxic to tomato cells and caused cell death when infiltrated into tomato leaves. A similar effect was also found by Itkin and co-workers in mutant tomato plants accumulating tomatidine (Itkin et al., 2011). These results suggest that the reduction in virulence of the $\Delta cfTom1$ mutants is only due to an increased sensitivity to α -tomatine.

The fate of the tomatidine produced by the fungus in the tomato apoplast still needs to be elucidated, as it seems to be suicidal for the biotrophic fungus to accumulate phytotoxic degradation products. The hierarchical cluster analysis showed a strong association between stachydrine and the aglycon forms of the various GAs. Here we postulate that stachydrine is a degradation product of tomatidine and other aglycons of GAs. The strong association was evident at both the early and late stages after inoculation. In the incompatible interaction this metabolite had significantly accumulated in both WLTEs and AF at 4dpi. At this stage of infection, it is less likely for stachydrine to be a degradation product of GA, as the *CfTom1* gene, necessary for producing tomatidine, was only weakly expressed. Hence, we assume that elicitation of tomato plants could contribute to *de novo* biosynthesis of stachydrine. Further work, which utilizes ^{14}C - and ^{15}N -labeled α -tomatine, may help to elucidate the fate of both the lycotetraose and the aglycon part of α -tomatine. The lycotetraose and the aglycone parts of GA could be potential carbon and nitrogen sources for the fungus. Like mannitol, stachydrine is reported to be osmo-protective suggesting that enrichment of osmo-protectant is a common strategy adopted by fungi to overcome harsh conditions associated with plant

defense (McNeil et al., 1999; Shen et al., 1999; Clark et al., 2003).

Altogether, our results clearly show that an early reprogramming of the metabolome of both the mesophyll cells and the apoplast play a crucial role in the resistance response of tomato against *C. fulvum*. At the later stages of infection, the majority of the alterations are the result of the manipulation of the host metabolism by the fungus to breach the defense line and get access to the carbon reserves of the host. The intercellular tomato pathogen *C. fulvum* encounters α -tomatine and other GAs during colonization of the apoplast of tomato leaves and CfTom1 is the major, and possibly only, α -tomatine-detoxifying enzyme that contributes to full virulence of this fungus on tomato. This activity certainly contributed to the adaptation of *C. fulvum* to tomato after divergence from its close relative *Dothistroma septosporum* that is pathogenic on pine and lacks a homologue of the *CfTom1* gene (de Wit et al., 2012). The present work shows how powerful the combined use of metabolomics and genome mining is to elucidate the major metabolic alterations occurring at the interface of the host and microbe when the biotrophic relationship is established.

Materials and Methods

Plant Materials and *C. fulvum* Disease Assays

Susceptible Money Maker (MM)-Cf-0 and resistant (Cf-0: *Hcr9-4D* (*Cf-4*)) tomato lines were grown in the greenhouse at 70% relative humidity, at 23-25°C during daytime and at 19-21°C at night, with a light/dark regime of 16/8 h and 100Watt m⁻² supplemental light when light intensity was less than 150 Watt m⁻². Plants were inoculated with race 5 of *C. fulvum* secreting Avr4 (de Wit, 1977). From *C. fulvum*-inoculated susceptible and resistant plants, leaflets were harvested at 4, 6, 10 and 14 days post inoculation (dpi) with the fungus and at the same time points leaflets were harvested from the non-inoculated (mock-treated) plants. Three biological replicates were performed, while each biological replicate was represented by four plants. Furthermore, we monitored the dynamics of the apoplastic glycoalkaloids upon inoculation of an additional six resistant and seven susceptible tomato genotypes with *C. fulvum* (Supplementary Figure S4).

Large Scale Untargeted Metabolomics Profiling during Tomato Infection

Metabolite extraction and their analysis by LC (RP-C18)-PDA-LTQ-Orbitrap-FTMS (C18-LCMS)

Sample preparation

Apoplastic fluid was isolated from tomato leaves as described by Joosten (2012) and 2 ml aliquots were freeze-dried (2 ml of AF is obtained from 4 g (fresh weight (FW))

of leaves) and extracted with 300 μ l of 75% methanol (MeOH) in water containing 0.1% formic acid (FA). For the analysis of the whole leaf tissue metabolome, 0.1g FW of frozen leaf powder was used and extracted with 300 μ l of 99.9% MeOH containing 0.1% FA. Samples were briefly mixed, sonicated for 30 min and centrifuged at 21,000g. Supernatants were filtered through a 0.2 μ m inorganic membrane filter and transferred to HPLC vials.

Metabolite analysis using C18-LCMS

The LC-PDA-LTQ-Orbitrap-FTMS instrument consisted of an Accela HPLC system (Accela photodiode array (PDA) and auto-sampler), interfaced to an LTQ/Orbitrap hybrid mass spectrometer (Thermo Fisher Scientific) that was equipped with an ESI source (van der Hooft et al., 2011). A Luna RP-C18 (2) analytical column (Phenomenex, USA) was used for chromatographic separation. The mobile phase consisted of a binary eluent solvent system of degassed ultra-pure water (solvent A) and acetonitrile (solvent B), both containing 0.1% v/v FA. The sample injection volume was 5 μ l, while keeping the flow rate of the eluents at 0.19 ml/min and keeping the column temperature at 40 °C. The HPLC gradient started at 5% B and linearly increased to 35% B in 45 min. The column was re-equilibrated for 15 min following the separation of each sample (van der Hooft et al., 2011). The mass chromatograms that were generated by the Orbitrap-FTMS were processed (peak picking and baseline correction) using the MetAlign software package (Lommen, 2009). Extraction and reconstitution of compound mass spectra were performed according to the method described by Tikunov et al. (2012). From the processed data, information on the relative peak height of the representative masses $[M+H]^+$ for α -tomatine, dehydro-tomatine and their degradation products, tomatidine and tomatidenol, was extracted at their recorded retention time for tomato fruit (Supporting Information, Table S2), according to the MOTO database (Moco et al., 2006) and the Komics database (<http://webs2.kazusa.or.jp/komics/>) (Iijima et al., 2008). Quantification of α -tomatine was done using a standard curve of commercial α -tomatine (Sigma Aldrich). Genemath XT was used to compute the principal component analysis (PCA), hierarchical cluster analysis (HCA) and similarity matrix analysis as described by (Etalo et al., 2013).

Extraction of and analysis of metabolites by LC (HILIC)-QTOF-MS (HILIC-LCMS)

Sample preparation

For the measurements of both apoplastic fluids and whole leaf tissue extracts, freeze-dried samples of 2 mg were used. The extraction solvent was prepared by mixing methanol/chloroform/water at a ratio of 5:2:2 (v/v/v) and degassing this mixture by directing a gentle stream of nitrogen through the solvent for 5 min. One ml of precooled solvent (-20°C) was added, the mixture was vortexed for 20 sec and shaken at 4 °C for 6 min to extract the metabolites and simultaneously precipitate the proteins.

After centrifugation at 14,000g for 2 min, the supernatant was transferred into a new Eppendorf tube, dried in a vacuum concentrator and kept at -20°C until further use.

Metabolite analysis using HILIC-LCMS

The instrumentation consisted of an Agilent 1200 LC stack (binary pump SL, degasser, auto-sampler, thermostat and column oven) interfaced to an Agilent 6530 accurate-mass quadrupole time-of-flight (Q-TOF) with a JetStream ESI source. The HPLC system was equipped with a Waters Acquity BEH HILIC column (2.1×150 mm, 1.7 µm particle size, Waters Corporation, Milford, MA) at 40 °C. The mobile phase consisted of (A) water with 5mM ammonium acetate and 0.2% acetic acid, and (B) 9:1 acetonitrile/water with 5mM ammonium acetate and 0.2% acetic acid. The gradient method was: 0 to 4 min: 100% B, 4 to 12 min: linear gradient to 45% B and 12 to 20 min: 45% B. The column was re-equilibrated for 20 min following the separation of each sample and the flow-rate was 0.25 ml/min. MS and MS/MS data were collected with a scan rate of 0.25 sec in both profile and centroid modes, and mass calibration was maintained by constant infusion of reference ions at m/z 121.0509 and 922.0098. MS/MS data were generated utilizing data-dependent MS/MS triggering with dynamic exclusion. Precursor ions, with a minimum 1 k signal intensity were isolated with a 4 m/z isolation width (medium setting), and a variable collision energy was applied based on precursor ion m/z ($10 \text{ eV} + 0.03 \text{ eV} \times \text{ion } m/z$). Ions were excluded from data-dependent MS/MS analysis for 30 sec following acquisition of two spectra. Data were exported into the open exchange format mzXML. Samples were measured in both negative and positive mode. Additionally, blank runs were acquired to determine background contaminations. The mass chromatograms that were generated by the QTOF-MS were processed using the MZmine software package (Pluskal et al., 2010). For identification of lipid species, the accurate mass and MS/MS information in the LipidBlast library was used (Kind et al., 2013).

Functional characterization of *CfTom1* in vitro and in vivo

Fungal materials

Cladosporium fulvum race 0WU (CBS131901)(de Wit et al., 2012) was grown on half-strength potato dextrose agar (19.5 g l⁻¹ PDA and 15 g l⁻¹ technical agar, Oxoid) at 20 °C for 2-3 weeks for conidia production and DNA isolation. Stocks of conidia were maintained in 25% glycerol at -80°C. For tomatinase activity assays, the fungus was grown in liquid CA medium (10 g l⁻¹ casamino acids, 10 mM ammonium sulfate and 0.5 g l⁻¹ yeast nitrogen base, pH 6.5). To induce the expression of the *CfTom1* gene, *C. fulvum* was pre-incubated in Gamborg B5 medium supplemented with 20 g l⁻¹ sucrose at 22°C and incubated in an orbital shaker at 200 rpm for 6 days. Mycelium was then transferred to several B5 induction media at pH 4, pH 7, in the absence or presence of 50 µM α-tomatine, and cultured for 24 h.

DNA extraction, quantitative PCRs and Southern blotting

DNA was isolated from freeze-dried mycelia of *C. fulvum* strains, which were scraped from PDA plates, or from ground *C. fulvum*-inoculated tomato leaves frozen in liquid nitrogen, using the DNeasy plant mini kit (Qiagen Benelux bv, Venlo, The Netherlands), according to the manufacturer's instructions. Total RNA was isolated from ground mycelia or *C. fulvum*-inoculated tomato leaves using the hybrid method as described by van Esse et al. (2008).

cDNA was synthesized from 5 µg of total RNA using the SuperScript II reverse transcriptase kit (Invitrogen) as previously described (Bolton et al., 2008). Quantitative PCR was performed with the 7300 System (Applied Biosystems, Foster City, U.S.A.). Each reaction was performed in 25 µl, containing 12.5 µl Sensimix (Biolab), 1 µl of 10 µM dNTPs, 1 µl of each forward and reverse oligonucleotide (5 µM), 100 ng of template cDNA and 9.5 µl ddH₂O. The thermal profile included an initial 95°C denaturation step for 10 min, followed by denaturation for 15 s at 95°C and annealing/extension for 45 s at 60°C for 40 cycles. qCfActin_F and qCfActin_R, and qCfTom1_F and qCfTom1_R oligonucleotide pairs were designed with Primer3 Plus (Supporting Information, Table S1) (Untergasser et al., 2007). The efficiency and specificity of the oligonucleotide pairs were determined with a dilution series of genomic DNA prior to use. The *C. fulvum actin* gene was used as a reference gene for normalization and results were analyzed using the 2^{-ΔCt} method (Livak and Schmittgen, 2001). Results are the average of three biological repeats.

All PCRs were performed in 25 µl using Pfu or GoTaq DNA polymerase (Promega) following the manufacturer's recommendations, and using 100 ng of genomic DNA as template. The PCR program was initiated by a denaturation step at 94°C for 5 min, followed by 32 cycles of denaturation at 94°C for 1 min, annealing at 55°C for 45 s, and extension at 72°C for 1 min, with a final extension step at 72°C for 7 min.

Southern blotting was performed with digoxigenin-labeled probes using a DIG DNA Labeling and Detection Kit (Roche, Basel, Switzerland) according to the manufacturer's instructions. The probe was generated using the pCfTom1_US_F and pCfTom1_US_R primer pair (Supporting Information, Table S1).

Identification and cloning of the *CfTom1* gene and its expression by the Potato Virus X expression system in tomato

Amino acid sequences of GH3 and GH10 tomatinases were aligned with ClustalW2 (Larkin et al., 2007) and edited in GeneDoc software (Nicholas et al., 1997). A consensus phylogenetic tree was constructed using the minimum-evolution algorithm with default parameters and 1000 bootstrap replications in the MEGA5 software (Tamura et al., 2011).

The GH10 tomatinase gene (*CfTom1*; jgiID 188986) from *C. fulvum* was amplified by PCR using the following oligonucleotide set; the *CfTom1_F* oligonucleotide excludes the native signal peptide sequence of the tomatinase gene and includes a 15-nucleotide overhang sequence corresponding to the *PR1A* signal peptide sequence; the *CfTom1_R* oligonucleotide contains the *NotI* restriction site (Supporting Information, Table S1). A second PCR was performed to amplify the *PR1A* signal peptide sequence by using the *PR1A_F* oligonucleotide containing a *Clal* restriction site and *PR1A_R* oligonucleotide. Overlapping PCR was performed to fuse the *PR1A* signal peptide sequence to the *CfTom1* coding sequence using the *PR1A_F* and *CfTom1_R* oligonucleotides (Supporting Information, Table S1). The amplified *PR1A-CfTom1* fragment was purified from the agarose gel using the Illustra™ GFX™ PCR DNA and Gel Band Purification Kit (GE Healthcare). The purified *PR1A-CfTom1* fragment was cloned into the pGEM-T Easy vector (Promega) according to the manufacturer's instructions. The recombinant pGEM-T vector was introduced into chemically-competent *Escherichia coli* cells (DH5α) by the standard heat shock transformation protocol. The plasmid was retrieved from a positive clone using the Miniprep plasmid isolation kit (Qiagen) and the insert was sequenced by MacroGen Inc. The correct *PR1A-CfTom1* insert was isolated using *Clal* and *NotI* restriction enzymes (Promega) and was ligated (Promega) into the binary Potato Virus X (PVX)-based vector pSfinx (Hammond-Kosack et al., 1995; Takken and Lu, 2001) that was digested with the same restriction enzymes. The product of the ligation reaction was introduced into *E. coli* and the obtained *pSfinx::PR1A-CfTom1* plasmid was finally introduced into *Agrobacterium tumefaciens* (GV3101) by electroporation. A positive *A. tumefaciens* clone containing the *pSfinx::PR1A-CfTom1* construct was cultured on plates containing modified LB medium (10 g l⁻¹ bacto-peptone; 5 g l⁻¹ yeast extract; 5 g l⁻¹ NaCl) supplemented with 100 µg ml⁻¹ kanamycin and 25 µg ml⁻¹ rifampicin for 48 h at 28°C. Heterologous expression of *pSfinx::PR1A-CfTom1* in tomato seedlings was performed as described previously (Stergiopoulos et al., 2010).

Construction of the *cftom1* targeted deletion plasmid

The gene replacement vector *pR4R3Δcftom1* was constructed using the MultiSite Gateway® Three-Fragment Vector Construction Kit (Invitrogen™) according to the manufacturer's instructions. The upstream (US, 1.8kb) and downstream (DS, 1.55kb) flanking regions of *CfTom1* were amplified using oligonucleotides with overhang sequences homologous to the *AttB4*, *AttB1r*, *AttB2r* or *AttB3* recombination sites (Supporting Information, Table S1). Purified US and DS fragments were cloned into *pDONR™ P4-P1R* and *pDONR™ P2R-P3*, respectively, using 1 µl of BP clonase™ II enzyme mix (Invitrogen™), 70 ng of insert DNA and 70 ng of pDONR™ in a 5 µl reaction volume, and introduced into *E. coli*. The *p221_GFP_HYG* pENTRY vector was kindly provided by Rafael Arango Isaza (Plant Research International, Wageningen). To construct the final replacement vector, an LR reaction was performed with 50 ng of *pDONR™ P4-P1R_cftom1US*, 50 ng of *pDONR™ P2R-P_cftom1DS*, 50 ng of *p221_GFP_HYG* and 70 ng of

pDESTTMR4-R3 destination vector in the presence of 1 µl of LR clonaseTM II enzyme mix (Invitrogen) in a 5 µl total volume. The product of the LR reaction was introduced into *E. coli* to obtain the final *pR4R3Δcftom1* plasmid. Insertion of all fragments was confirmed by PCR using insert-specific primers (Supporting Information, Table S1).

***Agrobacterium tumefaciens*-mediated fungal transformation and mutant screening**

The *pR4R3Δcftom1* construct was transformed into *Agrobacterium tumefaciens* AGL1 by electroporation. *A. tumefaciens*-mediated transformation of *C. fulvum* was performed as described previously (Zwiers and De Waard, 2001) with the following modifications. *A. tumefaciens* AGL1 cells containing the *pR4R3Δcftom1* construct were grown in minimal medium (MM) (10 mM K₂HPO₄, 10 mM KH₂PO₄, 2.5 mM NaCl, 2 mM MgSO₄, 0.7 mM CaCl₂, 9 µM FeSO₄, 4 mM NH₄SO₄, and 10 mM glucose; adjusted to pH 5.5) supplemented with 100 µg ml⁻¹ spectinomycin and 10 µg ml⁻¹ rifampicin for 2-3 days at 28°C. *A. tumefaciens* AGL1 cells were collected by centrifugation at 3363×*g* for 8 min and resuspended in induction medium (IM) [MM; 40 mM 2-(N-morpholino) ethanesulfonic acid, pH 5.3; 0.5% glycerol (w/v); 200 µM acetosyringone] supplemented with appropriate antibiotics to the final OD₆₀₀ of 0.15. Prior to co-cultivation, the *A. tumefaciens* AGL1 culture was incubated at 28°C for 4-6 h to an OD₆₀₀ of 0.25. *C. fulvum* conidia were collected from half-strength PDA plates with sterile water and passed through two layers of miracloth to remove mycelium. The *A. tumefaciens* AGL1 culture (200 µl; OD₆₀₀ 0.25) was co-cultivated with 200 µl conidia suspension (1×10⁷ conidia ml⁻¹). The co-cultivation mixture was plated on H Bond-nitrocellulose membrane that was previously placed on IM plates and incubated for 2 days at 20°C. After 2 days co-incubation, membranes were transferred to MM plates supplemented with 100 µg ml⁻¹ hygromycin and 200 µM cefotaxime. Transformed fungal colonies (2-3-week-old) were transferred onto PDA plates supplemented with 100 µg ml⁻¹ hygromycin and 200 µM cefotaxime, and incubated at 20°C for 2-3 weeks. Fungal transformants were sub-cultured twice on selective PDA plates and once on non-selective PDA plates. Subsequently, transformants were tested on PDA plates containing 100 µg ml⁻¹ hygromycin.

α-Tomatine sensitivity assay

Conidia from wild-type *C. fulvum*, one ectopic transformant and two independent *Δcftom1* mutants were collected and diluted to a final concentration of 2×10⁴ conidia ml⁻¹. Agar plugs were prepared on sterile microscope slides by addition of 250 µl CA medium (CA medium supplemented with 1% technical agar). Conidia (20 µl) were mixed with 10 mM α-tomatine (in methanol) (Sigma Aldrich) to obtain a final concentration of 100 µM, and incubated on the CA agar plugs at 20°C for 2 days. As a negative control, conidia were incubated in methanol (1% v/v) but without α-tomatine. For each sample, the germination of 100 conidia was analyzed. The results are the average of two biological repeats.

Tomatinase activity monitoring by LC-MS

For *in vitro* α -tomatine degradation, 1×10^6 conidia of *C. fulvum* wild-type strain, ectopic transformant and $\Delta cftom1$ mutants were cultured in 30 ml liquid CA medium at 22°C with shaking at 200 rpm for 5-6 days, using three biological replicates. The fungal cultures were filtered to remove mycelia and the supernatants were used to determine tomatinase activity. Culture filtrate (4 ml) of each strain was incubated with 100 $\mu\text{g ml}^{-1}$ α -tomatine (Sigma Aldrich) for 24 h with shaking at 28°C. After 24 h incubation, samples were prepared for Liquid Chromatography-Quadrupole Time of Flight-Mass Spectrometry (LC-QTOF-MS) analysis to determine α -tomatine, and its degradation products tomatidine and β -tomatine following the method described by (De Vos et al., 2007). This experiment was performed with three biological replicates.

A. tumefaciens strains containing the *pSfinx::CfTom1* and the original *pSfinx* (empty virus) vectors were inoculated on 10-day-old MM-Cf-0 tomato seedlings for transient heterologous *CfTom1* gene expression. This experiment was performed in three biological replicates. After 5 weeks, *pSfinx::CfTom1* or *pSfinx::Empty* construct-transformed tomato leaves were collected for AF isolation. AF isolation was performed by vacuum infiltration according to the method described by de Wit and Spikman (1982). 15 ml of AF for each sample was freeze-dried and re-suspended in 6 ml methanol containing 0.1% FA. Prior to LC-MS analysis, 1 ml of each sample was filtered through 0.45 μm pore size filters and samples were analyzed by LC-MS in positive ionization mode to determine depletion of α -tomatine and accumulation of tomatidine. This experiment was also performed for wild-type, ectopic and $\Delta cftom1$ mutants-inoculated tomato plants. Here, AF was isolated from inoculated tomato plants at 10 dpi with the different strains (this experiment was performed with two biological replicates).

C. fulvum virulence assays

Wild-type *C. fulvum* (race 0WU; CBS131901), one ectopic and two independent $\Delta cftom1$ mutants ($\Delta cftom1$ -2.6 and $\Delta cftom1$ -5.1) were grown on half-strength PDA plates for 2-3 weeks at 20°C. Conidia were collected from the plates with water and subsequently passed through one layers of miracloth to remove fungal mycelium. The suspension of conidia was diluted to a final concentration of 5×10^5 conidia ml^{-1} . Five-week-old MM-Cf-0 tomato plants were inoculated with conidia from the wild-type, the ectopic mutant and the two $\Delta cftom1$ mutants via spray-inoculation on the abaxial side of the tomato leaves. *C. fulvum*-inoculated tomato plants were kept in plastic-covered cages for two days to ensure 100% relative humidity for conidial germination. After two days, plastic covers were removed and disease development of the wild-type, ectopic transformant and $\Delta cftom1$ mutants were assayed every two days. Inoculated leaves were collected at different days after inoculation (2, 4, 8, 10 and 12 dpi) (the experiment was performed with three biological replicates). Fungal biomass quantification was performed using quantitative PCR analysis as described previously but using genomic DNA. Genomic

DNAs were isolated from wild-type, ectopic transformant and $\Delta cftom1$ mutants infected leaves and were diluted to final concentration of $100 \text{ ng } \mu\text{l}^{-1}$. A standard curve was constructed by using serial dilutions of *C. fulvum* genomic DNA ($10 \text{ ng } \mu\text{l}^{-1}$; $1 \text{ ng } \mu\text{l}^{-1}$; $0.1 \text{ ng } \mu\text{l}^{-1}$; $0.01 \text{ ng } \mu\text{l}^{-1}$; $0.001 \text{ ng } \mu\text{l}^{-1}$) and using *actin* as a reference gene. Logarithms (base 10) of DNA concentrations were plotted against crossing point of Ct values.

The effect of tomatidine on H_2O_2 accumulation

Cell suspensions of MSK8 tomato (*Lycopersicon esculentum* Mill.) were grown in Murashige and Skoog plant salt base (4.3 g l^{-1}) liquid medium supplemented with B5 vitamins (myo-inositol (100 g l^{-1}), nicotinic acid (1 g l^{-1}), pyridoxine.HCl (1 g l^{-1}) and thiamine.HCl (10 g l^{-1}), sucrose (3%) and kinetin (0.1 mg ml^{-1}). The MSK8 cells were continuously rotated at 125 rpm in the dark at 25°C . Five-day-old MSK8 cell suspensions were used for the H_2O_2 accumulation assay. 2 ml of MSK8 cell suspensions were transferred to 12 well-plates and stabilized for two hours in a rotary shaker before further use. These cells were co-incubated either with α -tomatine (final concentration of $40 \text{ } \mu\text{M}$) or tomatidine (final concentration of $40 \text{ } \mu\text{M}$) in the presence of the histochemical stain DAB ($100 \text{ } \mu\text{g ml}^{-1}$) and with or without $1 \text{ } \mu\text{M}$ chitin-hexamer. The MSK8 cell suspensions treated with same dilution range of methanol (0.8% v/v) were used as a control. Pictures were taken at 15 h post co-incubation. A reddish-brown precipitate indicates the accumulation of H_2O_2 .

Assessing phytotoxic effects of α -tomatine and tomatidine towards tomato

100, 250 and $500 \text{ } \mu\text{M}$ of α -tomatine and tomatidine (diluted from a 5 mM stock of α -tomatine and tomatidine in methanol) (Sigma Aldrich) were infiltrated into 5- or 6-week-old tomato leaves. The same dilution range of methanol (10%, 5% and 2% v/v) was used as a negative control. Pictures were taken at 3 days after treatment with α -tomatine or tomatidine. The experiment was performed with three biological replicates.

In vitro* degradation of α -tomatine in tomato leaf powder by *C. fulvum

For *in vitro* α -tomatine degradation, conidia of *C. fulvum* race 5 were cultured in 50 ml of liquid Aspergillus medium at 22°C with shaking at 200 rpm for 5-6 days, using three biological replicates. The expanded mycelium was filtered in sterile cheese close and transferred to the same liquid medium, containing 50 mg of ground frozen tomato leaf powder and incubated for 48 h, while shaking at 22°C . After 48 h of incubation, the culture filtrate was collected and 2 mL aliquots of freeze-dried samples were extracted with 75% MeOH (containing 0.1% FA) and subjected to LC-LTQ-Orbitrap-FTMS analysis to determine the levels of α -tomatine, and its degradation products tomatidine and $\text{C}_7\text{H}_{13}\text{NO}_2$, following the method used by van der Hooft et al. (2011). This experiment was performed using three biological replicates.

Acknowledgements

We thank Bert Schipper for his help with the C18-LCMS analysis of the apoplast metabolome. We extend our gratitude to all metabolomics group members of Plant Research International (PRI) and the Laboratory of Plant Physiology (Wageningen University) for their invaluable technical and intellectual contributions. We acknowledge Bert Essenstam for excellent plant care. This project was (co)financed by the Centre for BioSystems Genomics (CBSG) and The Netherlands Metabolomics Centre (specifically DWE and RCHDV), who are both part of the Netherlands Genomics Initiative/Netherlands Organisation for Scientific Research.

References

- Abu-Nada Y, Kushalappa AC, Marshall WD, Al-Mughrabi K, Murphy A (2007) Temporal dynamics of pathogenesis-related metabolites and their plausible pathways of induction in potato leaves following inoculation with *Phytophthora infestans*. *Eur J Plant Pathol* **118**: 375-391
- Allwood JW, Ellis DI, Goodacre R (2008) Metabolomic technologies and their application to the study of plants and plant–host interactions. *Physiol Plant* **132**: 117-135
- Allwood JW, Ellis DI, Heald JK, Goodacre R, Mur LAJ (2006) Metabolomic approaches reveal that phosphatidic and phosphatidyl glycerol phospholipids are major discriminatory non-polar metabolites in responses by *Brachypodium distachyon* to challenge by *Magnaporthe grisea*. *Plant J* **46**: 351-368
- Arneson PA, Durbin RD (1967) Hydrolysis of tomatine by *Septoria lycopersici* - a detoxification mechanism. *Phytopathology* **57**: 1358-1360
- Bell E (2007) Apoptosis: Recognizing 'eat-me' signals. *Nat Rev Immunol* **7**: 917-917
- Bolton MD, van Esse HP, Vossen JH, de Jonge R, Stergiopoulos I, Stulemeijer IJ, van den Berg GC, Borrás-Hidalgo O, Dekker HL, de Koster CG, de Wit PJGM, Joosten MHAI, Thomma BP (2008) The novel *Cladosporium fulvum* lysin motif effector Ecp6 is a virulence factor with orthologues in other fungal species. *Mol Microbiol* **69**: 119-136
- Bouarab K, Melton R, Peart J, Baulcombe D, Osbourn A (2002) A saponin-detoxifying enzyme mediates suppression of plant defences. *Nature* **418**: 889-892
- Bowyer P, Clarke BR, Lunness P, Daniels MJ, Osbourn AE (1995) Host-range of a plant-pathogenic fungus determined by a saponin detoxifying enzyme. *Science* **267**: 371-374
- Caillaud MC, Wirthmueller L, Fabro G, Piquerez SJ, Asai S, Ishaque N, Jones JD (2012) Mechanisms of nuclear suppression of host immunity by effectors from the Arabidopsis downy mildew pathogen *Hyaloperonospora arabidopsidis* (Hpa). *Cold Spring Harb Symp Quant Biol* **77**: 285-293
- Clark AJ, Blissett KJ, Oliver RP (2003) Investigating the role of polyols in *Cladosporium fulvum* during growth under hyper-osmotic stress and in planta. *Planta* **216**: 614-619
- de Jong CF, Laxalt AM, Bargmann BOR, de Wit PJGM, Joosten MHAI, Munnik T (2004) Phosphatidic acid accumulation is an early response in the Cf-4/Avr4 interaction. *Plant J* **39**: 1-12
- de Jonge R, van Esse HP, Kombrink A, Shinya T, Desaki Y, Bours R, van der Krol S, Shibuya N, Joosten MHAI, Thomma BP (2010) Conserved fungal LysM effector Ecp6 prevents chitin-triggered immunity in plants. *Science* **329**: 953-955
- de Wit PJGM (1977) A light and scanning-electron microscopic study of infection of tomato plants by virulent and avirulent races of *Cladosporium fulvum*. *Neth J Plant Path* **83**: 109-122
- de Wit PJGM, Spikman G (1982) Evidence for the occurrence of race and cultivar-specific elicitors of necrosis in intercellular fluids of compatible interactions of *Cladosporium fulvum* and tomato. *Physiol Plant Pathol* **21**: 1-11

- de Wit PJGM, van der Burgt A, Ökmen B, Stergiopoulos I, Abd-Elsalam K, Aerts AL, Bahkali AHA, Beenen H, Chettri P, Cox MP, Datema E, de Vries RP, Dhillon B, Ganley AR, Griffiths S, Guo Y, Hamelin RC, Henrissat B, Kabir MS, Jashni MK, Kema G, Klaubauf S, Lapidus A, Lévassieur A, Lindquist E, Mehrabi R, Ohm RA, Owen TJ, Salamov A, Schwelm A, Schijlen E, Sun H, van den Burg HA, van Ham RCHJ, Zhang S, Goodwin SB, Grigoriev IV, Collemare J, Bradshaw RE (2012) The genomes of the fungal plant pathogens *Cladosporium fulvum* and *Dothistroma septosporum* reveal adaptation to different hosts and lifestyles but also signatures of common ancestry. *PLOS Genet* **8**: 1-22
- Dow JM, Callow JA (1978) A possible role for α -tomatine in the varietal-specific resistance of tomato to *Cladosporium fulvum*. *Phytopath. Z.* **92**: 211-216
- Draper J, Rasmussen S, Zubair H (2011) Metabolite analysis and metabolomics in the study of biotrophic interactions between plants and microbes. In *Annual Plant Reviews Volume 43*. Wiley-Blackwell, pp 25-59
- Dulermo T, Rasclé C, Billon-Grand G, Gout E, Bligny R, Cotton P (2010) Novel insights into mannitol metabolism in the fungal plant pathogen *Botrytis cinerea*. *Biochem J* **427**: 323-332
- Etalo DW, Stulemeijer IJE, van Esse HP, de Vos RCH, Bouwmeester HJ, Joosten MHAJ (2013) System-wide hypersensitive response-associated transcriptome and metabolome reprogramming in tomato. *Plant Physiol* **162**: 1599-1617
- Ford JE, McCance DJ, Drysdale RB (1977) The detoxification of α -tomatine by *Fusarium oxysporum* f. sp. lycopersici. *Phytochemistry* **16**: 545-546
- Fraser CM (2004) Insights into the evolution of phytopathogens. *Trends Microbiol* **12**: 482-483
- Gründemann D, Harlfinger S, Golz S, Geerts A, Lazar A, Berkels R, Jung N, Rubbert A, Schömig E (2005) Discovery of the ergothioneine transporter. *Proc Nat Acad Sci USA* **102**: 5256-5261
- Hammond-Kosack KE, Staskawicz BJ, Jones JDG, Baulcombe DC (1995) Functional expression of a fungal avirulence gene from a modified potato-virus-x genome. *Mol Plant-Microbe Interact* **8**: 181-185
- Hann DR, Dominguez-Ferreras A, Motyka V, Dobrev PI, Schornack S, Jehle A, Felix G, Chinchilla D, Rathjen JP, Boller T (2013) The Pseudomonas type III effector HopQ1 activates cytokinin signaling and interferes with plant innate immunity. *New Phytol* **201**: 585-598
- Hématy K, Cherk C, Somerville S (2009) Host-pathogen warfare at the plant cell wall. *Curr Opin Plant Biol* **12**: 406-413
- Holub EB (2006) Evolution of parasitic symbioses between plants and filamentous microorganisms. *Curr Opin Plant Biol* **9**: 397-405
- Howden AJM, Huitema E (2012) Effector-triggered post-translational modifications and their role in suppression of plant immunity. *Front Plant Sci* **3**: 1-6
- Huckelhoven R (2007) Cell wall-associated mechanisms of disease resistance and susceptibility. *Annu Rev Phytopathol* **45**: 101-127
- Iijima Y, Nakamura Y, Ogata Y, Tanaka Ki, Sakurai N, Suda K, Suzuki T, Suzuki H, Okazaki K, Kitayama M, Kanaya S, Aoki K, Shibata D (2008) Metabolite annotations based on the integration of mass spectral information. *Plant J* **54**: 949-962
- Itkin M, Rogachev I, Alkan N, Rosenberg T, Malitsky S, Masini L, Meir S, Iijima Y, Aoki K, de Vos R, Prusky D, Burdman S, Beekwilder J, Aharoni A (2011) Glycoalkaloid metabolism1 is required for steroidal alkaloid glycosylation and prevention of phytotoxicity in tomato. *Plant Cell* **23**: 4507-4525
- Ito S-I, Ihara T, Tamura H, Tanaka S, Ikeda T, Kajihara H, Dissanayake C, Abdel-Motaal FF, El-Sayed MA (2007) α -Tomatine, the major saponin in tomato, induces programmed cell death mediated by reactive oxygen species in the fungal pathogen *Fusarium oxysporum*. *FEBS Letters* **581**: 3217-3222
- Joosten MHAJ (2012) Isolation of apoplastic fluid from leaf tissue by the vacuum infiltration-centrifugation technique. *Methods Mol Biol* **835**: 603-610
- Joosten MHAJ, Hendrickx LM, Wit PJGM (1990) Carbohydrate composition of apoplastic fluids isolated from tomato leaves inoculated with virulent or avirulent races of *Cladosporium fulvum* (syn. *Fulvia fulva*). *Neth J Plant Pathol.* **96**: 103-112
- Kachroo A, Lapchuk L, Fukushige H, Hildebrand D, Klessig D, Kachroo P (2003) Plastidial fatty acid signaling modulates salicylic acid- and jasmonic acid-mediated defense pathways in the arabidopsis *ssi2* mutant. *Plant Cell* **15**: 2952-2965
- Kachroo P, Shanklin J, Shah J, Whittle EJ, Klessig DF (2001) A fatty acid desaturase modulates the activation of defense signaling pathways in plants. *Proc Natl Acad Sci U S A* **98**: 9448-9453

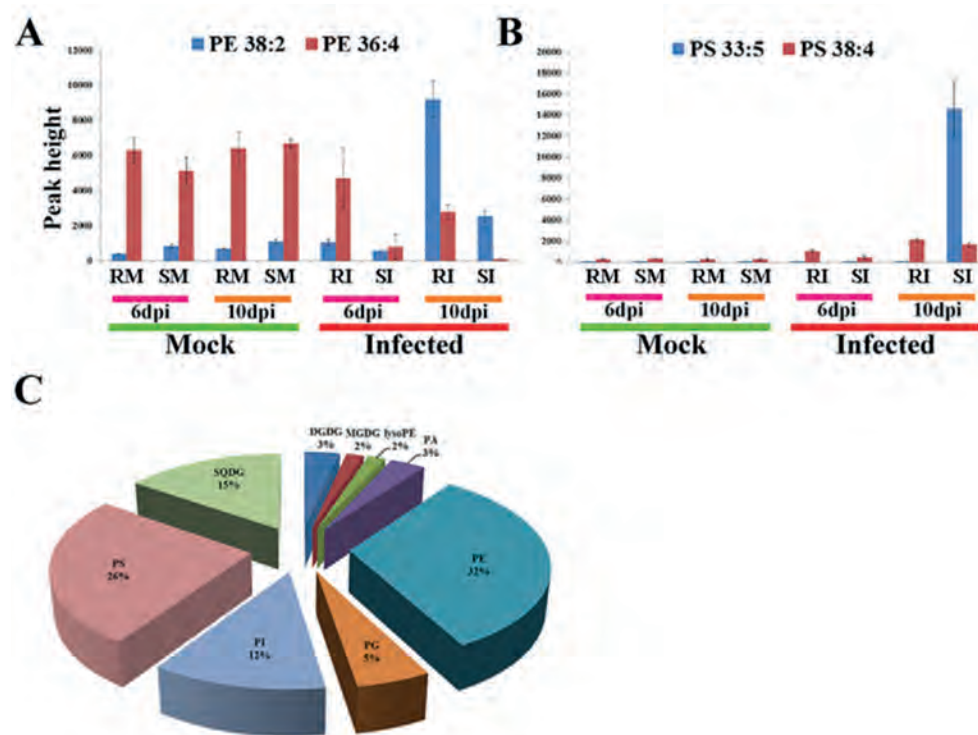
- Kaup O, Grafen I, Zellermann EM, Eichenlaub R, Gartemann KH** (2005) Identification of a tomatinase in the tomato-pathogenic actinomycete *Clavibacter michiganensis* subsp *michiganensis* NCPPB382. *Mol Plant-Microbe Interact* **18**: 1090-1098
- Keukens EAJ, de Vrije T, van den Boom C, de Waard P, Plasman HH, Thiel F, Chupin V, Jongen WME, de Kruijff B** (1995) Molecular basis of glycoalkaloid induced membrane disruption. *BBA- Biomembranes* **1240**: 216-228
- Kind T, Liu KH, Lee do Y, DeFelice B, Meissen JK, Fiehn O** (2013) LipidBlast in silico tandem mass spectrometry database for lipid identification. *Nat Methods* **10**: 755-758
- Kliebenstein DJ, Rowe HC, Denby KJ** (2005) Secondary metabolites influence Arabidopsis/Botrytis interactions: variation in host production and pathogen sensitivity. *Plant J* **44**: 25-36
- Lam E, Kato N, Lawton M** (2001) Programmed cell death, mitochondria and the plant hypersensitive response. *Nature* **411**: 848-853
- Larkin MA, Blackshields G, Brown NP, Chenna R, McGettigan PA, McWilliam H, Valentin F, Wallace IM, Wilm A, Lopez R, Thompson JD, Gibson TJ, Higgins DG** (2007) Clustal W and clustal X version 2.0. *Bioinformatics* **23**: 2947-2948
- Laxalt AM, Munnik T** (2002) Phospholipid signalling in plant defence. *Curr Opin Plant Biol* **5**: 332-338
- Lewis DH, Smith DC** (1967) Sugar alcohols (polyols) in fungi and green plants . Distribution physiology and metabolism. *New Phytol* **66**: 143-&
- Li B, Wu J, Li X** (2013) Simultaneous determination and pharmacokinetic study of stachydrine and leonurine in rat plasma after oral administration of Herba Leonuri extract by LC-MS/MS. *J Pharm Biomed Anal* **76**: 192-199
- Liebrand TWH, van den Berg GCM, Zhang Z, Smit P, Cordewener JHG, America AHP, Sklenar J, Jones AME, Tameling WIL, Robatzek S, Thomma BPHJ, Joosten MHAJ** (2013) Receptor-like kinase SOBIR1/EVR interacts with receptor-like proteins in plant immunity against fungal infection *Proc Natl Acad Sci U S A* **110**: 13228-13228
- Livak KJ, Schmittgen TD** (2001) Analysis of relative gene expression data using real-time quantitative PCR and the 2(T)(-Delta Delta C) method. *Methods* **25**: 402-408
- Lommen A** (2009) MetAlign: Interface-driven, versatile metabolomics tool for hyphenated full-scan mass spectrometry data preprocessing. *Anal Chem* **81**: 3079-3086
- Manoharan K, Chae HS, Myoung J, Cho SH, Shin SH, Cho BH, Lee WS** (2000) Synthesis of phosphatidylserine in carrot cells cultured under carbon-source starvation. *Plant Cell Physiol* **41**: 1143-1148
- Markham KR, Gould KS, Ryan KG** (2001) Cytoplasmic accumulation of flavonoids in flower petals and its relevance to yellow flower colouration. *Phytochemistry* **58**: 403-413
- Marrs KA, Alfenito MR, Lloyd AM, Walbot V** (1995) A glutathione-S-transferase involved in vacuolar transfer encoded by the maize gene Bronze-2. *Nature* **375**: 397-400
- Martin-Hernandez AM, Dufresne M, Hugouvieux V, Melton R, Osbourn A** (2000) Effects of targeted replacement of the tomatinase gene on the interaction of *Septoria lycopersici* with tomato plants. *Mol Plant-Microbe Interact* **13**: 1301-1311
- McNeil SD, Nuccio ML, Hanson AD** (1999) Betaines and related osmoprotectants. Targets for metabolic engineering of stress resistance. *Plant Physiol* **120**: 945-950
- Meijer HJG, Munnik T** (2003) Phospholipid-based signaling in plants *Annu Rev Plant Biol* **54**: 265-306
- Melton RE, Flegg LM, Brown JKM, Oliver RP, Daniels MJ, Osbourn AE** (1998) Heterologous expression of *Septoria lycopersici* tomatinase in *Cladosporium fulvum*: Effects on compatible and incompatible interactions with tomato seedlings. *Mol Plant-Microbe Interact* **11**: 228-236
- Moco S, Bino RJ, Vorst O, Verhoeven HA, de Groot J, van Beek TA, Vervoort J, de Vos CHR** (2006) A liquid chromatography-mass spectrometry-based metabolome database for tomato. *Plant Physiol* **141**: 1205-1218
- Nicholas KB, Nicholas HB, Deerfield DW** (1997) GeneDoc: Analysis and visualization of genetic variation. *EMBNEW NEWS* **4**: 14
- O'Connell RJ, Panstruga R** (2006) Tete a tete inside a plant cell: establishing compatibility between plants and biotrophic fungi and oomycetes. *New Phytol* **171**: 699-718
- OBrien IEW, Reutelingsperger CPM, Holdaway KM** (1997) Annexin-V and TUNEL use in monitoring the progression of apoptosis in plants. *Cytometry* **29**: 28-33
- Osborn A** (1996) Saponins and plant defence - A soap story. *Trends Plant Sci* **1**: 4-9

- Osbourn A, Bowyer P, Lunness P, Clarke B, Daniels M** (1995) Fungal pathogens of oat roots and tomato leaves employ closely related enzymes to detoxify different host plant saponins. *Mol Plant-Microbe Interact* **8**: 971-978
- Osbourn AE** (1999) Antimicrobial phytoprotectants and fungal pathogens: a commentary. *Fungal Genet Biol* **26**: 163-168
- Pareja-Jaime Y, Roncero MIG, Ruiz-Roldan MC** (2008) Tomatinase from *Fusarium oxysporum* f. sp *lycopersici* is required for full virulence on tomato plants. *Mol Plant-Microbe Interact* **21**: 728-736
- Park J, Gu Y, Lee Y, Yang Z, Lee Y** (2004) Phosphatidic acid induces leaf cell death in Arabidopsis by activating the Rho-related small G protein GTPase-mediated pathway of reactive oxygen species generation. *Plant Physiol* **134**: 129-136
- Perfect SE, Green JR** (2001) Infection structures of biotrophic and hemibiotrophic fungal plant pathogens. *Mol Plant Pathol* **2**: 101-108
- Pluskal T, Castillo S, Villar-Briones A, Oresic M** (2010) MZmine 2: Modular framework for processing, visualizing, and analyzing mass spectrometry-based molecular profile data. *Bmc Bioinformatics* **11**
- Quidde T, Osbourn AE, Tudzynski P** (1998) Detoxification of α -tomatine by *Botrytis cinerea*. *Physiol Mol Plant Pathol* **52**: 151-165
- Ravichandran KS** (2010) Find-me and eat-me signals in apoptotic cell clearance: progress and conundrums. *J Exp Med* **207**: 1807-1817
- Roddick JG** (1977) Subcellular localization of steroidal glycoalkaloids in vegetative organs of *Lycopersicon esculentum* and *Solanum tuberosum*. *Phytochemistry* **16**: 805-807
- Roddick JG, Drysdale RB** (1984) Destabilization of liposome membranes by the steroidal glycoalkaloid α -tomatine. *Phytochemistry* **23**: 543-547
- Roldan-Arjona T, Perez-Espinosa A, Ruiz-Rubio M** (1999) Tomatinase from *Fusarium oxysporum* f. sp *lycopersici* defines a new class of saponinases. *Mol Plant-Microbe Interact* **12**: 852-861
- Sandrock RW, Vanetten HD** (2001) The relevance of tomatinase activity in pathogens of tomato: disruption of the beta(2)-tomatinase gene in *Colletotrichum coccodes* and *Septoria lycopersici* and heterologous expression of the *Septoria lycopersici* beta(2)-tomatinase in *Nectria haematococca*, a pathogen of tomato fruit. *Physiol Mol Plant Pathology* **58**: 159-171
- Segawa K, Suzuki J, Nagata S** (2012) Constitutive exposure of phosphatidylserine on viable cells P *Natl Acad Sci USA* **109**: 995-995
- Seipke RF, Loria R** (2008) *Streptomyces scabies* 87-22 possesses a functional tomatinase. *J Bacteriol* **190**: 7684-7692
- Servillo L, Giovane A, Balestrieri ML, Ferrari G, Cautela D, Castaldo D** (2011) Occurrence of pipercolic acid and pipercolic acid betaine (Homostachydrine) in citrus genus plants. *J Agric Food Chem* **60**: 315-321
- Shen B, Hohmann S, Jensen RG, Bohnert a H** (1999) Roles of sugar alcohols in osmotic stress adaptation. Replacement of glycerol by mannitol and sorbitol in yeast. *Plant Physiol* **121**: 45-52
- Shen B, Jensen RG, Bohnert HJ** (1997) Increased resistance to oxidative stress in transgenic plants by targeting mannitol biosynthesis to chloroplasts. *Plant Physiol* **113**: 1177-1183
- Shi Q, Liu Z, Yang Y, Geng P, Zhu Y-y, Zhang Q, Bai F, Bai G** (2009) Identification of anti-asthmatic compounds in *Pericarpium citri reticulatae* and evaluation of their synergistic effects. *Acta Pharmacol Sin*. **30**: 567-575
- Shimajima M** (2011) Biosynthesis and functions of the plant sulfolipid. *Prog Lipid Res* **50**: 234-239
- Steel CC, Drysdale RB** (1988) Electrolyte leakage from plant and fungal tissues and disruption of liposome membranes by α -tomatine. *Phytochemistry* **27**: 1025-1030
- Stergiopoulos I, de Wit PJGM** (2009) Fungal effector proteins. *In Annu Rev Phytopathol*, Vol 47, pp 233-263
- Stergiopoulos I, van den Burg HA, Ökmen B, Beenen HG, van Lier S, Kema GHJ, de Wit PJGM** (2010) Tomato Cf resistance proteins mediate recognition of cognate homologous effectors from fungi pathogenic on dicots and monocots. *Proc Natl Acad Sci U S A* **107**: 7610-7615
- Stulemeijer IJ, Joosten MHAI, Jensen ON** (2009) Quantitative phosphoproteomics of tomato mounting a hypersensitive response reveals a swift suppression of photosynthetic activity and a differential role for hsp90 isoforms. *J Proteome Res* **8**: 1168-1182
- Sugimoto K, Sato N, Tsuzuki M** (2007) Utilization of a chloroplast membrane sulfolipid as a major internal sulfur source for protein synthesis in the early phase of sulfur starvation in *Chlamydomonas reinhardtii*. *FEBS Letters* **581**: 4519-4522

- Sugimoto K, Tsuzuki M, Sato N** (2010) Regulation of synthesis and degradation of a sulfolipid under sulfur-starved conditions and its physiological significance in *Chlamydomonas reinhardtii*. *New Phytol* **185**: 676-686
- Takken FLW, Lu R** (2001) A functional cloning strategy, based on a binary PVX-expression vector, to isolate HR-inducing cDNAs of plant pathogens *Plant J* **26**: 363-363
- Tamura K, Peterson D, Peterson N, Stecher G, Nei M, Kumar S** (2011) MEGA5: Molecular evolutionary genetics analysis using maximum likelihood, evolutionary distance, and maximum parsimony methods. *Mol Biol Evol* **28**: 2731-2739
- Thordal-Christensen H, Zhang Z, Wei Y, Collinge DB** (1997) Subcellular localization of H₂O₂ in plants. H₂O₂ accumulation in papillae and hypersensitive response during the barley—powdery mildew interaction. *Plant J* **11**: 1187-1194
- Tikunov YM, Laptinok S, Hall RD, Bovy A, de Vos RCH** (2012) MSCLust: a tool for unsupervised mass spectra extraction of chromatography-mass spectrometry ion-wise aligned data. *Metabolomics* **8**: 714-718
- Untergasser A, Nijveen H, Rao X, Bisseling T, Geurts R, Leunissen JAM** (2007) Primer3Plus, an enhanced web interface to Primer3. *Nucleic Acids Res* **35**: W71-W74
- van der Hooft JJ, Vervoort J, Bino RJ, Beekwilder J, de Vos RC** (2011) Polyphenol identification based on systematic and robust high-resolution accurate mass spectrometry fragmentation. *Anal Chem* **83**: 409-416
- van Meer G, Voelker DR, Feigenson GW** (2008) Membrane lipids: where they are and how they behave. *Nat Rev Mol Cell Bio* **9**: 112-124
- Vance JE, Steenbergen R** (2005) Metabolism and functions of phosphatidylserine. *Prog Lipid Res* **44**: 207-234
- Voegelé RT, Hahn M, Lohaus G, Link T, Heiser I, Mendgen K** (2005) Possible roles for mannitol and mannitol dehydrogenase in the biotrophic plant pathogen *Uromyces fabae*. *Plant Physiol* **137**: 190-198
- Vossen JH, Abd-El-Hallem A, Fradin EF, Van Den Berg GCM, Ekengren SK, Meijer HJG, Seifi A, Bai Y, Ten Have A, Munnik T, Thomma BPHJ, Joosten MHJ** (2010) Identification of tomato phosphatidylinositol-specific phospholipase-C (PI-PLC) family members and the role of PLC4 and PLC6 in HR and disease resistance. *Plant J* **62**: 224-239
- Walley JW, Kliebenstein DJ, Bostock RM, Dehesh K** (2013) Fatty acids and early detection of pathogens. *Curr Opin Plant Biol* **16**: 520-526
- Ward JL, Forcat S, Beckmann M, Bennett M, Miller SJ, Baker JM, Hawkins ND, Vermeer CP, Lu C, Lin W, Truman WM, Beale MH, Draper J, Mansfield JW, Grant M** (2010) The metabolic transition during disease following infection of *Arabidopsis thaliana* by *Pseudomonas syringae* pv. tomato. *Plant J* **63**: 443-457
- Welti R, Wang X, Williams TD** (2003) Electrospray ionization tandem mass spectrometry scan modes for plant chloroplast lipids. *Anal. Biochem* **314**: 149-152
- Wink M** (1988) Plant-breeding - importance of plant secondary metabolites for protection against pathogens and herbivores. *Theor Appl Genet* **75**: 225-233
- Wright KM, Duncan GH, Pradel KS, Carr F, Wood S, Oparka KJ, Cruz SS** (2000) Analysis of the N gene hypersensitive response induced by a fluorescently tagged tobacco mosaic virus. *Plant Physiol* **123**: 1375-1386
- Zacares L, Lopez-Gresa MP, Fayos J, Primo J, Belles JM, Conejero V** (2007) Induction of p-coumaroyldopamine and feruloyldopamine, two novel metabolites, in tomato by the bacterial pathogen *Pseudomonas syringae*. *Mol Plant Microbe Interact* **20**: 1439-1448
- Zwiers LH, De Waard MA** (2001) Efficient *Agrobacterium tumefaciens*-mediated gene disruption in the phytopathogen *Mycosphaerella graminicola*. *Current Genetics* **39**: 388-393

Supplemental information

Supplementary figures



Supplementary Figure S1. Dynamics of the lipidome of tomato leaves upon challenge with *C. fulvum*.

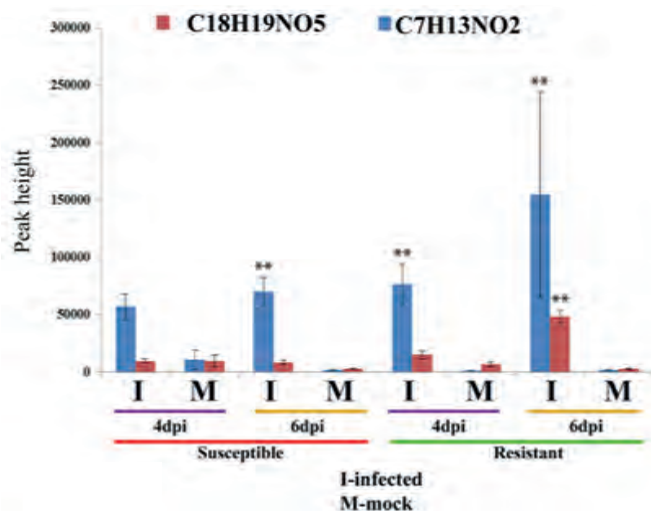
(A) Differentially accumulating phospholipid species (phosphatidylethanolamine (PE)) that are detected in both the whole leaf tissue extract (WLTE) and apoplastic fluid (AF) of tomato plants challenged with *C. fulvum*.

(B) Differentially accumulating phosphatidyl-serine (PS) that is detected only in the AF of tomato leaves challenged with *C. fulvum*. The error bar indicates the standard error of the mean of three independent biological replicates.

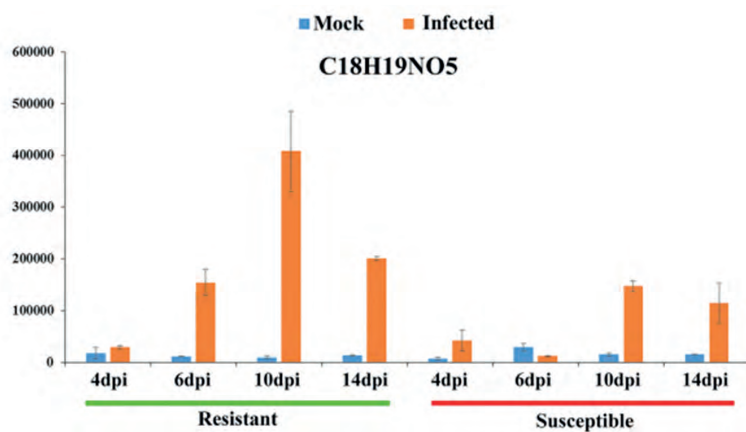
(C) Composition of identified phospholipids that are predominantly found in the WLTEs, as depicted in Figure 1B.

SM, susceptible, mock-treated; RM, resistant, mock-treated; SI, susceptible, *C. fulvum*-inoculated; RI, resistant, *C. fulvum*-inoculated.

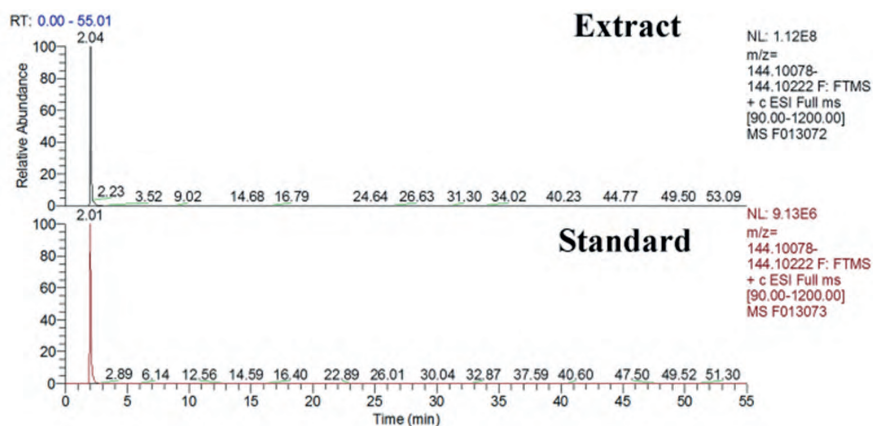
A



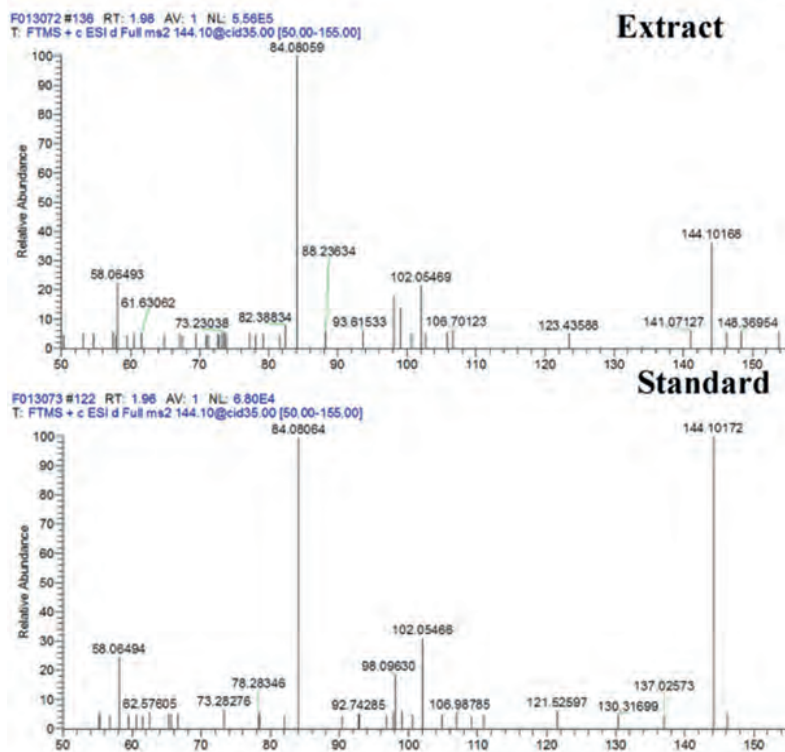
B



C



D



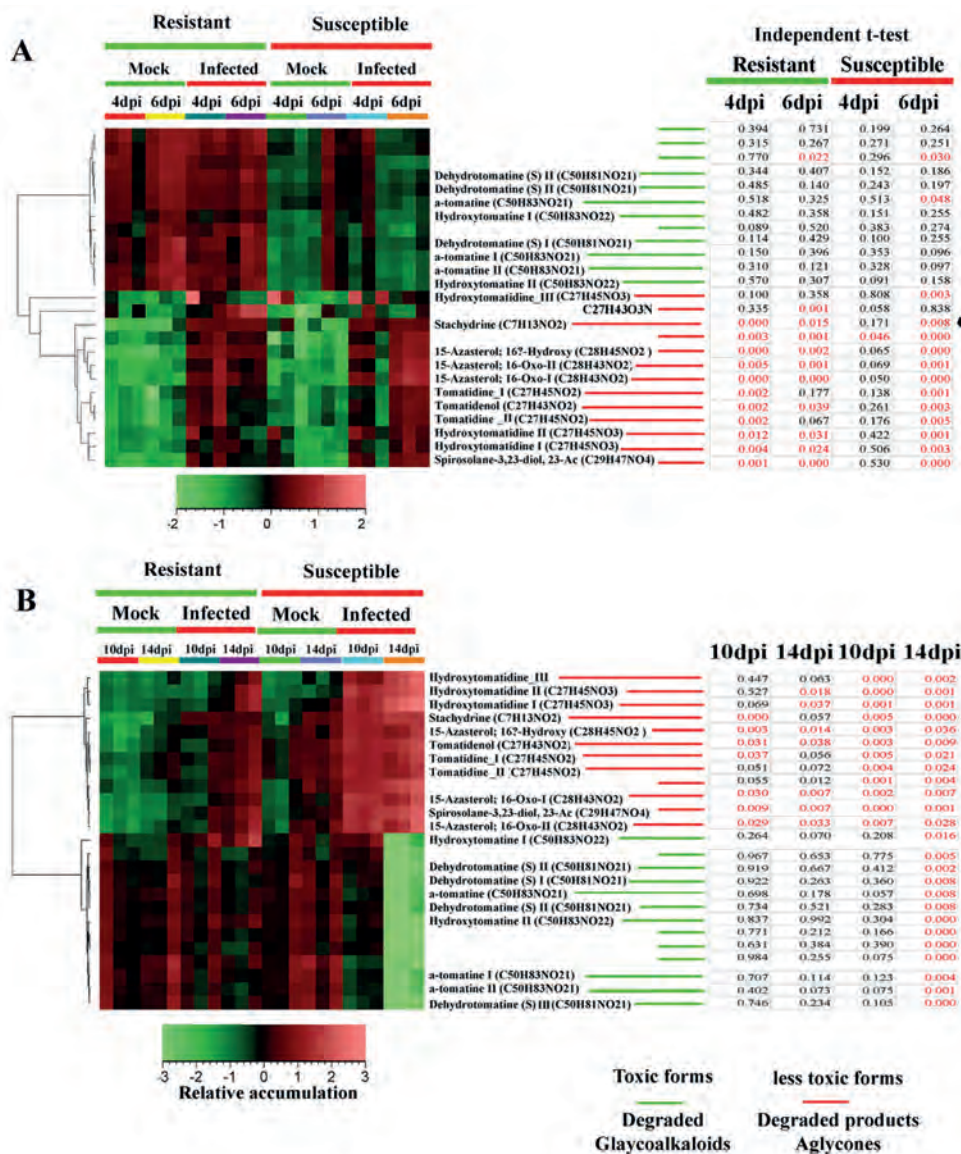
Supplementary Figure S2. Metabolites that show differential accumulation in tomato whole leaf extracts (WLTEs) obtained from plants inoculated with *C. fulvum*, as compared to the respective mock-treated plants. Samples were analysed by C18-LCMS in the positive ion mode.

(A) Significantly accumulating metabolites in tomato leaves in response to *C. fulvum* inoculation.

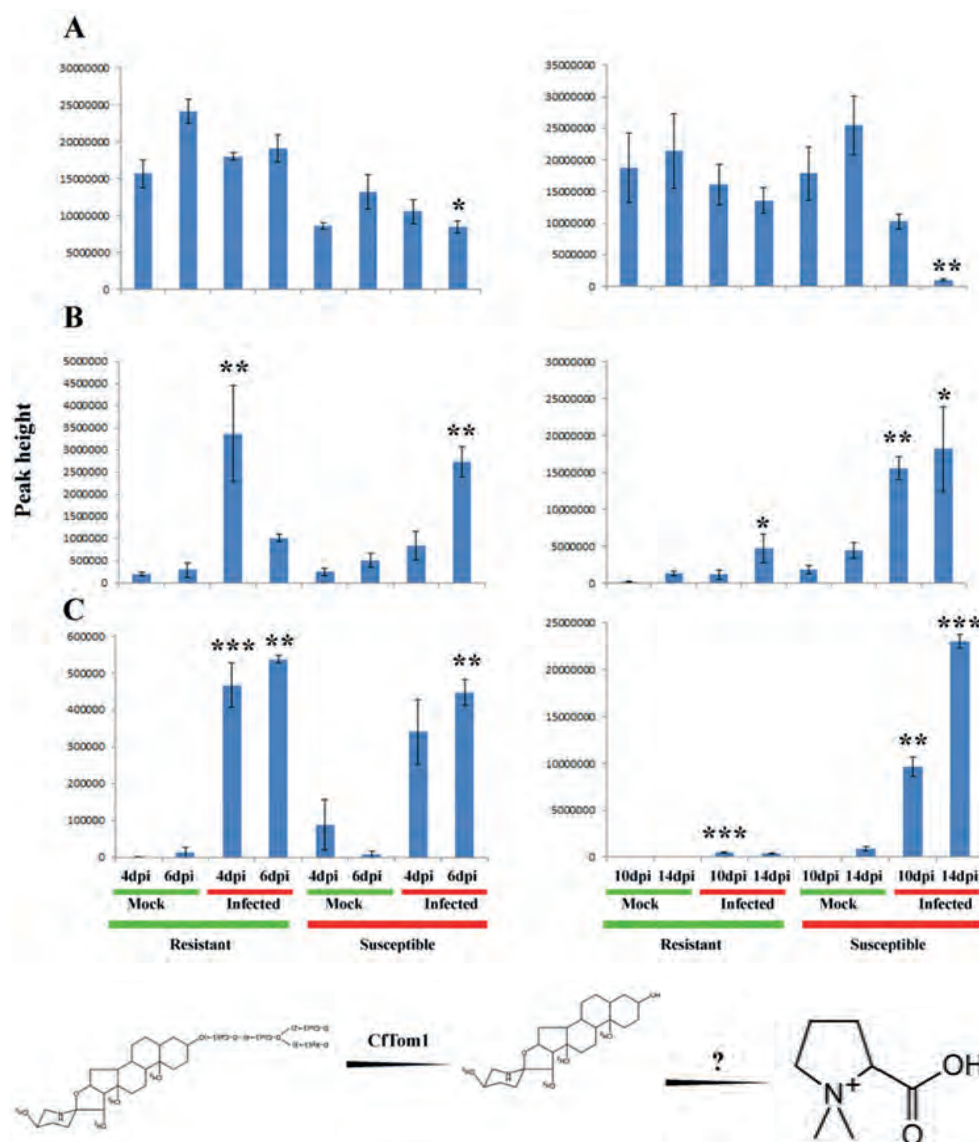
(B) Inoculation-associated changes in the profile of the $C_{18}H_{19}NO_5$ compound in the AF of resistant and susceptible plants.

(C) Chromatogram showing the elution profile of stachydrine ($C_7H_{13}NO_2$) in AF extract of susceptible plants 14dpi and from authentic standard.

(D) MS/MS spectrum of stachydrine ($C_7H_{13}NO_2$) from sample extract and stachydrine standard.



Supplementary Figure S3. Temporal dynamics of glycoalkaloids and their aglycones in the tomato leaf apoplast upon inoculation with *C. fulvum*. Each time point is represented by three independent biological repeats. **A** and **B** represent the early (4 and 6 dpi) and later (10 and 14 dpi) stages after inoculation, respectively. An independent t-test was computed by comparing inoculated plants with their respective controls at each time point. In the table, GAs and their aglycone derivatives of which the inoculation is significantly different between *C. fulvum*-inoculated and control samples at the specified time points, are marked in red.



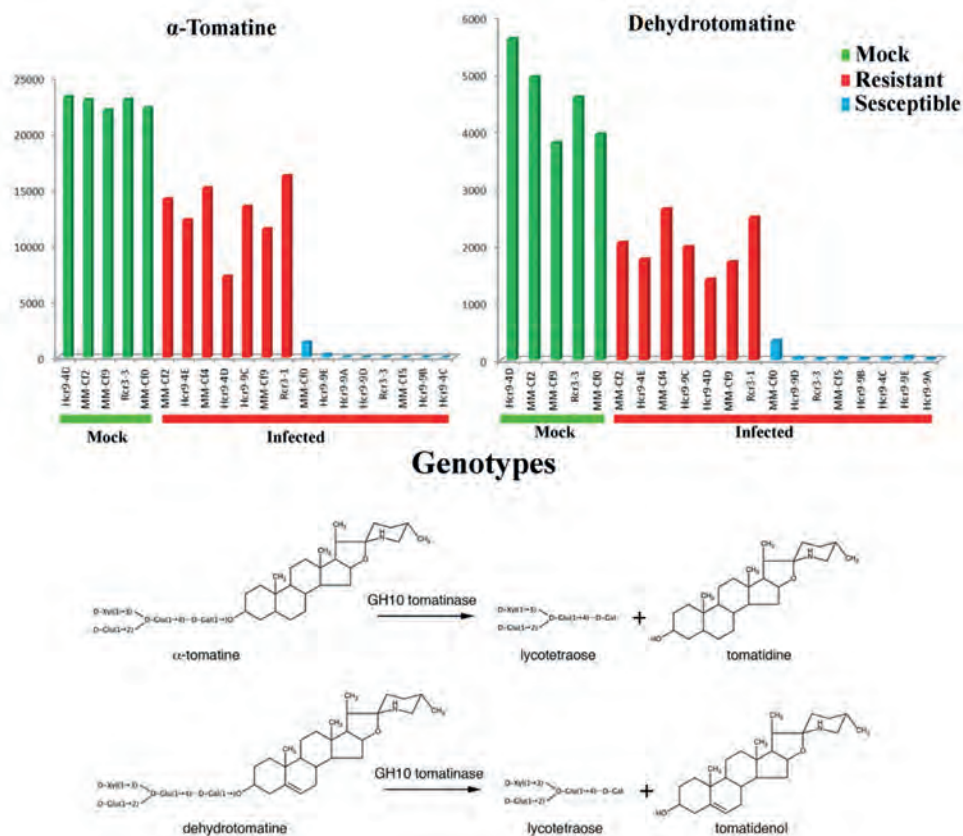
Supplementary Figure S4. Time-course of the dynamics of α -tomatine degradation. Panels on the left and on the right represent the temporal dynamics of α -tomatine and its degradation products at the early (4 and 6 dpi) and later (10 and 14 dpi) stages after inoculation of resistant and susceptible tomato plants with *C. fulvum* and in the mock-treated controls.

(A) Dynamics of α -tomatine accumulation.

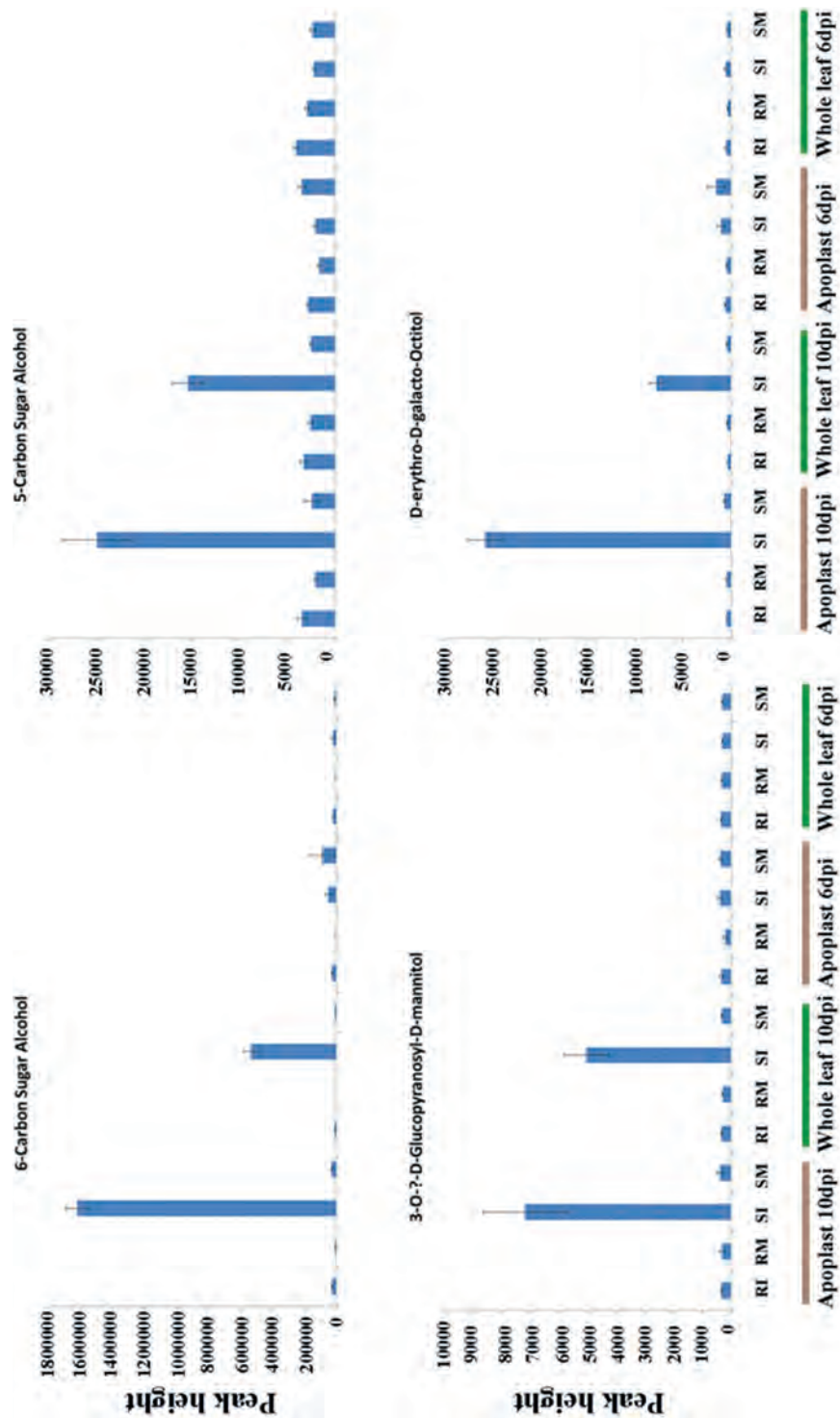
(B) Dynamics of tomatidine accumulation

(C) Dynamics of stachydrine ($C_7H_{13}NO_2$) accumulation. Stachydrine is a likely degradation product of tomatidine and other aglycones of GAs, accumulation during colonization of tomato leaflets by *C. fulvum*.

The identity of α -tomatine, tomatidine and stachydrine has been confirmed with authentic standards. Significant differences are indicated as (* $P < 0.05$; ** $P < 0.01$ and *** $P < 0.001$), when *C. fulvum*-inoculated plants are compared with the respective control at each time point.



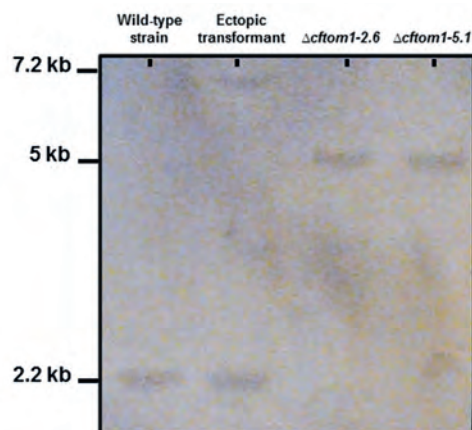
Supplementary Figure S5. Degradation of the two major glycoalkaloids (α -tomatine and dehydro-tomatine) in resistant and susceptible tomato genotypes, at 14 dpi with race 5 of *C. fulvum*. The *C. fulvum* GH10 tomatinase hydrolyses the lycotetraose from tomatine and dehydro-tomatine, resulting in the accumulation of the less toxic derivatives tomatidine and tomatidenol, respectively.



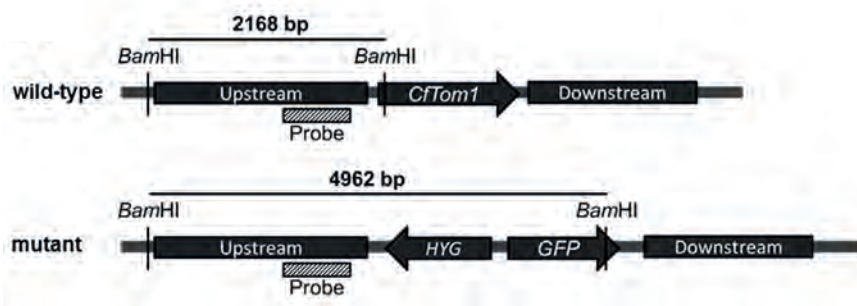
Supplementary Figure S6. LC (HILIC)-QTOF-MS profiles of sugar alcohols in the apoplastic fluids (AFs) and whole leaf tissue extracts (WLTEs) from tomato plants that were mock-treated or inoculated with *C. fulvum* at 6 and 10 dpi.

SM, susceptible, mock-treated; RM, resistant, mock-treated; SI, susceptible, *C. fulvum*-inoculated; RI, resistant, *C. fulvum*-inoculated.

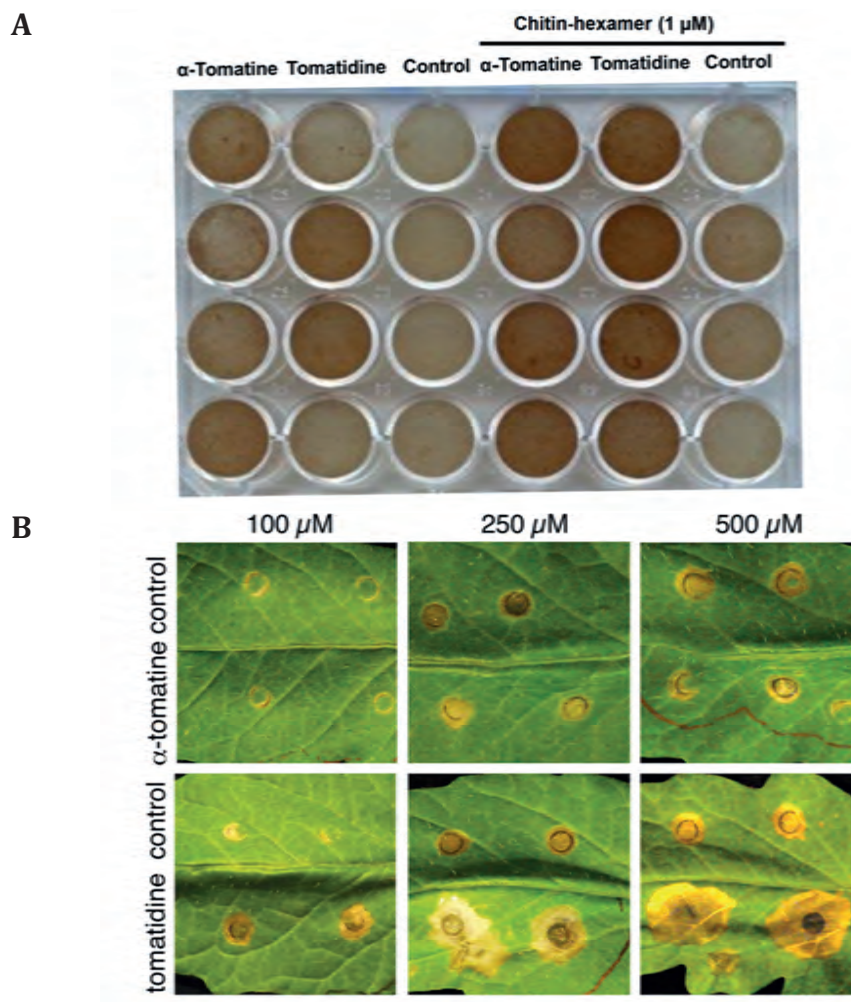
A



B



Supplementary Figure S7. Southern blot analysis of the $\Delta cfTom1$ mutants. (A) Targeted gene deletion of *C. fulvum CfTom1*. Genomic DNA preparations of wild-type *C. fulvum*, an ectopic transformant and two $\Delta cfTom1$ mutants were digested with *Bam*HI, the obtained fragments were separated on gel, blotted and hybridized with the indicated probe. (B) *Bam*HI restriction map of the *CfTom1* genomic region in wild-type and $\Delta cfTom1$ mutants. The *CfTom1*, *HYG* and *GFP* coding regions are shown as gray arrows indicating the orientation of the genes, while 5' and 3' flanking regions of *CfTom1* that are used for homologous recombination are shown as gray boxes.



Supplementary Figure S8. The phytotoxic effect of α -tomatine and tomatidine on tomato MSK8 cell suspensions and on tomato leaves.

(A) Effects of α -tomatine and tomatidine on H_2O_2 accumulation in MSK8 cell suspensions either treated with chitin or not.

(B) Phytotoxic effects of α -tomatine and tomatidine on tomato leaves. Tomato leaves were infiltrated with different concentrations of α -tomatine and tomatidine (100, 250 and 500 μ M) and with a control solution containing the same dilution series of methanol (10%, 5% and 2% v/v). Pictures were taken at 3 dpi.



Chapter 6

General Discussion

The *Cladosporium fulvum* - tomato interaction, a model for biological integration of multilayer information: a systems biology perspective



Technology meets biology in the systems-wide analysis of plant-microbe interactions

Systems biology and systems-wide studies in plant-microbe interactions

Although defining and labelling things is not what I like, it is tradition in science to give a definition to the subjects that we are dealing with. Hence, I searched the web for the definition of “systems biology”. Numerous definitions appeared and in some cases, for example, digging for its definition in a commentary of renowned systems biologist Marc W. Kirschner, entitled the “meaning of systems biology” (Kirschner, 2005)/, one can easily lose patience as it took him two pages to finally state that the explicit definition of systems biology should not come from him, but we should await the words of the first great modern systems biologist. Here, it is not my intention to take the reader to the end of this discussion to provide a brief definition of systems biology. Most of the definitions that have been proposed share a common view and I would like to mention the definition given by Athel Cornish-Bowden, who shared the same points of view with two other highly esteemed scientists, Hans Westerhoff and Denis Noble. He stated, and I quote: “Systems biology or systems thinking is beyond collecting of a huge amount of data, more than just moving from a focus on the elements of a system towards a focus on the interactions between them; it means seeking a vision of the system as a whole: not just its components, not just the connections between them, but a vision of how the whole system works” (Cornish-Bowden, 2011).

The other major hurdle of defining systems biology is that of the question: What is a system itself? Is it a cell, an organ, an organism, a species, a species and its functioning by itself and in combination with other species and/or its interaction with its environment? We could keep going on and on, with no sight of the horizon. However, the statement given about what a system is, by Francois Jacob is impressive and is worth mentioning, as he put forward: “Every object that biology studies is a system of systems” (Jacob, 1974).

As other emerging scientific fields, the infant research area of systems biology also faced fierce resistance from the scientific community. One of the most out-spoken critics of systems biology is the renowned scientist and Nobel laureate Sydney Brenner. In an interview in *Nature Molecular Cell Biology*, he described ~omics-assisted systems biology studies as “low-input, high-throughput, no-output biology” (Friedberg, 2008). According to Brenner, the claims of systems biology cannot be met, and a weaker version is just a new name for physiology. I personally do not want to put myself in the camp of Cornish-Bowden or Sydney Brenner. However, the humble statements given by Cornish-Bowden are remarkable and deserve to be appreciated by the scientific community (Cornish-Bowden, 2011). With great respect and appreciation for Sydney Brenner, both as a person and as a fellow scientist, with all due respect I do not agree with his point of view on systems biology.

Systems biology in fact is not more than a tool that has tremendous potential to contribute to our quest towards the understanding of life and existence, and the scientific community should realize that none of the specific scientific fields will bring the silver bullet to solve the challenges that our planet is facing. It is only the integration of systems and components of biology with physical, social and material sciences that could help us broaden our understanding of the mystery and complexity behind life and existence. The question therefore is not: Does systems or integrative biology work, or not? Rather, the question should be: How can we make it work? What are the most important technological and biological considerations? Here, I will propose some changes that to my opinion are required to make systems biology successful. This starts with a number of prerequisites before data are being generated, and an integration procedure is followed to ultimately obtain the general picture of the functioning of a system at the cellular level. To mention some: a robust biological system, a solid method to synchronically perturb the system, precise and temporal sampling and reliable sampling techniques, support by high-throughput technologies and most of all, the availability of integrative data mining bioinformatics-based methods. I will also put some emphasis on spatial sampling to show its potential contribution to systems biology studies, in the concluding remarks of the discussion.

The *Cladosporium fulvum*-tomato pathosystem: a versatile model for plant-microbe interaction studies

The *Cladosporium fulvum*-tomato interaction is a well-studied and versatile pathosystem that has significantly contributed to the expansion of our understanding of the molecular basis of plant-microbe interactions (de Wit, 1977; Joosten et al., 1997; van Esse et al., 2008; de Jonge et al., 2010; de Jonge et al., 2012; Sato et al., 2012; Etalo et al., 2013; Liebrand et al., 2013). The interaction can be divided into a compatible and an incompatible interaction between the pathogenic fungus and tomato, which is referring to the interaction of either susceptible or resistant tomato plants with *C. fulvum*, respectively (Joosten and de Wit, 1999; de Wit et al., 2009).

Any biological, within or among species, interaction involves alterations in the transcriptome, proteome and eventually the metabolome of the organisms that are involved. These terms are referring to the presence and abundance of (1) RNA transcripts, (2) proteins encoded by the genome and (3) small molecules in a system, respectively. Interestingly, however, it is not always straightforward to identify the cause of these alterations when the interaction involves more than one organism. This is mainly because various proteins and metabolites that originate from the interacting organisms will influence the rate of alteration of the global transcriptome, proteome and metabolome of the system, which in most cases includes both organisms during sampling. This problem is solved in the “dying seedlings” system used in my thesis,

in which defence-associated responses are induced in the absence of the fungus, by only introducing the avirulence factor (Avr) from the fungus into a resistant plant that expresses the matching *Cf* resistance gene. Under permissive conditions these seedlings undergo a synchronized and systemic defence response that leads to the induction of the hypersensitive response (HR) (Cai et al., 2001; de Jong et al., 2002; Stulemeijer et al., 2007; Etalo et al., 2013).

In **chapters 3 and 4** of this thesis we showed that at the transcriptome level, the dying seedlings reliably mimic the (local) response of resistant tomato plants to inoculation by *C. fulvum*. Hence, any changes in the transcriptome, proteome and metabolome can be directly linked to the activation of the defence response of the host plant upon recognition of the fungal avirulence factor (Stulemeijer et al., 2009; Etalo et al., 2013). In **chapter 2** of this thesis, a temporal study of such a synchronized and systemic response revealed the dynamic changes in a multitude of biological processes that are linked to signal perception and transduction, and the resulting defence response that is ultimately manifested by the massive reprogramming of the host metabolome (Etalo et al., 2013). For a comprehensive understanding of the molecular and metabolic alterations that occur during the interaction, we combined this highly robust “dying seedlings” system with state-of-the-art transcriptomics and metabolomics technologies.

The availability of these powerful technologies, together with the recent release of the full genome sequence of tomato (Sato et al., 2012) and *C. fulvum* (de Wit et al., 2012), renders the *C. fulvum*-tomato pathosystem an ideal model for systems biology studies. For example, *Avr5* (*C. fulvum* avirulence factor 5) has successfully been identified by comparing two RNA-seq data sets, both obtained from a compatible interaction between tomato and *C. fulvum* (Mesarich et al., unpublished data). One of the datasets was obtained by RNA-seq analysis of *Cf-0* tomato plants colonised by a race 5 of *C. fulvum*, which secretes all avirulence factors, except *Avr5* (we used this RNA-seq dataset in **chapters 3 and 4**). The other dataset was obtained by RNA-seq analysis of *Cf-0* plants that were colonised by a race 0 of *C. fulvum*, secreting all avirulence factors. A comparative analysis of all genes expressed by *C. fulvum*, eventually resulted in the identification of a specific transcript that was abundant in the RNA-seq dataset obtained from the race 0-inoculated *Cf-0* tomato plants, whereas this transcript was not present in the transcriptome of the *Cf-0* tomato plants that had been inoculated with race 5 of *C. fulvum*. Eventually, it was proven that this transcript indeed codes for the avirulence factor *Avr5* of *C. fulvum* (Mesarich et al., unpublished data). The success of this approach shows that parallel integration of RNA-seq data obtained from two highly complex biological systems that theoretically only differ in one gene, by using state-of-the-art bioinformatics, can sieve-out information from such complex datasets, a task comparable with finding a needle in a haystack.

Choice of ~omics technologies

~Omics technologies allow the exact and simultaneous quantitative monitoring of the abundance of thousands of genes, proteins and metabolites in a high-throughput way. It should be noted that no single ~omics analysis can fully unravel the complexity of the fundamental changes that occur during the progress of a plant-microbe interaction. Hence, the integration of multiple layers of information is not an alternative but rather an obligatory procedure if one wants to explore the interconnected real-time changes that take place when a system is perturbed. Hence, in this thesis we followed an integrated approach involving metabolomics and transcriptomics for a system-wide understanding of the interaction between tomato and *C. fulvum*.

Genome-wide transcriptome profiling technologies used in this study

At the start of the project, microarrays were the traditional and most widely used transcriptome profiling tools for systems-wide analysis of plant-microbe interactions (Maleck et al., 2000; Thilmony et al., 2006). In **chapter 2** of this thesis, we used data generated using the Affymetrix tomato genome array (a microarray that only contains about one third of all tomato genes), to elucidate the major HR-associated transcriptional alterations occurring in the dying seedlings. Recent advances in Next Generation Sequencing technologies and bioinformatics tools revolutionized the use of RNA-seq analysis in systems biology studies and we used this exciting technology to perform whole transcriptome profiling of the tomato-*C. fulvum* pathosystem (both the dying seedlings, as well as the compatible and incompatible interaction between tomato and the fungus). When the two technologies are compared, as expected the number of differentially regulated transcripts identified in the RNA-seq analysis was nearly five times higher than in the Affymetrix tomato genome array analysis (**Chapters 2 and 3**). This figure would have been much higher if we had not used highly stringent filtering criteria on the RNA-seq dataset. Nevertheless, this technology has provided a huge amount of information that was used in almost all chapters of this thesis to obtain insight into the complex and versatile regulatory mechanisms that are underlying the maintenance of the homeostasis of the system.

Metabolic profiling technologies used in this study

The output from the cellular integration of the transcriptome and proteome is the metabolome, which consists of chemically diverse small molecules and represents a functional readout of the cellular state (Joyce and Palsson, 2006). Bacteria, representing the simplest form of life, still produce at least 600 different metabolites, whereas for plants this is estimated to be more than 200,000 (Oldiges et al., 2007). Unlike the genome, the transcriptome and the proteome, capturing a representative part of the metabolome of a complex system requires a series of extraction, separation and detection techniques. We have used several metabolomics platforms that enabled us to monitor the dynamics of metabolites with a wide range of chemical and physical properties.

These metabolites include volatile organic compounds (VOCs) (identified by TD-GC-MS, **chapter 3**), semipolar metabolites (for which we employed C18-LC-MS and HILIC-LC-MS **chapters 2, 4 and 5**), polar and apolar metabolites (identified by GC-TOF-MS and HILIC-LC-MS, **chapters 2 and 5**). Here I want to mention some biologically important metabolic processes occurring in the tomato-*C. fulvum* interaction that were revealed by the use of these platforms. In **chapter 3** measurement of the VOCs showed the massive emission of α -copaene, a sesquiterpene, by the dying seedlings during mounting of the HR. Similarly, in **chapter 2** our discovery of the accumulation of aromatic amino acids (identified by GC-TOF-MS) and secondary metabolites that are derived from them (shown by LC-MS), was an important milestone in establishing a biological connection between datasets that had been obtained from various measurements. Furthermore, extraction of non-volatile compounds combined with HILIC-MS analysis showed important changes in the lipidome. The results from these complementary integrated platforms clearly showed how complex the defence metabolome is in tomato.

The Hypersensitive Response: a Cause or a Consequence of Host Defence? A systems perspective

It has been nearly a century since Elvin C Stakman's observation on black stem rust (*Puccinia graminis*) resulted in the establishment of the concept of the hypersensitive response (HR) of a resistant host plant to infection (Stakman, 1915). This response, which is considered to be one of the hallmarks of the immunity of plants to pathogens, involves a type of programmed cell death (PCD) and occurs at the site of pathogen entry, resulting in efficient containment of the pathogen (Lam et al., 2001). Since the formulation of the concept of the HR, the following question remained unanswered. Is the HR causal to disease resistance or is it a consequence of the defence response?

In **chapters 2, 3 and 4**, the multilayer information obtained by transcriptome and metabolome analysis suggested that the HR represents the final stage invoked by tomato plants to resist *C. fulvum* infection. In **chapter 2**, the observed metabolome reprogramming in the dying seedlings prior to the temperature shift that induces the HR, strongly suggests that the system is slightly leaky and that there is already an induction of the defence response, without the execution of the HR. Projection of the HR from the observed response in the dying seedlings suggests that the HR is most likely the consequence of the escalated signalling response at the site of infection. This escalated signalling results in massive reprogramming of the transcriptome and the metabolome, a highly carbon- and energy-demanding process (**Chapters 2 and 3**). In both chapters, the role of energy homeostasis during the HR was discussed. In conclusion, although the HR is often associated with induced defence, in line with a number of other reports, our results suggest that the HR is not causal for disease resistance (Kiraly et al., 1972; Lehnackers and Knogge, 1990; Goulden and Baulcombe, 1993; Jakobek and Lindgren,

1993; Hammond-Kosack and Jones, 1996; Schiffer et al., 1997; Bendahmane et al., 1999; Bulgarelli et al., 2010; Etalo et al., 2013).

In **chapter 2**, the combined metabolome and transcriptome analysis suggests that the HR potentially contributes to fuel the defence response by acting as a bio-recycler. In the dying seedlings, the massive up-regulation of genes involved in the final step of aromatic amino acid biosynthesis (**Chapter 2**), the accumulation of phenylalanine and tyrosine (**Chapter 2**), the accumulation of secondary metabolites that are derived from these aromatic amino acids and the activation of genes that are involved in their biosynthesis (**Chapter 2**) are examples of the profound changes that occur during mounting of the HR. On the other hand, the activation of a number of catabolic pathways that converge to produce acetyl-CoA (**Chapters 2 and 3**) and the massive up-regulation of genes involved in the cellular energetics (**Chapter 3**), are indicators of the role of the HR as a bio-recycler for the generation of energy and carbon skeletons to sustain the activation of the defence response.

Finally, my suggestion about the HR is that it should not be treated as a process having only one origin following predefined routes and playing a predefined role. The HR is simply the ultimate manifestation of various developmental- and stress-related responses. For example, in plants programmed cell death (PCD) plays a vital role in the differentiation of vascular bundles (Fukuda, 2000) and in the hypersensitivity response of plants to pathogens and cell death is induced even by PAMPs (Naito et al., 2008) and low temperature (Wolter et al., 1993). Hence, the attempts to put the HR in a box need rethinking by the scientific community. Refocussing from the final manifestation, which in this case is the HR, to the differences and similarities between the associated pathways in fact leading to the HR, will provide an important contribution to understanding the significance of the HR in a particular situation. Such comparative analysis contributes to the identification of the point where various stress signalling pathways converge to enforce the HR. Most importantly, in experiments that focus on the identification of genes important for plant defence, utilization of the HR as marker for induced defence responses has its limitations, as the activation of defence may not always end up with the HR. Altogether, our integrated analysis suggests that the HR is a highly controlled biological demolition process that takes place in parallel with biosynthetic processes, thus reaffirming that the HR does not only involve cellular degradation but requires active transcription to take place (He et al., 1994). In relation to this, regulatory mechanisms that underlie the plant defence response in general and the HR in particular will be discussed below.

Regulation of the defense transcriptome

Uncontrolled defense costs life

The absence of specialized immune cells imposes a tight control of the immune response of plants, as complete tissues are able to mount this response and can potentially undergo an HR. Furthermore, the allocation of energy and other resources has to be balanced between various biological processes, such as development and defence, and an efficient use of energy eventually determines the overall fitness and chances of survival of plants (Kliebenstein and Rowe, 2008; Denance et al., 2013; Neilson et al., 2013). Hence, any response to a perturbation of plant homeostasis should be accompanied by a fast switch to the appropriate gene transcription programme and suppression of other programmes to ensure an economic and efficient reaction. In **chapter 2** of this thesis we have shown the parallel transcriptional activation of genes associated with defence response activation and genes involved in its suppression, suggesting that a parallel and tight regulation is essential to keep the fine balance between plant defence and other biological processes, such as growth and development. Furthermore, in **chapter 4**, simultaneous virus-induced gene silencing (VIGS) of genes encoding defence repressor WRKY transcription factors (*SIWRKY-39/40/45/46*), resulted in constitutive defence activation at the expense of plant growth. All together, these results indicate that defence is costly and if uncontrolled, it could even cost life. Therefore, factors that are involved in the regulation of this response are essential for plant survival and are subject of study in systems biology (Moore et al., 2011; Etalo et al., 2013). Transcription factors, like the WRKYs, play an important role in the regulation of the defence transcriptome (Rushton and Somssich, 1998; Pozo et al., 2008; Rushton et al., 2010; Berr et al., 2012; Chang et al., 2013; Meng et al., 2013). **Chapter 4** of this thesis is exclusively dedicated to the functional characterization of these defence-related TFs.

The role of WRKY transcription factors in regulating the defence transcriptome and beyond

Guilt by Association (GBA); from a social perspective to systems biology

“Birds of a feather flock together” is a saying often used to express: “tell me your friends and I will tell you who you are”. Similarly, most of the data analyses involving ~omics-based datasets highly depend on the assumption that genes, proteins and metabolites that have similar expression or accumulation patterns across many samples, are regulated in the same way. This analogy is not accepted by most reductionists and it is also one of the seemingly weak points of systems biology that are mentioned by its fierce critic Sydney Brenner. In principle, it is obvious that correlation does not necessarily indicate a causal relationship. The confounding of direct and indirect associations is also

another setback for correlation-based inferences (Opgen-Rhein and Strimmer, 2007). Hence, any inference that is made based on correlation needs to be substantiated by additional analysis, including the targeting of the implicated components for example through the use of reverse genetics tools.

In **chapter 2**, the co-expression network analysis indicated a prominent role of WRKY transcription factors in the orchestration of the HR in tomato. Over-representation analysis of the promoter regions of clusters of genes that were all massively upregulated during mounting of the HR, indicated that there was a significantly high incidence of the W-box motif, which is a WRKY-binding domain, at 1kb upstream of the promoter region of these genes. Furthermore, in **chapter 3**, our RNA-seq analysis revealed that in the dying seedlings and in an incompatible interaction between tomato and *C. fulvum*, a large number of genes encoding WRKY transcription factors (TFs) showed up-regulation. Furthermore, a Wilcoxon rank sum test indicated that, as compared to other TFs, WRKYs are the most over-represented amongst the regulated genes, suggesting that WRKYs are the key regulators of the defence transcriptome in tomato plants. Based on results from our co-expression analyses, we targeted a number of genes encoding WRKY transcription factors using VIGS. We used a strategy of simultaneous gene silencing through the use of chimeric constructs aimed at targeting multiple genes encoding WRKY TFs that have functional redundancy (**Chapter 4**). This is a useful strategy for use in (crop) plant species, like tomato, for which there is no or less availability of mutants and T-DNA insertion lines. The VIGS analysis of several WRKY TFs confirmed their prominent role as both defence activators and repressors (**Chapter 4**). The constitutive defence activation, in combination with a dramatic reduction in growth of tomato plants targeted for *SIWRKY-39/40/45/46*, suggests that these TFs also play an important role in the regulation of the trade-off between defence and growth. Further system-based studies aimed at unravelling the exact targets of these transcription factors should further unravel the tomato WRKY defence network. In conclusion, based on the analysis of the dying seedlings and an incompatible and compatible interaction, WRKY TFs appear to act as key regulators of the defence response in tomato. These TFs have both positive and negative roles in the regulation of the two interconnected layers of plant innate immunity, which are PAMP-triggered immunity (PTI) and effector-triggered immunity (ETI), and have also been shown to strongly influence the defence metabolome of the host (**Chapters 2, 3 and 4**).

Envisioning the defence versus growth trade off, following a 'hypothetico-deductive' process

The traditional hypothesis generation is referred to as the 'hypothetico-deductive' process. First, it involves scientific expertise and imagination to formulate possible hypotheses and then the deductive consequences of these hypotheses are tested by

experiments (King et al., 2004). As I have already indicated in the initial statements of this General Discussion, the validity of systems biology should not be judged only based on its ability to provide conclusive information. As important as providing a holistic explanation of our scientific questions, systems biology plays an important role in the generation of new hypotheses. As expected, numerous hypotheses could be generated from our integrated analysis of the *C. fulvum*-tomato pathosystem. For example, **chapter 2** of this thesis provided the hypothesis for the work presented in **chapters 3** and **4**. These two chapters gave a broad insight into the significance of energy homeostasis and the need for a tight regulation of defence. Beyond broadening of our understanding of the energy homeostasis and its possible regulatory processes, these chapters further generated numerous questions that led to the formulation of additional systems-based hypotheses. One of these hypotheses deals with the growth/defence trade-off and the role of the circadian clock and the isoprenoid pathway in this.

The circadian clock and the isoprenoid pathway: at the cross roads of understanding growth/defence trade-off

In **chapter 2**, a time-dependent co-expression analysis of the dying seedlings and the parental control lines, revealed the presence of a cluster of genes with significant SORLIP4 (phytochrome A-regulated gene expression) motif enrichment in their promoter regions (Etalo et al., 2013). This cluster represents genes mostly associated with the circadian clock and light signalling in plants. Interestingly, in **chapter 3**, genes involved in the circadian clock were significantly down-regulated during mounting of the HR. Furthermore, in the dying seedlings all eight differentially regulated genes encoding TCP transcription factors, which are involved in development, were found to be down regulated (**Chapter 3**) and the major pathways that are involved in the regulation of differentiation and growth were also suppressed during mounting of the HR (**Figure 1**). The activity of TCP TFs is postulated to be related to the control of growth and development, providing a mechanism to link the circadian clock with hormonal, environmental (light, temperature, stress conditions) and nutritional/metabolic stress (Harmer, 2009; Pruneda-Paz and Kay, 2010).

Based on these observations, I propose an unknown factor-1 “UF1” as crucial regulator, which is induced upon pathogen-associated molecular pattern (PAMP) or pathogen avirulence factor perception. UF1 represses the activity of TCP transcription factors, resulting in the repression of the circadian clock. The suppression of the circadian clock in turn represses the MEP/DOXP pathway and the production of growth hormones derived from this pathway (such as cytokinins, gibberellic acid and strigolactones) (Dudareva et al., 2005) (**Figure 1**). Furthermore, the circadian clock is reported to regulate auxin biosynthesis, transport and signalling (Covington and Harmer, 2007) and our transcriptome data also showed that the genes involved in nearly every step of the auxin-signalling pathway, from its biosynthesis to the actual auxin-triggered response,

were down-regulated (**Chapter 3**). Although there is activation of the MVA pathway, our RNA-seq analysis indicated that the steroid- and brassinosteroid- pathways were suppressed (**Chapter 3**). Altogether, this coordinated repression of anabolic processes, like photosynthesis and energy-consuming growth- and development-related processes, in combination with the induction of energy-conserving and -generating catabolic processes, replenishes the cellular energy levels to fuel defence at the expense of growth.

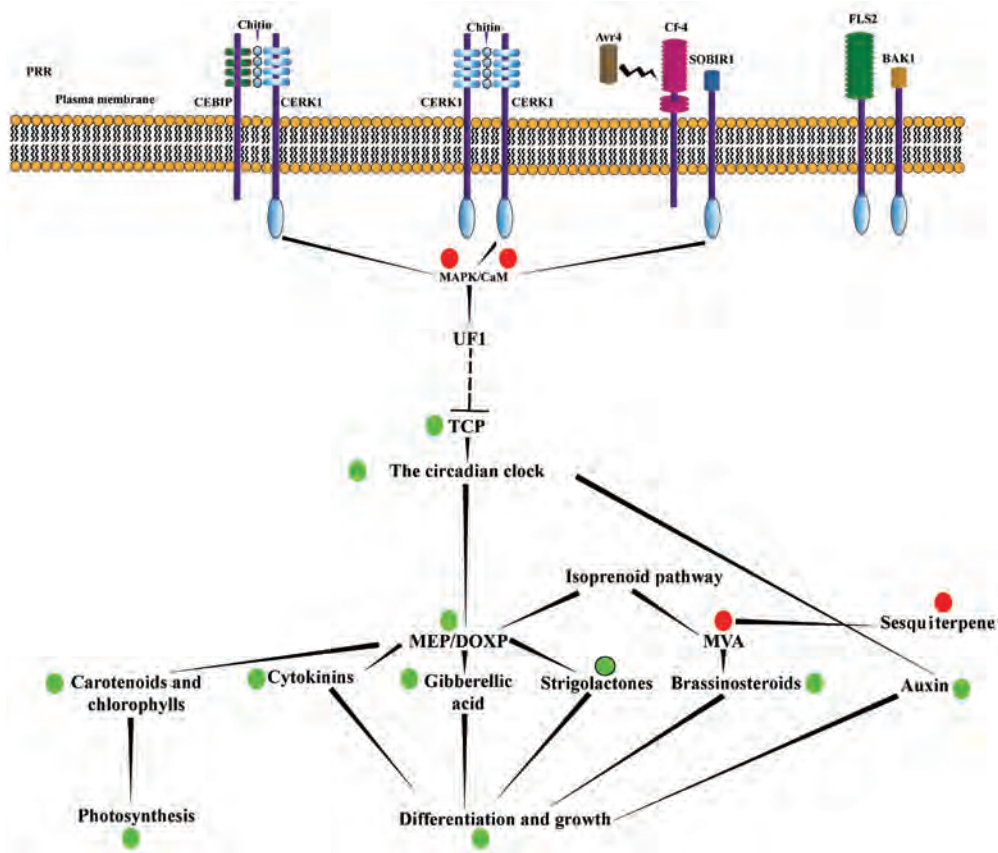


Figure 1. Proposed model for growth/defence trade-off in plant-microbe interactions.

The green and red dots indicate respectively down- and up-regulation of genes involved in the indicated biological processes. “Unknown factor-1” (UF1) is proposed to be induced upon pathogen perception and acts as suppressor(s) of TCP TFs, resulting in the repression of the circadian rhythm.

CEBIP (chitin elicitor-binding protein) and CERK (chitin elicitor receptor kinase) are involved in perception of the pathogen-associated molecular pattern (PAMP) chitin (Petutschnig et al., 2010; Kouzai et al., 2014), whereas FLS2 (flagellin-sensing-2) and BAK1 (BRI1-associated kinase-1) mediate perception of the PAMP flagellin (Gómez-Gómez and Boller, 2000; Lu et al., 2010). The receptor-like kinase SOBIR1 (Suppressor of BIR1-1) was recently shown to be required for triggering defence responses upon perception of Avr4 by the Cf-4 resistance protein (Liebrand et al., 2013).

Piriformospora indica is a mutualistic fungus that colonizes a broad range of mono- and dicotyledonous plants. Recently, using systems biology approaches, the deployment of an “inverse” strategy by the fungus to manipulate barley innate immunity during colonization of the roots has been shown (Schafer et al., 2009). In this study, a stage-specific upregulation of genes involved in the metabolism of phytohormones, mainly encompassing gibberellin, brassinosteroids, auxin and abscisic acid is shown, whereas interestingly, salicylic acid (SA)-associated gene expression was suppressed. Further genetic studies showed a reduced fungal colonization of mutants that are impaired in gibberellin synthesis as well as in its perception (Schafer et al., 2009). Overall, these results show that the isoprenoid pathway forms the backbone of the plant defence signalling pathway and therefore is a potential target for fungi with mutualistic association with the plant. Hence, the circadian clock and isoprenoid pathway should be the focus of studies that aim to unravel the mystery behind the trade-off between growth and plant immune responses. Furthermore, it will be interesting to determine which effectors of pathogens are targeting these pathways.

Metabolomics: the revival of the interest in the role of small molecules in plant-microbe interactions

Metabolomics as a tool for the discovery of novel biomarkers for resistance and susceptibility of plants to pathogens

Chapter 5 of this thesis demonstrates the power of metabolomics for the elucidation of the (bio) chemical changes that are taking place upon successful colonization of the host by a pathogen on the one hand and successful activation of the plant defense response on the other. The degradation of a number of antimicrobial glycoalkaloids (α -tomatine, dehydrotomatine and hydroxytomatine), sulpholipids (sulfoquinovosyl diacylglycerols; SQDGs), in combination with the accumulation of the sugar alcohols mannitol and xylitol and the phosphatidylserine (PS) 38:3, can be considered as indicators of susceptibility. On the other hand, the early accumulation of specific phospholipids (PSs, PEs and PIs) (**Chapter 5**) and the production of hydroxycinnamic acid amides (**Chapter 2**) are indicators of induced defense responses. In my study, the metabolomics work has revealed novel metabolites associated with susceptibility. One of these is the partially characterized fatty acid, amino acid-conjugated compound (FAC), hydroxyphenylglycinoyl alkyl glycine, of which the predicted structure, obtained by MS/MS analysis, is shown in **Figure 2A**. This compound is only detected in the leaf apoplast originating from compatible interactions at the later stages of colonization (10-14 days post inoculation), while analysis of the dying seedlings showed that the compound is not part of the plant-induced defense response. In the same way, the analysis of *in vitro* grown mycelium of *C. fulvum* showed that the metabolite is not constitutively present in the fungus. Hence, we can conclude that the compound is produced by *C. fulvum*, but only upon successful colonization of the leaves of tomato (**Figure 2B**).

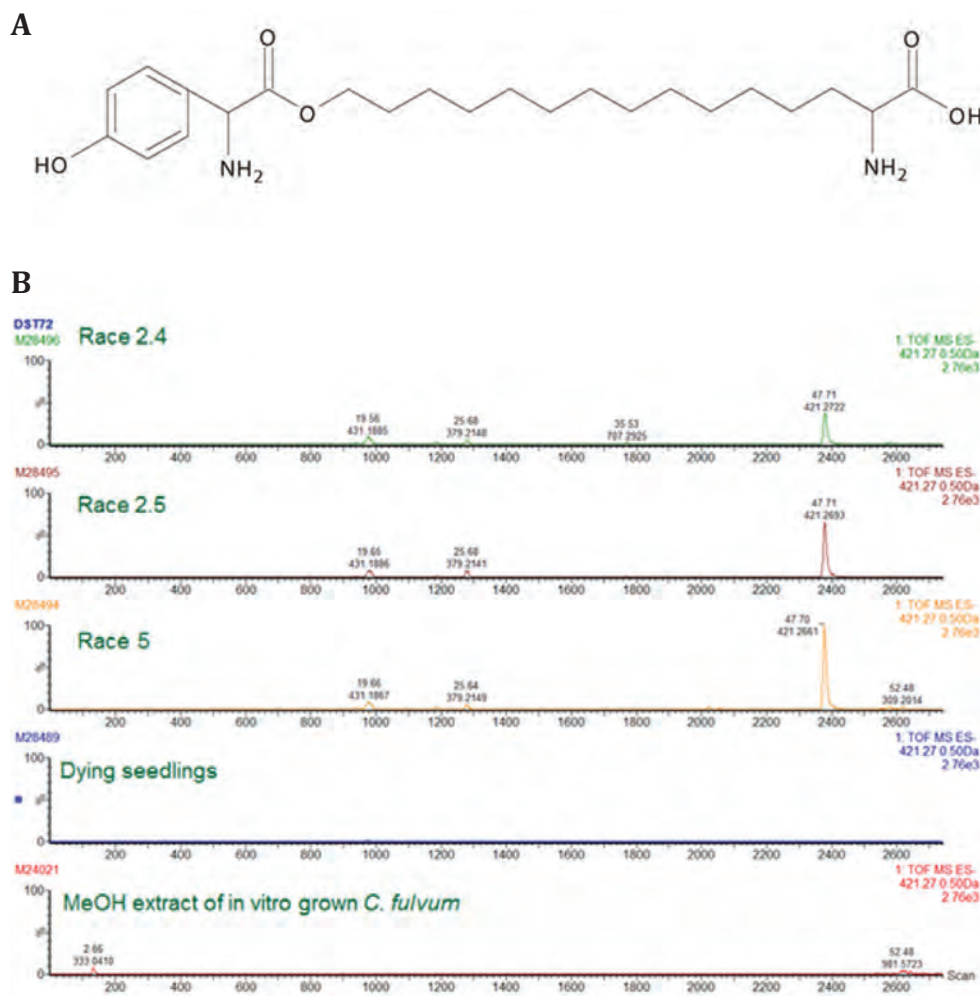


Figure 2. Hydroxyphenylglycinoyl alkyl glycine, a novel metabolite specific to a compatible interaction between tomato and *C. fulvum*.

(A) Predicted structure of hydroxyphenylglycinoyl alkyl glycine.

(B) LC-MS analysis of the abundance of hydroxyphenylglycinoyl alkyl glycine, in compatible interactions of tomato with races 2.4, 2.5 and 5 of *C. fulvum*, in the dying seedlings and in a MeOH extract of *in vitro*-grown *C. fulvum*.

Fatty acid amino acid conjugates have been shown to be implicated in the induction of jasmonic acid (JA) signaling and one of the classical examples is volicitin, a molecule present in the oral secretion of the armyworm. Upon recognition by the plant, volicitin induces JA-signalling that results in the activation of direct defence (such as the formation of protease inhibitors) and the release of a range of volatiles by the attacked plant that recruit the natural enemy of the armyworm (Schmelz et al., 2003). Several reports showed that JA

and SA have an antagonistic relationship in the defense response of plants (Niki et al., 1998; Thaler et al., 2002; Takahashi et al., 2004; Thaler et al., 2012). This suggests that the hydroxyphenylglycinoyl alkyl glycine that is produced by *C. fulvum* may suppress tomato SA-triggered defense signaling through the activation of JA-signalling. A similar strategy is employed by pathogenic strains of the bacterium *Pseudomonas syringae*, as these use the JA mimic coronatine to suppress host SA signaling (Katsir et al., 2008). In contrast, the necrotrophic pathogen *Botrytis cinerea* exploits this antagonism by secreting SA, thereby inducing exopolysaccharide formation, as a strategy to facilitate disease development (El Oirdi et al., 2011). Such mechanisms are part of the ongoing arms race between plants and microbes. Although quite some effort and time was spent on the purification of this compound by preparative and analytical LCMS, unfortunately, we were so far unable to obtain sufficient pure material for unambiguous structure elucidation by NMR.

C. fulvum-mediated degradation of glycoalkaloids: phytochemical detoxification and nutrient generation

One of the proposed roles of secondary metabolites in plants is that they allow resources to be temporarily stored as defensive compounds and, upon demand, be remobilized and reallocated to growth and development (Neilson et al., 2013). The sequestration of any free amino acids, sugars, or other nutrients that are not immediately required for growth and development in an unpalatable form, effectively lowers the nutritional value of the plant tissues while at the same time enhancing chemical defense (Lieberei et al., 1985; Selmar et al., 1988; Rosenthal, 1990; Selmar, 1993; Augner, 1995; Kongsawadworakul et al., 2009). In tomato fruit ripening glycoalkaloids showed a drastic reduction in abundance with subsequent accumulation of the aglycones, suggesting that turnover of GAs is also part of the regular carbon and nitrogen sequestration/recycling in plants in the absence of pathogenic micro-organisms (Eltayeb and Roddick, 1985; Kozukue and Friedman, 2003; Kozukue et al., 2004). In **chapter 5** I show that *C. fulvum* has hijacked this mechanisms of nutrient sequestration/recycling as it hydrolyzes most of the GAs that are present in tomato leaves, and are toxic to the fungus, into nitrogen-containing aglycones and carbon-rich lycotetraose (Okmen et al., 2013).

The concentration of α -tomatine in tomato leaves can reach levels as high as 1 mM, and that is assuming uniform distribution over all cells (Arneson and Durbin, 1967). Such an abundant nitrogen- and carbon-rich secondary metabolite would be a good nutrient source for pathogens if they would be able to overcome its toxicity. Indeed, *C. fulvum* is able to hydrolyze GAs into their harmless aglycones and lycotetraose. The final fate of these derivatives was so far unknown. In **chapter 5**, I propose stachydrine as the most likely degradation product of the GAs. Like sugar alcohols, stachydrine has been reported to have antioxidant activity and play a role in osmo-protection (**Figure 3**). Fungal infection also results in the formation of the osmo-protectant sugar alcohols, manitol and xylitol, suggesting that the formation of such protecting, energy-rich molecules is a common strategy of fungi (Amin et al., 1995; McNeil et al., 1999; Shen et al., 1999; Clark

et al., 2003; Friedberg, 2008). Further studies, which should for example utilize ^{14}C - and ^{15}N -labeled α -tomatine, may help to elucidate the fate of both the lycotetraose and the aglycon part of α -tomatine. Furthermore, comparative and integrative studies involving genomics, transcriptomics and metabolomics, of the degradation pathway of GAs during tomato fruit ripening and during the establishment of a biotrophic relationship between tomato and *C. fulvum* should shed light on the common genes involved, and metabolite intermediates produced, during GA turnover in the presence and absence of the fungus. Such studies will be powered by the recently released tomato (Sato et al., 2012) and *C. fulvum* (de Wit et al., 2012) genome sequences.

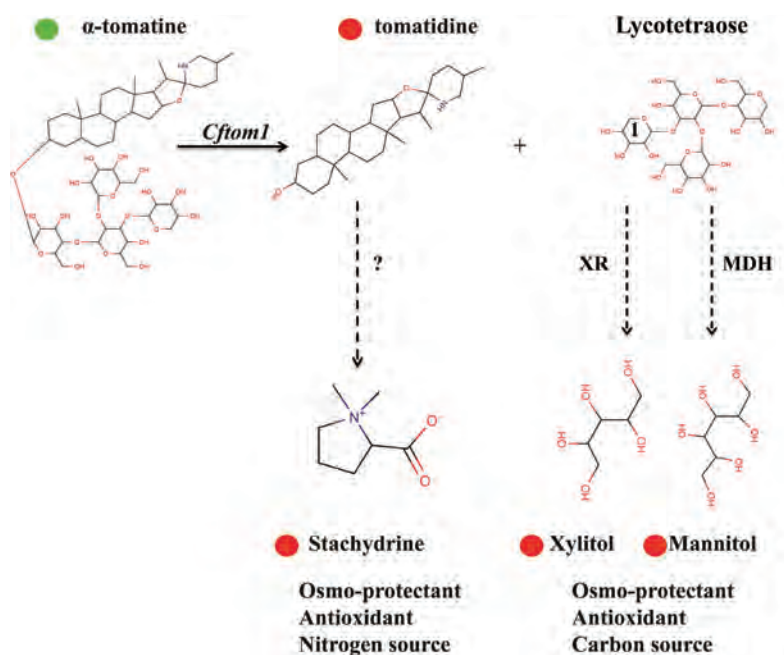


Figure 3. Proposed strategy used by *C. fulvum* to detoxify anti-microbial phytochemicals and produce carbon- and nitrogen-containing multipurpose metabolites upon establishment of a biotrophic relationship with tomato. Green and red dots indicate the degradation and accumulation, respectively, of the corresponding metabolites during a compatible interaction between tomato and *C. fulvum*. In the structure of lycotetraose, xylose is marked with a "1" and proposed to be converted to xylitol by xylose reductase (XR), whereas the six-carbon sugars are proposed to be converted to mannitol by mannitol dehydrogenase (MDH). *Cftom1* refers to the gene encoding *C. fulvum* tomatinase-1, which is the enzyme that converts α -tomatine into its non-antimicrobial aglycone tomatidine.

Concluding remarks

This thesis reflects the power of integrative systems biology for the elucidation of the molecular mechanisms underpinning host resistance and the subsequent countermeasures taken by the pathogen during the establishment of a biotrophic relationship. The availability of transcriptome and metabolome data on a range of samples enabled us to identify many important components of the host defense response. The remarkable correlations between primary and secondary metabolites, lipids and plant hormones (SA and ethylene) on the one hand, and the regulation of genes involved in the biosynthesis and signaling of these small molecules, on the other, suggests that the different technological platforms can now take us to the point of biological integration. Further advances can be made through statistical integration of the multilayer information, for example through combined gene expression-metabolic networks, which could help with gene function prediction and metabolite identification. It should be noted, though, that for such an approach large numbers of samples of different plant-fungal genotype combinations sampled over time are needed, in order to obtain sufficient statistical power in the correlation analysis. Furthermore, the success of statistical and biological integration is vital for developing mathematical models to describe the system dynamics. Such models will give leads for “fluxomics” studies (Winter and Kromer, 2013) and will create a bridge between systems and synthetic biology.

To obtain a high level of integration between the various systems, local sampling and sampling technologies will play an increasingly important role. The results obtained using the dying seedlings and the apoplastic metabolome reflect the power of local sampling. Further utilization of laser micro-dissection technologies for the highly localized sampling of tissues for transcriptome and metabolome analysis, will make a paramount contribution to the generation of high quality data for integration. Another important area is to obtain knowledge on the exact cellular localization of metabolites at the infection sites. For that, *in situ* MS technologies with high spatial resolution, such as Laser Ablation Electro Spray Ionization (LAESI), will provide the metabolome read out of a tissue at around 200µm (10-15 plant cells) resolution (Nemes et al., 2010; Rubakhin et al., 2010). These technological advances will allow us to capture the biological changes at the tissue and cellular level. The next challenge will be to understand a living system at the level of cellular compartmentalization of biological processes, a daunting challenge for systems biology for the coming decades. However, looking back to the technological advances that we made during the past 5 decades, I would say that although it is not easy, it will not be impossible to ultimately capture the real sense of cellular networking.

References

- Amin U, Lash T, Wilkinson B (1995) Proline betaine is a highly effective osmoprotectant for *Staphylococcus aureus*. *Arch Microbiol* **163**: 138-142
- Arneson PA, Durbin RD (1967) Hydrolysis of tomatine by *Septoria lycopersici* - a detoxification mechanism. *Phytopathology* **57**: 1358-1360
- Augner M (1995) Low nutritive quality as a plant defence: Effects of herbivore-mediated interactions. *Evol Ecol* **9**: 605-616
- Bendahmane A, Kanyuka K, Baulcombe DC (1999) The Rx gene from potato controls separate virus resistance and cell death responses. *Plant Cell* **11**: 781-791
- Berr A, Menard R, Heitz T, Shen WH (2012) Chromatin modification and remodelling: a regulatory landscape for the control of Arabidopsis defence responses upon pathogen attack. *Cell Microbiol* **14**: 829-839
- Bulgarelli D, Biselli C, Collins NC, Consonni G, Stanca AM, Schulze-Lefert P, Vale G (2010) The CC-NB-LRR-type Rdg2a resistance gene confers immunity to the seed-borne barley leaf stripe pathogen in the absence of hypersensitive cell death. *PLoS One* **5**
- Cai XZ, Takken FLW, Joosten MHAI, De Wit PJGM (2001) Specific recognition of AVR4 and AVR9 results in distinct patterns of hypersensitive cell death in tomato, but similar patterns of defence-related gene expression. *Mol Plant Pathol* **2**: 77-86
- Chang C, Yu D, Jiao J, Jing S, Schulze-Lefert P, Shen QH (2013) Barley MLA immune receptors directly interfere with antagonistically acting transcription factors to initiate disease resistance signaling. *Plant Cell* **25**: 1158-1173
- Clark AJ, Blissett KJ, Oliver RP (2003) Investigating the role of polyols in *Cladosporium fulvum* during growth under hyper-osmotic stress and in planta. *Planta* **216**: 614-619
- Cornish-Bowden A (2011) Systems biology. How far has it come. *Biochemist* **33**: 16-18
- Covington MF, Harmer SL (2007) The circadian clock regulates auxin signaling and responses in Arabidopsis. *PLoS Biol* **5**: e222
- de Jong CF, Takken FLW, Cai XH, de Wit PJGM, Joosten MHAI (2002) Attenuation of Cf-mediated defense responses at elevated temperatures correlates with a decrease in elicitor-binding sites. *Mol Plant Microbe Interact* **15**: 1040-1049
- de Jonge R, van Esse HP, Kombrink A, Shinya T, Desaki Y, Bours R, van der Krol S, Shibuya N, Joosten MH, Thomma BP (2010) Conserved fungal LysM effector Ecp6 prevents chitin-triggered immunity in plants. *Science* **329**: 953-955
- de Jonge R, van Esse HP, Maruthachalam K, Bolton MD, Santhanam P, Saber MK, Zhang Z, Usami T, Lievens B, Subbarao KV, Thomma BPHJ (2012) Tomato immune receptor Ve1 recognizes effector of multiple fungal pathogens uncovered by genome and RNA sequencing. *P Natl Acad Sci USA* **109**: 5110-5115
- de Wit PGM (1977) A light and scanning-electron microscopic study of infection of tomato plants by virulent and avirulent races of *Cladosporium fulvum*. **83**: 109-122
- de Wit PJGM, van der Burgt A, Okmen B, Stergiopoulos I, Abd-Elsalam KA, Aerts AL, Bahkali AH, Beenen HG, Chettri P, Cox MP, Datema E, de Vries RP, Dhillon B, Ganley AR, Griffiths SA, Guo YA, Hamelin RC, Henrissat B, Kabir MS, Jashni MK, Kema G, Klaubauf S, Lapidus A, Levasseur A, Lindquist E, Mehrabi R, Ohm RA, Owen TJ, Salamov A, Schwelm A, Schijlen E, Sun H, van den Burg HA, van Ham RCHJ, Zhang SG, Goodwin SB, Grigoriev IV, Collemare J, Bradshaw RE (2012) The genomes of the fungal plant pathogens *Cladosporium fulvum* and *Dothistroma septosporium* reveal adaptation to different hosts and lifestyles but also signatures of common ancestry. *Plos Genet* **8**: 1-22
- de Wit PJGMd, Joosten MHAI, Thomma BPHJ, Stergiopoulos I (2009) Gene for gene models and beyond: the *Cladosporium fulvum*-tomato pathosystem. In *Plant Relationships*. Springer, Berlin Heidelberg, pp 135-156
- Denance N, Sanchez-Vallet A, Goffner D, Molina A (2013) Disease resistance or growth: the role of plant hormones in balancing immune responses and fitness costs. *Front Plant Sci* **4**: 155
- Dudareva N, Andersson S, Orlova I, Gatto N, Reichelt M, Rhodes D, Boland W, Gershenzon J (2005) The nonmevalonate pathway supports both monoterpenes and sesquiterpene formation in snapdragon flowers. *Proc Natl Acad Sci USA* **102**: 933-938
- El Oirdi M, El Rahman TA, Rigano L, El Hadrami A, Rodriguez MC, Daayf F, Vojnov A, Bouarab K (2011) *Botrytis cinerea* manipulates the antagonistic effects between immune pathways to promote disease development in tomato. *Plant cell* **23**: 2405-2421
- Eltayeb EA, Roddick JG (1985) Biosynthesis and degradation of alpha-tomatine in developing tomato fruits. *Phytochemistry* **24**: 253-257

- Etalo DW, Stulemeijer IJ, van Esse HP, de Vos RC, Bouwmeester HJ, Joosten MAHJ** (2013) System-wide hypersensitive response-associated transcriptome and metabolome reprogramming in tomato. *Plant Physiol* **162**: 1599-1617
- Friedberg EC** (2008) Sydney Brenner. *Nat Rev Mol Cell Biol* **9**: 8-9
- Fukuda H** (2000) Programmed cell death of tracheary elements as a paradigm in plants. *Plant Mol Biol* **44**: 245-253
- Gómez-Gómez L, Boller T** (2000) FLS2: An LRR Receptor-like Kinase Involved in the Perception of the Bacterial Elicitor Flagellin in Arabidopsis. *Mol Cell* **5**: 1003-1011
- Goulden MG, Baulcombe DC** (1993) Functionally homologous host components recognize potato virus X in *Gomphrena globosa* and potato. *Plant Cell* **5**: 921-930
- Hammond-Kosack KE, Jones JD** (1996) Resistance gene-dependent plant defense responses. *Plant Cell* **8**: 1773-1791
- Harmer SL** (2009) The circadian system in higher plants. *Annu Rev Plant Biol* **60**: 357-377
- He SY, Bauer DW, Collmer A, Beer SV** (1994) Hypersensitive response elicited by *Erwinia amylovora* harpin requires active-plant metabolism. *Mol Plant Microbe Interact* **7**: 289-292
- Jacob F** (1974) The logic of living systems. London: Allen Lane
- Jakobek JL, Lindgren PB** (1993) Generalized induction of defense responses in bean is not correlated with the induction of the hypersensitive reaction. *Plant Cell* **5**: 49-56
- Joosten MAHJ, de Wit PJGM** (1999) The tomato-*Cladosporium fulvum* interaction : A versatile experimental system to study plant-pathogen interactions. *Annu Rev Phytopathol* **37**: 335-367
- Joosten MAHJ, Vogelsang R, Cozijnsen TJ, Verberne MC, DeWit PJGM** (1997) The biotrophic fungus *Cladosporium fulvum* circumvents Cf-4-mediated resistance by producing unstable AVR4 elicitors. *Plant Cell* **9**: 367-379
- Joyce AR, Palsson BO** (2006) The model organism as a system: integrating 'omics' data sets. *Nat Rev Mol Cell Bio* **7**: 198-210
- Katsir L, Schilmiller AL, Staswick PE, He SY, Howe GA** (2008) COI1 is a critical component of a receptor for jasmonate and the bacterial virulence factor coronatine. *P Natl Acad Sci USA* **105**: 7100-7105
- King RD, Whelan KE, Jones FM, Reiser PGK, Bryant CH, Muggleton SH, Kell DB, Oliver SG** (2004) Functional genomic hypothesis generation and experimentation by a robot scientist. *Nature* **427**: 247-252
- Kiraly Z, Barna B, Ersek T** (1972) Hypersensitivity as a consequence, not cause, of plant resistance to infection. *Nature* **239**: 456-&
- Kirschner MW** (2005) The meaning of systems biology. *Cell* **121**: 503-504
- Kliebenstein DJ, Rowe HC** (2008) Ecological costs of biotrophic versus necrotrophic pathogen resistance, the hypersensitive response and signal transduction. *Plant Sci* **174**: 551-556
- Kongsawadworakul P, Viboonjun U, Romruensukharom P, Chantuma P, Ruderman S, Chrestin H** (2009) The leaf, inner bark and latex cyanide potential of *Hevea brasiliensis*: Evidence for involvement of cyanogenic glucosides in rubber yield. *Phytochemistry* **70**: 730-739
- Kouzai Y, Nakajima K, Hayafune M, Ozawa K, Kaku H, Shibuya N, Minami E, Nishizawa Y** (2014) CEBiP is the major chitin oligomer-binding protein in rice and plays a main role in the perception of chitin oligomers. *Plant Mol Biol* **84**: 519-528
- Kozukue N, Friedman M** (2003) Tomatine, chlorophyll, β -carotene and lycopene content in tomatoes during growth and maturation. *J Sci Food Agric* **83**: 195-200
- Kozukue N, Han JS, Lee KR, Friedman M** (2004) Dehydrotomatine and alpha-tomatine content in tomato fruits and vegetative plant tissues. *J Agr Food Chem* **52**: 2079-2083
- Lehnackers H, Knogge W** (1990) Cytological studies on the infection of barley cultivars with known resistance genotypes by *Rhynchosporium-Secalis*. *Can J Bot* **68**: 1953-1961
- Lieberrei R, Selmar D, Biehl B** (1985) Metabolization of Cyanogenic Glucosides in *Hevea-Brasiliensis*. *Plant Syst Evol* **150**: 49-63
- Liebrand TWH, van den Berg GCM, Zhang Z, Smit P, Cordewener JHG, America AHP, Sklenar J, Jones AME, Tameling WIL, Robatzek S, Thomma BPHJ, Joosten MAHJ** (2013) Receptor-like kinase SOBIR1/EVR interacts with receptor-like proteins in plant immunity against fungal infection. *P Natl Acad Sci USA* **110**: 13228-13228
- Lu D, Wu S, Gao X, Zhang Y, Shan L, He P** (2010) A receptor-like cytoplasmic kinase, BIK1, associates with a flagellin receptor complex to initiate plant innate immunity. *Proc Natl Acad Sci U S A* **107**: 496-501
- Maleck K, Levine A, Euglem T, Morgan A, Schmid J, Lawton KA, Dangl JL, Dietrich RA** (2000) The transcriptome of *Arabidopsis thaliana* during systemic acquired resistance. *Nat Genet* **26**: 403-410
- McNeil SD, Nuccio ML, Hanson AD** (1999) Betaines and related osmoprotectants. Targets for metabolic engineering of stress resistance. *Plant Physiol* **120**: 945-950

- Meng X, Xu J, He Y, Yang KY, Mordorski B, Liu Y, Zhang S (2013) Phosphorylation of an ERF transcription factor by Arabidopsis MPK3/MPK6 regulates plant defense gene induction and fungal resistance. *Plant Cell* **25**: 1126-1142
- Moore JW, Loake GJ, Spoel SH (2011) Transcription dynamics in plant immunity. *Plant Cell* **23**: 2809-2820
- Naito K, Taguchi F, Suzuki T, Inagaki Y, Toyoda K, Shiraishi T, Ichinose Y (2008) Amino acid sequence of bacterial microbe-associated molecular pattern flg22 is required for virulence. *Mol Plant Microbe Interact* **21**: 1165-1174
- Neilson EH, Goodger JQD, Woodrow IE, Moller BL (2013) Plant chemical defense: at what cost? *Trends Plant Sci* **18**: 250-258
- Nemes P, Woods AS, Vertes A (2010) Simultaneous imaging of small metabolites and lipids in rat brain tissues at atmospheric pressure by laser ablation electrospray ionization mass spectrometry. *Anal Chem* **82**: 982-988
- Niki T, Mitsuhashi I, Seo S, Ohtsubo N, Ohashi Y (1998) Antagonistic effect of salicylic acid and jasmonic acid on the expression of pathogenesis-related (PR) protein genes in wounded mature tobacco leaves. *Plant Cell Physiol* **39**: 500-507
- Okmen B, Etalo DW, Joosten MH, Bouwmeester HJ, de Vos RCH, Collemare J, de Wit PJGM (2013) Detoxification of -tomatine by *Cladosporium fulvum* is required for full virulence on tomato. *New Phytol* **198**: 1203-1214
- Oldiges M, Lütz S, Pflug S, Schroer K, Stein N, Wiendahl C (2007) Metabolomics: current state and evolving methodologies and tools. *Appl Microbiol Biotechnol* **76**: 495-511
- Opge-Rhein R, Strimmer K (2007) From correlation to causation networks: a simple approximate learning algorithm and its application to high-dimensional plant gene expression data. *Bmc Syst Biol* **1**: 1-10
- Petutschnig EK, Jones AME, Serazetdinova L, Lipka U, Lipka V (2010) The Lysin Motif Receptor-like Kinase (LysM-RLK) CERK1 Is a Major Chitin-binding Protein in Arabidopsis thaliana and Subject to Chitin-induced Phosphorylation. *J Biol Chem* **285**: 28902-28911
- Pozo MJ, Van Der Ent S, Van Loon LC, Pieterse CMJ (2008) Transcription factor MYC2 is involved in priming for enhanced defense during rhizobacteria-induced systemic resistance in *Arabidopsis thaliana*. *New Phytol* **180**: 511-523
- Pruneda-Paz JL, Kay SA (2010) An expanding universe of circadian networks in higher plants. *Trends Plant Sci* **15**: 259-265
- Rosenthal GA (1990) Metabolism of L-canavanine and L-canaline in leguminous plants. *Plant Physiol* **94**: 1-3
- Rubakhin SS, Sweedler JV, Nemes P, Vertes A (2010) Laser ablation electrospray ionization for atmospheric pressure molecular imaging mass spectrometry. *In* Mass Spectrometry Imaging, Vol 656. Humana Press, pp 159-171
- Rushton PJ, Somssich IE (1998) Transcriptional control of plant genes responsive to pathogens. *Curr Opin Plant Biol* **1**: 311-315
- Rushton PJ, Somssich IE, Ringler P, Shen QJ (2010) WRKY transcription factors. *Trends Plant Sci* **15**: 247-258
- Sato S, Tabata S, Hirakawa H, Asamizu E, Shirasawa K, Isobe S, Kaneko T, Nakamura Y, Shibata D, Aoki K, Egholm M, Knight J, Bogden R, Li CB, Shuang Y, Xu X, Pan SK, Cheng SF, Liu X, Ren YY, Wang J, Albiero A, Dal Pero F, Todesco S, Van Eck J, Buels RM, Bombarely A, Gosselin JR, Huang MY, Leto JA, Menda N, Strickler S, Mao LY, Gao S, Tecle IY, York T, Zheng Y, Vrebalov JT, Lee J, Zhong SL, Mueller LA, Stiekema WJ, Ribeca P, Alioto T, Yang WC, Huang SW, Du YC, Zhang ZH, Gao JC, Guo YM, Wang XX, Li Y, He J, Li CY, Cheng ZK, Zuo JR, Ren JF, Zhao JH, Yan LH, Jiang HL, Wang B, Li HS, Li ZJ, Fu FY, Chen BT, Han B, Feng Q, Fan DL, Wang Y, Ling HQ, Xue YBA, Ware D, McCombie WR, Lippman ZB, Chia JM, Jiang K, Pasternak S, Gellay L, Kramer M, Anderson LK, Chang SB, Royer SM, Shearer LA, Stack SM, Rose JKC, Xu YM, Eannetta N, Matas AJ, McQuinn R, Tanksley SD, Camara F, Guigo R, Rombauts S, Fawcett J, Van de Peer Y, Zamir D, Liang CB, Spannagl M, Gundlach H, Bruggmann R, Mayer K, Jia ZQ, Zhang JH, Ye ZBA, Bishop GJ, Butcher S, Lopez-Cobollo R, Buchan D, Filippis I, Abbott J, Dixit R, Singh M, Singh A, Pal JK, Pandit A, Singh PK, Mahato AK, Dogra V, Gaikwad K, Sharma TR, Mohapatra T, Singh NK, Causse M, Rothan C, Schiex T, Noirot C, Bellec A, Klopp C, Delalande C, Berges H, Mariette J, Frasse P, Vautrin S, Zouine M, Lathe A, Rousseau C, Regad F, Pech JC, Philippot M, Bouzayen M, Pericard P, Osorio S, del Carmen AF, Monforte A, Granell A, Fernandez-Munoz R, Conte M, Lichtenstein G, Carrari F, De Bellis G, Fuligni F, Peano C, Grandillo S, Termolino P, Pietrella M, Fantini E, Falcone G, Fiore A, Giuliano G, Lopez L, Facella P, Perrotta G, Daddiego L, Bryan G, Orozco M, Pastor X, Torrents D, van Schriek KNMGM, Feron RMC, van Oeveren J, de Heer P, daPonte L, Jacobs-Oomen S, Cariaso M, Prins M, van Eijk MJT, Janssen A, van Haaren MJJ, Jo SH, Kim J, Kwon SY, Kim S, Koo DH, Lee S, Hur CG, Clouser C, Rico A, Hallab A, Gebhardt C, Klee K, Jocker A, Warfsmann J, Gobel U, Kawamura S, Yano K, Sherman JD,

- Fukuoka H, Negoro S, Bhutty S, Chowdhury P, Chattopadhyay D, Datema E, Smit S, Schijlen EWM, van de Belt J, van Haast JC, Peters SA, van Staveren MJ, Henkens MHC, Mooyman PJW, Hesselink T, van Ham RCHJ, Jiang GY, Droege M, Choi D, Kang BC, Kim BD, Park M, Kim S, Yeom SI, Lee YH, Choi YD, Li GC, Gao JW, Liu YS, Huang SX, Fernandez-Pedrosa V, Collado C, Zuniga S, Wang GP, Cade R, Dietrich RA, Rogers J, Knapp S, Fei ZJ, White RA, Thannhauser TW, Giovannoni JJ, Botella MA, Gilbert L, Gonzalez R, Goicoechea JL, Yu Y, Kudrna D, Collura K, Wissotski M, Wing R, Schoof H, Meyers BC, Gurazada AB, Green PJ, Mathur S, Vyas S, Solanke AU, Kumar R, Gupta V, Sharma AK, Khurana P, Khurana JP, Tyagi AK, Dalmay T, Mohorianu I, Walts B, Chamala S, Barbazuk WB, Li JP, Guo H, Lee TH, Wang YP, Zhang D, Paterson AH, Wang XY, Tang HB, Barone A, Chiusano ML, Ercolano MR, D'Agostino N, Di Filippo M, Traini A, Sanseverino W, Frusciante L, Seymour GB, Elharam M, Fu Y, Hua A, Kenton S, Lewis J, Lin SP, Najari F, Lai HS, Qin BF, Qu CM, Shi RH, White D, White J, Xing YB, Yang KQ, Yi J, Yao ZY, Zhou LP, Roe BA, Vezzi A, D'Angelo M, Zimbello R, Schiavon R, Caniato E, Rigobello C, Campagna D, Vitulo N, Valle G, Nelson DR, De Paoli E, Szinay D, de Jong HH, Bai YL, Visser RGF, Lankhorst RMK, Beasley H, McLaren K, Nicholson C, Riddle C, Gianese G, Consortium TG (2012) The tomato genome sequence provides insights into fleshy fruit evolution. *Nature* **485**: 635-641
- Schafer P, Pfiffi S, Voll LM, Zajic D, Chandler PM, Waller F, Scholz U, Pons-Kuhnemann J, Sonnewald S, Sonnewald U, Kogel KH (2009) Manipulation of plant innate immunity and gibberellin as factor of compatibility in the mutualistic association of barley roots with *Piriformospora indica*. *Plant J* **59**: 461-474
- Schiffer R, Gorg R, Jarosch B, Beckhove U, Bahrenberg G, Kogel KH, Schulze-Lefert P (1997) Tissue dependence and differential cordycepin sensitivity of race-specific resistance responses in the barley powdery mildew interaction. *Mol Plant Microbe Interact* **10**: 830-839
- Schmelz EA, Alborn HT, Tumlinson JH (2003) Synergistic interactions between volicitin, jasmonic acid and ethylene mediate insect-induced volatile emission in *Zea mays*. *Physiol Plant* **117**: 403-412
- Selmar D (1993) Transport of cyanogenic glucosides - linustatin Uptake by hevea cotyledons. *Planta* **191**: 191-199
- Selmar D, Lieberei R, Biehl B (1988) Mobilization and utilization of cyanogenic glycosides - the linustatin pathway. *Plant Physiol* **86**: 711-716
- Shen B, Hohmann S, Jensen RG, Bohnert A H (1999) Roles of sugar alcohols in osmotic stress adaptation. Replacement of glycerol by mannitol and sorbitol in yeast. *Plant Physiol* **121**: 45-52
- Stakman EC (1915) Relation between *Puccinia graminis* and plants highly resistant to its attack. *J Agric Res* **4**: 193-200
- Stulemeijer IJ, Joosten MH, Jensen ON (2009) Quantitative phosphoproteomics of tomato mounting a hypersensitive response reveals a swift suppression of photosynthetic activity and a differential role for hsp90 isoforms. *J Proteome Res* **8**: 1168-1182
- Stulemeijer IJE, Stratmann JW, Joosten MHJ (2007) Tomato mitogen-activated protein kinases LeMPK1, LeMPK2, and LeMPK3 are activated during the cf-4/Avr4-induced hypersensitive response and have distinct phosphorylation specificities. *Plant Physiol* **144**: 1481-1494
- Takahashi H, Kanayama Y, Zheng MS, Kusano T, Hase S, Ikegami M, Shah J (2004) Antagonistic interactions between the SA and JA signaling pathways in Arabidopsis modulate expression of defense genes and gene-for-gene resistance to cucumber mosaic virus. *Plant Cell Physiol* **45**: 803-809
- Thaler J, Fidantsef A, Bostock R (2002) Antagonism between jasmonate- and salicylate-mediated induced plant resistance: Effects of concentration and timing of elicitation on defense-related proteins, herbivore, and pathogen performance in tomato. *J Chem Ecol* **28**: 1131-1159
- Thaler JS, Humphrey PT, Whiteman NK (2012) Evolution of jasmonate and salicylate signal crosstalk. *Trends Plant Sci* **17**: 260-270
- Thilmony R, Underwood W, He SY (2006) Genome-wide transcriptional analysis of the *Arabidopsis thaliana* interaction with the plant pathogen *Pseudomonas syringae* pv. tomato DC3000 and the human pathogen *Escherichia coli* O157:H7. *Plant J* **46**: 34-53
- van Esse HP, van't Klooster JW, Bolton MD, Yadeta KA, van Baarlen P, Boeren S, Vervoort J, de Wit PJGM, Thomma BPHJ (2008) The *Cladosporium fulvum* virulence protein Avr2 inhibits host proteases required for basal defense. *Plant Cell* **20**: 1948-1963
- Winter G, Kromer JO (2013) Fluxomics - connecting 'omics analysis and phenotypes. *Environ Microbiol* **15**: 1901-1916
- Wolter M, Hollricher K, Salamini F, Schulze-Lefert P (1993) The mlo resistance alleles to powdery mildew infection in barley trigger a developmentally controlled defence mimic phenotype. *Mol Gen Genet* **239**: 122-128

Summary

Reductionist approaches have been dominating studies on plant defense against invading pathogens and have resulted in a profound insight into the complexity of the molecular warfare between plants and pathogens. To further deal with this complexity, the joining of forces between component biology and systems biology has proven to be a viable strategy. Although the field of systems biology is rapidly evolving, the use of this discipline as a tool to integrate high-throughput -omics technologies to study plant-microbe interactions, is just beginning to be explored. In the work described in this thesis, an integrated approach involving transcriptomics and metabolomics was used to explore the mechanisms underpinning tomato resistance to the leaf mold fungus *Cladosporium fulvum* and the counter measures taken by the fungus, leading to host susceptibility.

Chapter 1 provides a brief overview of the various systems biology approaches in studies aimed at deciphering plant-microbe interactions. The chapter also introduces the tomato-*C. fulvum* pathosystem and describes the different layers of the plant immune system, with special emphasis on chemical defense.

Chapter 2 describes the analysis of the transcriptional and metabolic changes associated with mounting of the hypersensitive response (HR), which is a form of programmed cell death that occurs at the site of pathogen entry in resistant plants. For this study, tomato plants that express both a *Cf* gene for resistance to *C. fulvum* and the matching avirulence (*Avr*) gene of this pathogen, are used. In these so-called dying seedlings, a massive reprogramming of both the transcriptome (microarray-based) and the metabolome occurred upon mounting of the *Cf/Avr*-induced HR. The multilayer information that was obtained showed that the aromatic amino acid (AAA) biosynthesis pathway and AAA-derived phenylpropanoid accumulation were highly induced in these *Cf/Avr* plants. In addition to the induction of the biosynthesis of primary and secondary metabolites, there was a massive induction of energy-generating and energy-conserving catabolic processes. Co-expression analysis pointed to WRKY transcription factors as the most prominent orchestrators of the HR.

Chapter 3 provides a systems view on the regulatory mechanisms involved in the growth/defence trade-off. Using RNA-seq analysis, the global change in the transcriptome of the dying seedlings, also employed in chapter 2, was compared to that of resistant and susceptible tomato plants inoculated with *C. fulvum*. This analysis revealed that plants that are mounting a resistance response to the fungus undergo massive transcriptional reprogramming resulting in a shift towards energy generation at the expense of growth. For example, a number of catabolic processes that generate acetyl-CoA, an important intermediate for the energy cycle and the biosynthesis of a wide

range of defence-associated primary and secondary metabolites, were up-regulated. The induction of these catabolic processes coincides with a significant reduction in the levels of trehalose-6-phosphate, which plays a central role in the maintenance of energy homeostasis during carbon starvation, and is accompanied by the accumulation of trehalose.

Chapter 4 deals with the functional characterization of tomato WRKY transcription factors (*SIWRKYs*) in the regulation of the defense transcriptome and metabolome. Both in the microarray-based (chapter 2) and in the RNA-seq-based (chapter 3) transcriptional profiling studies, genes encoding tomato WRKYs (*SIWRKYs*) showed the most pronounced changes upon activation of the defence response of tomato resistant to *C. fulvum*. In the RNA-seq analysis 36, out of a total of 59 expressed *SIWRKYs*, were transcriptionally up-regulated, whereas the transcription of only two of them was suppressed. Virus-induced gene silencing (VIGS) of selected differentially regulated, and possibly functionally redundant, *SIWRKYs* showed that this class of transcription factors consists of a group of key regulators, some of which are activating and some of which are suppressing the plant immune response. Untargeted metabolomics showed that suppression of the expression of *SIWRKY31/33* and *SIWRKY80* (an ortholog of *AtWRKY70*) by VIGS in resistant *Cf-4*-expressing tomato plants resulted in an increase in plant susceptibility, which is similar to the increased susceptibility that is observed when the expression of the resistance gene *Cf-4* itself is knocked-down. Targeting of the expression of defence repressors (*SIWRKY39/40/45/46*) boosted basal defence in susceptible plants, resulting in a drastic reduction of *C. fulvum* proliferation. Compared to the control (*GUS*-silenced) plants, targeting of (combinations of) the genes encoding these *SIWRKYs* in resistant plants, followed by inoculation with *C. fulvum*, resulted in significant changes in the apoplast metabolome. This supports their involvement in the defence-associated metabolome reprogramming of tomato upon its colonisation by *C. fulvum*.

Chapter 5 provides a detailed analysis of the major alterations that occur in the metabolome of tomato leaves upon successful and unsuccessful colonization by *C. fulvum*. For this, we performed a comprehensive untargeted metabolic profiling of whole leaf, as well as of leaf apoplastic extracts of resistant (incompatible interaction) and susceptible (compatible interaction) tomato plants challenged with *C. fulvum*. In whole leaf extracts, substantial changes were detectable for a large variety of metabolites, including polar, semi-polar and apolar compounds, while in the apoplast only the more polar and semi-polar compounds changed in abundance. In the incompatible interaction, an early (4-6 days post inoculation) increase in the accumulation of a number of phospholipids and secondary metabolites was apparent. Interestingly, in the compatible interaction the major change that was observed was the conversion of a number of antimicrobial glycoalkaloids into their less toxic derivatives and the accumulation of several sugar

alcohols in both the whole leaf and the apoplast. Although α -tomatine, the most abundant tomato glycoalkaloid, was thought to be localized in the vacuole, for the first time we show that this compound is also present in the apoplast. Furthermore, we show that α -tomatine is hydrolyzed by *C. fulvum* tomatinase-1 (CfTom1), upon colonization of the leaf apoplast by the fungus. CfTom1 belongs to the *glycosyl hydrolase (GH)-10* gene family and encodes a tomatinase, for which we showed that it can degrade α -tomatine into its non-toxic aglycone, tomatidine, *in vitro* as well as *in planta* during successful colonization of tomato leaves. Functional analysis of Δ cftom1 knock-out mutants of *C. fulvum* showed that degradation of α -tomatine is required for full virulence of the fungus on tomato. We observed that this must be due to the higher level of the toxic α -tomatine, rather than to the presumed suppression of basal defense by α -tomatine breakdown products. Finally, based on experimental evidence, we propose stachydrine, a pyrrolidine alkaloid reported to be present in several plant species, to be a possible degradation product of α -tomatine.

Chapter 6 provides a systems biology perspective on the biological integration of multilayer information obtained from \sim omics data. Based on the integration of all this information, inferences are made about the possible role of the HR in the resistance response of tomato. Furthermore, this chapter provides insight into the possible key regulatory components that govern the growth/defense trade-off. The potential of metabolomics studies in the discovery of pathogen effectors and biomarkers associated with susceptibility and resistance is discussed. Chapter 6 also provides insight into the possible implications of the comprehensive metabolic changes that occur during the interaction of *C. fulvum* with tomato, with an emphasis on the strategies that enable *C. fulvum* to establish a successful biotrophic relationship with its host. The importance of biological integration and the need for statistical integration and mathematical modeling of a system are discussed and they are suggested to form a bridge between systems and synthetic biology. Finally, the contribution of spatial sampling technologies to complement a meaningful integration of multilayer information is discussed.

Samenvatting

Wetenschappelijke studies gericht op de afweer van planten tegen binnendringende ziekteverwekkers zijn tot nu toe voornamelijk uitgevoerd vanuit een reductionistische benadering. Deze studies hebben geleid tot een gedetailleerd inzicht in de complexiteit van de strijd tussen planten en ziekteverwekkers op moleculair niveau. Een combinatie van deze reductionistische benadering met een meer moderne systeem-biologische benadering, gebaseerd op “high-throughput” “-omics” technologieën zou moeten helpen deze complexiteit beter te begrijpen. Echter, het gebruik van een dergelijke geïntegreerde benadering bij onderzoek aan de interactie tussen planten en micro-organismen is nog maar net begonnen. In het onderzoek beschreven in dit proefschrift is gebruik gemaakt van een combinatie van transcriptomics (genexpressie analyse) en metabolomics (metaboliet analyse) om meer inzicht te krijgen in de mechanismen die ten grondslag liggen aan de resistentie van tomaat tegen het bladpathogeen *Cladosporium fulvum* en de strategie van de schimmel om die afweer af te slaan en de plant te infecteren.

Hoofdstuk 1 geeft een kort overzicht van de verschillende, op systeembioologie gebaseerde studies gericht op het ontcijferen van de interacties tussen planten en hun microbiële ziekteverwekkers. Het hoofdstuk introduceert ook het tomaat - *C. fulvum* pathosysteem en beschrijft de diverse lagen van het immuunsysteem van de plant, met speciale nadruk op de chemische afweer van planten tegen de binnendringende schimmel.

Hoofdstuk 2 beschrijft de analyse van de transcriptionele en metabolische veranderingen die geassocieerd zijn met het activeren van de zogenaamde overgevoelighedsreactie (“hypersensitieve response”). Dit is een vorm van geprogrammeerde celdood die specifiek in resistente planten plaatsvindt op de plaats waar de ziekteverwekker het plantenweefsel binnen probeert te dringen en verdere kolonisatie door de schimmel effectief tegengaat. Voor deze studie werden tomatenplanten gebruikt die zowel een gen voor resistentie tegen *C. fulvum* als het bijbehorende avirulentie (*Avr*) gen van de ziekteverwekker tot expressie brengen. In deze zogenaamde ‘doodgaande zaailingen’ vindt de geïnduceerde celdood (als gevolg van het activeren van de *Cf/Avr*-interactie) plaats in de gehele plant zonder dat inoculatie met de schimmel nodig is. Met deze transgene planten kunnen de processen bestudeerd worden die normaal in resistente planten bij schimmelinfectie slechts zeer lokaal plaatsvinden en daardoor moeilijk te onderzoeken zijn. Het bleek dat er tijdens deze *Cf/Avr*-geïnduceerde celdood een massale herprogrammering plaatsvindt op zowel transcriptioneel niveau (gebaseerd op microarrays) als metabolisch niveau (gebaseerd op massaspectrometrie). Met name de aromatische aminozuur biosynthese en de hiervan afgeleide phenyl-propanoïden biosynthese werden sterk geïnduceerd in deze *Cf/Avr* planten. Naast de inductie van de

biosynthese van deze primaire en secundaire metabolieten was er een sterke activering van energie producerende en energie besparende katabolische processen. Co-expressie analyse liet zien dat zogenaamde “WRKY” transcriptiefactoren belangrijke regulatoren zijn bij deze overgevoelighedsreactie.

Hoofdstuk 3 geeft een overzicht van de mechanismen die betrokken zijn bij het negatieve effect van het activeren van de resistentiereactie op de groei van de plant. Met behulp van transcriptoom sequentieanalyse (RNA-seq) werden de veranderingen in het transcriptoom van de ‘doodgaande zaailingen’ vergeleken met die van resistente (incompatibele interactie) en vatbare (compatibele interactie) tomatenplanten die waren geïnoculeerd met *C. fulvum*. Dit onderzoek liet zien dat ook resistente planten door hun lokale overgevoelighedsreactie een zeer sterke transcriptionele herprogrammering ondergaan. De veranderingen in het transcriptoom wezen op een verschuiving naar het opwekken van energie ten koste van de groei. Een aantal katabolische processen die acetyl-CoA genereren - dat een belangrijk tussenproduct is in de energiecycclus en in de biosynthese van een breed scala aan afweer-gerelateerde primaire en secundaire metabolieten - waren sterk geactiveerd. De inductie van deze katabolische processen viel samen met een duidelijke vermindering van de hoeveelheid trehalose-6-fosfaat, dat een centrale rol speelt in het behoud van de energie homeostase gedurende een koolstoftekort, en een accumulatie van trehalose.

Hoofdstuk 4 behandelt de functionele karakterisering van tomaat WRKY transcriptiefactoren die een belangrijke rol lijken te spelen bij de regulatie van het transcriptoom en metabooloom tijdens de resistentiereactie. Uit de Hoofdstukken 2 en 3 bleek dat genen die coderen voor tomaat WRKYs (*SIWRKYs*) de meest uitgesproken veranderingen op transcriptieel niveau vertonen tijdens de activering van de afweerreactie van tomatenplanten tegen *C. fulvum*. Uit de RNA-seq analyse bleek dat 36 van de 59 *SIWRKYs* transcriptieel waren geactiveerd, terwijl de transcriptie van slechts twee van hen was onderdrukt. Virus-geïnduceerde gen “silencing” (VIGS) in tomaat van geselecteerde differentieel gereguleerde, en eventueel functioneel redundante, *SIWRKYs* toonde aan dat deze familie van transcriptiefactoren bestaat uit een groep van centrale regulatoren, waarvan sommige de afweerreactie van de plant activeren en anderen deze juist onderdrukken. De onderdrukking van de expressie van *SIWRKY31/33* en *SIWRKY80* (een ortholoog van *AtWRKY70*) met behulp van VIGS in tomaat met het *Cf-4* resistentiegen, resulteerde in een verhoogde gevoeligheid voor *C. fulvum* en een metabolietprofiel dat vergelijkbaar was met dat van planten waarvan de expressie van het resistentiegen *Cf-4* zelf wordt onderdrukt. Anderzijds resulteerde de verlaging van de expressie van afweer-onderdrukkende WRKYs (*SIWRKY39/40/45/46*) in een metabolietprofiel dat wijst op een stimulatie van de basale afweerreactie van vatbare planten. Deze planten vertoonden inderdaad een sterk verminderde vatbaarheid voor *C. fulvum*. Vergeleken met controleplanten waarin VIGS van *GUS* plaatsvond, leidde VIGS

van (combinaties van) de genen die coderen voor deze *SIWRKYs* in resistente planten, gevolgd door inoculatie met *C. fulvum*, tot sterke veranderingen in het metaboloom van de apoplast, wat de ruimte tussen de cellen is waarin de schimmel groeit. Deze resultaten ondersteunen de betrokkenheid van de diverse *SIWRKYs* bij de afweer-gerelateerde herprogrammering van het metaboloom van tomaat tijdens de kolonisatie van het bladweefsel door *C. fulvum*.

Hoofdstuk 5 geeft een gedetailleerde analyse van de belangrijkste veranderingen die optreden in het metaboloom van tomatenbladeren na succesvolle en niet-succesvolle kolonisatie door *C. fulvum*. Hiervoor is een uitgebreide metaboliet analyse toegepast op gehele bladeren, evenals op de apoplast van resistente en vatbare tomatenplanten, die waren geïnoculeerd met *C. fulvum*. In het totale bladextract waren sterke wijzigingen meetbaar in de hoeveelheden van een grote verscheidenheid aan metabolieten, waaronder polaire, semi-polaire en apolaire verbindingen, terwijl in de apoplast alleen de meer polaire en semi-polaire verbindingen sterk in hoeveelheid veranderden. In de incompatibele interactie was er al vroeg (binnen 4 tot 6 dagen na inoculatie) een sterke accumulatie van een aantal fosfolipiden en secundaire metabolieten waar te nemen. Interessant is dat in de compatibele interactie omzettingen plaatsvonden van antimicrobiële glyco-alkaloïden in hun minder toxische derivaten en dat accumulatie optrad van verschillende suiker-alcoholen in zowel het hele blad als in de apoplast. Er werd tot nu toe aangenomen dat α -tomatine, het meest voorkomende tomaat glyco-alkaloïd, enkel aanwezig is in de vacuole van de plantencel. In dit onderzoek kon echter voor het eerst worden aangetoond dat deze verbinding (ook) in de apoplast aanwezig is en *C. fulvum* hiermee dus direct in contact kan komen. Daarnaast werd aangetoond dat bij de kolonisatie het α -tomatine dat aanwezig in de apoplast wordt gehydrolyseerd door *C. fulvum* met behulp van het enzym tomatinase-1 (CfTom1). CfTom1 behoort tot de glycosyl hydrolase (GH) -10 gen familie en codeert voor een tomatinase, waarvoor nu is aangetoond dat het α -tomatine kan afbreken tot het voor de schimmel minder of niet-toxische aglycon, tomatidine. Dit gebeurt zowel *in vitro*, als ook *in planta* bij een succesvolle kolonisatie van de plant. Verder bleek uit een functionele analyse van Δ cftom1 “knock-out” mutanten van *C. fulvum* dat voor een volledige virulentie van de schimmel op tomaat de afbraak van het voor de schimmel giftige α -tomatine vereist is. Gebaseerd hierop, wordt verondersteld dat de eerder gepostuleerde onderdrukking van de basale plantafweer door afbraakproducten van α -tomatine, onjuist is. Daarnaast lijkt stachydrine, een pyrrolidine-alkaloïd dat in verschillende plantensoorten aanwezig is, in tomaat een schimmel-geïnduceerd afbraakproduct van α -tomatine te zijn.

Hoofdstuk 6 schetst een systeem-biologisch perspectief op de integratie van informatie van “omics” data verkregen op meerdere niveaus. Gebaseerd op de integratie van alle informatie beschreven in de voorafgaande hoofdstukken zijn conclusies getrokken over de mogelijke rol van de overgevoeligheidsreactie in de resistentie van tomaat

tegen *C. fulvum*. Bovendien geeft dit hoofdstuk inzicht in de belangrijkste componenten die de balans tussen groei en afweer kunnen reguleren. De potentie van metaboliet analyses voor het karakteriseren van effectoren van ziekteverwekkers en het opsporen van bio-merkers die geassocieerd zijn met gevoeligheid en resistentie, wordt hier ook besproken. Tevens geeft dit hoofdstuk inzicht in de mogelijke gevolgen van de sterke veranderingen die optreden in het metabooloom tijdens de interactie van *C. fulvum* met tomaat, met een nadruk op de strategieën die het *C. fulvum* mogelijk maken om een succesvolle biotrofe relatie (compatibele interactie) met zijn gastheer te verkrijgen. Verder wordt ingegaan op het belang van een goede integratie van statistische analyses en mathematische modellering van het systeem, omdat deze een brug zouden kunnen vormen tussen systeembioïogie en synthetische biologie. Tenslotte wordt de bijdrage van de manier van bemonstering aan een zinvolle integratie van de informatie die verkregen is op de diverse niveaus, besproken.

ማጠቃለያ

ተክሎች ከበሽታ አምጪ ህዋሳት ጋር የሚያደርጉት እልህ አስጨራሽ ግብ ግብ ለረጅም ጊዜ ሲጠና የነበረው እያንዳንዱን የተክል ባህሪ ወሳኝ የሆኑትን ህብላ ዘሮች አንድ በአንድ ነጥሎ በማጥናት ነበር። ዪሄ የሳይንስ ዘዴ ለግንዛቤአችን ከፍተኛ አስተዋዕዞ እያደረገ ቢገኝም በተክሎች እና በበሽታ አምጪ ህዋሳት መካከል የሚካሄደውን የተወሰነ ትግል በበለጠ ለማብራራት ተጨማሪ የሳይንስ ዘዴ አስፈላጊ ነው። ይህ ግንዛቤ ሁሉን አቀፍ የሰነ ሕይወት የሳይንስ ዘርፍ አንዲወለድ መንገዱን ከፍቷል። ይህ ሁሉን አቀፍ የሰነ ሕይወት የሳይንስ ዘርፍ እያንዳንዱ ህብላ ዘሮች እንዴት እርስ በርሳቸው እንደተያያዙና በተክሉ የጤና መከላከያ ዘዴ ላይ ተፅዕኖ እንደሚያረጉ ያጠናል። ከህብላ ዘሮች በተጨማሪም በጥናቱ ተክሎች በሚያመርቷቸው ኬሚካሎች እንዴት በሽታ አምጪ ህዋሳትን እንደሚከላከሉ እና በተጨማሪም እንዴት በሽታ አምጪ ህዋሳት ከነዚህ መርዛማ የተክል ኬሚካሎች ራሳቸውን እንደሚከላከሉ አሳይቻለሁ።

ምዕራፍ ፩ ይህ ምዕራፍ ስለ ተክሎች የጤና መከላከያ ዘዴ አደረጃጀት በሰፊው ያብራራል። ለበሽታ በቀላሉ ተጋላጭ በሆኑ ፣ በሽታውን መቋቋም በሚችሉ የቲማቲም ተክሎች እና በበሽታ አምጪ ተህዋሲው ክላይስፖሪም መካከል ያለውን ግብ ግብ ያብራራል። በተጨማሪም ስለ አጠቃላይ የተክል የኬሚካል ይዘት ስለሚያጠናው አዲሱ የሳይንስ ዘርፍ ሜታቦሎሚክስ እና ስለ አጠቃላይ ተገላጭ ህብላ ዘሮች የሚያጠናውን የሳይንስ ዘርፍ ትራንስክሪፕቶሚክስ በሰፊው ያብራራል።

ምዕራፍ ፪ ይህ ምዕራፍ በሽታ ተጃጃሚ ተክሎች በሽታው በተከሰተበት አካባቢ የሚገኙ የተወሰኑ የራሳቸውን ሴሎች በመግደል እንዴት በሽታው ወደሌላው ጤነኛ ክፍል እንዳይስፋፋ እንደሚያደርጉ ያብራራል። ከዚህ ሂደት ጋር የተያያዙ የአጠቃላይ የህብላ ዘር መገለጽ ለውጦችንና የተክሉ አጠቃላይ ኬሚካላዊ ለውጦችን በሰፊው ይዳስሳል። ውርኪ የተባሉ የህብላ ዘር መገለጽ አቀነባባሪዎች በለውጡ ላይ ከፍተኛ ሚና እንደሚጫወቱ ጥናቱ በቂ መረጃ ይሰጣል። ከዚህም በተረፈ በሽታን መከላከል ተክሉን ከፍተኛ ጉልበት እንደሚጠይቀው ጥናቱ ያመለክታል። ተክሉ የራሱን የተወሰነ ክፍል በመግደል በሽታው ወደጤነኛ ክፍል እንዳይስፋፋ ከማረጋገጥም በተጨማሪ የሞተውን አካሉን የኬሚካል ይዘቱን መልሶ ጸረ ተህዋሲያን ኬሚካሎች ለመስሪያ ሊጠቀምበት እንደሚችል ጥናቱ ያመለክታል።

ምዕራፍ ፫ ይህ ምዕራፍ ተክሎች በሽታን በሚከላከሉበት ወቅት ያላቸውን የሃይል ምጣኔ ሃብት አጠቃቀምን ሂደት ይዳስሳል። በዋናነት ተክሎች በሽታን በሚከላከሉበት ወቅት እንዴት ከእድገት ጋር የተያያዙ ሂደቶችን በማስቆም ተክሉ ያለውን ውሱን ሃይል ለበሽታ መከላከል እንደሚያውሉት ያብራራል።

ምዕራፍ ፬ ይህ ምዕራፍ ቀደም ብሎ በምዕራፍ ፪ ላይ አንደተገለጸው ውርኪ የተባሉ የህብላ ዘር መገለጽ አቀነባባሪዎች በተክሉ የበሽታ መከላከያ አወቃቀር ላይ ያላቸውን ሚና ያጠናል። ሚናቸውን ለማወቅም ሻይረስ በመጠቀም የተወሰኑትን ተክሉ በሽታ በሚከላከልበት ወቅት እንዳይገለጹ በማድረግ ሚናቸውን ለማወቅ ተችሏል። የተወሰኑት የተክሉ የበሽታ መከላከያ አቅም እንዲነቃቃ ሲያደርጉ የተቀሩት ደግሞ የተክሉ የበሽታ መከላከያ አቅም ከመጠን በላይ እንዳይነቃቃ ይቆጣጠሩታል። በተጨማሪም የተክሉ አጠቃላይ የኬሚካል ይዘት ላይ ተጽኖ እንደሚያሳድሩም ጥናቱ ያመለክታል።

ምዕራፍ ፭ ይህ ምዕራፍ በተክሎችና በበሽታ አምጪ ተህዋሲያን መካከል የሚደረገውን የኬሚካል የጦር መሳሪያ እሽቅድድም በሰፊው ያብራራል። የቲማቲም ተክል በሽታ አምጪ የሆኑ ባክቴሪያ እና ፈንገሶችን ቶማቲን የተባለ ኬሚካል በመጠቀም ይከላከላል። ይህ ቶማቲን የተባለው ኬሚካል

የፈንገሱን ህዋስ ሽፋን በመበጣጠስ ይገለጻል። በአንጻሩ ፈንገሱ ደግሞ ይህንን አደገኛ ኬሚካል ኢንዱስትሪ በመጠቀም መርዛማ ወዳልሆኑ የኬሚካል አይነቶች ይለውጣቸዋል። ቶማቲካን እና ስታቺድሪን የተባሉት ኬሚካሎች ለበሽታው ተጋላጭ በሆኑ የቲማቲም ዝርያዎች ላይ ከፍተኛ ክምጭት አሳይተዋል። ባጠቃላይ ተክሎች ራሳቸውን ከበሽታ አምጪ ተህዋሲያን ለመከላከል አያሌ ኬሚካሎችን ሲጠቀሙ ጠላት ተህዋሲያን ደግሞ የተለያዩ ኢንዱስትሪዎቻቸውን በመጠቀም እነዚህን አደገኛ ኬሚካሎች ያወድማሉ።

ምዕራፍ ፯ ይህ ምዕራፍ ቀደም ብለው የተጠቀሱት ምዕራፎች ያላቸውን ተያያዥነት ጠቅለል አድርጎ ያብራራል። ማብራሪያው የተደረጉት ጥናቶች ከሁሉን አቀፍ የስነ ህይወት ሳይንስ አንጻር እንዴት ይታያሉ ሚላውን ይዳስሳል። በተጨማሪም ከተለያዩ ቴክኖሎጂዎች የመጡ መረጃዎች አንዴት ሊዋቀሩና የተክሉን መሰረታዊ የበሽታ መከላከያ ዘዴ በበለጠ ሊያብራሩ አንደሚችሉ ሃሳቦችን ይሰጣል። በስተመጨረሻም የሁሉን አቀፍ የስነ ህይወት ሳይንስ እንዴት ከተለያዩ ቴክኖሎጂዎች የመጡ መረጃዎችን አዋቅሮ ወደ ስነ ህይወታዊ ሂሳባዊ ማሳያዎች(ሞዴል)መለወጥ የሚቻልበትን መንገድ ይገልጻል። ብሎም እንዴት የሁሉን አቀፍ የስነ ህይወት ሳይንስ እና ስነ ህይወታዊ ሂሳባዊ ማሳያዎች ሲጣመሩ አዲስ ለተወለደው የሳይንስ ዘርፍ ሰው ሰራሽ (ሲንተቲክ) የስነ ህይወት የጥናት ዘርፍ አስተዋጾ እንደሚያደርጉ ያብራራል።

Acknowledgements

A number of people have helped and taught me immensely throughout my personal and educational life and I am very grateful for all of them. For convenience, only a handful of them are mentioned below in the acknowledgement and those who are not listed will always be in my heart and remembered. This thesis is the result of many years of experiences that I have accumulated at Wageningen University and it is attributed to all remarkable individuals who invested on me, believed in me, and gave me the opportunity to explore all possibilities and the combination of these factors remarkably contributed to the successful completion of this project.

First of all, special acknowledgement goes to Harro; my promoter, mentor, friend, and above all a wonderful human being. I witnessed your ability to give guidance without compromising my freedom which was crucial in finding my way without getting lost into the wildness. Especially in the last stage of writing, you showed your organizational skills and it was the moment that I clearly understood why you destined to be a professor. I am also thankful for the opportunity you gave me to spend some time with you in University of California, Davis during your sabbatical. In just one month, I managed to learn and do a number of metabolomics analysis and its success was strongly attributed to your personal and financial commitment. Beyond science, our stay at Davis also gave me the opportunity to get to know you well as a person. I am sure you will remember how impressed I was when we visited Yosemite National Park. It was such an awesome experience and most of all while camping, the delicious breakfast that you made with your rudimentary cooking utensils was delicious and it is unforgettable experience. Here I would like to confess to the world that the Professor also knows how to survive in the jungle. I am very grateful for having the opportunity to work with you and continue our collaboration in the future. Thank you Harro!

It was during my MSc thesis that I got to know Matthieu (Matt), my co-promoter. He has been my inspiration and tutor who introduced me to the world of phytopathology and molecular sciences. Matt, who would care about me like you do? Who would believe in me and my ability to make things happen like you do? Who would potentially give me such an opportunity to grow myself in the field of science like you do? And of course who would serve me such a nice BBQ with the most prestigious wines like you do? I shall extend my deepest and heartfelt appreciation to this wonderful soul! I am blessed to have your presence in my life and you are not only a scientist but also a good man with a good heart and that makes working with you very enjoyable experience. Without you, I would find it difficult to imagine for things to happen in a way they happen in this project. Thanks Matt! You are all-in-one!

Ric, my co-promoter is the busiest person around and yet he manages to allot time to everyone who needs his help while maintaining his smile and cheerful conversation. In that sense, I would say he is an evergreen person! He baptized me and let the spirit of metabolomics to get into my veins and he continues to give me the inspiration that helped me to dive deep into the world of small molecules. Especially at the final writing stage of my thesis, I have realized that for my project the combination of Harro, Matthieu, and Ric brought a peculiar flavor to the project and for sure that made us a dream team.

Thanks to Robert Hall, currently I am working on mass spectrometer imaging (LAESI) using a state-of-the-art technology. What I can say is that it is fascinating technology and it is a privilege to be chosen to handle this project. Robert, you believe in me and supported me in many ways. The dinner we had at your place was prestigious and I, Fe and Carlos were really impressed with your kindness and care at the dinner table. Our trip to the flower bulb fields was also memorable and I am grateful for having the opportunity to work with you.

During my PhD, I collaborated with a number of individuals in WUR and outside of WUR. I would like to thank Wladimir Tameling for continuous support I got from him when I was performing VIGS experiment on WRKY transcription factors. Your ability to explain things in very understandable manner makes life easier and it shows how deeply you understand the subject matter. Thank you Wlad for everything! Similarly, the help I got from Thierry Delatte in the analysis of trehalose -6-phosphate was remarkable. My good friend Bilal, his promoter and supervisors; Pierre and Jérôme are great people to work with. I am very grateful for all the experience we shared during the course of this work.

Anna Undas was the first person who taught me the practical aspect of Gas Chromatography Mass Spectrometry (GCMS). That also gave a good foundation for our friendship. Anna, the dinner and the discussion we had at your place were magnificent and most of all I am very much entertained by the way your cute rabbit cleans its face. Thanks Anna! You are a true friend and I treasure our friendship. At the beginning of my PhD, Francel was my other mentor in the lab and had it not been for him, it would probably took me significantly more time to get used to the situation in the lab. Furthermore, his cheerful face and positive outlook were like a morning coffee that helped me to have a fresh start of the day. Francel you give color to these who are around you! Without Bert I would probably find it difficult to analyze my samples in LCMS and you taught me a lot about the practical aspect of LCMS. Your patience, smiley face, and friendly character make working with you a pleasant experience. Bert, thank you for the unreserved support and friendship you showed me during the course of my PhD.

My friendship with Mahdere and Abiy dates back to a decade and started when we were studying at Jimma University, Ethiopia. Fortunately, we got the opportunity to move to Wageningen to continue our study. This further strengthened our friendship and has

ACKNOWLEDGEMENTS

enriched us with memorable moments. This year they have their first daughter Edna; the little angel and the most adorable being. She even makes our bond stronger. Although staying abroad for many years is a bit challenging, the close relation I have with you makes me feel at home. Your family has a special place in my heart. Furthermore, the Friday evening small party with Mahi, Abelo, Rutta will always be remember and I am glad that we have a story to tell and to remember.

Often describing what Natalia means to me is challenging. The problem is that words are limited and shallow and they often describe what mind can see or conditioned to see. My connection with Natalia transcends all the barriers and what I see is the expansion of myself in her and the expansion of herself in me. This glorify our oneness and that realization ridicule the fact that time and space exist and her presence in my life can be felt at any moment of time. Nati, thank you for being you and I am fortunate to have you and your friendship in my life!

Jules and Catja, what a wonderful office mates! Sitting with you was refreshing and a lot of fun. The Friday afternoon soft drink session was one of the best moments of our friendship. The way our team popularize Rakia is threatening Coca-Cola and other soft drink producers. Our expertise expands from molecular biology and metabolomics to the Rakiomics. The post cards from Vicky, our beloved friend in France gave our office a grace. Vicky's move on the dance floor is one of a kind and will drive anyone crazy. Vicky you've got the move! My friends, one who gets the opportunity to sit with you in that office finds the key to happiness! As it has been said; "one who brings happiness to others will find it".

I would like to thank Rina, she is an outstanding secretary, and she dealt with all my administrative-related issues promptly and make sure that things are done accordingly and on time. Rina, you are the best and thank you for your help and kindness.

All shengo (ሸንጎ) members and friends in Wageningen; Dugshu, Arabu, Gecho, Mahdi, Byo, Mahi, Tuta, Sinte, Eske, Dele, Abelo, Asfshe, Tade, Mule, Wess, Dani, Ashu bret, Gicho, Fredi and Jembe; Saturday evening will always be remembered. All the philosophical, political, social, economic.....issues that were discussed and all the laughter that we shared were refreshing and will remain to be a memorable moment of our life. Our Saturday night gathering gave relief to mind and made us ready for the upcoming productive working days. My friends back in Ethiopia; Ben, Siraw, Ngsti, Dave, Brooke melese, Heluye, Fanni, Ade, Habtsh; your continuous support from a distance was important to keep my spirit high. Thank you so much for your friendship. Habtshe, Selamina and Brooke you are true friends!

My friends in wageningen; Anna (green), Viviane, Manickam, Neli, Lemeng, Aldana, Julio, Wei song, Jimmy, Rik Padraic, Charles, Daniela, Ralph, Thomas, Chunxu and all others

that are not listed here made my stay in Wageningen enjoyable. All the ideas, beer, fun and laughter we shared made my stay in Wageningen a pleasurable experience. The wolf screaming on our way back from the international club (the way Julio and wei were screaming and laughing), the train party we had on our way back from Rotterdam (the pole dancer and the meditator) and the movember cave-manship are some of the memorable moments we had together. Thank you guys, you gave color to my life!

Kangmo Lee, my best friend, our stay in Wageningen was full of adventure. Our friendship created a bridge that helped me to explore Korea, its magnificent culture and most of all the delicious foods. Kimchi, the fried rice, the korean BBQ, tattorita, Bibimpap... are all delicious and as I write, I am salivating. Your foods have great influence on my cooking and the fusion Ethio-Korean foods brought the fourth dimension to the taste. Many thanks to my longtime friends Jhamna, Luis, Alina, Loes and Yodit. You guys are awesome.

Working with all members of plant physiology, phytopathology, and plant research international PRI (bioscience) was one of the most interesting experiences I had in Wageningen. I couldn't imagine a place where there is such deep rooted scientific collaboration between groups while maintaining a very good interpersonal relationship. I am proud to be associated with Wageningen University. Wageningen gave me all the challenges and opportunities that I need for the evolution of my consciousness and that profoundly affect me both as a person and a scientist.

Last but not the least, I would like to thank my family; mama, papa, Atse, Tade, Jhon, Azi and my nephew DD (Robel); your love is like a food to my soul! Most of all I am very grateful for my brother Tade who invested too much on me. I am very happy that you will be traveling all ways long to attend on my defense ceremony. Tade, I would like to say from the bottom of my heart, it is all because of you!



Curriculum vitae

Desalegn Woldeesenbet Etalo was born on March 8 1982 in Addis Ababa, Ethiopia. His great desire was to be an electric engineer and at some point of his life he found himself studying biology and with no doubt he fall in love with it. He got his Bachelor degree in Horticultural science from Jimma University, Ethiopia. As a partial fulfilment of his thesis, he studied the role of 2, 4-D (2,4-Dichlorophenoxyacetic acid) on promoting the rooting potential of rose cuttings (*Rosa hybrida*). His research was nominated second from the top three best Bachelor thesis in plant science by the Jimma University Research and Publication office. After completing his study, he served at Jimma University as a graduate assistance and involved in a number of teaching and research activities.

In 2006, he moved to Wageningen to continue his MSc studies in Plant Sciences under the Netherlands Fellowship Programme (NUFFIC). During his study he found the plant world to be even more exciting than he previously taught. He undertook two thesis; the first one on systemic distribution of wound induced reactive oxygen species (ROS) in *Arabidopsis* (*Arabidopsis thaliana*) under the supervision of Dr. Jeremy Harbinson and Dr. Uulke van Meeteren. This work resulted into publication. His second thesis was on dynamics of reactive oxygen species (ROS) and reactive nitrogen species (RNS) during plant-pathogen interactions under the supervision of Dr. Wladimir Tameling, Dr. Jeremy Harbinson and Dr. Matthieu Joosten. The work resulted into a number of exiting results which with some additional effort can be developed into scientific publication.

Upon completion of his MSc on 2008, he got an opportunity to work on PhD project that intend to use an integrated approach of transcriptomics and metabolomics to study the molecular interaction between tomato and *C. fulvum* under the supervision of Prof. Harro Bouwmeester, Dr. Matthieu Joosten and Dr. Ric de Vos. The project opened the door for him to learn different cutting edge ~omics technologies and management of high-throughput data sets from these technologies. This work is one of the first few that showed the potential of combined omics analysis in dissecting the major biological components of a system involved in plant-pathogen interactions. The work produces extensive data and two impressive publications in respected journals (Plant Physiology and New phytologist). Furthermore, three articles will be submitted for publication soon. Since November 2013, Desalegn is working as postdoctoral researcher in Plant Research International in the application of small-scale metabolomics in plant researches. Primarily, he is focusing on the application of Laser Ablation Electrospray Ionization (LAESI) technique in plant researches.

Publications

- Etalo DW**, Stulemeijer IJE, Peter van Esse H, de Vos RCH, Bouwmeester HJ, Joosten MHAJ (2013) System-wide hypersensitive response-associated transcriptome and metabolome reprogramming in tomato. *Plant Physiol.* **162**: 1599-1617
- Ökmen B., **Etalo D.W.**, Joosten M. H.A.J., Bouwmeester H. J., De Vos R. C.H, Collemare J. and de Wit P.J.G.M (2013). Detoxification of tomatine by *Cladosporium fulvum* is required for full virulence on tomato. *New Phytol* **198**: 1203-1214
- Etalo, D.W.**, Harbinson, J. and van Meeteren, U. (2009). Could wound-induced xylem peroxide Contribute to the Hydraulic Conductivity in Stems? *Acta Hort* **847**:287-294.

**Education Statement of the Graduate School
Experimental Plant Sciences**



Issued to: Desalegn Etalo
Date: 20 March 2014
Group: Plant Physiology, Wageningen University & Research Centre

1) Start-up phase		<i>date</i>
▶ First presentation of your project		
Metabolomics X Transcriptomics in tomato caldosporium interaction for gene discovery		Mar 30, 2009
▶ Writing or rewriting a project proposal		
Combined Metabolomic and Transcriptional Profiling of the Molecular Interaction between the Plant Host Tomato (<i>Lycopersicum esculentum</i> L.) and the Pathogen Tomato Leaf Mold Disease (<i>Cladosporium fulvum</i>) as a Tool to Clone Secondary Metabolite Pathway Genes		Jan 28, 2009
▶ Writing a review or book chapter		
▶ MSc courses		
Genomics (ABG-30306)		2009
▶ Laboratory use of isotopes		
<i>Subtotal Start-up Phase</i>		<i>13.5 credits*</i>
2) Scientific Exposure		<i>date</i>
▶ EPS PhD student days		
European Retreat of PhD students in Plant Sciences, Cologne (Germany)		Apr 15-17, 2010
EPS PhD student day, Utrecht University		Jun 01, 2010
EPS PhD student day, Wageningen UR		May 20, 2011
▶ EPS theme symposia		
EPS theme 2 symposium 'Interactions between Plants and Biotic Agents', Utrecht University		Jan 22, 2009
EPS theme 3 symposium 'Metabolism and Adaptation', University of Amsterdam		Feb 18, 2009
EPS theme 3 symposium 'Metabolism and Adaptation', Leiden University		Feb 19, 2010
EPS theme 2 symposium 'Interactions between Plants and Biotic Agents', University of Amsterdam		Feb 03, 2011
EPS theme 3 symposium 'Metabolism and Adaptation', Wageningen UR		Feb 10, 2011
EPS theme 2 symposium 'Interactions between Plants and Biotic Agents', Wageningen UR		Feb 10, 2012

EPS theme 3 symposium 'Metabolism and Adaptation' Utrecht University	Apr 26, 2012
► NWO Lunteren days and other National Platforms	
ALW meeting 'Experimental Plant Sciences', Lunteren	Apr 06-07, 2009
ALW meeting 'Experimental Plant Sciences', Lunteren	Apr 19-20, 2010
ALW meeting 'Experimental Plant Sciences', Lunteren	Apr 02-05, 2011
ALW meeting 'Experimental Plant Sciences', Lunteren	Apr 02-03, 2012
► Seminars (series), workshops and symposia	
CBSG_summit 2009	Mar 16-17 2009
CBSG_summit 2010	Mar 15-16 2010
CBSG_summit 2011	Jan 31-Feb 01, 2011
► Seminar plus	
► International symposia and congresses	
Metabolomics conference 2010 Amsterdam	Jun 27-Jul 01, 2010
Metabolomics conference 2013 Glasgow	Jul 01-04, 2013
► Presentations	
Omics assisted gene hunting in cladosporiumx tomato pathosysntem- cologne_Germany (Oral)	Apr 15-17, 2010
Combined metabolomic and transcriptomics profiling of the tomatoxcladosporium pathosysntem: a tool to clone seconday metabolite genes: Amsterdam metabolomics conference 2010 (Poster)	Jun 27-Jul 01, 2010
System wide analysis of the defense response of resistant (Cf-4) tomato lines during recongnition of the avirulence (Avr4) factor of cladosporium fulvum using high-throughput omics technology _Annual EPS Theme Meeting 3 Symposium (Oral)	Feb 19, 2010
Systems Biology of Plant-Pathogen Interactions: temporal dissection of the hypersensitive response in tomato dying seedlings (Cf-4/Avr4) using cutting-edge ~omics technologies-Annual EPS Theme 3 Symposium (Oral)	Feb 10, 2011
The Arms race between tomato and C. fulvum at metabolome level, Metabolomics conference, Glasgow	Jul 02, 2013
► IAB interview	Feb 17, 2011
► Excursions	
CBSG matchmaking event (excursion to Rijk Zwaan and Monsanto)	

Subtotal Scientific Exposure

*16.5 credits**

3) In-Depth Studies

date

► **EPS courses or other PhD courses**

Summerschool on Environmental Signaling	Aug 24-26, 2009
Comparative label-free LC-MS for Quantitative Proteomics	Apr 21-23 2010
Systems Biology; Statistical analysis of ~omics data'	Dec 13-17, 2010

EDUCATION STATEMENT

Bioinformatics-A User's Approach	Aug 29-Sep 2 2011
CBSG Bioinformatics 'Plant genome mining'	Oct 2011
EPS Autumn School 'Host-Microbe Interactomics'	Nov 01-03, 2011
► Journal club	
member of literature discussion group at Plant Physiology	2009-2012
► Individual research training	
Traning in Metabolomics and metabolomics data analysis, University of California Davis, Oliver Fiehn Lab	July14-Aug 14, 2011

Subtotal In-Depth Studies

*12.0 credits**

4) Personal development	<u><i>date</i></u>
► Skill training courses	
Scientific Writing, WGS course	Jun 2011
Intellectual property rights in a breeding contexts, CBSG workshop	Apr 2012
► Organisation of PhD students day, course or conference	
► Membership of Board, Committee or PhD council	

Subtotal Personal Development

*2.1 credits**

TOTAL NUMBER OF CREDIT POINTS*	44.1
---------------------------------------	-------------

Herewith the Graduate School declares that the PhD candidate has complied with the educational requirements set by the Educational Committee of EPS which comprises of a minimum total of 30 ECTS credits

** A credit represents a normative study load of 28 hours of study.*

The research described in this thesis was carried out at the Laboratories of Plant Physiology, Phytopathology and Plant Research International at Wageningen University, Wageningen, The Netherlands, and it was financially supported by the Centre for BioSystems Genomics (CBSG 2012), an initiative under the auspices of the Netherlands Genomics Initiative (NGI).

Financial support from Wageningen University for printing this thesis is gratefully acknowledged.

Cover and layout design: Agilecolor Design Studio/Atelier || www.agilecolor.com

Printed by: Proefschriftmaken.nl || Uitgeverij BOXPress